

1-1-2012

# New adaptations of analytical tools for the study of dynamic interactions of lanthanide-based catalysis in aqueous media

Prabani Lakmanthi Dissanayake  
*Wayne State University,*

Follow this and additional works at: [http://digitalcommons.wayne.edu/oa\\_dissertations](http://digitalcommons.wayne.edu/oa_dissertations)

 Part of the [Chemistry Commons](#)

---

## Recommended Citation

Dissanayake, Prabani Lakmanthi, "New adaptations of analytical tools for the study of dynamic interactions of lanthanide-based catalysis in aqueous media" (2012). *Wayne State University Dissertations*. Paper 434.

This Open Access Dissertation is brought to you for free and open access by DigitalCommons@WayneState. It has been accepted for inclusion in Wayne State University Dissertations by an authorized administrator of DigitalCommons@WayneState.

**NEW ADAPTATIONS OF ANALYTICAL TOOLS FOR  
THE STUDY OF DYNAMIC INTERACTIONS OF  
LANTHANIDE-BASED CATALYSIS IN AQUEOUS MEDIA**

by

**PRABANI LAKMANTHI DISSANAYAKE**

**DISSERTATION**

Submitted to the Graduate School

of Wayne State University,

Detroit, Michigan

in partial fulfillment of the requirements

for the degree of

**DOCTOR OF PHILOSOPHY**

2012

MAJOR: CHEMISTRY

Approved by:

\_\_\_\_\_  
Advisor

\_\_\_\_\_  
Date

\_\_\_\_\_

\_\_\_\_\_

\_\_\_\_\_

## **DEDICATION**

*To my loving parents*

## ACKNOWLEDGEMENTS

First and foremost, I would like to express my heartfelt gratitude to my graduate advisor Professor Matthew J. Allen for his insightful guidance, motivation, generous support and encouragement throughout the period of my research work. I greatly appreciate his patience and valuable comments in the preparation of this manuscript. Without his help and mentoring through my research carrier, I would not have been able to accomplish my goals. I really appreciate his personal qualities such as being an efficient worker, having exceptional writing skills and possessing great critical thinking.

I am thankful to all of my committee members; Professor Colin F. Poole, Professor Jeremy J. Kodanko, and Professor Anne J. McNeil for their precious time and academic advice.

I would also like to extend my thanks to all our group members for their support and knowledge sharing discussions. I am truly grateful to have such wonderful lab mates, and I am grateful to Buddhima, Sashi, Derek, Akhila, and Jeremy for their time and valuable comments given to me for proofreading my thesis chapters.

I acknowledge LIC (Lumigen Instrument Center) staff, Chemistry Department, especially Dr. Bashar for his help and support given to me for my  $^{17}\text{O}$  NMR spectroscopic studies. Support from Nestor Ocampo and Marty Krol is greatly acknowledged.

Additionally, I want to express my cordial thanks to Melissa Barton and I thank all the staff in the chemistry department for truly making the department a friendly place.

I would like to express my appreciation towards Wayne State University for giving me the opportunity to earn my Ph.D. and for the great support during my stay.

I am forever indebted to my husband Nirodha Abeywardana for his endless love, moral support and care given to me all times which made this dissertation possible. I thank my little

son, Nisith Abeywardana for his innocent smile and love which made my life beautiful and complete.

I would like to express my deepest gratitude to my parents for their support, endless love and education given to me, that built the foundation for all my achievements. Without them I wouldn't be here today.

# TABLE OF CONTENTS

Dedication.....	ii
Acknowledgements.....	iii
List of Tables.....	ix
List of Figures.....	xii
List of Schemes.....	xvi
List of Abbreviations.....	xviii
List of Symbols.....	xix
<b>CHAPTER ONE: Introduction to chemistry of lanthanides.....</b>	<b>1</b>
1.1 Introduction .....	1
1.2 Photophysical and magnetic properties .....	1
1.3 Chemistry of the aqueous lanthanides.....	3
<b>CHAPTER TWO: Solvation and dynamics of lanthanides.....</b>	<b>7</b>
2.1 Lanthanides as water-tolerant Lewis acids.....	7
2.2 Solvation and dynamics of lanthanides in non-aqueous conditions.....	8
2.3 Lanthanides in aqueous medium.....	15
<b>CHAPTER THREE: Mukaiyama Aldol Reaction.....</b>	<b>22</b>
3.1 Introduction.....	22
3.2 Transition states of the Mukaiyama aldol reaction.....	23

3.3	Synthetic applications of the Mukaiyama aldol reaction.....	24
3.4	Lanthanide catalysts for the Mukaiyama aldol reaction.....	25
3.5	Conclusion.....	34

#### **CHAPTER FOUR: Dynamic Measurements of Aqueous Lanthanide**

##### **Triflate-Catalyzed Reactions Using Luminescence Decay ..... 36**

4.1	Introduction.....	36
4.2	Examining triflate dissociation using luminescence-decay measurements.....	37
4.2.1	Determination of $q$ values for reaction coordinates of a catalytic cycle.....	40
4.2.2	Water-coordination numbers for reaction coordinates of the catalytic cycle.....	42
4.3	Luminescence-decay measurements of a new class of aqueous-stable chiral ligands coordinated to lanthanides.....	44
4.3.1	Determination of $q$ values of metalated chiral ligands.....	46
4.3.2	Derivation of an equation for $K$ .....	50
4.3.3	Proposed transition state for the studied asymmetric Mukaiyama aldol reaction....	52
4.4	Effect of counter anion identity on the inner-sphere hydration of lanthanides.....	53
4.5	Conclusions.....	58
4.6	Experimental Section.....	59
4.6.1	Synthetic Procedures and Characterization of Eu-complex <b>4.3</b> .....	60
4.6.2	Procedure for metalation of chiral ligands <b>4.6–4.12</b> with lanthanides.....	62

#### **CHAPTER FIVE: Luminescence-Decay as an Easy-to-Use Tool for the Study of**

##### **Lanthanide-Containing Catalysts in Aqueous Solutions..... 63**

5.1	Introduction.....	63
-----	-------------------	----

5.2	Inner- and outer-sphere coordination environments of lanthanide ions in binary solvents.....	63
5.3	The six-step procedure to determine $q'$ and $n$ .....	67
5.4	Derivation of $\alpha$ and $A$ for binary solvent systems.....	86
5.5	Validation of empirically derived $\alpha$ equations.....	89
5.6	Conclusion.....	93
5.7	Experimental Section.....	94
<b>CHAPTER SIX: Adaptations of <math>^{17}\text{O}</math> NMR spectroscopy to the determination of exchange rates of the Ln-based catalytic cycles.....</b>		
6.1	Introduction.....	99
6.2	$^{17}\text{O}$ nuclear properties.....	99
6.2.1	$^{17}\text{O}$ transverse relaxation in the presence of paramagnetic ions.....	101
6.2.2	Determination of substrate- and product-exchange rates of lanthanide catalytic cycles using $^{17}\text{O}$ transverse relaxation.....	112
6.3	Conclusion.....	126
6.4	Experimental Section.....	128
	Summary of findings.....	130
	Future Outlook.....	132
	Appendix A.....	136
	Appendix B.....	145
	Appendix C.....	174
	References.....	202
	Abstract.....	210



Autobiographical Statement.....213

## LIST OF TABLES

<b>Table 2.1</b> Concentrations and chemical shifts for different lanthanide salts and their relative stability constants .....	9
<b>Table 2.2</b> Calculated apparent equilibrium constants for Ln <sup>3+</sup> ions.....	13
<b>Table 3.1</b> Mukaiyama aldol reactions with different conditions.....	23
<b>Table 3.2</b> Mukaiyama aldol reaction conditions.....	26
<b>Table 3.3</b> Reaction conditions for Mukaiyama aldol reactions catalyzed by Ytterbium trifluoromethanesulfonate in aqueous conditions.....	27
<b>Table 3.4</b> Reaction conditions used for <b>Scheme 3.5</b> .....	28
<b>Table 3.5</b> Reaction conditions used for <b>Scheme 3.6</b> .....	29
<b>Table 3.6</b> Reaction conditions used for <b>Scheme 3.7</b> .....	31
<b>Table 3.7</b> Reaction condition used for <b>Scheme 3.8</b> .....	32
<b>Table 3.8</b> Reaction conditions used for <b>Scheme 3.9</b> .....	34
<b>Table 4.1</b> Excitation and emission wavelengths used in the determination of <i>q</i> values.....	47
<b>Table 4.2</b> Number of H <sub>2</sub> O molecules, <i>q</i> , coordinated to complexes of Eu <sup>3+</sup> with chiral ligands <b>4.6–4.12</b> .....	48
<b>Table 4.3</b> Relationships among yield and water-coordination number.....	50
<b>Table 4.4</b> Published yields of Yb <sup>3+</sup> salts used to catalyze the Mukaiyama aldol reaction in <b>Scheme 1.1</b> .....	54
<b>Table 4.5</b> Yields of a Eu <sup>3+</sup> -salt-catalyzed Mukaiyama aldol reaction at 19 h (The rest of the reaction mixture contained unreacted starting material).....	55

<b>Table 5.1</b> Mean $ \tau_H^{-1} - \tau_D^{-1} _m$ values for MeOH and methanol- $d_4$ .....	68
<b>Table 5.2</b> Mean $ \tau_H^{-1} - \tau_D^{-1} _m$ values for EtOH and ethanol- $d$ .....	69
<b>Table 5.3</b> Mean $ \tau_H^{-1} - \tau_D^{-1} _m$ values for DMSO.....	70
<b>Table 5.4</b> Mean $ \tau_H^{-1} - \tau_D^{-1} _m$ values for acetone.....	71
<b>Table 5.5</b> Mean $ \tau_H^{-1} - \tau_D^{-1} _m$ values for THF.....	72
<b>Table 5.6</b> Mean $ \tau_H^{-1} - \tau_D^{-1} _m$ values for acetonitrile.....	73
<b>Table 5.7</b> Mean $ \tau_H^{-1} - \tau_D^{-1} _m$ values for DMF and DMF- $d_7$ .....	74
<b>Table 5.8</b> Mean $ \tau_H^{-1} - \tau_D^{-1} _{IS}$ values for MeOH and methanol- $d_4$ .....	76
<b>Table 5.9</b> Mean $ \tau_H^{-1} - \tau_D^{-1} _{IS}$ values for EtOH and ethanol- $d$ .....	77
<b>Table 5.10</b> Mean $ \tau_H^{-1} - \tau_D^{-1} _{IS}$ values for DMSO.....	78
<b>Table 5.11</b> Mean $ \tau_H^{-1} - \tau_D^{-1} _{IS}$ values for acetone.....	79
<b>Table 5.12</b> Mean $ \tau_H^{-1} - \tau_D^{-1} _{IS}$ values for THF.....	80
<b>Table 5.13</b> Mean $ \tau_H^{-1} - \tau_D^{-1} _{IS}$ values for acetonitrile.....	81
<b>Table 5.14</b> Mean $ \tau_H^{-1} - \tau_D^{-1} _{IS}$ values for DMF and DMF- $d_7$ .....	81
<b>Table 5.15</b> Calculated decay per inner-sphere solvent molecule.....	83
<b>Table 5.16</b> values of $w'$ for complexes <b>5.1–5.5</b> and Eu(OTf) <sub>3</sub> .....	85
<b>Table 5.17</b> Calculated $q'$ and $n$ values for DMSO binary systems.....	86
<b>Table 5.18</b> $\alpha$ values for each binary solvent system studied.....	88

<b>Table 5.19</b>	Equations describing $\alpha$ as a function of water percentage for each binary solvent system studied. The variable $x$ is the water percentage (v/v)...	89
<b>Table 5.20</b>	Recalculated $\alpha$ values and number of inner-sphere water molecules in 100% H <sub>2</sub> O for all the complexes.....	91
<b>Table 5.21</b>	Wavelengths ( $\lambda_{ex}$ and $\lambda_{em}$ ) used in the determination of inner-sphere water-coordination numbers.....	98
<b>Table 6.1</b>	Line widths for <sup>17</sup> O NMR peaks in paramagnetic solutions.....	102
<b>Table 6.2</b>	Comparison of $k_1$ values obtained from samples containing <sup>17</sup> O -enriched water versus natural abundance water. ....	104
<b>Table 6.3</b>	Calculated water-exchange rates for Ln <sup>3+</sup> perchlorate solutions at 298.15 K.....	110
<b>Table 6.4</b>	Measured <sup>17</sup> O spectral linewidths. ....	117
<b>Table 6.5</b>	Measured <sup>17</sup> O spectral linewidths.....	125

## LIST OF FIGURES

<b>Figure 1.1</b>	Radial distribution of the 4f, 5d, and 6s orbitals .....	2
<b>Figure 1.2</b>	Inner- and outer-sphere coordination of solvent molecules of aqueous Ln <sup>3+</sup> ions. The wedge around the metal ion represents non-water ligands.....	4
<b>Figure 2.1</b>	IR spectra for solutions of lutetium triflate (—) and tetraethylammonium triflate (...) in acetonitrile (lower traces in absorbance) and acetonitrile (upper trace in transmittance.) <sup>14</sup> Reprinted from <i>Inorganica Chimica Acta</i> , 207, Plinio Di Bernardo, Gregory R. Choppin, Roberto Portanova, Pier Luigi Zanonato, Lanthanide(III) trifluoromethanesulfonate complexes in anhydrous acetonitrile, 85–91, Copyright 1993, with permission from Elsevier.....	12
<b>Figure 2.2</b>	Conductivity ( $\Lambda_M$ ) of solutions of lutetium triflate (10 mM) solutions containing different concentrations of water (X) and DMSO (+). <sup>14</sup> Reprinted from <i>Inorganica Chimica Acta</i> , 207, Plinio Di Bernardo, Gregory R. Choppin, Roberto Portanova, Pier Luigi Zanonato, Lanthanide(III) trifluoromethanesulfonate complexes in anhydrous acetonitrile, 85–91, Copyright 1993, with permission from Elsevier.....	14
<b>Figure 2.3</b>	Simplified Jablonski diagram depicting the mechanism of quenching of the phosphorescence of Eu <sup>3+</sup> ions by surrounding H <sub>2</sub> O and D <sub>2</sub> O. <b>Step 1:</b> The excitation from <sup>7</sup> F <sub>J</sub> → <sup>5</sup> L <sub>J</sub> states; <b>step 2:</b> vibrational relaxation to long lived <sup>5</sup> D <sub>0</sub> energy state; <b>step 3:</b> emission; <b>step 4:</b> <sup>5</sup> D <sub>0</sub> energy state quenching by O–H and O–D vibrational oscillators of H <sub>2</sub> O and D <sub>2</sub> O, respectively. When the quenching occurs, decay in the phosphorescence occurs from the <sup>5</sup> D <sub>0</sub> → <sup>7</sup> F <sub>J</sub> states.....	17
<b>Figure 3.1</b>	General Mukaiyama aldol reaction.....	22
<b>Figure 4.1</b>	Control complex, <b>4.3</b> , with a water-coordination number of one.....	39
<b>Figure 4.2</b>	Luminescence-decay curve of complex <b>4.3</b> in D <sub>2</sub> O.....	40
<b>Figure 4.3</b>	Luminescence decay curve of complex <b>4.3</b> in H <sub>2</sub> O.....	41
<b>Figure 4.4</b>	Water-coordination number, <i>q</i> , of Eu <sup>3+</sup> in solvents containing different amounts of H <sub>2</sub> O before (•) and after (o) the addition of benzaldehyde. Standard error bars are smaller than the data points..	43

<b>Figure 4.5</b> Structures of (4.4) a common gadolinium-containing polyaminopolycarboxylate-based contrast agent and (4.5) the ligands with two types of water-binding sites labeled.....	44
<b>Figure 4.6</b> Proposed transition state in the asymmetric Mukaiyama aldol reaction using the new ligand 4.6–4.11.....	53
<b>Figure 4.7</b> Effect of Ln salts on $q$ : Eu(OTf) <sub>3</sub> (●), EuCl <sub>3</sub> (○), Eu(NO <sub>3</sub> ) <sub>3</sub> (▲), and Eu(OAc) <sub>3</sub> (■). .....	54
<b>Figure 4.8</b> Yields of the reaction shown in Scheme 1.1 catalyzed by Eu(OTf) <sub>3</sub> or Eu(NO <sub>3</sub> ) <sub>3</sub> after 48 h as a function of solvent composition.....	57
<b>Figure 5.1</b> Coordination environments of lanthanide ions in pure solvent (left) and binary solvents (right). The symbols $q$ , $q'$ , and $n$ represent the number of inner-sphere water molecules in pure water, the number of inner-sphere water molecules in binary solvent systems, and the number of inner-sphere solvent molecules in binary solvent systems, respectively.....	64
<b>Figure 5.2</b> Complexes with $w$ values ranging from 0 to 3, where $w$ represents the remaining coordination sites after ligand binding.....	65
<b>Figure 5.3</b> Plot of $ \tau_H^{-1} - \tau_D^{-1} _m$ versus $q'$ used to determine $\alpha$ and $A$ . The intercept of the plot equals $\alpha$ and reciprocal of the slope is the proportionality constant, $A$ .....	66
<b>Figure 5.4</b> $ \tau_H^{-1} - \tau_D^{-1} _m$ versus $q'$ for 60% H <sub>2</sub> O (v/v) in DMSO.....	87
<b>Figure 5.5</b> Comparison between published $q$ values taken from reference 7 (●) and recalculated $q'$ (○) of Eu <sup>3+</sup> in the first reaction coordinate of the catalytic cycle. Standard error bars are smaller than the size of the dots.....	92
<b>Figure 5.6</b> Flowchart description of my method to determine the number of inner-sphere water molecules of a Eu <sup>3+</sup> complex in a binary solvent system.....	93

<b>Figure 6.1</b>	Chemical shift range for $^{17}\text{O}$ nuclei in different functional groups.....	100
<b>Figure 6.2</b>	Cross section of the all-glass sample holder employed in the temperature studies, drawn bolted into an NMR probe. The lettered parts are (A) a brass block; (B) a brass bolt welded to the probe; (C) a rubber gasket; (D) a glass coil (2 mm outer diameter); (E) a nonsilvered Dewar; (F) a receiver coil; (G) a thermocouple well; (H) a solution surface; and (I) a orifice for filling and evacuating. Reprinted with permission from <i>J. Chem. Phys.</i> <b>1962</b> , <i>37</i> , 307–320; Copyright 1962, American Institute of Physics.....	105
<b>Figure 6.3</b>	The concentration dependence of the $^{17}\text{O}$ linewidth in acidified solutions of $\text{La}^{3+}$ , $\text{Lu}^{3+}$ , and $\text{Y}^{3+}$ perchlorates. Adapted with permission from <i>J. Chem. Phys.</i> <b>1969</b> , <i>51</i> , 4918–4927 ; doi: 10.1063/1.1671884. Copyright 1969 American Institute of Physics.....	108
<b>Figure 6.4</b>	‘Normalized’ $^{17}\text{O}$ linewidth in perchlorate solutions containing paramagnetic ions versus $1000/T$ . Adapted with permission from <i>J. Chem. Phys.</i> <b>1969</b> , <i>51</i> , 4918–4927; doi: 10.1063/1.1671884. Copyright 1969, American Institute of Physics.....	109
<b>Figure 6.5</b>	Temperature dependence of $^{17}\text{O}$ NMR transverse relaxation rates due to the presence of $[\text{Gd}(\text{DTPA})(\text{H}_2\text{O})]^{2-}$ (●, ○), $[\text{Gd}(\text{DOTA})(\text{H}_2\text{O})]^-$ (■, □), and $[\text{Gd}(\text{TETA})]^-$ (▲, Δ). Filled and open symbols correspond to measurements at 9.4 and 4.7 T, respectively. Adapted with permission from Micskei, K.; Helm, L.; Brücher, E.; Merbach, A. E. <i>Inorg. Chem.</i> <b>1993</b> , <i>32</i> , 3844–3850. Copyright 1993 American Chemical Society.....	111
<b>Figure 6.6</b>	Schematic drawing of an NMR tube with a coaxial insert.....	116
<b>Figure 6.7</b>	Reduced transverse $^{17}\text{O}$ relaxation rates versus temperature for $\text{Gd}(\text{DOTA})^-$ (○) and $\text{Gd}(\text{OTf})_3$ (●).....	118
<b>Figure 6.8</b>	(Left) Schematic drawing of an NMR tube containing sample <b>6.1</b> ; (Right) $^{17}\text{O}$ NMR spectrum obtained for solution <b>6.1</b> where the insert shows portion of the spectrum that contains peaks B, C, and D.....	120
<b>Figure 6.9</b>	(a) Schematic of an NMR tube containing sample <b>6.2</b> (water only), (b) $^{17}\text{O}$ NMR spectrum obtained for sample <b>6.1</b> , (c) schematic of an NMR tube containing sample <b>6.3</b> (water and $\text{D}_2\text{O}$ only), (d) $^{17}\text{O}$ NMR spectrum obtained for sample <b>6.2</b> . The letters C and D correspond to the peak labels in <b>Figure 6.8</b> .....	121

**Figure 6.10** Observed linewidths for the  $^{17}\text{O}$ -labeled benzaldehyde peak in sample **6.1** plotted as a function of temperature..... 122

**Figure 6.11** Observed linewidths obtained for  $^{17}\text{OH}_2$  in  $\text{H}_2\text{O}-\text{CH}_3\text{CN}$  ( $\bullet$ ),  $^{17}\text{OH}_2$  in  $\text{H}_2\text{O}-\text{C}_2\text{H}_5\text{OH}$  ( $\circ$ ), and  $^{17}\text{OH}_2$  in  $\text{H}_2\text{O}-\text{THF}$  ( $\blacktriangle$ ). Error bars represents the standard error of the measurements for the  $\text{H}_2\text{O}-\text{THF}$  system. Measurements for the  $\text{H}_2\text{O}-\text{CH}_3\text{CN}$  and  $\text{H}_2\text{O}-\text{C}_2\text{H}_5\text{OH}$  systems were not repeated. The regression type for the  $\text{H}_2\text{O}-\text{C}_2\text{H}_5\text{OH}$  system is linear..... 126



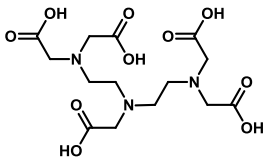
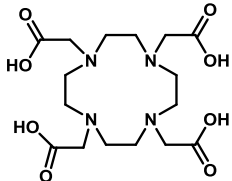
## LIST OF SCHEMES

<b>Scheme 1.1</b>	The Mukaiyama aldol reaction between a silyl enol ether and benzaldehyde in the presence of a $\text{Ln}(\text{OTf})_3$ precatalyst that was studied in this thesis. The specific reaction is between cyclohexenyloxytrimethylsilane and benzaldehyde to synthesize 2-(hydroxyphenylmethyl)cyclohexanone.....	5
<b>Scheme 3.1</b>	Possible transition states for Z-enol silanes, LA represents the Lewis acid..	24
<b>Scheme 3.2</b>	Mukaiyama aldol reaction for the synthesis of C12–C13 aldol bond in Rutamycin B, and Oligomycin C.....	25
<b>Scheme 3.3</b>	Mukaiyama aldol reactions catalyzed by lanthanide catalysts.....	26
<b>Scheme 3.4</b>	Mukaiyama aldol reactions catalyzed by ytterbium trifluoromethanesulfonate in aqueous conditions.....	27
<b>Scheme 3.5</b>	The Mukaiyama aldol reaction catalyzed by a ytterbium trifluoromethanesulfonate–surfactant combined precatalyst.....	28
<b>Scheme 3.6</b>	Mukaiyama aldol reactions catalyzed by Lanthanide Trifluoromethanesulfonate Lewis acid–surfactant combined precatalysts....	29
<b>Scheme 3.7</b>	Mukaiyama aldol reactions catalyzed by lanthanide complexes.....	30
<b>Scheme 3.8</b>	Mukaiyama aldol reactions catalyzed by a lanthanide–pybox complex.....	31
<b>Scheme 3.9</b>	Synthesis of optically active $\beta$ -hydroxycarbonyl compounds in aqueous solvent using chiral crown ether–lanthanide trifluoromethanesulfonate complexes.....	33
<b>Scheme 4.1</b>	Hydration of lanthanide triflates.....	37
<b>Scheme 4.2</b>	Catalytic cycle of an aqueous $\text{Eu}(\text{OTf})_3$ -catalyzed Mukaiyama aldol reaction.....	38

<b>Scheme 4.3</b>	Metalation of chiral ligands (4.6–4.12) with $\text{Eu}^{3+}$ to form chiral lanthanide-based precatalysts (4.6'–4.12').....	46
<b>Scheme 4.4</b>	Proposed equilibrium leading to activation of 4.6 for nucleophilic attack by benzaldehyde.....	49
<b>Scheme 4.5</b>	Equilibrium between hydrated chiral lanthanide and benzaldehyde-coordinated chiral lanthanide complex.....	51
<b>Scheme 4.6</b>	Synthesis of $q = 1$ Eu-complex (4.3) via compound 4.1–4.2.....	60
<b>Scheme 5.1</b>	Synthetic route to complex 5.4.....	96
<b>Scheme 6.1</b>	The equilibrium for water exchange between bulk and inner-sphere water, where $k_1$ is the rate constant for water exchange.....	103
<b>Scheme 6.2</b>	Simplified catalytic cycle of the Mukaiyama aldol reaction showing rates of exchange between bound and unbound substrate ( $k_{\text{substrate}}$ ) and product ( $k_{\text{product}}$ ).....	113
<b>Scheme 6.3</b>	Possible equilibria in a solution of $^{17}\text{O}$ -labeled benzaldehyde in 15% $\text{H}_2\text{O}$ in THF (v/v) containing 10 mM $\text{Eu}(\text{OTf})_3$ . Charges have been omitted for simplicity. Oxygen atoms not labeled as $^{17}\text{O}$ represent $^{16}\text{O}$ .....	120
<b>Scheme 6.4</b>	Route used to synthesize $^{17}\text{O}$ -labeled benzaldehyde.....	123

## LIST OF ABBREVIATIONS

Abbreviation	Term
Ln	lanthanide
FT	fourier-transform
MRI	magnetic resonance imaging
VT	variable-temperature
OTf	triflate
TLC	thin-layer chromatography
s	singlet
d	doublet
t	triplet
m	multiplet
HRESIMS	high-resolution electrospray ionization mass spectra
equiv	equivalents
$R_f$	retention factor
calcd	calculated
DMF	<i>N,N</i> -dimethylformamide
DMSO	dimethylsulfoxide
MeOH	methanol
THF	tetrahydrofuran
HPLC	high-Performance Liquid Chromatography
LC-MS	liquid chromatography and mass spectrometry

Abbreviation	Term	Structure
DTPA	diethylenetriaminepentaacetic acid	
DOTA	1,4,7,10-tetraazacyclododecane-1,4,7,10-tetraacetic acid	

## LIST OF SYMBOLS

Symbol	Name
$T_1$	longitudinal relaxation
$T_2$	transverse relaxation
$r_i$ ( $i = 1, 2$ )	longitudinal ( $i = 1$ ) and transverse ( $i = 2$ ) relaxivity
$q$	number of inner-sphere water molecules
$\delta$	chemical shift
$k_{ex}$	exchange rate of coordinated- and bulk-water molecules
$\tau_m$	mean residency lifetime of coordinated water molecules
$T_{1e}$	electronic spin relaxation time
$r_1^{IS}$	inner sphere longitudinal relaxation rate
$c$	concentration of the paramagnetic contrast agent
$A^{\max}$	maximum Absorbance
$g$	electron g factor
$\mu_B$	bohr magneton
$\mu_0$	magnetic constant
$S$	total spin of the paramagnetic metal ion
$\tau_{ci}$ ( $i = 1, 2$ )	longitudinal ( $i = 1$ ) and transverse ( $i = 2$ ) correlation times
$\omega_I$	nuclear Larmor frequency
$\omega_S$	electron Larmor frequency
$\gamma_I$	nuclear gyromagnetic ratio
$T_{ie}$ ( $i = 1, 2$ )	longitudinal ( $i = 1$ ) and transverse ( $i = 2$ ) electronic relaxation times
$\omega$	larmor frequency
$\gamma$	gyromagnetic ratio
$B_0$	magnetic field strength
$m$	mass
$z$	charge
$w$	weight
$v$	volume
$A$	pre-exponential factor
$\Delta E_a$	activation energy
$R$	universal gas constant
$T$	temperature
$1/T_1$	longitudinal relaxation rate
$1/T_2$	transverse relaxation rate
$\Delta E$	energy gap
$\tau_{D_2O}^{-1}$	rate of luminescence decay in $D_2O$
$\tau_{H_2O}^{-1}$	rate of luminescence decay in $H_2O$
$\alpha$	empirically derived proportionality constant
$\Delta q$	Difference of water coordination number before and after addition of

	the substrate
$A$	empirically derived proportionality constant
$q_e$	measured number of water molecules coordinated to $\text{Eu}^{3+}$ at equilibrium
$q_i$	measured number of water molecules coordinated to $\text{Eu}^{3+}$ prior to the addition of benzaldehyde
$B$	benzaldehyde
$q_b$	number of water molecules coordinated to $\text{Eu}^{3+}$ after the addition of benzaldehyde
$q'$	number of inner-sphere water molecules coordinated to $\text{Eu}^{3+}$ in binary solvent systems
$n$	number of inner-sphere solvent molecules coordinated to $\text{Eu}^{3+}$ in binary solvent systems
$ \tau_H^{-1} - \tau_D^{-1} _m$	difference of the measured decay rates in protic and deuterated solvent systems
$ \tau_H^{-1} - \tau_D^{-1} _{IS}$	absolute value of the difference of luminescence quenching rate due to inner-sphere solvent molecules
$ \tau_H^{-1} - \tau_D^{-1} _{OS}$	absolute value of the difference of luminescence quenching rate due to outer-sphere solvent molecules
$Q$	quadrupole moment
$E$	electric field gradient
$\tau_c$	rotational correlation time
$e$	charge of the electron

## CHAPTER ONE

### Introduction to chemistry of lanthanides

#### 1.1 Introduction

To pursue an analytical Ph.D., I have enabled the investigation of reaction mechanisms of water-tolerant lanthanide catalytic systems in aqueous media by studying new applications of two analytical techniques: luminescence-decay studies and variable-temperature  $^{17}\text{O}$  NMR spectroscopy. I will discuss these studies throughout my thesis in the appropriate chapters. However, the application of these techniques depends on the properties of the lanthanides; consequently, this chapter begins with a brief introduction to the properties and uses of the lanthanides. This introduction ends with a focused review of the importance of the Lewis acidity of the lanthanides that highlights the need to acquire a deeper knowledge of the fundamental behavior of these elements in aqueous media.

#### 1.2 Photophysical and magnetic properties

The lanthanide elements ( $\text{Ln}$ 's), in the periodic table between barium (56) and hafnium (72), have been actively researched since the middle of the 18th century.<sup>1,2</sup> Because of the valence electron filling of the 4f orbitals across this series of elements, the lanthanides are also known as f-block elements. The 4f orbitals are shielded from the environment by the electrons in the 5d and 6s orbitals (**Figure 1.1**);<sup>3</sup> consequently, only small crystal-field effects are observed with  $\text{Ln}^{3+}$  ions relative to d-block elements. Another important consequence of this shielding of valence orbitals is that  $\text{Ln}^{3+}$  ions have sharp emission bands due to the transitions within the 4f<sup>n</sup> electronic energy levels, which are parity forbidden and have low molar absorption coefficients

( $<3 \text{ M}^{-1}\text{s}^{-1}$ ).<sup>4</sup> Furthermore, due to the presence of electronically shielded excited states, these excited state ions have long decay times ( $\sim 10 \text{ ms}$ ).<sup>4</sup>

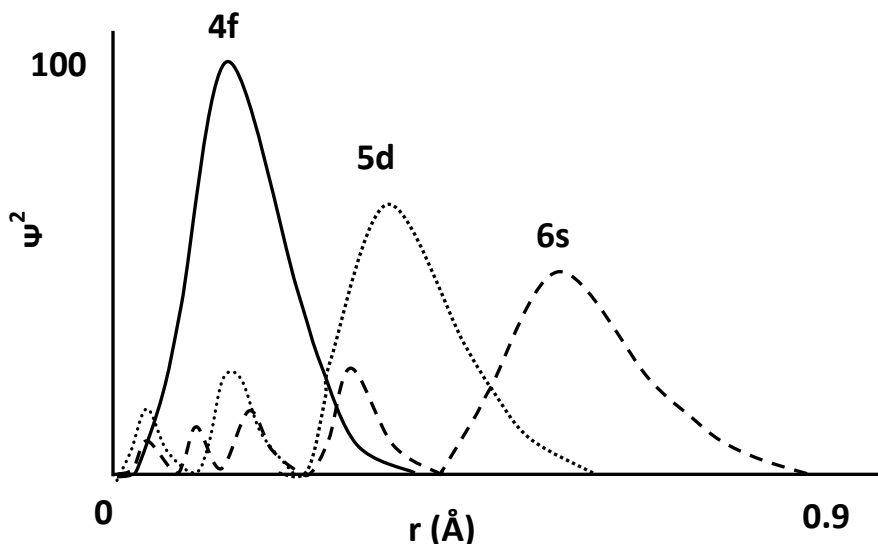


**Figure 1.1** Radial distribution of the 4f, 5d, and 6s orbitals.

Due to the photophysical properties of the lanthanides, many technologies like optical fibers, optical amplifiers, lasers, and luminescence stains use these ions for in vivo and in vitro applications including characterization in biotechnology, biomedical analysis, medical diagnosis, and cellular imaging.<sup>5,6</sup> Chapter two in this thesis contains a description of the mechanism of lanthanide luminescence, and chapter four contains a description of my research with luminescence-decay studies.

In addition to interesting luminescence properties, a consequence of having seven f orbitals is that the lanthanides are paramagnetic in their common +3 oxidation state, except for diamagnetic  $\text{La}^{3+}$  and  $\text{Lu}^{3+}$ , due to high-spin ground states. The magnetic properties of these ions are useful in magnetic applications like NMR spectroscopy and magnetic resonance imaging (MRI).<sup>5</sup> Chapter six contains a description of my research related to the magnetic properties of

lanthanides: studying the rate of ligand-exchange using variable-temperature  $^{17}\text{O}$  NMR spectroscopy.

### 1.3 Chemistry of the aqueous lanthanides

Upon solvating lanthanides, there is a strong propensity to form stable trivalent ions relative to divalent or tetravalent ions due to the stable electronic configuration of  $\text{Ln}^{3+}$  ions. These  $\text{Ln}^{3+}$  ions are hard Lewis acids, and they have a strong attraction for hard bases.<sup>7</sup> Furthermore, lanthanides have a wide-range of possible coordination numbers, 6–12.<sup>2</sup> However, compared to transition-metal ions, the coordination chemistry of these elements is less dependent on electronic configuration and more dependent on ionic radii. The low polarizing ability of  $\text{Ln}^{3+}$  ions lead to ionic interactions with ligands with less bonding strength compared to the covalent bonding characteristics of transition metals. With respect to  $\text{Ln}^{3+}$  ions, I was interested in solvated lanthanide ions, because my intention was to investigate reaction mechanisms of water-tolerant lanthanide catalytic systems in aqueous media.

Trivalent lanthanide ions readily form hydrated complexes due to their hydration energies ( $-\Delta H_{\text{hydr}} = 3300\text{--}3700 \text{ KJ mol}^{-1}$ ) and ionic radii (173–204 pm).<sup>3</sup> When lanthanide ions are solvated, the space that the directly coordinated solvent molecules occupies is called the inner-coordination sphere or inner-sphere. The next nearby layer of space outside of the inner-coordination sphere is ordered with hydrogen-bond interactions with the inner-sphere and is called the second-sphere, and the space outside of the second-sphere with freely diffusing water molecules is called the outer-sphere (**Figure 1.2**). The second- and outer-spheres are often grouped together and collectively called the outer-sphere, and I will use this convention throughout this thesis.



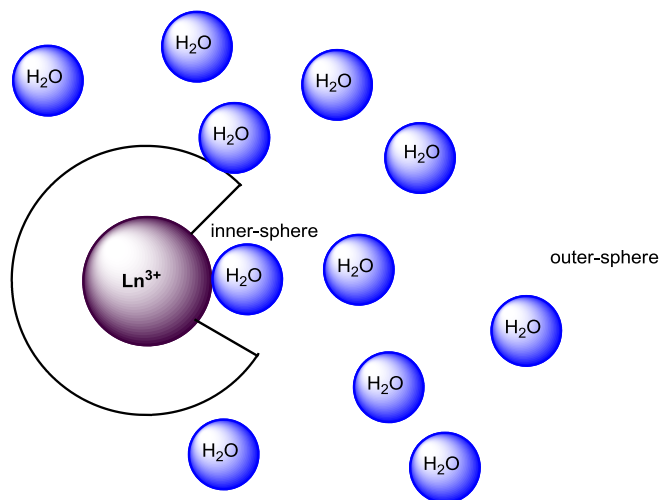
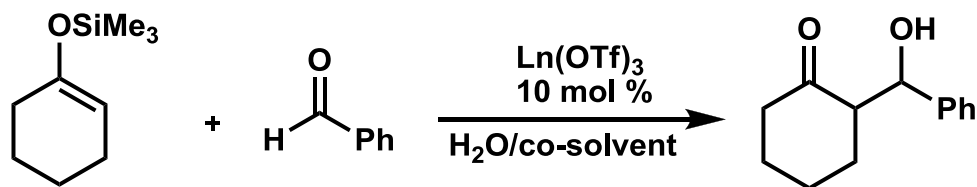


**Figure 1.2** Inner- and outer-sphere coordination of solvent molecules of aqueous  $\text{Ln}^{3+}$  ions. The wedge around the metal ion represents non-water ligands.

The use of lanthanides as Lewis acid precatalysts in aqueous solution has several advantages over traditional Lewis acid precatalysts like  $\text{BF}_3$  and  $\text{TiCl}_4$  that include the potential to work with unprotected functional groups, ease of product separation and catalyst recovery, and avoidance of costly solvent-drying procedures.<sup>7,8</sup> However, details of the lanthanide coordination spheres are not well understood in aqueous systems with respect to solvent and counter ions during catalysis. This lack of knowledge hampers the ability to rationally design and study new catalysts. Many attempts have been made to gain a detailed understanding of the aqueous properties of lanthanides via different analytical techniques—including Fourier-transform (FT)IR, NMR spectroscopy, conductivity measurements, and luminescence-decay studies—and the use of these techniques prior to my research are described in the second chapter of this thesis followed by a brief introduction to the analytical techniques that I have used to build upon and complement the techniques used by others. Due to the Lewis acidic properties of

the lanthanides, there are many important carbon–carbon and carbon–heteroatom bond-forming reactions catalyzed by lanthanides including the Diels–Alder, aldol, retro-aldol, aza-Diels–Alder, and Mukaiyama aldol reactions.<sup>9</sup> Because the Mukaiyama aldol reaction (**Scheme 1.1**) is water-tolerant, potentially stereoselective, and a synthetically important carbon–carbon bond-forming reaction,<sup>9</sup> I performed my research using this reaction as a test case. In the third chapter of this thesis, I summarize the common reaction conditions used with the Mukaiyama aldol reaction,<sup>10</sup> and my new mechanistic investigations of this reaction acquired by adapting luminescence-decay measurements are in the fourth chapter.

**Scheme 1.1** The Mukaiyama aldol reaction between a silyl enol ether and benzaldehyde in the presence of a  $\text{Ln}(\text{OTf})_3$  precatalyst that was studied in this thesis. The specific reaction is between cyclohexenyloxytrimethylsilane and benzaldehyde to synthesize 2-(hydroxyphenylmethyl)cyclohexanone.



In the fourth chapter, I also describe my research that unveils mechanistic information regarding the catalytic reaction of aqueous, lanthanide-catalyzed, asymmetric Mukaiyama aldol reactions for the synthesis of chiral  $\beta$ -hydroxy ketones via changes in water-coordination number. At the end of the fourth chapter, I describe a mechanistic study of the relationships between the rates of catalysis and water-coordination numbers of a series of lanthanide-based catalysts. This study involved the combination of high-performance liquid chromatography (HPLC) and luminescence-decay

measurements to investigate the potential use of other lanthanide salts in aqueous media including nitrates and triflates as catalysts.

In chapter five, I describe the influence of solvents other than water on inner-sphere coordination. This research is important because many organic reactions are carried out in aqueous binary solvent systems when lanthanide-based precatalysts are used.<sup>11</sup> In this study, I used the luminescence-decay rates of  $\text{Eu}^{3+}$ -containing complexes to elucidate the coordination environment of  $\text{Eu}^{3+}$  in several binary solvent systems. The end of this chapter describes how my research can be used to determine the average number of inner-sphere-water and solvent molecules in different binary aqueous solvent systems. I used the results of this chapter to make a web calculator that can be found at <http://chem.wayne.edu/allengroup/teaching.html>.

Although I have used luminescence-decay studies to determine changes in inner-sphere coordination, the mechanistically important water-, substrate-, and product-exchange rates could not be obtained using this technique. In the sixth chapter, I describe  $^{17}\text{O}$  NMR spectroscopy as the second analytical tool that I have used to elucidate mechanistic details of water-tolerant, lanthanide-catalyzed organic reactions. This technique is commonly used to study water-exchange rates with lanthanide ions, and I worked toward its application to study substrate-binding and product-inhibition rates.

The final two chapters summarize my investigations and describe future directions to explore water-tolerant lanthanide-based catalysis with respect to structure–activity relationships and novel adaptations of analytical techniques to study these catalytic systems.

## CHAPTER TWO

### Solvation and dynamics of lanthanides

Portions of this chapter were reprinted or adapted with permission from Dissanayake, P.; Mei, Y.; Allen, M. J. Luminescence-Decay as an Easy-to-Use Tool for the Study of Lanthanide-Containing Catalysts in Aqueous Solutions. *ACS Catal.* **2011**, *1*, 1203–1212. Copyright 2011 American Chemical Society.

#### 2.1 Lanthanides as water-tolerant Lewis acids

Lanthanide ions are widely used as water-tolerant Lewis acid precatalysts because they do not undergo hydrolysis and avoid the difficulties associated with recovery and reuse compared to many non-water-tolerant Lewis acids. The advantages of using aqueous-stable catalysts include the ability to use unprotected functional groups, ease of product separation and catalyst recovery, and avoidance of costly solvent drying procedures.<sup>7,8</sup> To gain the advantages of lanthanide-based precatalysts especially with respect to enantioselectivity, because many enantioselective Lewis acid catalysts must be used under strictly anhydrous conditions,<sup>10</sup> lanthanide catalysts in aqueous medium should be well understood. This understanding includes knowledge of both the inner- and outer-sphere environments of lanthanide-based precatalysts with respect to changes in the  $\text{Ln}^{3+}$  ion, counter ions, and cosolvents. A thorough understanding of these properties is helpful in understanding the kinetic and thermodynamic properties of these precatalysts in aqueous solution. However, over last two decades studies have been performed to correlate the knowledge of lanthanide salts with respect to changes in the  $\text{Ln}^{3+}$  ion, counter ions, and cosolvents to determine kinetic and thermodynamic properties of these salts in both non-aqueous and aqueous medium. Studies done initially in anhydrous conditions were important to

determine the techniques, optimum conditions which can be used to gain information regarding  $\text{Ln}^{3+}$  behavior, and this knowledge is important to study  $\text{Ln}^{3+}$  ions in aqueous media. Sub-topic 2.2 explains the past studies done to study the coordination environment of  $\text{Ln}^{3+}$  ions in non-aqueous medium, and sub-topic 2.3 describes related studies in aqueous media.

## 2.2 Solvation and dynamics of lanthanides in non-aqueous conditions

Nielson and coworkers used  $^{139}\text{La}$  NMR spectroscopy to study several  $\text{La}^{3+}$  salts including triflate, perchlorate, bromide, chloride, and nitrate in methanol, where the water content was less than 40 ppm.<sup>11</sup> They measured the chemical shift of  $^{139}\text{La}$ , to determine the relative stability constants between  $\text{Ln}^{3+}$  and counter ions ( $\text{X}^-$  and  $\text{Y}^-$ ) shown in following equilibrium in methanol at 23 °C (**Eq 2.1**).



When  $\text{La}^{3+}$  is in equilibrium with the two different anions,  $\text{X}^-$  and  $\text{Y}^-$ , only one resonance for  $^{139}\text{La}$  was observed due to rapid anion exchange (**Eq 2.2**). In **Eq 2.2**,  $x$  is the mole fraction of the  $\text{LaX}^{2+}$  complex (**Eq 2.3**) and total concentration of La at time =  $t$  is shown in **Eq 2.4**. The relative equilibrium constant for 1:1 complexes can be described by **Eq 2.5**, and by substituting **Eqs 2.2–2.4**, to **Eq 2.5**, the final **Eq 2.6** can be obtained to calculate relative equilibrium constant.

$$\text{Eq 2.2} \quad \delta_{obs} = x\delta_{\text{LaX}^{2+}} + (1-x)\delta_{\text{LaY}^{2+}}$$

$$\text{Eq 2.3} \quad x = \frac{(\delta_{obs} - \delta_{\text{LaY}^{2+}})}{(\delta_{\text{LaX}^{2+}} - \delta_{\text{LaY}^{2+}})}$$

$$\text{Eq 2.4} \quad [\text{La}]_t = [\text{LaX}_3]_t + [\text{LaY}_3]_t$$

$$\text{Eq 2.5} \quad K_{Y,X} = \frac{[\text{LaY}^{2+}][\text{X}^-]}{[\text{LaX}^{2+}][\text{Y}^-]}$$

$$\text{Eq 2.6} \quad K_{Y,X} = \frac{(1-x)(3[LaX_3]_t - [La]_t)x}{x\{3[LaY_3]_t - [La]_t(1-x)\}}$$

Nielson and coworkers used these equations with the chemical shift of the  $^{139}\text{La}$  resonance at different concentrations (**Table 2.1**).<sup>11</sup> They observed a large variation of chemical shift for different anions. These results indicate that when different anions are used, the environment of the  $^{139}\text{La}$  ion changes, indicating the inner-sphere interactions between  $\text{La}^{3+}$  and anions exist.

**Table 2.1** Concentrations and chemical shifts for different lanthanide salts and their relative stability constants.<sup>a</sup>

<i>X</i>	<i>Y</i>	[ <i>LaX</i> <sub>3</sub> ] (M)	[ <i>LaY</i> <sub>3</sub> ] (M)	$\delta X^a$ (ppm)	$\delta Y^a$ (ppm)	$\delta_{obs}$ (ppm)	<i>K</i> <sub><i>Y,X</i></sub>
$\text{ClO}_4^-$	$\text{Cl}^-$	0.247	0.244	-28	272	185	3.82
$\text{ClO}_4^-$	$\text{Br}^-$	0.213	0.213	-28	233	113	1.27
$\text{ClO}_4^-$	$\text{NO}_3^-$	0.242	0.263	-28	4.5	0.4	13.2
$\text{Cl}^-$	$\text{NO}_3^-$	0.236	0.243	272	4.5	85	3.32
$\text{Br}^-$	$\text{NO}_3^-$	0.221	0.278	233	4.5	31	11.7
$\text{CF}_3\text{SO}_3^-$	$\text{Br}^-$	0.296	0.238	-31	233	89	1.06
$\text{CF}_3\text{SO}_3^-$	$\text{Cl}^-$	0.260	0.268	-31	272	180	3.26

<sup>a</sup> $\delta X$  and  $\delta Y$  are the chemical shifts for  $\text{LaX}_3$  and  $\text{LaY}_3$  respectively.

<sup>b</sup>Reprinted from *Inorganica Chimica Acta*, 139, Jean-Claude G Bünzli, André E Merbach, Roger M Nielson,  $^{139}\text{La}$  NMR and quantitative FT-IR investigation of the interaction between Ln(III) ions and various anions in organic solvents, 151–152, Copyright 1987, with permission from Elsevier.

The data in **Table 2.1** indicate that the interactions between  $\text{La}^{3+}$  and anions increase in the following order:  $\text{CF}_3\text{SO}_3^- \approx \text{ClO}_4^- < \text{Br}^- < \text{Cl}^- < \text{NO}_3^-$ .<sup>11</sup> This study demonstrates the

complexity of anion coordination in organic solvents, and it is evident that even ‘non-coordinating’ anions, tend to coordinate to  $\text{La}^{3+}$  in organic media. Another study was performed by Kasparek and coworkers using Fourier-transformed (FT) IR studies.<sup>12</sup> They determined that the number of uncoordinated perchlorate ions,  $\text{ClO}_4^-$ , per  $\text{Ln}^{3+}$  ion ( $\text{Ln}^{3+} = \text{La}^{3+}, \text{Pr}^{3+}, \text{Sm}^{3+}, \text{Gd}^{3+}, \text{Dy}^{3+}, \text{Ho}^{3+}, \text{Tm}^{3+}, \text{and Yb}^{3+}$ ) in anhydrous acetonitrile increases with the atomic number, 1.43, 1.78, 1.78, 1.89, 2.12, 2.13, 2.02, and 2.04, respectively. Additionally, the affinity of  $\text{Ln}^{3+}$  for chloride ions vs perchlorate ions has been further investigated with respect to  $\text{Nd}^{3+}, \text{Eu}^{3+}, \text{Tb}^{3+}, \text{and Er}^{3+}$ . The results of these two studies suggest that several different inner-sphere species are present with respect to the number of coordinated perchlorate ions, the coordination mode (bidentate or monodentate), and the number of coordinated acetonitrile molecules. Although these results do not enable a detailed quantitative analysis, using simple assumptions, the authors determined the equilibrium ratios for the formation of monoperchlorato species in  $\text{Ln}(\text{ClO}_4)_3$ ,  $\text{Ln} = \text{Tb}^{3+}, \text{Dy}^{3+}, \text{Ho}^{3+}, \text{Er}^{3+}, \text{Tm}^{3+}, \text{and Yb}^{3+}$  to be 1.9,<sup>13</sup> 1.8, 1.8, 2.1,<sup>13</sup> 2.7, and 2.4 M, respectively. Further, the authors determined that the chloride ion coordinates to lanthanide ions more readily than perchlorate and that the relative affinity of lanthanide ions for chloride is higher in acetonitrile than in methanol. These conclusions were important to understand the difference of  $\text{Ln}^{3+}$  coordination in the presence of different counter anions. This background knowledge on the interactions between  $\text{Ln}^{3+}$  and anions helped me to investigate the effect of counter ions on the catalytic activity of  $\text{Ln}^{3+}$  based precatalysts in aqueous medium, and section 4.4 in chapter four gives a full description of it.

Investigations by Zanonato and coworkers using FTIR studies determined the dissociation of the triflate anion from  $\text{Ln}^{3+}$  ( $\text{Ln}^{3+} = \text{La}^{3+}, \text{Pr}^{3+}, \text{Nd}^{3+}, \text{Sm}^{3+}, \text{Eu}^{3+}, \text{Gd}^{3+}, \text{Tb}^{3+}, \text{Dy}^{3+}, \text{Ho}^{3+}, \text{Er}^{3+}, \text{Tm}^{3+}, \text{Yb}^{3+}, \text{and Lu}^{3+}$ ) in anhydrous acetonitrile.<sup>14</sup> The authors obtained the IR

spectrum for tetraethylammonium triflate, which was considered to have completely solvated triflate ions, and compared this spectrum with the IR spectrum obtained for solutions of lanthanide triflates. As seen in **Figure 2.1**, acetonitrile is transparent in the IR region where free and coordinated triflate ions show peaks. The authors varied the concentration of tetraethylammonium triflate from 10 to 175 mM to confirm the absence of a difference in band shape, and they observed a linear relationship between the maximum absorbance peak at  $1270\text{ cm}^{-1}$  ( $A_{1270}^{\max}$ ) and tetraethylammonium triflate concentration. These results suggest that there is no coordinated triflate in the tetraethylammonium triflate solution in anhydrous acetonitrile. After comparing the peaks of solutions of lutetium triflate to tetraethylammonium triflate, they assigned free and metal-coordinated triflate stretching modes for the  $\text{SO}_3$  and  $\text{CF}_3$  groups. Using  $A_{1270}^{\max}$ , they quantitatively determined the concentration of free triflate ions in the lanthanide systems. Using these concentrations, they estimated the apparent equilibrium constants,  $K_3$ , for triflate dissociation from lanthanide triflate (**Eq 2.7** and **Table 2.2**).<sup>14</sup>





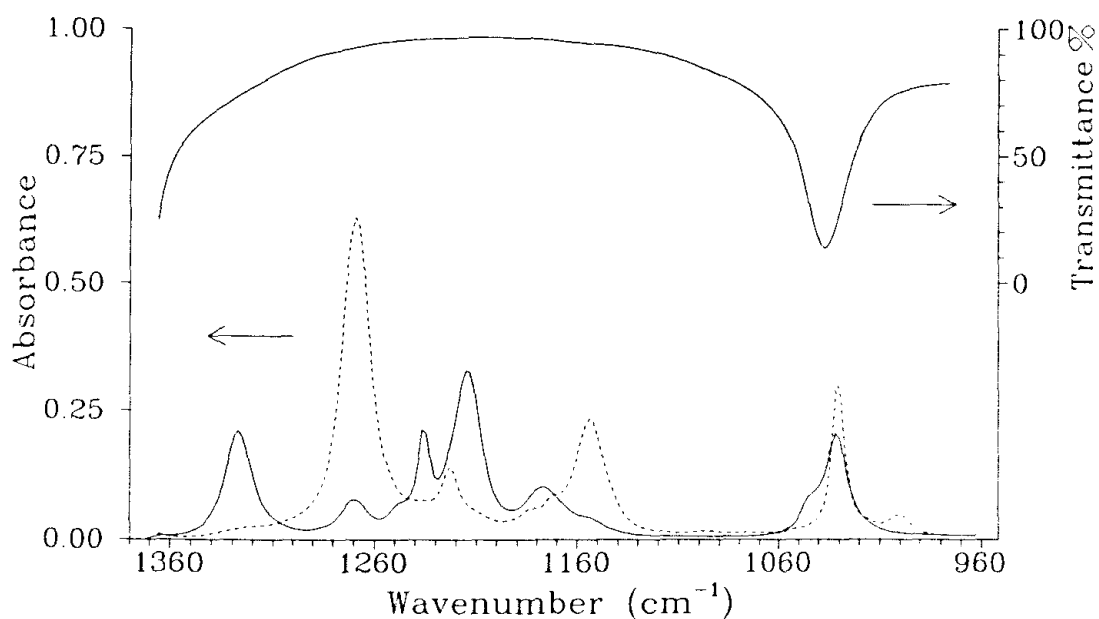


**Figure 2.1** IR spectra for solutions of lutetium triflate (—) and tetraethylammonium triflate ( - - ) in acetonitrile (lower traces in absorbance) and acetonitrile (upper trace in transmittance.)<sup>14</sup> Reprinted from *Inorganica Chimica Acta*, 207, Plinio Di Bernardo, Gregory R. Choppin, Roberto Portanova, Pier Luigi Zanonato, Lanthanide(III) trifluoromethanesulfonate complexes in anhydrous acetonitrile, 85–91, Copyright 1993, with permission from Elsevier.

**Table 2.2** Calculated apparent equilibrium constants for Ln<sup>3+</sup> ions.<sup>14</sup>

M <sup>3+</sup>	atomic number	log K <sub>3</sub>
Gd <sup>3+</sup>	64	2.52
Tb <sup>3+</sup>	65	2.58
Dy <sup>3+</sup>	66	2.53
Ho <sup>3+</sup>	67	2.53
Er <sup>3+</sup>	68	2.45
Tm <sup>3+</sup>	69	2.41
Yb <sup>3+</sup>	70	2.32
Lu <sup>3+</sup>	71	2.33

Adapted from *Inorganica Chimica Acta*, 207, Plinio Di Bernardo, Gregory R. Choppin, Roberto Portanova, Pier Luigi Zanonato, Lanthanide(III) trifluoromethanesulfonate complexes in anhydrous acetonitrile, 85–91, Copyright 1993, with permission from Elsevier.

A decrease of log K<sub>3</sub> values with increasing atomic number can be seen in **Table 2.2**. However, this result is the opposite of what would be expected based on the increasing charge density of these ions. The authors explained that this apparent contradiction was due to the steric crowding due to the addition of the third ligand to Ln(CF<sub>3</sub>SO<sub>3</sub>)<sup>2+</sup> resulting in the decreased opportunity to form Ln(CF<sub>3</sub>SO<sub>3</sub>)<sub>3</sub>. The authors extended their studies to determine the influence of the preferential solvation of lanthanide ions by a neutral ligand in acetonitrile on the dissociation of triflate. Using conductivity measurements they measured the conductance of solutions of lutetium triflate (10 mM) containing different concentrations of water and

dimethylsulfoxide (DMSO). When the ratio,  $R$ , between the moles of water or DMSO and the moles of metal ion in solution was higher than 20 (**Figure 2.2**), and two distinct plateaus in conductance were observed. This result was in accordance with previous observations.<sup>15</sup> When water was a competing ligand, two distinct plateaus with  $120\text{--}160\ \Omega^{-1}\ \text{cm}^2\ \text{mol}^{-1}$  were observed; however, when DMSO was present in a 1:2 electrolyte ratio of DMSO to  $\text{H}_2\text{O}$ , triflate dissociation continues until a second triflate is dissociated. This knowledge of preferential solvation of  $\text{Ln}^{3+}$  is important to determine the appropriate solvent conditions for efficient  $\text{Ln}^{3+}$  catalysis. Chapter 5 in this thesis describes how I have studied the preferential solvation of  $\text{Ln}^{3+}$  ions not only in DMSO, but also in other commonly used binary solvents.

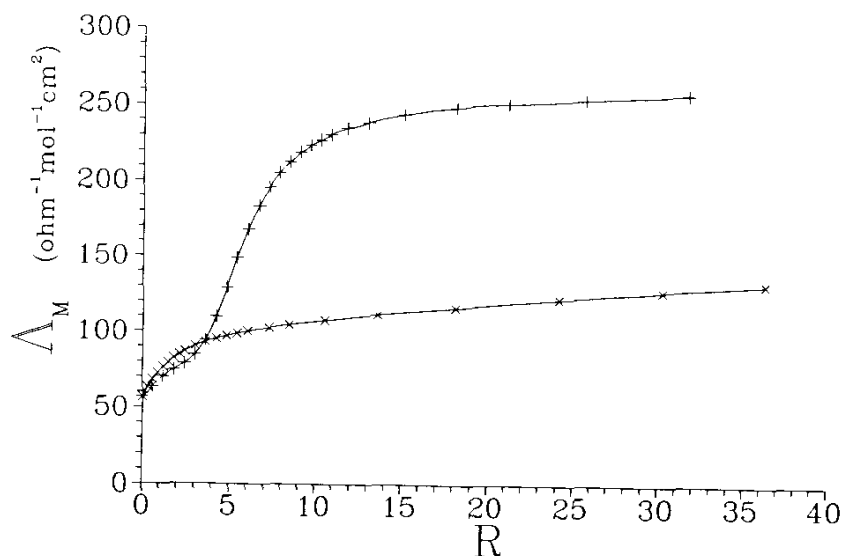


**Figure 2.2** Conductivity ( $\Lambda_M$ ) of solutions of lutetium triflate (10 mM) solutions containing different concentrations of water (X) and DMSO (+).<sup>14</sup> Reprinted from *Inorganica Chimica Acta*, 207, Plinio Di Bernardo, Gregory R. Choppin, Roberto Portanova, Pier Luigi Zanonato, Lanthanide(III) trifluoromethanesulfonate complexes in anhydrous acetonitrile, 85–91, Copyright 1993, with permission from Elsevier.

While informative, the studies discussed were performed in anhydrous conditions or in the presence of less than 40 ppm water. Therefore, these studies are not applicable, at best, to the  $\text{Ln}^{3+}$ -coordination environment when water or water-miscible organic solvents are used with larger amounts of water because the inner- and outer-sphere coordination environments of the lanthanide ions in binary solvents are different than the coordination environment in 100% water or 100% organic solvent. The difference arises from the possibility of more species in solution and of the equilibria between these species. Subtopic **2.3** explains the past studies done to determine the kinetic and thermodynamic properties of lanthanide salts with respect to changes in the  $\text{Ln}^{3+}$  ion, counter ions, and cosolvents in aqueous medium.

### **2.3 Lanthanides in aqueous medium**

Over last few decades, several groups investigated the coordination properties of  $\text{Ln}^{3+}$  in aqueous medium. Using liquid X-ray diffraction measurements, Spedding and coworkers measured the inner-sphere water-coordination numbers of  $\text{Tb}^{3+}$ ,  $\text{Dy}^{3+}$ ,  $\text{Er}^{3+}$ ,  $\text{Tm}^{3+}$ , and  $\text{Lu}^{3+}$  in concentrated (3.5–3.8 M) aqueous chloride solutions at 25 °C.<sup>16</sup> From quantitative X-ray studies followed by radial distribution functions, the inner-sphere water-coordination number of the  $\text{Ln}^{3+}$  ion studied was found to be eight. Another study was done by Narten and coworkers using neutron diffraction studies,<sup>17</sup> and their results are in close agreement with the studies of Spedding and coworkers. Narten and coworkers measured solutions of  $\text{NdCl}_3$  in  $\text{D}_2\text{O}$ , and observed that each  $\text{Nd}^{3+}$  ion is surrounded by inner-sphere water molecules, excluding chloride ions, and the average number of inner-sphere water molecules found to be  $8.5 \pm 0.2$ .<sup>18</sup> The oxygen atoms of the coordinated water molecules were directed towards  $\text{Ln}^{3+}$  ion while deuterium atoms were pointing away. To determine whether the preferential solvation of  $\text{Ln}^{3+}$  ions by water is affected

by the presence of concentrated  $\text{Cl}^-$  (10 N), Wartz and coworkers measured liquid X-ray diffraction patterns of concentrated aqueous  $\text{LaCl}_3$  solutions, where the ratio of chloride to lanthanide ion was 6:1. Even for these samples they observed Ln inner-spheres saturated with water.<sup>19</sup>

While  $^{139}\text{La}$  NMR measurements, FTIR studies,  $^{17}\text{O}$  NMR spectroscopic studies, and conductivity measurements were used to study  $\text{Ln}^{3+}$  ion interactions in solution, the limitations associated with these techniques, including the need for special instruments and complicated sample preparation, left a need for another technique to enable routine study of  $\text{Ln}^{3+}$  ions. One such technique is luminescence measurements. Luminescence is the common word to describe both fluorescence and phosphorescence. However, to determine  $\text{Ln}^{3+}$  coordination properties the decay rate of the phosphorescence is used.<sup>20</sup> To study the lanthanide phosphorescence decay, phosphorescent excited state ( $^5\text{D}_0$ ) should have a long-lived life time ( $\sim 10$  ms), and the energy gap between the  $^7\text{F}_0$  ground state and excited state should be relatively high (with  $\Delta E = 12,300\text{--}32,200\text{ cm}^{-1}$ ).<sup>4</sup> The long-lived life time enables the instrument (spectrophotometer) to detect quenching by surrounding vibrational oscillators, while energy gap requirement governs the non-radiative energy loss due to vibrational relaxation. The energy gap for  $\text{Eu}^{3+}$ ,  $\text{Gd}^{3+}$ , and  $\text{Tb}^{3+}$  are higher than that of other  $\text{Ln}^{3+}$  ions, however, because  $\text{Gd}^{3+}$  has a higher energy gap requirement ( $\Delta E = 32,200\text{ cm}^{-1}$ , it emits in the near UV region) and the fluorescence emission overlaps with the excitations and emissions of chelated organic molecules.<sup>4</sup> Further,  $\text{Eu}^{3+}$  is commonly used to represent the lanthanides series because it is centrally located in the series and, like all lanthanides, has a maximum water-coordination number,  $q$ , between 8 and 9.<sup>3,21</sup> When aqueous  $\text{Eu}^{3+}$  is excited from its  $^7\text{F}_0$  ground state to higher energy levels, a radiationless

energy transfer occurs to a long-lived  $^5D_0$  energy level.  $\text{Eu}^{3+}$  phosphorescence with the change of the spin state occurs from the  $^5D_0$  to the  $^7F_J$  states (**Fig 2.3**).

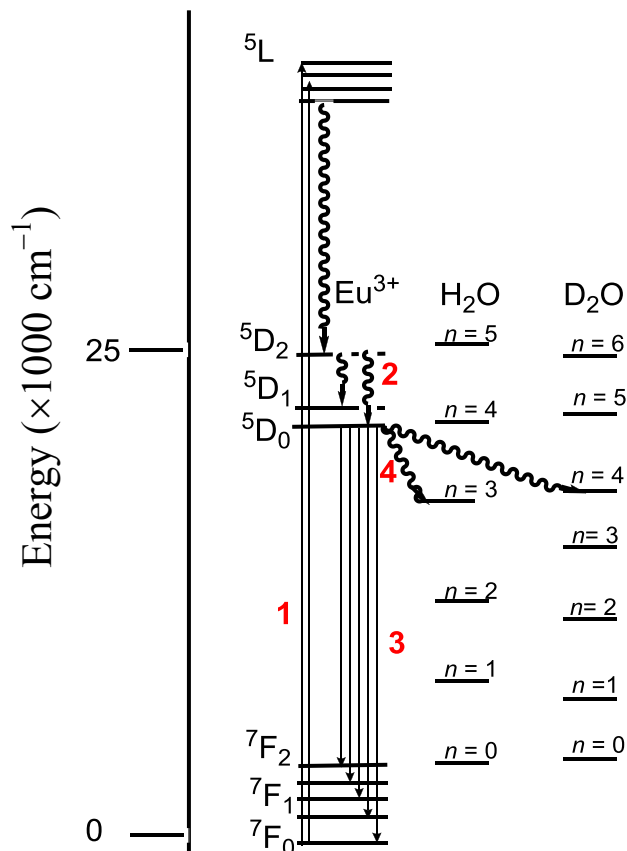


**Figure 2.3** Simplified Jablonski diagram depicting the mechanism of quenching of the phosphorescence of  $\text{Eu}^{3+}$  ions by surrounding  $\text{H}_2\text{O}$  and  $\text{D}_2\text{O}$ . **Step 1**: The excitation from  $^7F_J \rightarrow ^5L_J$  states; **step 2**: vibrational relaxation to long lived  $^5D_0$  energy state; **step 3**: emission; **step 4**:  $^5D_0$  energy state quenching by O-H and O-D vibrational oscillators of  $\text{H}_2\text{O}$  and  $\text{D}_2\text{O}$ , respectively. When the quenching occurs, decay in the phosphorescence occurs from the  $^5D_0 \rightarrow ^7F_J$  states.

The lifetime of the  $^5D_0$  excited state is directly related to the composition and structure of the inner-coordination sphere of the  $\text{Eu}^{3+}$  ion in solution. The excited-state energy can be

quenched either by the functional groups of counter ions, solvent molecules, or both depending on the energy transfer to the vibrational oscillators like O–H or N–H according to the Born–Oppenheimer principle.<sup>4,21</sup> Using this luminescence quenching, Horrocks and coworkers empirically derived an equation (**Eq 2.8**) to determine the inner-sphere water-coordination number of lanthanide ions in water.<sup>20</sup>

$$\mathbf{Eq\ 2.8} \quad q = A \left( \left| \tau_{H_2O}^{-1} - \tau_{D_2O}^{-1} \right| - \alpha + \beta n_{OH} + \gamma n_{NH} + \delta n_{O=CNH} \right)$$

In this equation,  $q$  is the number of inner sphere water molecules;  $A$  is an empirically derived proportionality constant;  $\tau_{H_2O}^{-1}$  is the rate of luminescence decay in  $H_2O$ ;  $\tau_{D_2O}^{-1}$  is the rate of luminescence decay in  $D_2O$ ;  $\alpha$  is the quenching of the excited state of  $Eu^{3+}$  by vibrational oscillators present in the outer-sphere;  $n_{OH}$  is the number of alcoholic OH oscillators in the inner-coordination sphere of  $Eu^{3+}$ ;  $n_{NH}$  is the number of amine NH oscillators in the inner-sphere sphere of  $Eu^{3+}$ ;  $n_{O=CNH}$  is the number of amide NH oscillators in which the amide carboxylic oxygen is in the inner-coordination sphere of  $Eu^{3+}$ ; and  $\beta$ ,  $\gamma$ , and  $\delta$  are empirically derived proportionality constants. Values of  $A$ ,  $\alpha$ ,  $\beta$ ,  $\gamma$ , and  $\delta$  are published for complexes with  $q$  values between 1 and 6.<sup>20</sup>

With OH oscillators in the first coordination sphere of the metal ion, there is an efficient pathway for radiationless de-excitation of  $Eu^{3+}$  via energy transfer to O–H vibrational overtones. If  $H_2O$  is replaced by  $D_2O$ , the energy transfer to O–D oscillators is about 200 times slower because the vibronic coupling of  $Eu^{3+}$  with the O–D oscillators is less efficient due to an isotopic effect. Using this quenching difference, the number of water molecules can be calculated from difference between the rates of luminescence decay in  $D_2O$  and  $H_2O$  (**Eq 2.8**).

Using this technique, Kimura and coworkers determined the number of inner-sphere water molecules of  $\text{Ln}^{3+}$  in different volume percentages of  $\text{H}_2\text{O}$  in binary solvent systems.<sup>22</sup> In this study using time-resolved laser-induced fluorescence spectroscopy, they measured luminescence decay constants  $K_{obs}$  ( $\text{ms}^{-1}$ ) of  $\text{Ln}^{3+}$ -polyaminopolycarboxylate complexes ( $\text{Ln} = \text{Sm}^{3+}, \text{Dy}^{3+}, \text{Eu}^{3+}, \text{and Tb}^{3+}$ ) of known ligand coordination numbers in different ratios of  $\text{H}_2\text{O}$  and  $\text{D}_2\text{O}$ . Using the linear relationship between  $K_{obs}$  and the inner-sphere coordination number ( $N_{\text{H}_2\text{O}}$ ), they derived the following empirical formulae to determine the inner-sphere coordination number ( $N_{\text{H}_2\text{O}}$ ) with an uncertainty of  $\pm 0.3$  water molecules (**Eqs 2.9–2.12**). With these equations, Kimura and coworkers extended their study to determine the inner-sphere hydration number and solvent composition in binary solvents composed of water and water-miscible-solvent mixed aqueous solvent systems. By changing the non-aqueous solvent mole fraction,  $X_s$ , they measured  $K_{obs}$ .

$$\text{Eq 2.9 for Sm}^{3+}: N_{\text{H}_2\text{O}} = 2.54 \times 10^{-5} k_{obs} - 0.37$$

$$\text{Eq 2.10 for Eu}^{3+}: N_{\text{H}_2\text{O}} = 1.05 \times 10^{-3} k_{obs} - 0.44$$

$$\text{Eq 2.11 for Tb}^{3+}: N_{\text{H}_2\text{O}} = 4.03 \times 10^{-3} k_{obs} - 0.87$$

$$\text{Eq 2.12 for Dy}^{3+}: N_{\text{H}_2\text{O}} = 2.11 \times 10^{-5} k_{obs} - 0.60$$

Using **Eq 2.10**, inner-sphere hydration numbers were calculated for twelve binary solvent systems: acetone, acetonitrile, *N,N*-dimethylacetamide, *N,N*-dimethylformamide (DMF), dimethylsulfoxide (DMSO), ethanol (EtOH), formamide, hexamethyl phosphoramidate, methanol (MeOH), *N*-methylformamide, pyridine, and tetrahydrofuran (THF). However, in their studies, the contribution of inner- and outer-sphere non-water solvent molecules was neglected; therefore, the calculated inner-sphere coordination number does not reflect an accurate



coordination sphere for  $\text{Eu}^{3+}$  because empirically derived **Eqs 2.9–2.12** do not account for binary solvent mixture dynamics. Consequently, these results are not optimal for use in studying catalysis. In another study,  $\text{Eu}^{3+}$  ions were used to determine a correlation between luminescence lifetime and water percentage.<sup>23</sup>  $\text{Eu}^{3+}$  luminescence lifetimes in DMF and DMSO with  $\leq 1\%$   $\text{H}_2\text{O}$  were measured. Using the correlation between  $\text{Eu}^{3+}$  luminescence lifetime and molar percentage of water in DMF, **Eqs 2.13** and **2.14** were derived, where  $t$  is the luminescence lifetime in ms. Using these equations, the water-concentration in binary solvents could be determined, but not inner- or outer-sphere water-coordination numbers. Therefore, these innovations cannot be applied to gain detailed mechanistic insights of lanthanide catalysts in solution.

**Eq 2.13** for DMF:  $H_2O \text{ mol}\% = (1.591 - t) / 0.588$

**Eq 2.14** for DMSO:  $H_2O \text{ mol}\% = (1.605 - t) / 0.112$

Due to the inapplicability of **Eqs 2.9–2.14** to study catalysis in binary solvent systems, I did not use these equations in my studies of the Mukaiyama aldol reaction. Chapter 4 contains a full account of this study. However, because **Eq 2.8** was empirically derived in water, it was not applicable to all solvent systems that are useful for catalysis because of differences in the inner- and outer-sphere luminescence quenching ability between water and other solvents. As a result of these differences, every experiment that I performed was validated when water is not the only solvent. For example, in determining the effect of THF on  $q$  values, I performed validation experiments using complexes with known coordination numbers.<sup>24</sup> The additional workload resulting from the need to validate each solvent composition renders the use of Horrocks's equation impractical for the routine study of carbon–carbon and carbon–heteroatom bond-forming reactions in the most commonly used aqueous solvent systems. Therefore, I expanded

upon my initial work to enable practical, routine analysis of lanthanide catalysts with respect to commonly used water-miscible solvents.<sup>25</sup> In Chapter 5, I report the results of my studies of the variations of inner- and outer-sphere dynamics with respect to commonly used organic solvents for Lewis acid-mediated catalytic systems including THF, EtOH, MeOH, DMF, DMSO, acetone, and acetonitrile. Furthermore, I describe the empirically derived equations that resulted from my studies that enable fast and accurate determination of inner-sphere coordination behavior in commonly used binary solvent systems.

## CHAPTER THREE

### Mukaiyama Aldol Reaction

Portions of this chapter were reprinted or adapted with permission from Dissanayake, P.; Averill, D. J.; Allen, M. J. Lanthanide-Catalyzed Mukaiyama Aldol Reactions. In *Science of Synthesis*, Knowledge Updates 2011/4; Marek, I., Ed.; Georg Thieme Verlag KG: Stuttgart, Germany, 2012; pp 1–9.

#### 3.1 Introduction

The Mukaiyama aldol reaction is the reaction between silyl enol ethers and aldehydes or ketones to form  $\beta$ -hydroxy carbonyls (**Figure 3.1**). This reaction was first reported by Mukaiyama in 1973.<sup>26</sup> In this reaction, the keto–enol form of the product is isolated using trimethylsilane to avoid cross aldol reactions resulting in chemoselective and stereoselective carbon–carbon bond formation. Mukaiyama used a stoichiometric amount of Lewis acids including  $\text{TiCl}_3$ ,  $\text{SnCl}_4$ ,  $\text{AlCl}_3$ . Later, alkali metals, alkaline earth metals, metalloids, transition metals, and lanthanide ions were used as Lewis acid catalysts.<sup>27</sup>

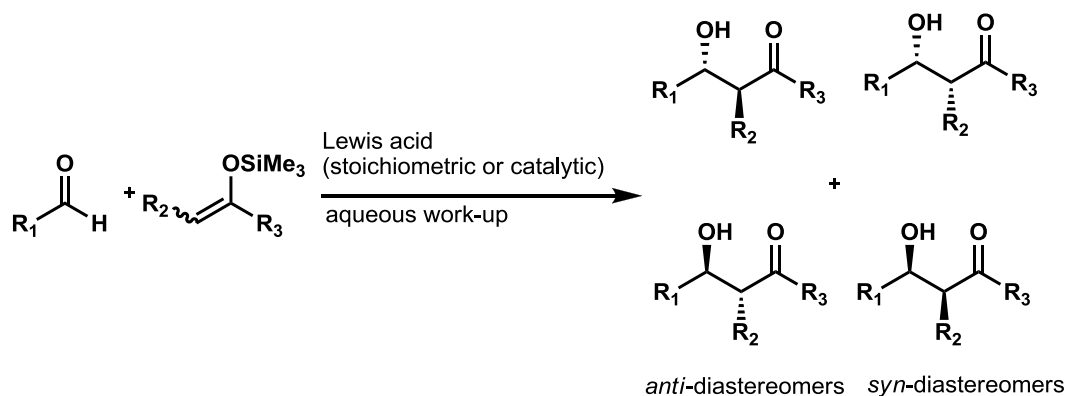


**Figure 3.1** General Mukaiyama aldol reaction.

### 3.2 Transition states of the Mukaiyama aldol reaction

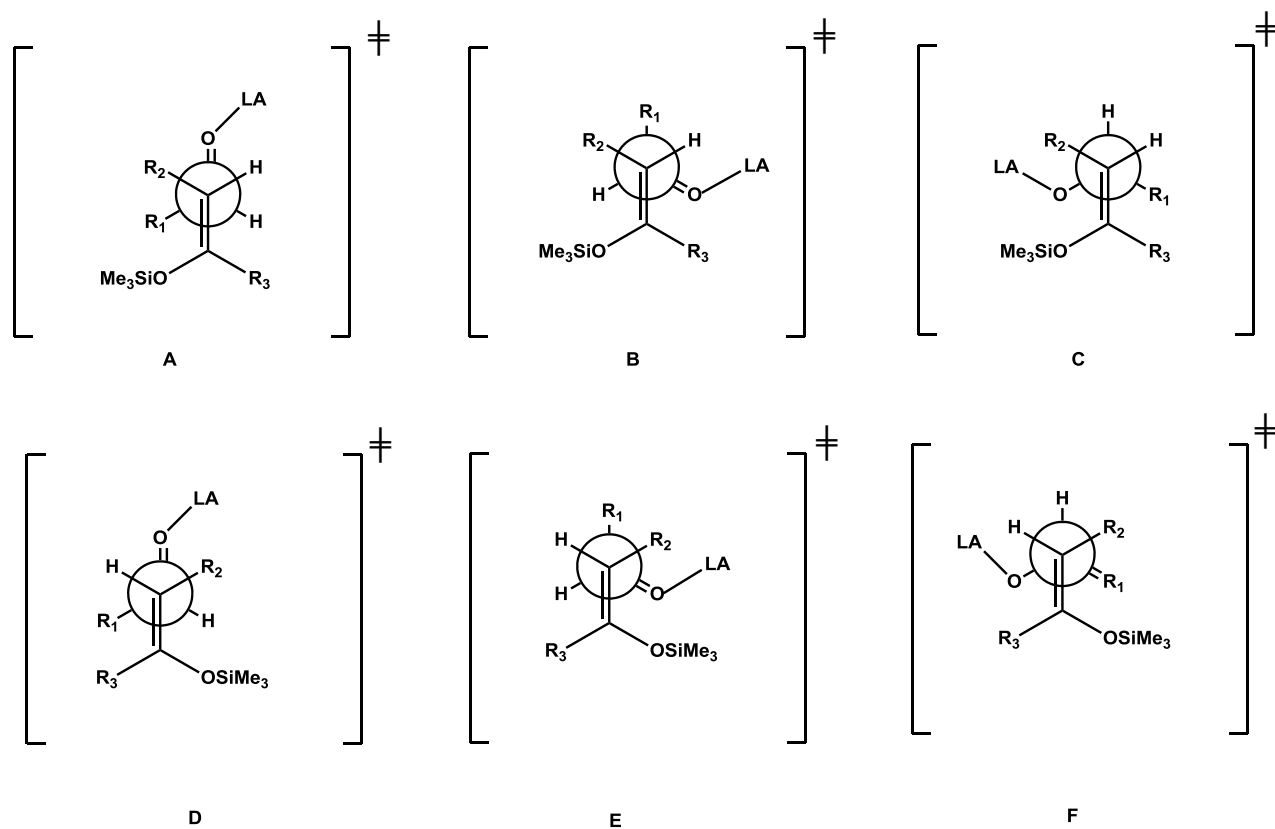
The stereoselectivity of the Mukaiyama aldol reaction changes with respect to Lewis acid catalyst, nature of the substituents ( $R_1$ ,  $R_2$ , and  $R_3$ ), and reaction conditions (**Table 3.1**).<sup>28–33</sup> This observation can be explained using an open model of the transition state. The possible transition states for *Z*-enol silanes are shown in **Scheme 3.1**, where LA represents the Lewis acid. Transition state B is unfavorable due to the steric hindrance between  $R_3$  and Lewis acid. Transition states C and E are unfavorable due to interactions between the O–LA moiety and OSiMe<sub>3</sub>. Transition state A produces *anti* diastereomers and is favored over D and F when  $R_2$  is small or  $R_3$  is bulky. The *syn* diastereomer is produced from transition states D and F. When  $R_2$  is bulky, transition state D is favored over transition state F because of the increased steric hindrance with  $R_1$  giving the *syn* diastereomer.<sup>34</sup>

**Table 3.1** Mukaiyama aldol reactions with different conditions.

$R_1$	$R_2$	$R_3$	Z/E	Lewis Acid	ratio of yield ( <i>anti/syn</i> )	yield (%)	ref
<i>i</i> -Pr	Me	OEt	15/85	TiCl <sub>4</sub>	93/7	75	28
<i>i</i> -Pr	Me	<i>t</i> -Bu	100/0	BF <sub>3</sub> ·OEt <sub>2</sub>	95/5	84	29
Ph	Me	OEt	25/75	TiCl <sub>4</sub> ·PPh <sub>3</sub>	91/9	79	30
Ph	Me	<i>t</i> -Bu	100/0	BF <sub>3</sub> ·OEt <sub>2</sub>	95/5	95	31
Ph	<i>t</i> -Bu	OEt	76/24	TiCl <sub>4</sub>	8/92	nr <sup>a</sup>	32
	Me	Ph	100/0	TiCl <sub>4</sub>	10/90	nr <sup>a</sup>	33

<sup>a</sup> not reported.

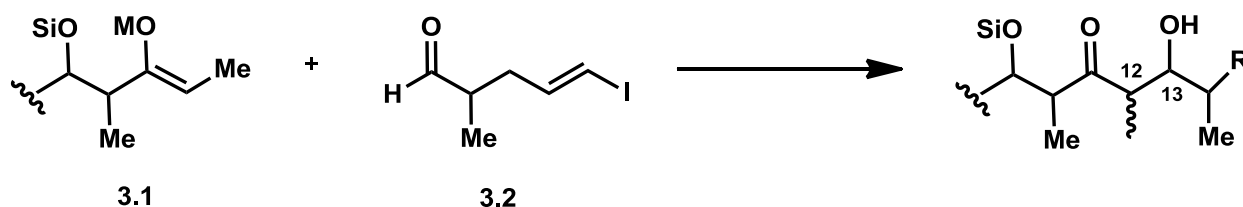
**Scheme 3.1** Possible transition states for Z-enol silanes, LA represents the Lewis acid.<sup>34</sup>



### 3.3 Synthetic applications of the Mukaiyama aldol reaction

The Mukaiyama aldol reaction has been used often in synthetic applications including the synthesis of two members of an oligomycin family that are commonly used as antibiotics: Rutamycin B and Oligomycin C. This reaction was used to synthesize the C12–C13 bond between (Z)-O-silyl enol ether, **3.1** and chiral  $\alpha$ -methyl aldehyde, **3.2**, by Jain and coworkers (**Scheme 3.2**).<sup>35</sup> They used different Lewis acid catalysts including BF<sub>3</sub>·OEt<sub>2</sub>, SnCl<sub>4</sub>, and TiCl<sub>4</sub> as well as different sizes of silicon groups such as Me<sub>3</sub>Si, Me<sub>2</sub>PhSi, *t*-BuMe<sub>2</sub>Si. With respect to yield and diastereoselectivity, the combination of BF<sub>3</sub>·OEt<sub>2</sub> and the sterically bulky Me<sub>2</sub>PhSi(Z)-O-silyl enol ether was found to be best.

**Scheme 3.2** Mukaiyama aldol reaction for the synthesis of the C12–C13 aldol bond in Rutamycin B and Oligomycin C.<sup>35</sup>



Another class of antifungal agents called SpHINGOFUNGINS B and F, were synthesized by Hanada and coworkers using the  $\text{Sn}^{2+}$ -catalyzed asymmetric Mukaiyama aldol reaction.<sup>36</sup> Roflamycoin antifungal antibiotics with a pentaene structure also were synthesized using a catalytic amount of a chiral titanium catalyst to introduce a stereocenter into roflamycoin via an asymmetric Mukaiyama aldol reaction.

Because of the importance of this reaction, it is important to study the reaction mechanism. In anhydrous conditions, the reaction mechanism is well understood.<sup>34</sup> However, in aqueous medium the reaction mechanism of this Mukaiyama aldol reaction is less well understood. Therefore, I was interested investigating the reaction mechanisms of lanthanide catalytic systems in aqueous media. To put my studies in context, section 3.4 summarizes the reaction conditions used for Mukaiyama aldol reactions since 1987.

### 3.4 Lanthanide catalysts for the Mukaiyama aldol reaction

In this section, reactions are categorized as follows: (1) non-enantioselective formation of  $\beta$ -hydroxycarbonyls; (2) enantioselective formation of  $\beta$ -hydroxycarbonyls in an organic solvents; and (3) enantioselective formation of  $\beta$ -hydroxycarbonyls in aqueous solvents. I focus first on non-enantioselective Mukaiyama Aldol reactions. Lanthanide-catalyzed Mukaiyama aldol reactions between aldehydes **3.3** and the trimethylsilyl methyl acetal **3.4** to obtain

Mukaiyama aldol products **3.5** and **3.6** were first reported using lanthanide trichlorides (**Scheme 3.3**).<sup>37</sup> Furthermore, when lanthanide tribromides are used as catalysts, the reactions proceed smoothly at room temperature.<sup>38</sup> In addition to lanthanides in the +3 oxidation state, samarium di-iodide is used as an efficient catalyst for this reaction, and the samarium di-iodide precatalyst is stable enough to be stored under argon without oxidation (**Scheme 3.3**).<sup>39</sup> **Table 3.2** summarizes the reaction conditions for **Scheme 3.3** and corresponding yields for different reactions.

**Scheme 3.3** Mukaiyama aldol reactions catalyzed by lanthanide catalysts.

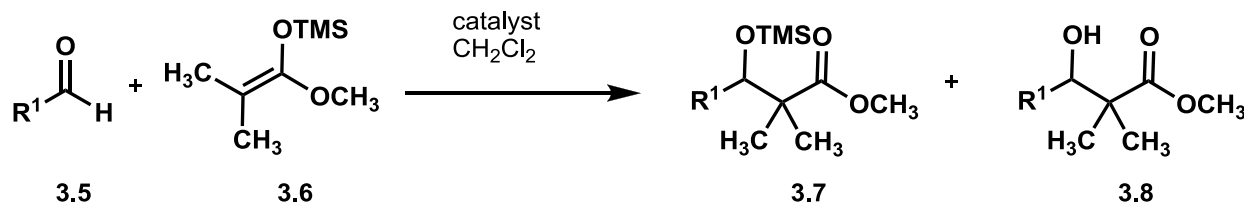


**Table 3.2** Mukaiyama aldol reaction conditions

R <sup>1</sup>	Ln Catalyst	Time	Temperature	Yield (%)		Ref
				R <sup>2</sup> = TMS	R <sup>2</sup> = H	
C <sub>6</sub> H <sub>5</sub>	SmCl <sub>3</sub>	12 h	rt	66	28	37
C <sub>6</sub> H <sub>5</sub>	CeCl <sub>3</sub>	24 h	rt	61	27	37
C <sub>6</sub> H <sub>5</sub>	LaCl <sub>3</sub>	4 d	rt	21	42	37
<i>n</i> -C <sub>5</sub> H <sub>11</sub>	SmCl <sub>3</sub>	36 h	rt	47	16	37
4-MeOC <sub>6</sub> H <sub>4</sub>	LnBr <sub>3</sub> (THF) <sub>2.6</sub> <sup>a</sup>	2 h	rt	86 <sup>b</sup>	nr <sup>c</sup>	38
3-O <sub>2</sub> NC <sub>6</sub> H <sub>4</sub>	LnBr <sub>3</sub> (THF) <sub>2.6</sub> <sup>a</sup>	4 h	rt	nr <sup>c</sup>	83 <sup>d</sup>	38
4-MeOC <sub>6</sub> H <sub>4</sub>	SmI <sub>2</sub> (THF) <sub>2</sub>	5 min	-78 °C	95	nr <sup>c</sup>	39
4-MeOC <sub>6</sub> H <sub>4</sub>	SmI <sub>3</sub> (THF) <sub>3</sub>	5 min	-78 °C	95	nr <sup>c</sup>	39
Ph	SmI <sub>2</sub> (THF) <sub>2</sub>	5 min	-78 °C	95	nr <sup>c</sup>	39
<i>n</i> -C <sub>7</sub> H <sub>15</sub>	SmI <sub>2</sub> (THF) <sub>2</sub>	4.5 h	-20 °C	90	nr <sup>c</sup>	39

<sup>a</sup> prepared from mischmetal, <sup>b</sup> LnBr<sub>3</sub>(THF)<sub>2.6</sub> (20 mol %), <sup>c</sup> not reported, <sup>d</sup> LnBr<sub>3</sub>(THF)<sub>2.6</sub> (10 mol %)

Another variation of the lanthanide-catalyzed Mukaiyama aldol reaction is carried out in aqueous media using a catalytic amount of ytterbium triflate. These aqueous reactions between formaldehyde and silyl enol ethers **3.7** to yield hydroxymethylated adducts **3.8** are shown in **Scheme 3.4** and results are shown in **Table 3.3**.<sup>40</sup>

**Scheme 3.4** Mukaiyama aldol reactions catalyzed by ytterbium trifluoromethanesulfonate in aqueous conditions.<sup>40</sup>

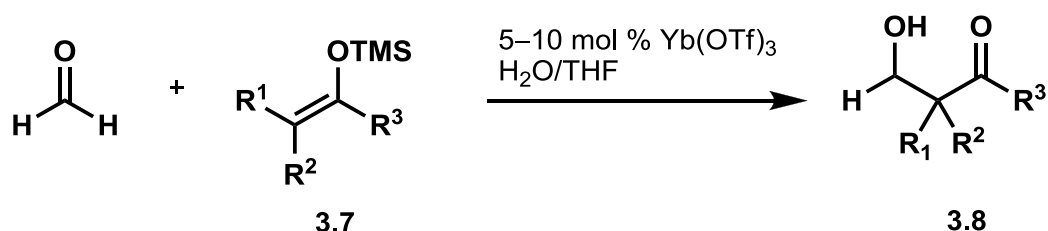


**Table 3.3** Reaction conditions for Mukaiyama aldol reactions catalyzed by ytterbium trifluoromethanesulfonate in aqueous conditions.

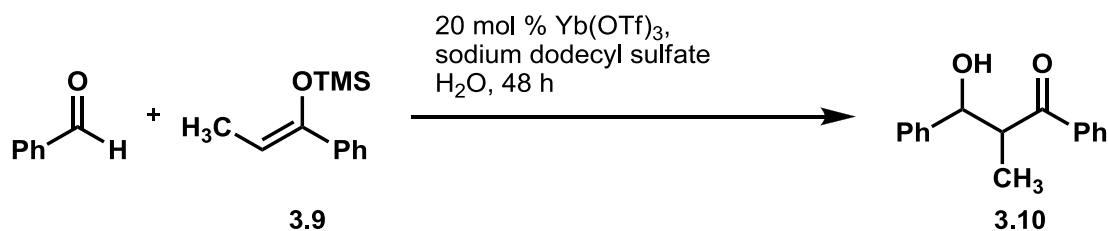
R <sup>1</sup>	R <sup>2</sup>	R <sup>3</sup>	yield (%)	Ref
Me	H	Ph	94	40
H	Me	Et	85	40
H		Me	86 <sup>a</sup>	40
Me			92	40
<i>i</i> Pr	H	Ph	92	40
Me		St-Bu	90	40

<sup>a</sup> dr 3:2; <sup>b</sup> dr (anti/syn) 9:1.



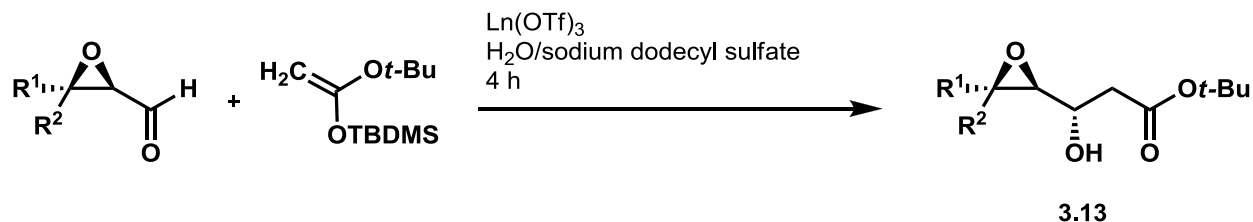
In addition to using cosolvents with water, lanthanide-Lewis-acid-surfactant-combined precatalysts are used for Mukaiyama aldol reactions in water (**Schemes 3.5** and **3.6**).<sup>41,42</sup> The reaction between benzaldehyde and silyl enol ether, **3.9**, to yield aldol adduct **3.10** (**Scheme 3.5**) suggests that the amount of surfactant, sodium dodecyl sulfate, influences the reaction yield (**Table 3.4**). The aqueous Mukaiyama aldol reactions of  $\alpha,\beta$ -epoxyaldehydes **3.11** with enol silane **3.12** to yield products **3.13** also have been reported using sodium dodecyl sulfate (**Scheme 3.5** and **Table 3.5**).<sup>42</sup>

**Scheme 3.5** The Mukaiyama aldol reaction catalyzed by a ytterbium trifluoromethanesulfonate-surfactant combined precatalyst.<sup>41</sup>



**Table 3.4** Reaction conditions used for **Scheme 3.5**.

sodium dodecyl sulfate (equiv)	yield (%)	Ref
none	17	41
0.04	12	41
0.1	19	41
0.2	50	41
1.0	22	41

**Scheme 3.6** Mukaiyama aldol reactions catalyzed by Lanthanide trifluoromethanesulfonateLewis acid–surfactant combined precatalysts.<sup>42</sup>**Table 3.5** Reaction conditions used for **Scheme 3.6**.

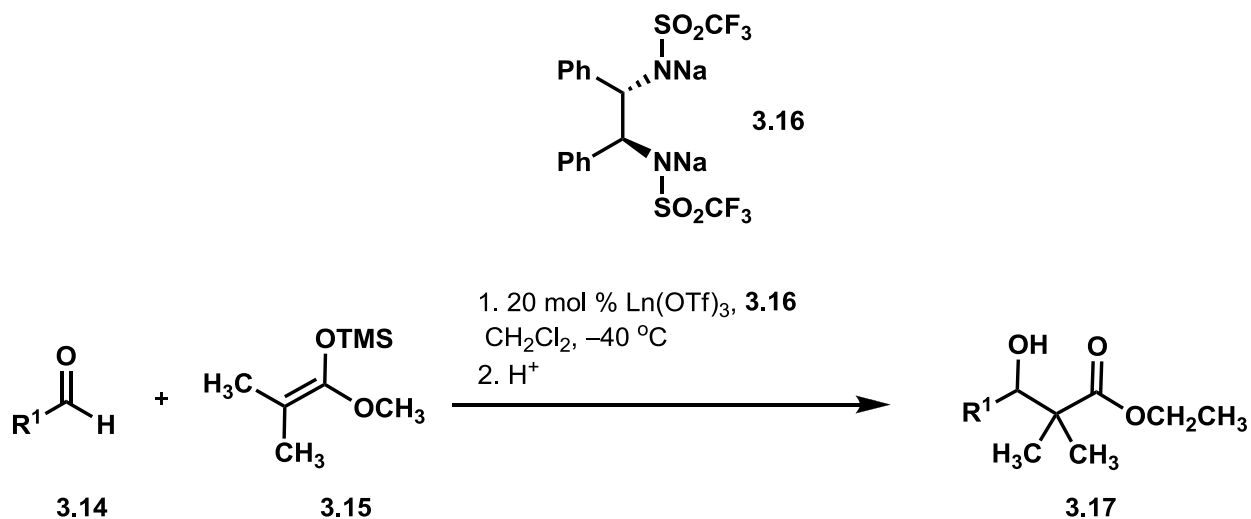
R <sup>1</sup>	R <sup>2</sup>	Lewis acid	yield (%)	anti:syn	Ref
H	CH <sub>2</sub> OTBDPS	Eu(OTf) <sub>3</sub>	25	90:10	42
H	CH <sub>2</sub> OTBDPS	La(OTf) <sub>3</sub>	46	91:9	42
H	CH <sub>2</sub> OTBDPS	Yb(OTf) <sub>3</sub>	33	94:6	42
CH <sub>2</sub> OTBDPS	H	La(OTf) <sub>3</sub>	33	67:33	42
H	OBn	La(OTf) <sub>3</sub>	35 <sup>a</sup>	90:10	42

<sup>a</sup> Starting material was used as a racemic mixture of R,R- and S,S-stereoisomers.

Another variation of the Mukaiyama Aldol reaction is the enantioselective formation of  $\beta$ -hydroxycarbonyls in organic solvents. As an example, a chiral lanthanide-containing catalyst has been used for the asymmetric Mukaiyama aldol reaction in nonaqueous media.<sup>43</sup> The precatalyst is prepared by reacting equimolar amounts of a lanthanide trifluoromethanesulfonate and bis(sulfonamide) disodium salt [prepared by deprotonation of the corresponding bis(sulfonamide) with excess sodium hydride] at 40 °C in tetrahydrofuran (THF) for 12 h. The THF is evaporated and replaced by dichloromethane before use in the Mukaiyama aldol reaction. The chiral Ln<sup>3+</sup>-catalyst catalyzes the Mukaiyama aldol reactions between aldehydes **3.14** and silyl acetal **3.15** to produce  $\beta$ -hydroxycarbonyls **3.17** (**Scheme 3.7**). The results (**Table 3.6**) demonstrate that yields increase from La<sup>3+</sup> to Eu<sup>3+</sup> to Yb<sup>3+</sup>. Interestingly, when the La<sup>3+</sup> complex of **3.16** is used, only  $\beta$ -hydroxycarbonyl products are observed as opposed to trimethylsilyl ether-

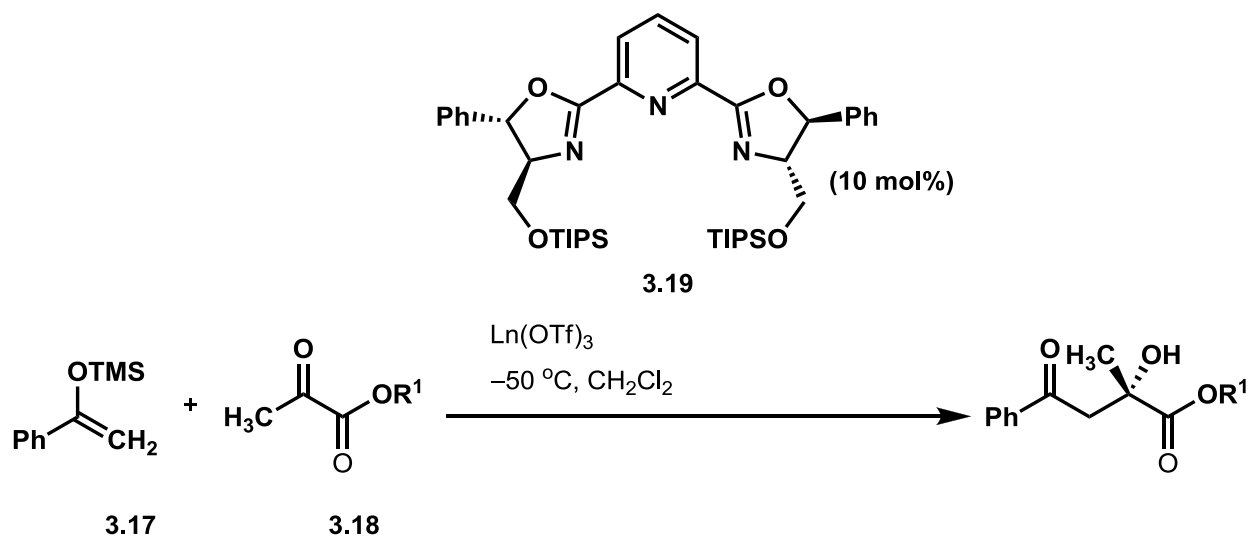
containing products.<sup>43</sup> However, when  $\text{Eu}^{3+}$  or  $\text{Yb}^{3+}$  complexes of **3.16** are used, both the hydroxy-containing product and the trimethylsilyl ether-containing products are observed. It seems that the reactivity difference among  $\text{Yb}^{3+}$ ,  $\text{Eu}^{3+}$ , and  $\text{La}^{3+}$  affects the reactivity of the corresponding metal alkoxide intermediates towards silylation. The yields observed with precatalyst **3.16** are inferior to those obtained using a combination of lanthanide triflate and pybox **3.19** (Scheme 3.8) to catalyze Mukaiyama aldol reactions between silyl enol ether **3.17** and pyruvic esters **3.18** to produce chiral products **3.20**. These results (Table 3.7) suggest that when pybox **3.19** is combined with lanthanides with smaller ionic radii, higher  $\text{er}$ 's and yields are obtained relative to when larger ions are used.

**Scheme 3.7** Mukaiyama aldol reactions catalyzed by lanthanide complexes.<sup>43</sup>



**Table 3.6** Reaction conditions used for **Scheme 3.7**.

R <sup>1</sup>	Ln(OTf) <sub>3</sub>	Yield (%)	er (S/R)	Ref
Ph	La(OTf) <sub>3</sub>	42	74:26	43
Ph	Eu(OTf) <sub>3</sub>	59	70:30	43
Ph	Yb(OTf) <sub>3</sub>	71	67:33	43
4-O <sub>2</sub> NC <sub>6</sub> H <sub>4</sub>	La(OTf) <sub>3</sub>	71	71:29	43
4-O <sub>2</sub> NC <sub>6</sub> H <sub>4</sub>	Eu(OTf) <sub>3</sub>	71	70:30	43
4-O <sub>2</sub> NC <sub>6</sub> H <sub>4</sub>	Yb(OTf) <sub>3</sub>	71	72:28	43
(CH <sub>2</sub> ) <sub>2</sub> Ph	La(OTf) <sub>3</sub>	19	70:30	43
(CH <sub>2</sub> ) <sub>2</sub> Ph	Eu(OTf) <sub>3</sub>	34	70:30	43
(CH <sub>2</sub> ) <sub>2</sub> Ph	Yb(OTf) <sub>3</sub>	55	70:30	43

**Scheme 3.8** Mukaiyama aldol reactions catalyzed by a lanthanide–pybox complex.<sup>44</sup>

**Table 3.7** Reaction conditions used for **Scheme 3.8**.

Ln <sup>3+</sup>	Ionic radius (Å)	R <sup>1</sup> = Et			R <sup>1</sup> = Me			R <sup>1</sup> = CHPh <sub>2</sub>			Ref
		Time (d)	Yield (%)	er (S:R)	Time (d)	Yield (%)	er (S:R)	Time (d)	Yield (%)	er (S:R)	
Lu <sup>3+</sup>	0.977	5	70	97.5:2.5	4	70	92.5:7.5	4	95	99.75:0.25	44
Yb <sup>3+</sup>	0.985	5	55	89.5:10.5	4	50	80.5:19.5	5	52	91:9	44
Ho <sup>3+</sup>	1.015	5	45	62:38	4	41	50:50	1.5 <sup>a</sup>	32	28:72	44
Y <sup>3+</sup>	1.019	5	41	74:26	4	37	50:50	1.5 <sup>a</sup>	30	20:80	44
Eu <sup>3+</sup>	1.066	5	39	69.5:30.5	4	40	69.5:30.5	1.5 <sup>a</sup>	30	16:84	44

<sup>a</sup> 20 °C

In addition to the reactions already described in this chapters, the asymmetric Mukaiyama aldol reaction can be carried out in aqueous media using lanthanide trifluoromethanesulfonates combined with chiral crown ethers such as **3.21** and **3.22** (**Scheme 3.9** and **Table 3.8**). Asymmetric β-hydroxycarbonyl compounds **3.25** can be obtained by the addition of aldehydes **3.23** and silyl enol ether **3.24** to a mixture containing the lanthanide–crown ether complex. Analogous chiral crown ethers which afford different selectivities can be used in place of **3.21** and **3.22**.<sup>45,46</sup>

**Scheme 3.9** Synthesis of optically active  $\beta$ -hydroxycarbonyl compounds in aqueous solvent using chiral crown ether–lanthanide trifluoromethanesulfonate complexes.

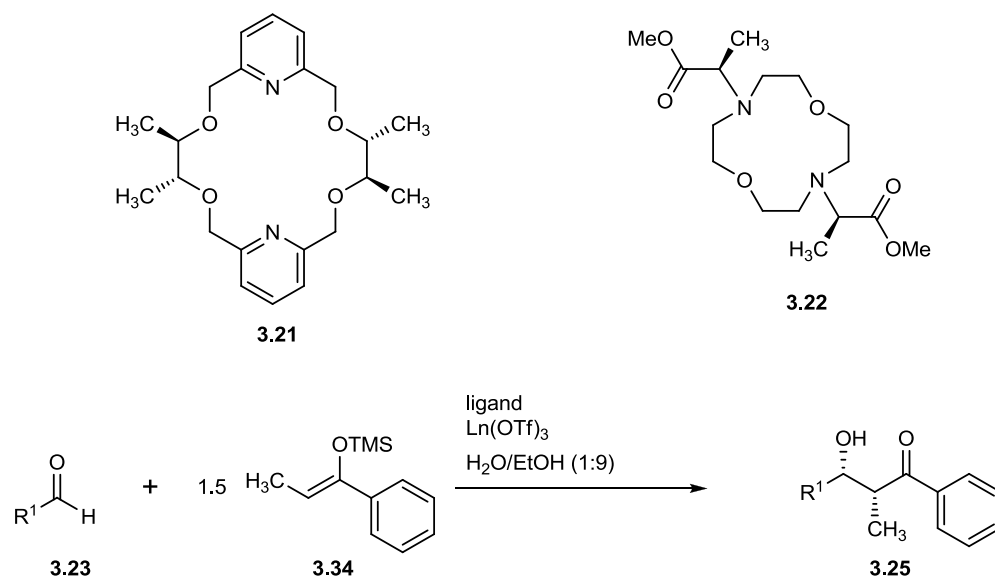


**Table 3.8** Reaction conditions used for **Scheme 3.9**.

R <sup>1</sup>	Temperature	Time	Catalyst	Yield (%)	syn:anti	er <sup>a</sup> (R:S) (syn)	Ref
Ph	0 °C	18 h	<b>3.21</b> (12 mol %) and Pr(OTf) <sub>3</sub> (10 mol %)	85	91:9	89:11	45
Ph	0 °C	18 h	<b>3.21</b> (24 mol %) and Ce(OTf) <sub>3</sub> (20 mol %)	78	93:7	91:9	46
4-MeOC <sub>6</sub> H <sub>4</sub>	0 °C	18 h	<b>3.21</b> (12 mol %) and Pr(OTf) <sub>3</sub> (10 mol %)	91	92:8	87.5:12.5	45
2-MeOC <sub>6</sub> H <sub>4</sub>	0 °C	18 h	<b>3.21</b> (12 mol %) and Pr(OTf) <sub>3</sub> (10 mol %)	96	95:5	91.5:8.5	45
4-ClC <sub>6</sub> H <sub>4</sub>	0 °C	18 h	<b>3.21</b> (12 mol %) and Pr(OTf) <sub>3</sub> (10 mol %)	87	90:10	91.5:8.5	45
1-naphthyl	0 °C	48 h	<b>3.21</b> (12 mol %) and Pr(OTf) <sub>3</sub> (10 mol %)	96	91:9	90.5:9.5	46
2-thienyl	0 °C	48 h	<b>3.21</b> (12 mol %) and Pr(OTf) <sub>3</sub> (10 mol %)	quantitative	91:9	86:14	45
2-pyridyl	0 °C	48 h	<b>3.21</b> (24 mol %) and Pr(OTf) <sub>3</sub> (20 mol %)	99	85:15	92.5:7.5	45
Ph	-25 °C	168 h	<b>3.22</b> (48 mol %) and Eu(OTf) <sub>3</sub> (20 mol %)	92	97:3	96.5:3.5	47
4-ClC <sub>6</sub> H <sub>4</sub>	-25 °C	168 h	<b>3.22</b> (48 mol %) and Eu(OTf) <sub>3</sub> (20 mol %)	75	95:5	95.5:4.5	47
4-Tol	-25 °C	168 h	<b>3.22</b> (48 mol %) and Eu(OTf) <sub>3</sub> (20 mol %)	73	96:4	95:5	47
( <i>E</i> ) CH <sub>3</sub> CH=CH (CH <sub>2</sub> ) <sub>5</sub> Me	-25 °C	168 h	<b>3.22</b> (48 mol %) and Eu(OTf) <sub>3</sub> (20 mol %)	65	95:5	96.5:3.5	47
( <i>E</i> ) CH <sub>3</sub> CH=CH (CH <sub>2</sub> ) <sub>5</sub> Me	-25 °C	168 h	<b>3.22</b> (48 mol %) and Eu(OTf) <sub>3</sub> (20 mol %)	22	96:4	98:2	47
Cy	-25 °C	168 h	<b>3.22</b> (48 mol %) and Eu(OTf) <sub>3</sub> (20 mol %)	12	2:98	97.5:2.5 <sup>b</sup>	47

<sup>a</sup> For syn isomer unless otherwise stated, <sup>b</sup> For anti isomer.

### 3.5 Conclusion

The knowledge of different conditions, catalysts, and substrates used for Mukaiyama aldol reaction was important for me in the design of my studies. The next chapter describes the

specific Mukaiyama aldol reaction that I used for my studies as well as my new mechanistic investigations of this reaction acquired by adapting luminescence-decay measurements.



## CHAPTER FOUR

### Dynamic Measurements of Aqueous Lanthanide Triflate-Catalyzed Reactions Using Luminescence Decay

Portions of the text in this chapter were reprinted or adapted with permission from:

(1) Dissanayake, P.; Allen, M. J. Dynamic Measurements of Aqueous Lanthanide Triflate-Catalyzed Reactions Using Luminescence Decay. *J. Am. Chem. Soc.* **2009**, *131*, 6342–6343. Copyright 2011 American Chemical Society. (2) Mei, Y.; Dissanayake, P.; Allen, M. J. A New Class of Ligands for Aqueous, Lanthanide-Catalyzed, Enantioselective Mukaiyama Aldol Reactions. *J. Am. Chem. Soc.* **2010**, *132*, 12871–12873. Copyright 2011 American Chemical Society. and (3) Averill, D. J.; Dissanayake, P.; Allen, M. J. The Role of Water in Lanthanide-Catalyzed Carbon–Carbon Bond Formation. *Molecules* **2012**, *17*, 2073–2081.

#### 4.1 Introduction

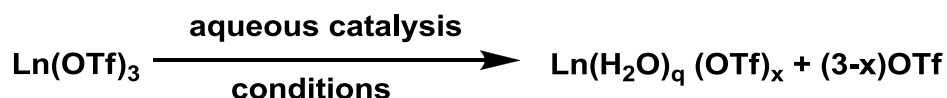
There is a great interest in water-compatible, lanthanide-triflate-based precatalysts for carbon–carbon bond-forming reactions; however, poor understanding of the mechanism of these precatalysts in aqueous systems severely limits the ability to increase their utility. In this chapter, I describe dynamic measurements of the water-coordination number of lanthanide-triflate-based catalysts using luminescence-decay measurements in a variety of aqueous systems. This characterization method is a reliable, convenient, and fast approach to analyze lanthanide-based catalysts in aqueous systems. Additionally, I describe my use of luminescence-decay measurements to unveil mechanistic information regarding a new precatalyst for the asymmetric Mukaiyama aldol reaction. This chapter ends with a description of the water-coordination

number measurements of a series of lanthanide salts to investigate the potential use of other lanthanide salts as catalysts in aqueous media.

#### 4.2 Examining triflate dissociation using luminescence-decay measurements

Although lanthanide triflates,  $\text{Ln}(\text{OTf})_3$ , are used as water-compatible precatalysts for a wide range of important carbon–carbon and carbon–heteroatom bond-forming reactions, attempts to use these water-tolerant precatalysts in stereoselective reactions have been successful only in cases of limited substrate scope.<sup>48–49</sup> I hypothesized that a major hindrance preventing the widespread use of lanthanide triflates in aqueous, asymmetric carbon–carbon bond formation was the nominal mechanistic understanding of the precatalysts in aqueous solution. Specifically, an unanswered question in aqueous lanthanide triflate-based catalysis was if complete loss of triflate from the precatalyst occurs during catalysis: is  $x$  greater than zero in **Scheme 4.1**?

**Scheme 4.1** Hydration of lanthanide triflates

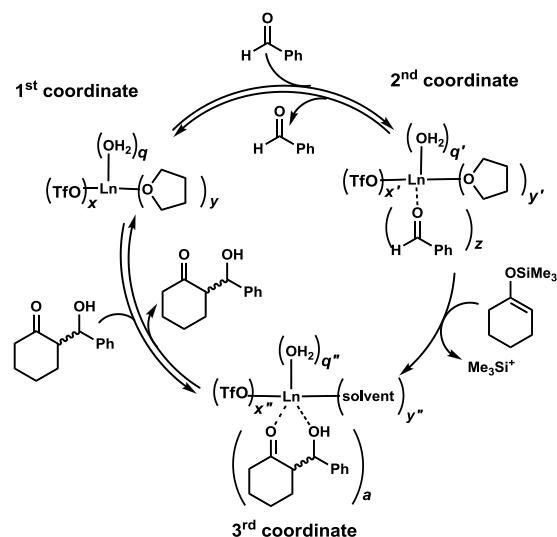


While knowledge of triflate dissociation should aid in the design of catalysts for aqueous asymmetric reactions, inconclusive support both for and against complete dissociation existed before I began my research.<sup>7,50</sup> My strategy for examining triflate dissociation was to use luminescence-decay measurements, which are commonly used to study water-coordination number with lanthanide-based contrast agents for magnetic resonance imaging.<sup>21,51</sup> Compared to other methods, such as X-ray crystallography and IR spectroscopy, this characterization method is advantageous because it allows for the direct, quantitative observation of reactions in aqueous solution. In addition to being water-tolerant, luminescence-decay measurements are fast (~10 ms) and dynamic, making them perfectly suited for the study of lanthanide-based aqueous

catalysis. I hypothesized that these properties would allow me to examine discrete reaction coordinates without perturbing the system being studied. The  $\text{Eu}^{3+}$  ion was used in these studies because it has a large energy gap between its emissive and ground states ( $\Delta E = 1.23 \times 10^4 \text{ cm}^{-1}$ ) and a long lived (9.67 ms) excited state in aqueous media.<sup>4</sup> Further,  $\text{Eu}^{3+}$  is commonly used to represent all of the lanthanides because it is centrally located in the series and, like all lanthanides, has a maximum water-coordination number,  $q$ , between 8 and 9.<sup>3,21</sup>

As demonstration of the applicability of luminescence-decay measurements to study lanthanide-based catalysts, I examined the Mukaiyama aldol reaction in **Scheme 1.1** because the Mukaiyama aldol reaction is one of the most important carbon–carbon bond-forming reactions.<sup>34,52</sup> To answer the question of triflate dissociation in the Mukaiyama aldol reaction using luminescence-decay measurements, I divided the catalytic cycle of the reaction into three reaction coordinates (**Scheme 4.2**).

**Scheme 4.2** Catalytic cycle of an aqueous  $\text{Eu}(\text{OTf})_3$ -catalyzed Mukaiyama aldol reaction<sup>a</sup>



<sup>a</sup> The subscripts  $a$ ,  $q$ ,  $x$ ,  $y$ , and  $z$  represent the number of 2-(hydroxyphenylmethyl) cyclohexanone, water, triflate, THF, and benzaldehyde ligands, respectively. Charges have been omitted for simplification.

This division made possible the separate examination of each reaction coordinate. The first reaction coordinate was generated by dissolving  $\text{Eu}(\text{OTf})_3$  in mixtures of water and tetrahydrofuran (THF). While many water-miscible solvents can be used for these reactions, I chose THF to avoid complications that could arise from solvents containing O–H or N–H oscillators.<sup>20</sup> The second and third reaction coordinates were generated by adding benzaldehyde or 2-(hydroxyphenylmethyl)cyclohexanone to the first reaction coordinate solutions, respectively. For each reaction coordinate, the concentration of precatalyst and substrate matched reported reaction conditions.<sup>7</sup> The amount of water was varied from 1 to 100%, and the validity of the method in each solvent was confirmed by measuring the water-coordination number of a control complex, **4.3**, 2,2',2''-(10-(2-hydroxyethyl)-1,4,7,10-tetraazacyclododecane-1,4,7-triyl)triaceto europium(III) (**Figure 4.1**). This complex has a water-coordination number of one,<sup>21</sup> and I obtained a water-coordination number of one for this complex using luminescence-decay measurements in every ratio of water to THF that I used (**Table A1, Appendix A**).

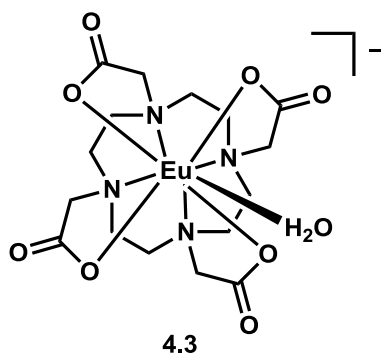


**Figure 4.1** Control complex, **4.3**, with a water-coordination number of one.

#### 4.2.1 Determination of $q$ values for reaction coordinates of a catalytic cycle

Luminescence decay measurements were acquired using a HORIBA Jobin Yvon Fluoromax-4 spectrofluorometer in decay-by-delay scan mode using the phosphorescence life time setting. For luminescence-decay measurements of control complex, **4.3**, an excitation wavelength of 395 nm and an emission wavelength of 594 nm were used. For measurements of  $\text{Eu}(\text{OTf})_3$ , an excitation wavelength of 394 nm and an emission wavelength of 591 nm were used. Other parameters were kept constant: excitation and emission slit width (5 nm), flash count (200), initial delay (0.01 ms), maximum delay (13 ms), and delay increment (0.01 ms). The natural log of the intensity of the scan was plotted against time, and the slope was used as the decay rate. This procedure was performed in  $\text{H}_2\text{O}$  and  $\text{D}_2\text{O}$  versions of each solvent (**Figures 4.2** and **4.3**).

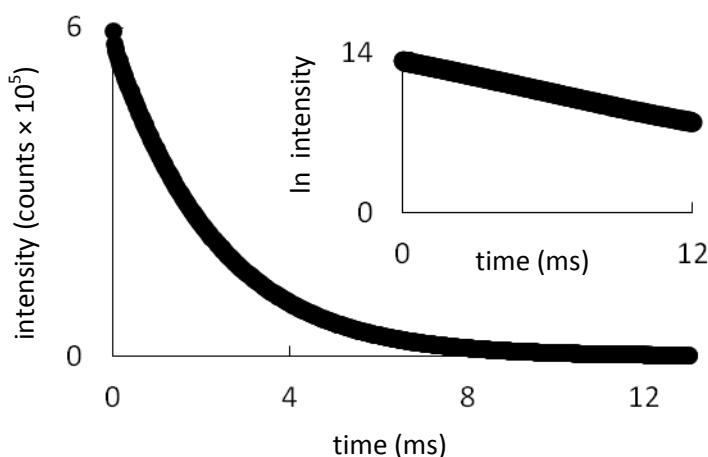


**Figure 4.2** Luminescence-decay curve of complex **4.3** in  $\text{D}_2\text{O}$ . The inset shows the natural log plot of the data, and the slope acquired from the natural log plot is the luminescence-decay rate

$$\tau_{\text{D}_2\text{O}}^{-1}.$$

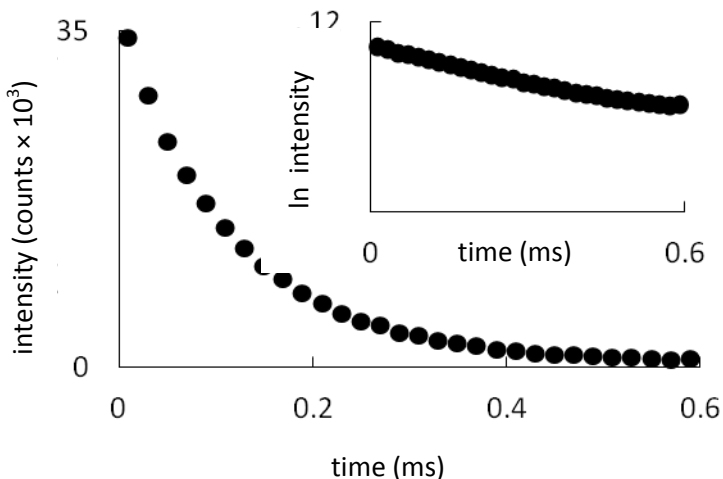


**Figure 4.3** Luminescence decay curve of complex **4.3** in H<sub>2</sub>O. The inset shows the natural log plot of the data, and the slope acquired from the natural log plot is the luminescence-decay rate

$$\tau_{H_2O}^{-1}$$

For each solvent, the decay rates in H<sub>2</sub>O ( $\tau_{H_2O}^{-1}$ ) and D<sub>2</sub>O ( $\tau_{D_2O}^{-1}$ ) were used in **Eq 4.1**, empirically derived by Horrocks and coworkers,<sup>21</sup> to determine the number of water molecules,  $q$ , coordinated to the Eu<sup>3+</sup> ion. For control complex, **3**, **Eq 4.2** was used because  $q$  is less than or equal to one for this complex.<sup>20</sup>

$$\mathbf{Eq\ 4.1}\quad q = 1.11 \left( \left| \tau_{H_2O}^{-1} - \tau_{D_2O}^{-1} \right| - 0.31 \right)$$

$$\mathbf{Eq\ 4.2}\quad q = 1.2 \left( \left| \tau_{H_2O}^{-1} - \tau_{D_2O}^{-1} \right| - 0.6666 \right)$$

For  $q$  measurements of the first reaction coordinate, solutions of Eu(OTf)<sub>3</sub> (1 mM) were prepared for each solvent studied (1–10, 20, 30, 40, 50, 60, 70, 80, 90, and 100% v/v of H<sub>2</sub>O in THF). The luminescence-decay measurements for the second reaction coordinate were acquired using the Eu(OTf)<sub>3</sub> solutions after addition of benzaldehyde in a 1:9 molar ratio of Eu<sup>3+</sup> to benzaldehyde (9 mM benzaldehyde). The third reaction coordinate measurements were acquired after addition

of 2-(hydroxyphenylmethyl)cyclohexanone to freshly prepared  $\text{Eu}(\text{OTf})_3$  solutions in a 1:9 molar ratio of  $\text{Eu}^{3+}$  to 2-(hydroxyphenylmethyl)-cyclohexanone. 2-Hydroxyphenylmethyl)cyclohexanone was not soluble in  $\text{H}_2\text{O}/\text{THF}$  ratios above 70%; thus, for 80–100%  $\text{H}_2\text{O}$  or  $\text{D}_2\text{O}$  in THF, a molar ratio of 1:1 ( $\text{Eu}^{3+}$  to 2-hydroxyphenylmethyl)cyclohexanone) was used. The solutions composed of 100%  $\text{H}_2\text{O}$  or  $\text{D}_2\text{O}$  were sonicated for 10 min after the addition of 2-(hydroxyphenylmethyl)cyclohexanone.

#### 4.2.2 Water-coordination numbers for reaction coordinates of the catalytic cycle

Water-coordination numbers,  $q$ , were determined for the three reaction coordinates using luminescence-decay measurements (**Tables A2–A4**). Data reported in these tables are the result of three to six replicates for each reaction coordinate. For the first reaction coordinate (**Figure 4.4**, solid dots), water saturation ( $q = 8.3$ )<sup>21</sup> of the  $\text{Eu}^{3+}$  containing precatalyst was determined by measurements in 100% water, and the results matched expected values.<sup>20</sup> Furthermore,  $q$  values near the saturation level were observed in solvents composed of 20–90% water. Below 20% water,  $q$  values decreased to 5.1 at 1% water. These results indicate that triflate is almost completely dissociated from the precatalyst in  $\text{H}_2\text{O}$ –THF solutions containing over 20%  $\text{H}_2\text{O}$  ( $x + y \approx 0$  in **Scheme 4.2**) and at least partially dissociated in solutions containing over 1%  $\text{H}_2\text{O}$  ( $x + y \geq 0$  in **Scheme 4.2**). Upon addition of benzaldehyde, a decrease of up to 0.34 in water-coordination number was observed for each solution containing greater than 1% water (**Figure 4.4**, hollow dots), indicating that water is partially displaced by benzaldehyde at water concentrations above 1% ( $z > 0$  in **Scheme 4.2**). The differences in water-coordination numbers between the first and second reaction coordinates are significant at a 95% confidence interval from 2 to 90%  $\text{H}_2\text{O}$  (Student  $t$  test). Finally, the water-coordination numbers of the third reaction coordinate were not different from the values of the first reaction coordinate (**Figure 4.4**, solid

dots). These data indicate that product inhibition does not occur to a measurable extent in the aqueous  $\text{Ln}(\text{OTf})_3$ -catalyzed Mukaiyama aldol reaction ( $a = 0$  in **Scheme 4.2**).

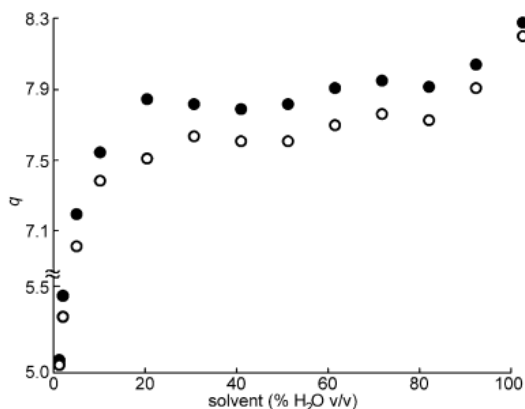


**Figure 4.4** Water-coordination number,  $q$ , of  $\text{Eu}^{3+}$  in solvents containing different amounts of  $\text{H}_2\text{O}$  before (●) and after (○) the addition of benzaldehyde. Standard error bars are smaller than the data points.

These observations of the reaction coordinates of the catalytic cycle of the Mukaiyama aldol reaction are important because they provide support for a reaction mechanism that involves triflate dissociation. These measurements represent time averaged values, and there may be minor amounts of other species that could be active catalysts in solution including hydroxides.<sup>53</sup> However, it has been shown that protons produced from aqua acid complexes of lanthanides are not active catalytic species in the reaction.<sup>7</sup> Interestingly, the maximum yield for the reaction that we studied was reported in a solution containing 20% water.<sup>7</sup> Our observations suggest that maximum yields are observed in 20% water solution because that is where the largest opportunity for benzaldehyde activation occurs; in our data, 20% water represents the largest difference in water-coordination number between the first and second reaction coordinates (**Figure 4.4**, largest difference between solid and hollow dots). Additionally, in this solvent the inner-sphere environment of  $\text{Eu}^{3+}$  is nearly saturated with water before the addition of substrate.



High yields in 20% water may also be because at this concentration of water an advantageous dynamic occurs leading to open coordination sites on the metal for benzaldehyde coordination.

Additionally, the use of this method to study asymmetric variations of these reactions should allow for the design of powerful water-tolerant asymmetric catalysts with wide substrate scopes which is described in **section 4.3**.

### 4.3 Luminescence-decay measurements of a new class of aqueous-stable chiral ligands coordinated to lanthanides

A new class of ligands for aqueous, lanthanide-catalyzed, asymmetric Mukaiyama aldol reactions for the synthesis of chiral  $\beta$ -hydroxy ketones was synthesized by Yujiang Mei, a former postdoctoral researcher in our laboratory. This set of ligands for generating enantiopure  $\beta$ -hydroxy carbonyl compounds is important because these subunits compose many bioactive compounds<sup>54</sup> and the ability to synthesize these groups in water has environmental and cost benefits.<sup>7</sup> The ligand design was inspired by macrocyclic gadolinium containing contrast agents for magnetic resonance imaging.<sup>21</sup> These complexes were chosen as his starting point because they are water-tolerant, and we hypothesized that the multidenticity of these ligands would allow for facile incorporation of chiral centers (**Figure 4.5**).

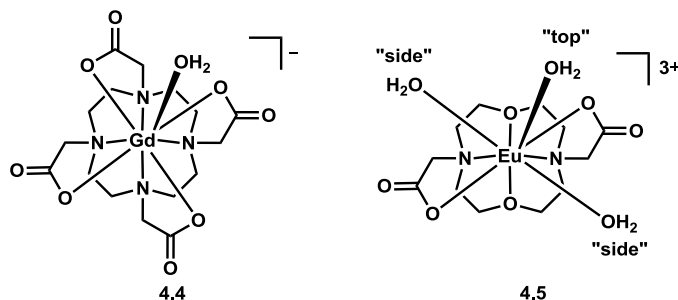


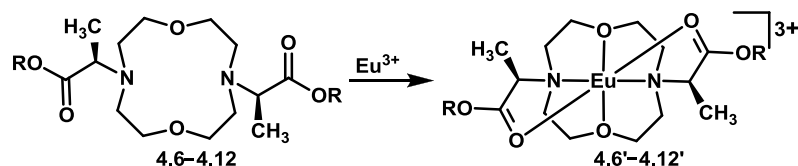
**Figure 4.5** Structures of (4.4) a common gadolinium-containing polyaminopolycarboxylate-based contrast agent and (4.5) the precatalyst with two types of water-binding sites labeled.

Yujiang modified the ligands because the contrast agents have only one open coordination site, and we hypothesized that a larger number of coordination sites is associated with higher turnover frequencies.<sup>24</sup> To increase the number of open coordination sites, he replaced two of the aminocarboxylic acid arms with ethers to yield a hexadentate  $C_2$ -symmetric system. The resulting complexes have three sites at which the substrate can coordinate: two “side” positions near the ethers in the macrocycle that are equivalent through a  $C_2$ -rotation and one “top” site between the two side sites. This new class of ligands takes advantage of the low degree of conformational flexibility and the water tolerance of lanthanide complexes of macrocyclic polyaminopolycarboxylate based ligands. Additionally, Yujiang stereospecifically introduced methyl groups at the methylene positions of the two remaining arms with the goal of imparting chirality. Furthermore, by converting the carboxylic acids into esters, possible binding sites for substrate molecules were controlled through changing the size of the R groups of the esters. We hypothesized that this feature would be a powerful tool for studying structure–activity relationships of these ligands with the goal of improving product enantioselectivity. My contribution to this research was the metalation of chiral ligands followed by the determination of  $q$  values of the resulting chiral lanthanide catalysts and ultimately the use of my  $q$  values to propose a mechanism of catalysis. Furthermore, I derived the equilibrium constant for the substrate-coordinated chiral ligand and water coordinated chiral ligand based on  $q$  values. This derivation is described in detail in the section **4.3.2**.

### 4.3.1 Determination of $q$ values of metalated chiral ligands.

The new  $C_2$ -symmetric ligands ( $R,R$ )-**4.6**–**4.12** were prepared in 97–98% yields by a simple two-step protocol starting from commercially available ( $S$ )-2-bromopropanoic acid (95% ee) by Yujiang (**Scheme 4.3**). The ligands were complexed with  $\text{Eu}(\text{OTf})_3$  in situ prior to catalysis.  $\text{Eu}^{3+}$  was chosen because it is an effective promoter of the activation of aldehydes in aqueous media<sup>7,55</sup> and because it enables luminescence-decay measurements.<sup>20,25</sup>

**Scheme 4.3** Metalation of chiral ligands (**4.6**–**4.12**) with  $\text{Eu}^{3+}$  to form chiral lanthanide-based precatalysts (**4.6'**–**4.12'**)\*.



\*  $R = \text{CH}_3, \text{C}_2\text{H}_5, n\text{-C}_3\text{H}_7, n\text{-C}_4\text{H}_9, i\text{-Pr}, t\text{-Bu}$ , and  $\text{H}$  for **4.6**–**4.12** or **4.6'**–**4.12'**, respectively.

The luminescence-decay measurements for the metalated chiral ligand solutions (1 mM) of **4.6'**–**4.12'** were acquired using following parameters which were kept constant during luminescence-decay measurements: excitation and emission slit width (5 nm), flash count (100), initial delay (0.001 ms), maximum delay (2.0 ms), and delay increment (0.02 ms). The excitation and emission wavelengths are listed in **Table 4.1**. Benzaldehyde (5 mM) was added to each solution, and the measurements were repeated. All solutions were prepared and measured 3–6 times, and the results of these measurements are listed in **Table 4.2**. The natural log of the intensity of the scan was plotted against time, and the resulting slope was used as the decay rate

( $\tau^{-1}$ ). The decay rates were used in **Eq 4.1** to determine the number of water molecules,  $q$ , coordinated to the  $\text{Eu}^{3+}$  ion.<sup>20</sup>

**Table 4.1** Excitation and emission wavelengths used in the determination of  $q$  values.

Sample	Excitation wavelength (nm)	Emission wavelength (nm)
<b>4.6'</b>	395	590
<b>4.6'</b> + benzaldehyde	395	590
<b>4.7'</b>	395	590
<b>4.7'</b> + benzaldehyde	395	590
<b>4.8'</b>	394	590
<b>4.8'</b> + benzaldehyde	394	590
<b>4.9'</b>	394	590
<b>4.9'</b> + benzaldehyde	394	590
<b>4.10'</b>	395	590
<b>4.10'</b> + benzaldehyde	395	590
<b>4.11'</b>	395	591
<b>4.11'</b> + benzaldehyde	395	591
<b>4.12'</b>	395	589
<b>4.12'</b> + benzaldehyde	395	589

**Table 4.2** Number of H<sub>2</sub>O molecules,  $q$ , coordinated to complexes of Eu<sup>3+</sup> with chiral ligands

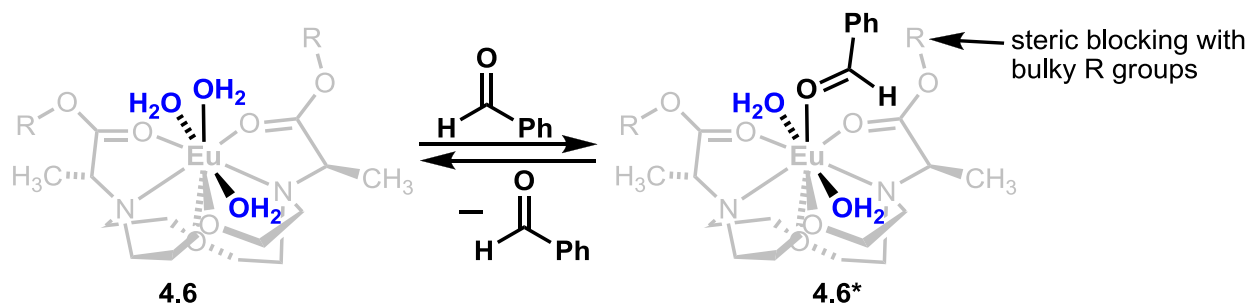
4.6–4.12.\*

Chiral ligand	$q$ (complex)	$q$ (complex plus benzaldehyde)	$\Delta q$
<b>4.6</b> ( <i>syn:anti</i> = 4:1)	2.39 ± 0.02	1.77 ± 0.01	−0.62
<b>4.6</b> ( <i>syn:anti</i> = 5:1)	2.49 ± 0.02	1.93 ± 0.01	−0.56
<b>4.6</b> ( <i>R,R</i> )	2.58 ± 0.02	1.90 ± 0.01	−0.68
<b>4.7</b> ( <i>syn:anti</i> = 4:1)	2.20 ± 0.02	1.80 ± 0.02	−0.40
<b>4.8</b> ( <i>syn:anti</i> = 4:1)	2.25 ± 0.02	1.80 ± 0.02	−0.45
<b>4.9</b> ( <i>syn:anti</i> = 4:1)	2.41 ± 0.01	1.92 ± 0.01	−0.49
<b>4.10</b> ( <i>syn:anti</i> = 4:1)	2.81 ± 0.01	2.62 ± 0.02	−0.19
<b>4.11</b> ( <i>syn:anti</i> = 1:1)	2.83 ± 0.01	2.69 ± 0.02	−0.14
<b>4.12</b> ( <i>syn:anti</i> = 3:1)	2.61 ± 0.04	2.52 ± 0.03	−0.09

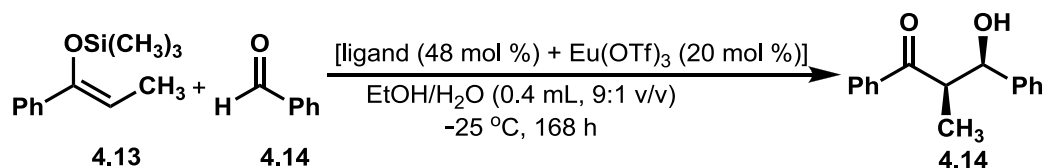
\* $q$  values are listed as mean ± standard error

Eu<sup>3+</sup> complexes of each ligand had water-coordination numbers between 2 and 3 prior to the addition of benzaldehyde. This range is expected for a hexadentate ligand. Upon addition of benzaldehyde, a decrease in water-coordination number was observed for each precatalyst. The change in water coordination number is listed as  $\Delta q$  in **Table 4.2**. A negative  $\Delta q$  value implies displacement of water by benzaldehyde (**Scheme 4.4**) and thus a shift in the equilibrium from the hydrated precatalyst (**4.6** in **Scheme 4.4**) toward coordinated (activated) benzaldehyde (**4.6\*** in **Scheme 4.4**).

**Scheme 4.4** Proposed equilibrium leading to activation of **4.6** for nucleophilic attack by benzaldehyde.



For linear R groups (ligands **4.6–4.12**), we observed displacements of 0.40–0.68 water molecules upon addition of benzaldehyde. These  $\Delta q$  values are larger than those observed for unchelated  $\text{Eu}^{3+}$  (**Table 4.2**).<sup>24</sup> This observation suggests that the ligands induce an interaction with the aldehyde, potentially hydrophobic or nonclassical hydrogen bonding,<sup>56</sup> that causes a favorable binding of aldehyde to the metal. Due to these binding interactions, we expected a correlation between  $\Delta q$  and yield percentage for the Mukaiyama aldol reaction shown in **Table 4.3**, larger absolute values of  $\Delta q$  can be used to account for increased yields in a set time. Much smaller  $\Delta q$  values were observed for bulkier R groups (ligands **4.10** and **4.11**), suggesting that the steric bulk hinders the binding of substrate and leads to lower yields. The equilibrium constant  $K$  listed in **Table 4.3** was calculated for the equilibrium shown in **Scheme 4.6**, and its derivation is shown in following section **4.3.2**.

**Table 4.3** Relationships among yield and water-coordination number.<sup>a</sup>

Ligand	R	yield (%) <sup>b</sup>	$\Delta q$	$K^c$
<b>4.6</b> ( <i>syn:anti</i> = 4:1)	$\text{CH}_3$	85	-0.62	0.38
<b>4.6</b> ( <i>syn:anti</i> = 5:1)	$\text{CH}_3$	88	-0.56	0.36
<b>4.6</b> ( <i>R,R</i> )	$\text{CH}_3$	92	-0.68	0.40
<b>4.7</b> ( <i>syn:anti</i> = 4:1)	$\text{C}_2\text{H}_5$	82	-0.40	0.29
<b>4.8</b> ( <i>syn:anti</i> = 4:1)	<i>n</i> - $\text{C}_3\text{H}_7$	83	-0.45	0.31
<b>4.9</b> ( <i>syn:anti</i> = 4:1)	<i>n</i> - $\text{C}_4\text{H}_9$	83	-0.49	0.33
<b>4.10</b> ( <i>syn:anti</i> = 4:1)	<i>i</i> -Pr	20	-0.19	0.16
<b>4.11</b> ( <i>syn:anti</i> = 1:1)	<i>t</i> -Bu	18	-0.14	0.12
<b>4.12</b> ( <i>syn:anti</i> = 3:1)	H	8	-0.09	0.08

<sup>a</sup> Reaction conditions: To a mixture of ligand (48 mol %) and  $\text{Eu}(\text{OTf})_3$  (20 mol %), which was stirred at  $50\text{ }^\circ\text{C}$  for 2 h and then cooled to  $-25\text{ }^\circ\text{C}$ , was added **4.13** (48.8  $\mu\text{mol}$ , 1.5 equiv) and **4.14** (32.5  $\mu\text{mol}$ , 1.0 equiv). <sup>b</sup> isolated yields. <sup>c</sup> based on the equation in **Scheme 4.6**.

### 4.3.2 Derivation of an equation for $K$

For the equilibrium shown in **Scheme 4.5**, B is benzaldehyde; L is the non- $\text{H}_2\text{O}$  ligands;  $q_i$  is the measured number of water molecules coordinated to  $\text{Eu}^{3+}$  prior to the addition of B;  $q_b$  is the number of water molecules coordinated to  $\text{Eu}^{3+}$  after the addition of B, and  $q_e$  is the measured number of water molecules coordinated to  $\text{Eu}^{3+}$  at equilibrium. Assuming that L is not labile; that B can replace  $\text{H}_2\text{O}$ ; that at equilibrium both B and  $\text{H}_2\text{O}$  are in excess; that no other  $\text{Eu}^{3+}$ -

containing species exist in solution; that the maximum number of B that can coordinate per  $\text{Eu}^{3+}$  is one ( $q_b = q_i - 1$ ); and that the volume change of the system upon addition of benzaldehyde is negligible; at equilibrium, **Eq. 4.3** is true. Because the volume is constant, **Eq. 4.3** reduces to **Eq. 4.4**, which is the ratio of the number of molecules of  $\text{LEuB}(\text{H}_2\text{O})_{q_e}$  and  $\text{LEu}(\text{H}_2\text{O})_{q_i}$ . Furthermore, the measured value  $q_e$  is the weighted average of the species in solution; thus, this term can be written as shown in **Eq 4.5**. Rearranging the equation yields **Eq 4.6**, and substituting  $(q_i - 1)$  for  $q_b$  changes **Eq 4.6** to **Eq 4.7**. Combining **Eq 4.7** with **Eq 4.4** and the definition of  $\Delta q$  in **Eq 4.8** yields **Eq 4.9**.

**Scheme 4.5** Equilibrium between hydrated chiral lanthanide and benzaldehyde-coordinated chiral lanthanide complex.



$$\text{Eq. 4.3} \quad K = \frac{\text{LEuB}(\text{H}_2\text{O})_{q_b}}{\text{LEu}(\text{H}_2\text{O})_{q_i}}$$

$$\text{Eq. 4.4} \quad K = \frac{\text{number of } \text{LEuB}(\text{H}_2\text{O})_{q_e} \text{ molecules}}{\text{number of } \text{LEu}(\text{H}_2\text{O})_{q_i} \text{ molecules}} \equiv \frac{N_b}{N_i}$$

$$\text{Eq. 4.5} \quad q_e = \frac{N_b(q_b) + N_i(q_i)}{(N_b + N_i)}$$

$$\text{Eq. 4.6} \quad \frac{N_b}{N_i} = \frac{q_i - q_e}{q_e - q_b}$$

$$\text{Eq. 4.7} \quad \frac{N_b}{N_i} = \frac{q_i - q_e}{q_e - q_i + 1}$$



$$\text{Eq. 4.8 } \Delta q = |q_e - q_i|$$

$$\text{Eq. 4.9 } K = \frac{\Delta q}{\Delta q + 1}$$

### 4.3.3 Proposed transition state for the studied asymmetric Mukaiyama aldol reaction

We have proposed a transition state for the asymmetric Mukaiyama aldol reaction with our new ligands **4.6–4.12 (Figure 4.6)**. In this model, benzaldehyde coordinates to the metal at the top position on the basis of the  $\Delta q$  data in **Table 4.3** (bulky R groups would block this position). When the aldehyde is coordinated in this position, the silyl enol ether can attack only from one side because the opposite face is blocked by an ester. Benzaldehyde is unlikely to bind with the H and Ph groups reversed from the arrangement in **Figure 4.6** because of unfavorable steric interactions between the phenyl ring and the macrocycle. If benzaldehyde were bound to the side positions, contradicting our  $\Delta q$  data, attack of the silyl enol ether would be blocked by the methyl group at the chiral center or by the ester.

The contribution I made to deduce structural information using my luminescence-decay studies and use of that structural information with the stereochemistry of the product to propose a mechanism was important to the scientific community to unveil mechanistic information regarding asymmetric Mukaiyama aldol reaction in aqueous media. Further, upon these achievements I was interested in studying other commercially available lanthanide salts other than lanthanide triflates to use as potential aqueous precatalysts and this research is explained in **section 4.4**.

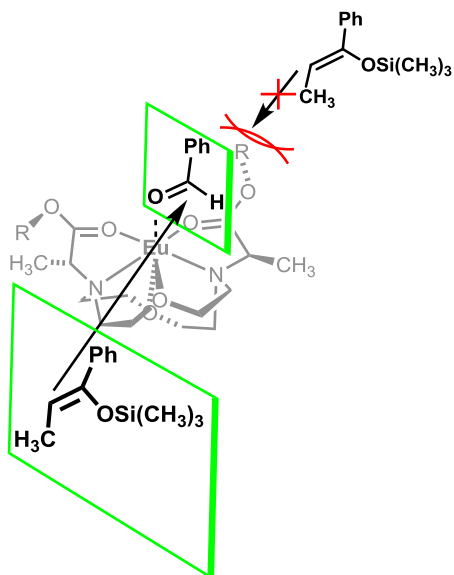


**Figure 4.6** Proposed transition state in the asymmetric Mukaiyama aldol reaction using the new ligands **4.6–4.11**.

#### 4.4 Effect of counter anion identity on the inner-sphere hydration of lanthanides

I studied the water-coordination numbers of solvated  $\text{Eu}^{3+}$  salts including  $\text{Eu}(\text{OTf})_3$ ,  $\text{Eu}(\text{NO}_3)_3$ ,  $\text{EuCl}_3$ , and  $\text{Eu}(\text{OAc})_3$  because these salts are commercially available. Although  $\text{Eu}_2(\text{CO}_3)_3$  and  $\text{Eu}_2(\text{SO}_4)_3$  can be purchased, I did not do further studies with these two salts because they are not water soluble. As shown in **Figure 4.7**,  $q$  values of  $\text{EuCl}_3$  are similar to those of  $\text{Eu}(\text{OTf})_3$  in solvents containing more than 3% water ( $\text{EuCl}_3$  was not soluble in solutions containing under 2% water).

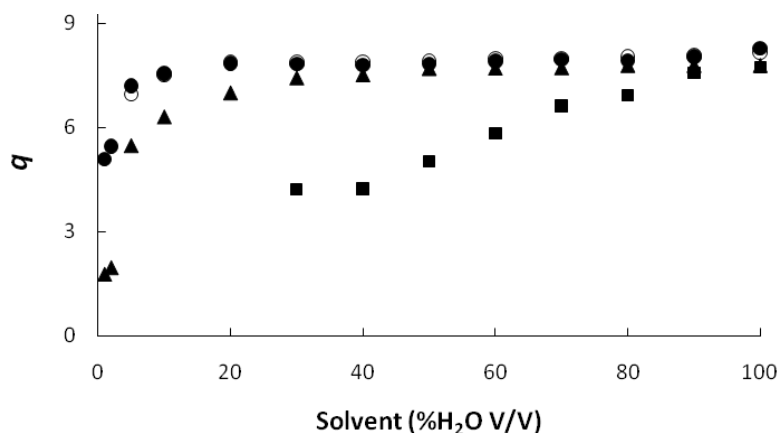


**Figure 4.7** Effect of Ln salts on  $q$ : Eu(OTf)<sub>3</sub> (●), EuCl<sub>3</sub> (○), Eu(NO<sub>3</sub>)<sub>3</sub> (▲), and Eu(OAc)<sub>3</sub> (■).

Due to the similarity of the obtained  $q$  values of EuCl<sub>3</sub> and Eu(OTf)<sub>3</sub>, it was my hypothesis that these ions should lead to similar yields in carbon–carbon bond-forming reactions. However, the published yields (**Table 4.4**) of the Mukaiyama aldol reaction in **Scheme 1.1** were not the same with these two salts. (In the literature, Yb<sup>3+</sup> was used in place of Eu<sup>3+</sup>, but with the same anions; therefore, I expect the trend in yield to be the same.)

**Table 4.4** Published yields of Yb<sup>3+</sup> salts used to catalyze the Mukaiyama aldol reaction in **Scheme 1.1**.<sup>7</sup>

Yb <sup>3+</sup> salt	Yield (%)
Yb(OTf) <sub>3</sub>	91
Yb(ClO <sub>4</sub> ) <sub>3</sub>	88
Yb(OAc) <sub>3</sub> · 8H <sub>2</sub> O	14
Yb(NO <sub>3</sub> ) <sub>3</sub> · 5H <sub>2</sub> O	7
YbCl <sub>3</sub>	3
Yb(SO <sub>4</sub> ) <sub>3</sub> · 5H <sub>2</sub> O	trace

This conflict between my hypothesis and the literature lead me to search for an explanation for this difference between my observations and reported yields. One possible explanation is the differences in yield are caused by a change in pH. I measured pH values of  $\text{EuCl}_3$  and  $\text{Eu}(\text{OTf})_3$  (1 mM) in  $\text{H}_2\text{O}$  and found them to be 5.77 and 6.23, respectively. Based on this pH difference, I hypothesized that if the pH value of the medium is maintained at 6.22, the water-tolerant catalytic ability of  $\text{EuCl}_3$  should be similar to that of  $\text{Eu}(\text{OTf})_3$ . Therefore, I carried out one set of reactions using  $\text{Eu}(\text{OTf})_3$  at pH values of 5.77 and 6.22. Another reaction was carried out using  $\text{EuCl}_3$  at pH 6.22. To maintain the pH of the medium, 2-(*N*-morpholino)ethanesulfonic acid (MES) buffer was used. Surprisingly, my data (**Table 4.5**) were almost the same despite the pH differences.

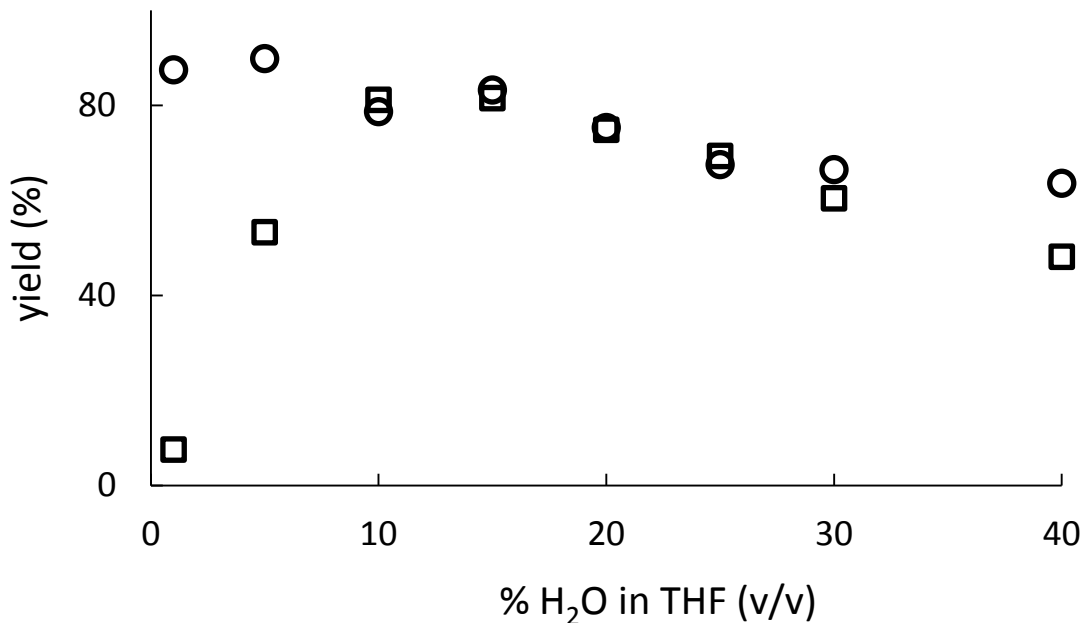
**Table 4.5** Yields of a  $\text{Eu}^{3+}$ -salt-catalyzed Mukaiyama aldol reaction at 19 h. (The rest of the reaction mixture contained unreacted starting material).

$\text{EuX}_3$	20% $\text{H}_2\text{O}$ pH = 6.22	20% $\text{H}_2\text{O}$ pH = 5.77	20% $\text{H}_2\text{O}$ no buffer
$\text{Eu}(\text{OTf})_3$	46	47	43
$\text{EuCl}_3$	45	46	44
No metal	5	3	5

These results prompted me to run both  $\text{EuCl}_3$  and  $\text{Eu}(\text{OTf})_3$  catalyzed reactions in 20% water without buffer. The pattern of the results that I obtained (**Table 4.7**) were in disagreement with the literature values (**Table 4.6**). Therefore, to further investigate this conflict, I used gas

chromatography coupled with mass spectrometry (GC–MS) as a quantitative analytical method. My purpose was to determine the yield for each salt at different water percentages using a GC–MS-derived calibration curve. Unfortunately, due to the high temperature in the GC–MS, a retro-aldol reaction lead to the decomposition of my product to cyclohexanone. To confirm that cyclohexanone production was due to the decomposition of the product and not to the decomposition of silyl enol ether, I analyzed product and silyl enol ether individually. The GC–MS data confirmed the appearance of cyclohexanone peak due to product decomposition and not from the silyl enol ether. My attempts to calculate yields by analyzing the unreacted limiting substrate benzaldehyde did not give promising results due to the retro-aldol reaction. Therefore, Derek Averill (Graduate Student in Allen lab) performed investigations using high-performance liquid chromatography (HPLC) coupled with a photodiode array detector. HPLC avoids the retro-aldol induced by heat of the GC–MS. Due to the limited water solubility of the silyl enol ether, we were unable to study the reaction at water percentages above 40% H<sub>2</sub>O in THF (v/v). To test our hypothesis that water-coordination numbers influence the final yield of this reaction, the yields of Eu(OTf)<sub>3</sub>- and Eu(NO<sub>3</sub>)<sub>3</sub>-catalyzed Mukaiyama aldol reactions were measured by Derek after 48 h in solvent mixtures ranging from 1 to 40% H<sub>2</sub>O in THF (v/v) using HPLC (**Figure 4.8**). We chose to use these two precatalysts from Eu(OTf)<sub>3</sub>, Eu(NO<sub>3</sub>)<sub>3</sub>, EuCl<sub>3</sub>, and Eu(OAc)<sub>3</sub> because of the wide range of water-coordination numbers (3.2 to 8.6) accessible under these conditions. Due to the incomplete solubility of the substrates with EuCl<sub>3</sub> and Eu(OAc)<sub>3</sub>, these precatalysts were not further studied.

**Figure 4.8** Yields of the reaction shown in **Scheme 1.1** catalyzed by  $\text{Eu}(\text{OTf})_3$  or  $\text{Eu}(\text{NO}_3)_3$  after 48 h as a function of solvent composition.\*<sup>57</sup>



\*Conditions: solvent mixtures of 1 to 40%  $\text{H}_2\text{O}/\text{THF}$  containing 7 mol %  $\text{Eu}(\text{OTf})_3$  (○) or  $\text{Eu}(\text{NO}_3)_3$  (□). Size of the standard error bars are smaller than the sizes of the dots, and squares, and not included for clarity. Figure courtesy of Derek Averill.

From these measurements, we found a correlation between water-coordination number as well as between yield and solvent composition. This observation can be rationalized based upon relative binding affinities of the anions for  $\text{Eu}^{3+}$ , which affect the water-coordination numbers of the precatalysts: triflate has a lower binding affinity for  $\text{Ln}^{3+}$  ions than nitrate.<sup>11</sup> This difference in europium binding affinities between triflate and nitrate results in higher water-coordination numbers for  $\text{Eu}(\text{OTf})_3$  compared to  $\text{Eu}(\text{NO}_3)_3$  and, ultimately, corresponds to higher europium accessibility because each water molecule coordinated to  $\text{Eu}^{3+}$  represents a potential site for benzaldehyde coordination and activation for reaction.

In general, increasing water percentage resulted in an increase of yield and reached a maximum and remained constant at solvent mixtures containing greater than 10%  $\text{H}_2\text{O}$  in THF

(v/v) (**Figure 4.8**). This solvent composition corresponds to the lowest H<sub>2</sub>O concentration at which the water-coordination number,  $q$ , is at a maximum value (**Figure 4.7**). The increase of yield percentage of Eu(NO<sub>3</sub>)<sub>3</sub>-catalyzed reactions over the entire range of solvents in this study can be attributed to the water-coordination number of Eu(NO<sub>3</sub>)<sub>3</sub> that increases without reaching a maximum with increasing H<sub>2</sub>O in THF from 1 to 40%.

#### 4.5 Conclusions

I demonstrated the applicability of luminescence-decay measurements as a dynamic tool that is useful in mechanistic studies of water-tolerant lanthanide-based catalytic systems. This method is widely applicable for the study of other important water tolerant lanthanide-catalyzed reactions, including solid-supported catalysts.<sup>58</sup> However, the major limitation of this study was the determination of the effect of THF on  $q$  values, which resulted the additional workload need to validate each solvent composition with the control complex **3**. The major reason for this validation was that **Eq 4.1** and **4.2** does not account for the differences in the inner- and outer-sphere luminescence quenching ability between water and other solvents because these equations were empirically derived in pure water. To overcome this major limitation, I investigated variations of inner- and outer-sphere dynamics with respect to commonly used organic solvents, and empirically derived equations that enable fast and accurate determination of inner-sphere coordination behavior in commonly used binary solvent systems. Chapter five in this thesis gives a full description of these studies.

I have demonstrated the further applicability of luminescence-decay measurements to study lanthanide-based chiral catalytic systems in aqueous medium that is the determination of a thermodynamic parameter,  $K$ . Furthermore, structural and mechanistic information was obtained

us these measurements for potent chiral precatalysts for carbon–carbon bond-forming reactions in aqueous media.

Finally, the use of luminescence-decay measurements to probe the coordination environment of europium-based precatalysts in solution enabled the study of the influence of precatalyst coordination-environment on reaction yield. These results are useful in the design of new precatalysts to be used for aqueous, enantioselective, lanthanide-catalyzed bond-forming reactions.

#### 4.6 Experimental Section

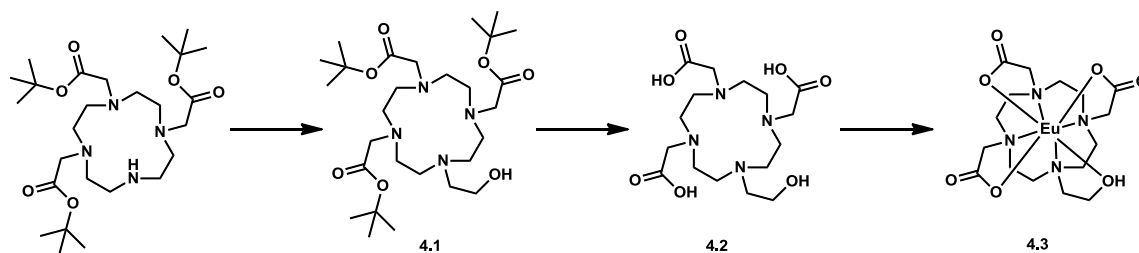
Commercial chemicals were of reagent-grade purity or better and were used without further purification. Water was purified using a PURELAB Ultra Mk2 water purification system (ELGA). Flash chromatography was performed using silica gel 60, 230–400 mesh (EMD Chemicals).<sup>59</sup> Analytical thin-layer chromatography (TLC) was carried out on ASTM TLC plates precoated with silica gel 60 F254 (250  $\mu\text{m}$  layer thickness). TLC visualization was accomplished using a UV lamp followed by charring with potassium permanganate stain (3 g  $\text{KMnO}_4$ , 20 g  $\text{K}_2\text{CO}_3$ , 5 mL 5% w/v aqueous NaOH, 300 mL  $\text{H}_2\text{O}$ ).  $^1\text{H}$  NMR spectra were obtained using a Varian Unity 300 (300 MHz) or a Varian Mercury 400 (400 MHz) spectrometer, and  $^{13}\text{C}$  NMR spectra were obtained using a Varian Mercury 400 (100 MHz) or a Varian Mercury 500 (125 MHz) spectrometer. Chemical shifts are reported relative to residual solvent signals unless otherwise noted ( $\text{CDCl}_3$ :  $^1\text{H}$ :  $\delta$  7.27,  $^{13}\text{C}$ :  $\delta$  77.23;  $\text{D}_2\text{O}$ :  $^1\text{H}$ :  $\delta$  4.79,  $^{13}\text{C}$ :  $\delta$  39.51 for an internal standard of dimethyl sulfoxide- $d_6$ ).  $^1\text{H}$  NMR data are assumed to be first order with apparent singlets and multiplets reported as “s” and “m”, respectively. Italicized elements are those that are responsible for the shifts. High-resolution electrospray ionization mass spectra (HRESIMS)



were obtained on an electrospray time of flight high-resolution Waters Micromass LCT Premier XE mass spectrometer. Liquid chromatography and mass spectrometry (LC–MS) analysis was performed on a Shimadzu LC–MS system equipped with a C18 column (Restek International, Viva C18, 5  $\mu\text{m}$ , 250  $\times$  4.6 mm) equilibrated with 0.4% v/v formic acid, using a binary gradient method (pump A: water; pump B: acetonitrile; 5–95% B over 70 min; flow rate: 1 mL/min). 2-(Hydroxyphenylmethyl)cyclohexanone was synthesized following a previously described procedure.<sup>7</sup>

#### 4.6.1 Synthetic Procedures and Characterization of Eu-complex 4.3

**Scheme 4.6** Synthesis of  $q = 1$  Eu-complex (4.3) via compound 4.1–4.2.



#### Synthesis of *tert*-Butyl 2,2',2''-(10-(2-hydroxyethyl)-1,4,7,10-tetraazacyclododecane-1,4,7-triyl)triacetate (4.1):

To a mixture of anhydrous acetonitrile (10 mL) and anhydrous  $\text{K}_2\text{CO}_3$  (247 mg, 1.79 mmol, 5 equiv) under an atmosphere of  $\text{N}_2$  was added *tert*-butyl-2,2',2''-(1,4,7,10-tetraazacyclododecane-1,4,7-triyl)triacetate (184 mg, 0.358 mmol, 1 equiv) followed by 2-bromoethanol (127  $\mu\text{L}$ , 1.79 mmol, 5 equiv). The resulting mixture was stirred at 70  $^\circ\text{C}$  for 12 h. After cooling to ambient temperature and removing excess  $\text{K}_2\text{CO}_3$  by filtration, the solvent was removed under reduced pressure. Purification was performed using silica gel chromatography (10:1 dichloromethane/methanol) to yield 198 mg (99%) of **4.1** as a light yellow oil.  $^1\text{H}$  NMR (400

MHz, CDCl<sub>3</sub>,  $\delta$ ): 1.45 (s, CH<sub>3</sub>, 27H), 2.54–2.57 (m, CH<sub>2</sub>, 4H), 2.72–2.77 (m, CH<sub>2</sub>, 12H), 2.79–2.82 (m, CH<sub>2</sub>, 4H), 3.32 (s, CH<sub>2</sub>C=O, 6H); <sup>13</sup>C NMR (100 MHz, CDCl<sub>3</sub>,  $\delta$ ): 28.8 (CH<sub>3</sub>), 48.1 (CH<sub>2</sub>), 51.3 (CH<sub>2</sub>), 52.8 (CH<sub>2</sub>), 57.8 (CH<sub>2</sub>), 81.4 (C(CH<sub>3</sub>)<sub>3</sub>), 171.9 (C=O); TLC: *R<sub>f</sub>* = 0.25 and 0.27 (18:1 dichloromethane/methanol); HRESIMS (*m/z*): [M + H]<sup>+</sup> calcd for C<sub>28</sub>H<sub>55</sub>N<sub>4</sub>O<sub>7</sub>, 559.4071; found, 559.4063.

**Synthesis of 2,2',2''-(10-(2-Hydroxyethyl)-1,4,7,10-tetraazacyclododecane-1,4,7-triyl)triacetic acid (4.2):**

A solution of **4.1** (180 mg, 0.322 mmol) in concentrated HCl (15 mL) was stirred at ambient temperature for 2 h. The reaction mixture was concentrated under reduced pressure, and the resulting residue was dissolved in H<sub>2</sub>O (3 mL) and freeze dried to afford 124 mg (99%) of **4.2** as a white solid. <sup>1</sup>H NMR (300 MHz, D<sub>2</sub>O,  $\delta$ ): 3.13 (m, CH<sub>2</sub>, 8H), 3.49 (m, CH<sub>2</sub>, 10H), 3.63–3.65 (m, CH<sub>2</sub>, 4H), 3.98–4.01 (m, CH<sub>2</sub>, 4H); <sup>13</sup>C NMR (125 MHz, D<sub>2</sub>O,  $\delta$ ): 49.5 (CH<sub>2</sub>), 49.8 (CH<sub>2</sub>), 52.1 (CH<sub>2</sub>), 53.4 (CH<sub>2</sub>), 54.5 (CH<sub>2</sub>), 56.4 (CH<sub>2</sub>), 56.5 (CH<sub>2</sub>), 56.9 (CH<sub>2</sub>), 60.9 (CH<sub>2</sub>), 61.1 (CH<sub>2</sub>), 64.1 (CH<sub>2</sub>), 67.6 (CH<sub>2</sub>), 68.1 (CH<sub>2</sub>), 170.4 (C=O); 174.3 (C=O); 175.8 (C=O); HRESIMS (*m/z*): [M – H]<sup>–</sup> calcd for C<sub>16</sub>H<sub>29</sub>N<sub>4</sub>O<sub>7</sub>, 389.2036; found, 389.2042.

**Synthesis of 2,2',2''-(10-(2-Hydroxyethyl)-1,4,7,10-tetraazacyclododecane-1,4,7-triyl)triacetoeuropium(III) (4.3):**

To a solution of **4.2** (18 mg, 47  $\mu$ mol, 1 equiv) in H<sub>2</sub>O (3 mL) was added EuCl<sub>3</sub> hexahydrate (35 mg, 96  $\mu$ mol, 2 equiv), and the resulting reaction mixture was stirred at ambient temperature for 24 h while maintaining the pH between 6.9 and 7.1 by the addition of 0.1 M aqueous NH<sub>4</sub>OH. The pH of the mixture was increased to 12 to precipitate excess Eu<sup>3+</sup> as Eu(OH)<sub>3</sub>. After

removing  $\text{Eu}(\text{OH})_3$  by filtration through a 0.2  $\mu\text{m}$  filter (Millipore, IC Millex-LG), the remaining filtrate was freeze dried. The resulting white solid was dissolved in  $\text{H}_2\text{O}$  (2 mL) and dialyzed against  $\text{H}_2\text{O}$  (cellulose ester, 100–500 Dalton molecular weight cut off, Spectra/Por Biotech). The entire dialysate volume was changed after 3, 7, and 17 h. After dialysis, the solution inside the membrane was freeze dried to yield 21 mg (85%) of **4.3** as a white solid. The purity of the product was confirmed by LC–MS characterization. HRESIMS ( $m/z$ ):  $[\text{M} + \text{H}]^+$  calcd for  $\text{C}_{16}\text{H}_{28}\text{N}_4\text{O}_7$   $^{151}\text{Eu}$ , 539.1173; found 539.1183.

#### 4.6.2 Procedure for metalation of chiral ligands 4.6–4.12 with lanthanides

**Metalated Chiral Ligand Solutions (4.6'–4.11')**: A mixture of chiral ligand (**4.6**, **4.7**, **4.8**, **4.9**, or **4.10** in **Scheme 4.3**) (1.2 mM, 1.2 equiv) and  $\text{Eu}(\text{OTf})_3$  (1 mM, 1 equiv) was stirred at ambient temperature for 5 h in a solution of  $\text{H}_2\text{O}$  and THF (10% v/v). This procedure was repeated using  $\text{D}_2\text{O}$  in THF (10% v/v). These solutions were used directly in the luminescence-decay measurements.

**Metalated Chiral Ligand Solution (4.11')**: A mixture of chiral ligand (**4.11** in **Scheme 4.3**) (3 mM, 3 equiv) and  $\text{Eu}(\text{OTf})_3$  (1 mM, 1 equiv) was stirred at 40 °C for 45 min and then at ambient temperature for 24 h in a solution of  $\text{H}_2\text{O}$  and THF (10% v/v). This procedure was repeated using  $\text{D}_2\text{O}$  and THF (10% v/v). The resulting solution was used directly in the luminescence-decay measurements.

**Metalated Chiral Ligand (4.12')**: This metalation of chiral ligand **4.12** (**Scheme 4.3**) was done by Yijiang Mei,<sup>65</sup> and solutions (1 mM in  $\text{H}_2\text{O}$  and THF (10% v/v) or  $\text{D}_2\text{O}$  and THF (10% v/v)) of this solid were used in the luminescence-decay measurements.

## CHAPTER FIVE

# Luminescence-Decay as an Easy-to-Use Tool for the Study of Lanthanide-Containing Catalysts in Aqueous Solutions

Portions of this chapter were reprinted or adapted with permission from Dissanayake, P.; Mei, Y.; Allen, M. J. Luminescence-Decay as an Easy-to-Use Tool for the Study of Lanthanide-Containing Catalysts in Aqueous Solutions. *ACS Catal.* **2011**, *1*, 1203–1212. Copyright 2011 American Chemical Society.

### 5.1 Introduction

This chapter describes my adaptation of luminescence-decay measurements into a simple and fast technique to determine inner-sphere water-coordination numbers of Ln<sup>3+</sup>-based complexes in binary solvent systems that are useful for catalysis. These solvents include tetrahydrofuran (THF), EtOH, MeOH, *N,N*-dimethylformamide (DMF), dimethylsulfoxide (DMSO), acetone, and acetonitrile as cosolvents with water. The luminescence-decay rates of well defined Eu<sup>3+</sup> containing complexes were used to perform this study. I expect that the increased knowledge regarding the inner-sphere coordination environment of precatalysts that my equations enable will be useful in the study of lanthanide-catalyzed reactions and new precatalysts.

### 5.2 Inner- and outer-sphere coordination environments of lanthanide ions in binary solvents

When water-miscible organic solvents are used with water in binary solvents in lanthanide-catalyzed organic transformations, the inner- and outer-sphere coordination

environments of the lanthanide ions become complex relative to the coordination environment in water (**Figure 5.1**). Specifically, when water-miscible solvents occupy the inner-coordination sphere, the luminescence quenching arising from inner-sphere vibrations and the number of inner-sphere water molecules is different than the quenching observed for the same complexes in only water.

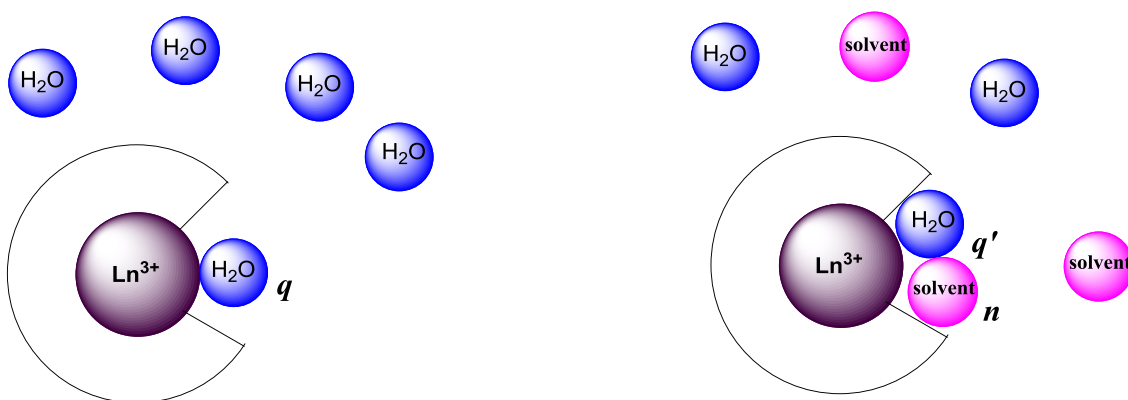


**Figure 5.1** Coordination environments of lanthanide ions in pure solvent (left) and binary solvents (right). The symbols  $q$ ,  $q'$ , and  $n$  represent the number of inner-sphere water molecules in pure water, the number of inner-sphere water molecules in binary solvent systems, and the number of inner-sphere solvent molecules in binary solvent systems, respectively.

To determine how  $q$  changes to  $q'$  in binary solvent systems, I chose well defined  $\text{Eu}^{3+}$  containing complexes (known  $q$  values in pure solvent) **5.1–5.6**, (**Figure 5.2**). While it is likely that these complexes exist as multiple species (hydroxides, hydrates, and oxides) in equilibrium in solution, these complexes displayed a single peak for the  ${}^7\text{F}_0 \rightarrow {}^5\text{D}_0$  transition; therefore, I made the assumption that the  $\text{Eu}^{3+}$  complexes in this study existed in a single form or that different forms were in equilibrium to give an average value of  $q'$ . The monoexponential luminescence decay values that I obtained for both  $\text{H}_2\text{O}$  and  $\text{D}_2\text{O}$  solutions ( $R^2 \geq 0.99$ ) further

support this assumption.<sup>20,60</sup> In this chapter, I explain the stepwise procedure that I developed to investigate inner-sphere water molecules in binary solvent systems. For the rest of this thesis, I will refer to the number of inner-sphere water molecules coordinated to  $\text{Eu}^{3+}$  in binary solvent systems as  $q'$ .

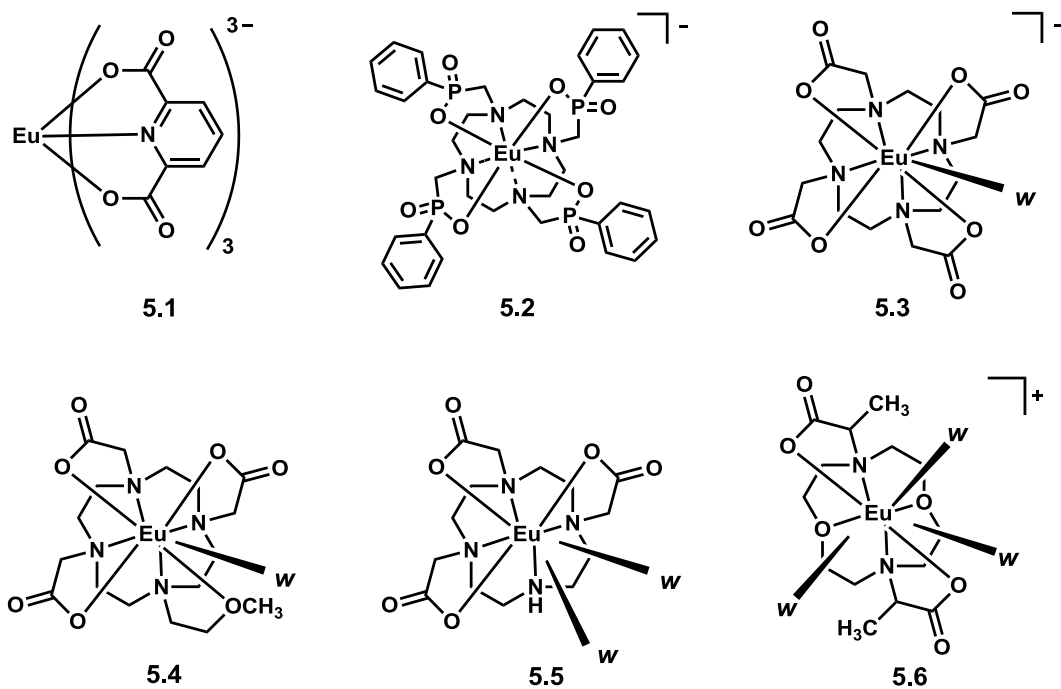


**Figure 5.2.** Complexes with  $w$  values ranging from 0 to 3, where  $w$  represents the remaining coordination sites after ligand binding.

Determination of  $q'$  is important because the number of inner-sphere water molecules plays an important role in the mechanism of the aqueous lanthanide-based catalysis.<sup>24,47</sup> However, application of the empirically derived Horrocks equation (**Eq 5.1**)<sup>20</sup> to determine  $q'$  is limited because **Eq 5.1** was derived in the absence of cosolvents. To determine  $q'$ , I examined changes to the parameters in Horrocks's equation ( $\alpha$  and  $A$ ) with respect to commonly used binary solvent systems. This determination was important because  $\alpha$  accounts for the influence

of non-coordinated molecules including binary solvents on luminescence decay, and consequently, the proportionality constant  $A$  (water molecules.ms) has an effect on  $\alpha$ . Using a similar strategy as Horrocks, I plotted  $|\tau_H^{-1} - \tau_D^{-1}|_m$ , which is the difference of the measured decay rates in protic and deuterated solvent systems, against  $q'$  (**Figure 5.3**). The data in **Figure 5.3** can be described by **Eq 5.2**, which enabled me to determine new  $\alpha$  and  $A$  values in binary solvents.

$$\text{Eq 5.1} \quad q = A(|\tau_{H_2O}^{-1} - \tau_{D_2O}^{-1}| - \alpha)$$

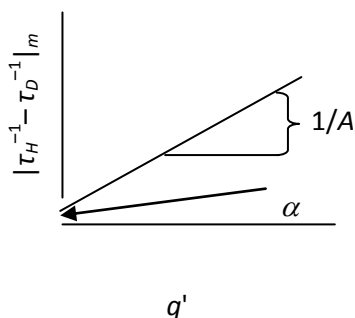


**Figure 5.3.** Plot of  $|\tau_H^{-1} - \tau_D^{-1}|_m$  versus  $q'$  used to determine  $\alpha$  and  $A$ . The intercept of the plot equals  $\alpha$  and reciprocal of the slope is the proportionality constant,  $A$ .

$$\text{Eq 5.2} \quad |\tau_H^{-1} - \tau_D^{-1}|_m = \frac{1}{A}q' + \alpha$$

However, I could not directly adapt Horrocks's method because the luminescence decay I measured arose from both inner- and outer-sphere nonwater solvent molecules. To overcome the

difficulties associated with non-water solvent molecules, I developed and implemented a six-step procedure to solve for  $q'$  and the non-water inner-sphere solvent-coordination number,  $n$ , in binary solvent systems. This stepwise procedure was applied to complexes **5.1–5.6** (**Figure 5.2**) as well as  $\text{Eu}(\text{OTf})_3$ . These complexes were chosen because they represent a range (0–3 and 9) of well-defined numbers of coordination sites that remain after ligand coordination, which I will define as  $w$ . The use of complexes that span a wide range of  $w$  values is important because it enables my results to be used for any lanthanide-based precatalysts. Values of  $w$  were obtained from published values,<sup>61–66</sup> but because complexes **5.4** and **5.6** did not have published coordination numbers, the number of open sites was established as 1 and 3, respectively, using  $q$  measurements in  $\text{H}_2\text{O}$ .<sup>20</sup> Additionally, because not all of the complexes were soluble in every solvent system studied, I used multiple complexes for some values of  $w$ : complex **5.1** or **5.2** for  $w$  values of zero and complex **5.3** or **5.4** for  $w$  values of one. The six-step procedure is described followed by a description of my validation of the resulting equations, an example of the use of my results to study a known system, and a flowchart that I expect will enable my results to be used routinely by the scientific community.

### 5.3 The six-step procedure to determine $q'$ and $n$

**Step 1:** Measure the luminescence-decay rates of  $\text{Eu}^{3+}$ -containing complexes of known values of  $w$  in commonly used binary solvent systems with water percentages ranging from 1 to 100% (**Figure 5.2**). The observed decay rates are a combination of both inner- and outer-sphere decay as illustrated by **Eq 5.3**, where  $|\tau_H^{-1} - \tau_D^{-1}|_{IS}$  is the absolute value of the difference of luminescence quenching rate due to inner-sphere solvent molecules and  $|\tau_H^{-1} - \tau_D^{-1}|_{OS}$  is the absolute value of the difference of luminescence quenching rate due to outer-sphere solvent



molecules. The measured values of  $|\tau_H^{-1} - \tau_D^{-1}|_m$  have maximum values in 100% water, and these values decrease with decreasing water concentration (**Tables 5.1–5.7**). This decrease is likely due to the presence of both inner- and outer-sphere non-water solvent molecules that have a lower decay rate per solvent molecule compared to water molecules.

$$\text{Eq 5.3 } |\tau_H^{-1} - \tau_D^{-1}|_m = |\tau_H^{-1} - \tau_D^{-1}|_{IS} + |\tau_H^{-1} - \tau_D^{-1}|_{OS}$$

**Table 5.1.** Mean  $|\tau_H^{-1} - \tau_D^{-1}|_m$  values for MeOH and methanol- $d_4$ .

% (v/v) of H <sub>2</sub> O in MeOH or D <sub>2</sub> O methanol- $d_4$	$ \tau_H^{-1} - \tau_D^{-1} _m$ (ms <sup>-1</sup> )				
	in <b>5.1 or 5.2</b> ( $w = 0$ )	<b>5.3</b> ( $w = 1$ )	<b>5.5</b> ( $w = 2$ )	<b>5.6</b> ( $w = 3$ )	Eu(OTf) <sub>3</sub> ( $w = 9$ )
100	0.35 <sup>a</sup>	1.15	1.99	2.79	7.84
90	0.35 <sup>a</sup>	1.11	1.87	2.66	7.56
80	0.35 <sup>a</sup>	1.08	1.80	2.64	7.43
70	0.33 <sup>a</sup>	1.07	1.64	2.63	7.21
60	0.30 <sup>a</sup>	1.06	1.52	2.50	7.13
50	0.30 <sup>a</sup>	0.98	1.45	2.49	7.12
40	0.30 <sup>a</sup>	0.96	1.35	2.38	7.09
30	0.29 <sup>a</sup>	0.96	1.30	2.37	6.96
20	0.25 <sup>a</sup>	0.96	1.31	2.34	6.81
10	0.22 <sup>a</sup>	0.93	1.32	2.31	6.48
9	0.21 <sup>a</sup>	0.93	1.28	2.31	6.36
8	0.16 <sup>a</sup>	0.92	1.22	2.25	6.31
7	0.14 <sup>a</sup>	0.91	1.20	2.29	6.21
6	0.12 <sup>a</sup>	0.89	1.20	2.24	6.21
5	0.12 <sup>b</sup>	0.85	1.17	2.24	5.93
4	0.12 <sup>b</sup>	0.84	1.16	2.13	5.44
3	0.10 <sup>b</sup>	0.82	1.17	1.92	5.35
2	0.10 <sup>b</sup>	0.81	1.08	1.86	5.00
1	0.10 <sup>b</sup>	0.80	1.01	1.84	4.87

<sup>a</sup>complex **5.1**; <sup>b</sup>complex **5.2**

**Table 5.2.** Mean  $|\tau_H^{-1} - \tau_D^{-1}|_m$  values for EtOH and ethanol-*d*.

% (v/v) of H <sub>2</sub> O in EtOH or D <sub>2</sub> O in ethanol- <i>d</i>	$ \tau_H^{-1} - \tau_D^{-1} _m$ (ms <sup>-1</sup> )				
	<b>5.1 or 5.2</b> ( <i>w</i> = 0)	<b>5.3</b> ( <i>w</i> = 1)	<b>5.5</b> ( <i>w</i> = 2)	<b>5.6</b> ( <i>w</i> = 3)	Eu(OTf) <sub>3</sub> ( <i>w</i> = 9)
100	0.35 <sup>a</sup>	1.15	1.99	2.79	7.84
90	0.28 <sup>a</sup>	1.07	1.82	2.70	7.56
80	0.27 <sup>a</sup>	1.05	1.68	2.66	7.46
70	0.25 <sup>a</sup>	1.03	1.66	2.64	7.35
60	0.21 <sup>a</sup>	1.01	1.61	2.60	7.29
50	0.22 <sup>a</sup>	0.98	1.59	2.60	7.26
40	0.20 <sup>a</sup>	0.97	1.54	2.56	7.10
30	0.20 <sup>a</sup>	0.97	1.55	2.50	7.04
20	0.27 <sup>a</sup>	0.93	1.50	2.43	6.79
10	0.25 <sup>a</sup>	0.87	1.45	2.46	6.56
9	0.24 <sup>a</sup>	0.87	1.35	2.46	6.41
8	0.13 <sup>a</sup>	0.87	1.33	2.50	6.40
7	0.12 <sup>a</sup>	0.83	1.34	2.48	6.39
6	0.11 <sup>b</sup>	0.86	1.32	2.45	6.40
5	0.11 <sup>b</sup>	0.76	1.32	2.35	6.09
4	0.10 <sup>b</sup>	0.75	1.15	2.22	5.56
3	0.10 <sup>b</sup>	0.77	1.18	1.90	5.23
2	0.10 <sup>b</sup>	0.76	1.16	1.88	5.15
1	0.10 <sup>b</sup>	0.75	1.15	1.87	5.15

<sup>a</sup>complex 5.1; <sup>b</sup>complex 5.2

**Table 5.3** Mean  $|\tau_H^{-1} - \tau_D^{-1}|_m$  values for DMSO.

% (v/v) of H <sub>2</sub> O or D <sub>2</sub> O in DMSO	$ \tau_H^{-1} - \tau_D^{-1} _m$ (ms <sup>-1</sup> )				
	<b>5.1</b> (w = 0)	<b>5.3</b> (w = 1)	<b>5.5</b> (w = 2)	<b>5.6</b> (w = 3)	Eu(OTf) <sub>3</sub> (w = 9)
100	0.35	1.15	1.99	2.79	7.84
90	0.30	1.08	1.47	1.91	6.66
80	0.24	0.88	1.33	1.46	6.25
70	0.22	0.87	1.21	1.52	5.40
60	0.20	0.81	0.98	1.56	4.46
50	0.19	0.76	0.84	1.36	3.82
40	0.18	0.67	0.74	1.27	3.42
30	0.17	0.58	0.66	0.94	2.64
20	0.14	0.33	0.44	0.72	1.21
10	0.12	0.22	0.26	0.35	0.68
9	0.12	0.17	0.23	0.35	0.68
8	0.10	0.14	0.20	0.32	0.68
7	0.08	0.13	0.17	0.30	0.64
6	0.06	0.13	0.17	0.31	0.64
5	0.04	0.12	0.16	0.23	0.49
4	0.01	0.03	0.04	0.10	0.29
3	0.01	0.02	0.04	0.08	0.21
2	0.01	0.01	0.03	0.05	0.16
1	0.01	0.01	0.03	0.05	0.14

**Table 5.4** Mean  $|\tau_H^{-1} - \tau_D^{-1}|_m$  values for acetone.

% (v/v) of H <sub>2</sub> O or D <sub>2</sub> O in acetone	$ \tau_H^{-1} - \tau_D^{-1} _m$ (ms <sup>-1</sup> )				
	<b>5.1</b> or <b>5.2</b> (w = 0)	<b>5.3</b> or <b>5.4</b> (w = 1)	<b>5.5</b> (w = 2)	<b>5.6</b> (w = 3)	Eu(OTf) <sub>3</sub> (w = 9)
100	0.35 <sup>a</sup>	1.15 <sup>d</sup>	1.99	2.79	7.84
90	0.30 <sup>a</sup>	1.05 <sup>d</sup>	1.84	2.77	7.60
80	0.29 <sup>a</sup>	1.04 <sup>d</sup>	1.80	2.70	7.53
70	0.30 <sup>a</sup>	1.04 <sup>d</sup>	1.77	2.66	7.51
60	0.29 <sup>a</sup>	1.04 <sup>d</sup>	1.75	2.61	7.36
50	0.28 <sup>a</sup>	1.02 <sup>d</sup>	1.72	2.60	7.17
40	0.26 <sup>a</sup>	1.02 <sup>d</sup>	1.70	2.54	6.94
30	0.25 <sup>a</sup>	0.98 <sup>d</sup>	1.69	2.49	6.77
20	0.21 <sup>b</sup>	0.96 <sup>d</sup>	1.64	2.47	6.79
10	0.20 <sup>b</sup>	0.96 <sup>d</sup>	1.59	2.44	6.79
9	0.19 <sup>b</sup>	0.95 <sup>d</sup>	1.46	2.39	6.80
8	0.18 <sup>b</sup>	0.94 <sup>d</sup>	1.37	2.34	6.80
7	0.18 <sup>b</sup>	0.87 <sup>d</sup>	1.30	2.25	6.69
6	0.16 <sup>b</sup>	0.84 <sup>d</sup>	1.29	2.22	6.62
5	0.16 <sup>b</sup>	0.86 <sup>d</sup>	1.26	2.20	6.63
4	ns <sup>c</sup>	0.84 <sup>e</sup>	ns <sup>c</sup>	2.01	6.35
3	ns <sup>c</sup>	0.73 <sup>e</sup>	ns <sup>c</sup>	1.98	5.98
2	ns <sup>c</sup>	0.71 <sup>e</sup>	ns <sup>c</sup>	1.94	5.85
1	ns <sup>c</sup>	0.69 <sup>e</sup>	ns <sup>c</sup>	1.89	5.76

<sup>a</sup>complex **5.1**; <sup>b</sup>complex **5.2**; <sup>c</sup>ns = not soluble; <sup>d</sup>complex **5.3**; <sup>e</sup>complex **5.4**

**Table 5.5.** Mean  $|\tau_H^{-1} - \tau_D^{-1}|_m$  values for THF.

% (v/v) of H <sub>2</sub> O or D <sub>2</sub> O in THF	$ \tau_H^{-1} - \tau_D^{-1} _m$ (ms <sup>-1</sup> )				
	<b>5.1</b> or <b>5.2</b> ( <i>w</i> = 0)	<b>5.3</b> or <b>5.4</b> ( <i>w</i> = 1)	<b>5.5</b> ( <i>w</i> = 2)	<b>5.6</b> ( <i>w</i> = 3)	Eu(OTf) <sub>3</sub> ( <i>w</i> = 9)
100	0.35 <sup>a</sup>	1.15 <sup>d</sup>	1.99	2.79	7.84
90	0.30 <sup>a</sup>	1.10 <sup>d</sup>	1.88	2.66	7.55
80	0.30 <sup>a</sup>	1.08 <sup>d</sup>	1.88	2.63	7.45
70	0.29 <sup>a</sup>	1.07 <sup>d</sup>	1.75	2.65	7.47
60	0.29 <sup>a</sup>	1.08 <sup>d</sup>	1.78	2.63	7.44
50	0.28 <sup>a</sup>	1.15 <sup>d</sup>	1.63	2.62	7.36
40	0.27 <sup>a</sup>	1.15 <sup>d</sup>	1.63	2.67	7.33
30	0.25 <sup>a</sup>	1.15 <sup>d</sup>	1.61	2.68	7.36
20	0.23 <sup>a</sup>	1.15 <sup>d</sup>	1.61	2.65	7.38
10	0.19 <sup>b</sup>	0.98 <sup>d</sup>	1.51	2.61	7.11
9	0.19 <sup>b</sup>	0.94 <sup>d</sup>	1.46	2.54	6.93
8	0.16 <sup>b</sup>	0.92 <sup>d</sup>	1.49	2.58	6.93
7	0.16 <sup>b</sup>	0.92 <sup>d</sup>	1.44	2.57	6.96
6	0.14 <sup>b</sup>	0.92 <sup>d</sup>	1.49	2.61	6.97
5	0.13 <sup>b</sup>	0.92 <sup>d</sup>	1.45	2.58	6.80
4	ns <sup>c</sup>	0.99 <sup>e</sup>	1.41	2.58	6.86
3	ns <sup>c</sup>	0.99 <sup>e</sup>	1.50	ns <sup>c</sup>	6.79
2	ns <sup>c</sup>	0.91 <sup>e</sup>	1.03	ns <sup>c</sup>	5.26
1	ns <sup>c</sup>	0.91 <sup>e</sup>	1.00	ns <sup>c</sup>	5.19

<sup>a</sup>complex **5.1**; <sup>b</sup>complex **5.2**; <sup>c</sup>ns = not soluble; <sup>d</sup>complex **5.3**; <sup>e</sup>complex **5.4**

**Table 5.6.** Mean  $|\tau_H^{-1} - \tau_D^{-1}|_m$  values for acetonitrile.

% (v/v) of H <sub>2</sub> O or D <sub>2</sub> O acetonitrile	$ \tau_H^{-1} - \tau_D^{-1} _m$ (ms <sup>-1</sup> )				
	in <b>5.1</b> or <b>5.2</b> (w = 0)	<b>5.3</b> or <b>5.4</b> (w = 1)	<b>5.5</b> (w = 2)	<b>5.6</b> (w = 3)	Eu(OTf) <sub>3</sub> (w = 9)
100	0.35 <sup>a</sup>	1.15 <sup>d</sup>	1.99	2.79	7.84
90	0.31 <sup>a</sup>	1.06 <sup>d</sup>	1.80	2.76	7.59
80	0.29 <sup>a</sup>	1.06 <sup>d</sup>	1.53	2.76	7.50
70	0.29 <sup>a</sup>	1.05 <sup>d</sup>	1.57	2.73	7.50
60	0.29 <sup>a</sup>	1.01 <sup>d</sup>	1.49	2.73	7.47
50	0.25 <sup>a</sup>	1.01 <sup>d</sup>	1.39	2.72	7.44
40	0.26 <sup>a</sup>	1.01 <sup>d</sup>	1.33	2.68	7.40
30	0.25 <sup>a</sup>	1.01 <sup>d</sup>	1.33	2.65	7.40
20	0.24 <sup>a</sup>	1.01 <sup>d</sup>	1.30	2.64	7.37
10	0.26 <sup>b</sup>	1.07 <sup>d</sup>	1.11	2.65	7.21
9	0.26 <sup>b</sup>	1.05 <sup>d</sup>	1.13	2.54	7.08
8	0.26 <sup>b</sup>	1.06 <sup>d</sup>	1.13	2.42	6.94
7	0.26 <sup>b</sup>	1.09 <sup>d</sup>	1.12	2.39	6.82
6	0.26 <sup>b</sup>	1.04 <sup>d</sup>	1.14	2.35	6.62
5	0.20 <sup>b</sup>	0.93 <sup>d</sup>	ns <sup>c</sup>	2.06	6.60
4	0.20 <sup>b</sup>	0.93 <sup>e</sup>	ns <sup>c</sup>	2.08	6.59
3	ns <sup>c</sup>	0.89 <sup>e</sup>	ns <sup>c</sup>	1.83	6.17
2	ns <sup>c</sup>	0.79 <sup>e</sup>	ns <sup>c</sup>	1.79	5.89
1	ns <sup>c</sup>	0.70 <sup>e</sup>	ns <sup>c</sup>	1.56	5.34

<sup>a</sup>complex **5.1**; <sup>b</sup>complex **5.2**; <sup>c</sup>ns = not soluble; <sup>d</sup>complex **5.3**; <sup>e</sup>complex **5.4**

**Table 5.7.** Mean  $|\tau_H^{-1} - \tau_D^{-1}|_m$  values for DMF and DMF- $d_7$ .\*

% (v/v) of H <sub>2</sub> O in DMF or D <sub>2</sub> O in DMF- $d_7$	$ \tau_H^{-1} - \tau_D^{-1} _m$ (ms <sup>-1</sup> )				
	<b>5.1</b> ( $w = 0$ )	<b>5.3</b> ( $w = 1$ )	<b>5.5</b> ( $w = 2$ )	<b>5.6</b> ( $w = 3$ )	Eu(OTf) <sub>3</sub> ( $w = 9$ )
100	0.35	1.15	1.99	2.79	7.84
90	0.35	1.07	1.67	2.13	6.58
60	0.31	0.93	1.29	1.63	5.16
20	0.29	0.61	0.88	1.25	4.18
9	0.24	0.49	0.73	1.09	4.02
5	0.24	0.44	0.69	1.10	3.89
3	0.14	0.23	0.52	0.67	2.43
1	0.10	0.21	0.47	0.64	2.17

\* Fewer measurements were performed with DMF-containing solutions because of the high price of DMF- $d_7$ .

**Step 2:** Measure the luminescence-decay rate caused by outer-sphere molecules using Eu<sup>3+</sup> complexes **5.1** and **5.2** that are composed of ligands that saturate the inner-coordination sphere of the metal. By completely blocking the inner-coordination sphere ( $|\tau_H^{-1} - \tau_D^{-1}|_{IS} = 0$  in **Eq 5.3**), I was able to isolate and measure luminescence decay caused by outer-sphere solvent molecules as illustrated in **Eq 5.4**.

$$\mathbf{Eq\ 5.4} \quad |\tau_H^{-1} - \tau_D^{-1}|_m = |\tau_H^{-1} - \tau_D^{-1}|_{OS}$$

The results obtained for Step 2 are included in **Tables 5.1–5.7** ( $w = 0$ ). The luminescence decay caused by outer-sphere solvent molecules were maximum in 100% water, and these values decreased with decreasing concentration of water. These results provide further evidence that non-water outer-sphere solvent molecules contribute less to luminescence quenching than water on a per-molecule basis.

**Step 3:** Calculate the inner-sphere decay component by subtracting the outer-sphere component (the data obtained from Step 2) from the measured data in Step 1. The isolated inner-sphere component is composed of decay arising from water molecules and non-water solvent molecules (**Eq 5.5**), where  $\left| \tau_H^{-1} - \tau_D^{-1} \right|_{IS_{water}}$  is the inner-sphere decay rate difference per water molecule and  $\left| \tau_H^{-1} - \tau_D^{-1} \right|_{IS_{solvent}}$  is the inner-sphere decay rate difference per non-water solvent molecule. The isolated value of  $\left| \tau_H^{-1} - \tau_D^{-1} \right|_{IS}$  is the sum of  $\left| \tau_H^{-1} - \tau_D^{-1} \right|_{IS_{water}}$  multiplied by the number of water molecules ( $q'$ ) and  $\left| \tau_H^{-1} - \tau_D^{-1} \right|_{IS_{solvent}}$  multiplied by the number of solvent molecules ( $n$ ). The results obtained for Step 3 are shown in **Tables 5.8–5.14**, where complexes **5.1** and **5.2** have been omitted because the value of  $\left| \tau_H^{-1} - \tau_D^{-1} \right|_{IS}$  for these complexes is 0 by definition.

$$\mathbf{Eq\ 5.5} \quad \left| \tau_H^{-1} - \tau_D^{-1} \right|_{IS} = q' \left| \tau_H^{-1} - \tau_D^{-1} \right|_{IS_{water}} + n \left| \tau_H^{-1} - \tau_D^{-1} \right|_{IS_{solvent}}$$



**Table 5.8.** Mean  $|\tau_H^{-1} - \tau_D^{-1}|_{IS}$  values for MeOH and methanol- $d_4$ .

% (v/v) of H <sub>2</sub> O in MeOH or D <sub>2</sub> O in methanol- $d_4$		$ \tau_H^{-1} - \tau_D^{-1} _{IS}$ (ms <sup>-1</sup> )			
		<b>5.3</b> ( $w = 1$ )	<b>5.5</b> ( $w = 2$ )	<b>5.6</b> ( $w = 3$ )	Eu(OTf) <sub>3</sub> ( $w = 9$ )
100		0.76	1.54	2.44	7.49
90		0.76	1.53	1.91	7.21
80		0.74	1.45	1.80	7.08
70		0.74	1.31	1.80	6.88
60		0.76	1.22	1.80	6.62
50		0.68	1.15	1.79	6.41
40		0.67	1.06	1.78	6.19
30		0.67	1.01	1.78	6.07
20		0.72	1.07	1.79	6.06
10		0.71	1.11	1.79	5.96
9		0.72	1.08	1.79	5.86
8		0.77	1.12	1.80	5.76
7		0.83	1.15	1.78	5.70
6		0.81	1.13	1.72	5.68
5		0.72	1.08	1.72	5.30
4		0.72	1.09	1.71	5.33
3		0.72	1.11	1.72	5.25
2		0.71	1.08	1.70	4.90
1		0.70	1.07	1.71	4.67

**Table 5.9.** Mean  $|\tau_H^{-1} - \tau_D^{-1}|_{IS}$  values for EtOH and ethanol-*d*.

% (v/v) of H <sub>2</sub> O in EtOH or D <sub>2</sub> O in ethanol- <i>d</i>	$ \tau_H^{-1} - \tau_D^{-1} _{IS}$ (ms <sup>-1</sup> )			
	<b>5.3</b> ( <i>w</i> = 1)	<b>5.5</b> ( <i>w</i> = 2)	<b>5.6</b> ( <i>w</i> = 3)	Eu(OTf) <sub>3</sub> ( <i>w</i> = 9)
100	0.80	1.64	2.44	7.49
90	0.73	1.48	2.36	7.22
80	0.73	1.36	2.34	7.14
70	0.68	1.31	2.29	7.00
60	0.70	1.30	2.29	6.98
50	0.66	1.27	2.28	6.94
40	0.68	1.25	2.27	6.81
30	0.69	1.27	2.22	6.76
20	0.66	1.23	2.16	6.52
10	0.62	1.20	2.21	6.31
9	0.63	1.11	2.22	6.17
8	0.74	1.20	2.37	6.27
7	0.71	1.22	2.36	6.27
6	0.75	1.21	2.34	6.29
5	0.65	1.21	2.24	5.98
4	0.65	1.05	2.12	5.46
3	0.67	1.08	1.80	5.13
2	0.66	1.06	1.78	5.05
1	0.65	1.05	1.77	5.05

**Table 5.10.** Mean  $|\tau_H^{-1} - \tau_D^{-1}|_{IS}$  values for DMSO.

% (v/v) of H <sub>2</sub> O or D <sub>2</sub> O in DMSO	$ \tau_H^{-1} - \tau_D^{-1} _{IS}$ (ms <sup>-1</sup> )			
	<b>5.3</b> (w = 1)	<b>5.5</b> (w = 2)	<b>5.6</b> (w = 3)	Eu(OTf) <sub>3</sub> (w = 9)
100	0.80	1.64	2.44	7.49
90	0.78	1.17	1.61	6.36
80	0.64	1.09	1.22	6.01
70	0.65	0.99	1.30	5.18
60	0.61	0.78	1.36	4.26
50	0.57	0.65	1.17	3.63
40	0.49	0.56	1.09	3.24
30	0.41	0.49	0.77	2.47
20	0.19	0.30	0.58	1.07
10	0.10	0.14	0.23	0.56
9	0.05	0.11	0.23	0.56
8	0.04	0.10	0.22	0.58
7	0.05	0.09	0.22	0.56
6	0.07	0.11	0.25	0.58
5	0.08	0.12	0.19	0.45
4	0.02	0.03	0.09	0.28
3	0.01	0.03	0.07	0.20
2	0.00	0.02	0.04	0.15
1	0.00	0.02	0.04	0.13

**Table 5.11.** Mean  $|\tau_H^{-1} - \tau_D^{-1}|_{IS}$  values for acetone.

% (v/v of H <sub>2</sub> O or D <sub>2</sub> O in acetone)	$ \tau_H^{-1} - \tau_D^{-1} _{IS}$ (ms <sup>-1</sup> )			
	<b>5.3 or 5.4</b> (w = 1)	<b>5.5</b> (w = 2)	<b>5.6</b> (w = 3)	Eu(OTf) <sub>3</sub> (w = 9)
100	0.80 <sup>a</sup>	1.64	2.44	7.49
90	0.75 <sup>a</sup>	1.54	2.47	7.30
80	0.75 <sup>a</sup>	1.51	2.41	7.24
70	0.74 <sup>a</sup>	1.47	2.36	7.21
60	0.75 <sup>a</sup>	1.46	2.32	7.07
50	0.74 <sup>a</sup>	1.44	2.32	6.89
40	0.76 <sup>a</sup>	1.44	2.28	6.68
30	0.73 <sup>a</sup>	1.44	2.24	6.52
20	0.75 <sup>a</sup>	1.43	2.26	6.58
10	0.76 <sup>a</sup>	1.39	2.24	6.59
9	0.76 <sup>a</sup>	1.27	2.20	6.61
8	0.76 <sup>a</sup>	1.19	2.16	6.62
7	0.69 <sup>a</sup>	1.12	2.07	6.51
6	0.68 <sup>a</sup>	1.13	2.06	6.46
5	0.70 <sup>a</sup>	1.10	2.04	6.47
4	nd <sup>b</sup>	nd <sup>b</sup>	nd <sup>b</sup>	nd <sup>b</sup>
3	nd <sup>b</sup>	nd <sup>b</sup>	nd <sup>b</sup>	nd <sup>b</sup>
2	nd <sup>b</sup>	nd <sup>b</sup>	nd <sup>b</sup>	nd <sup>b</sup>
1	nd <sup>b</sup>	nd <sup>b</sup>	nd <sup>b</sup>	nd <sup>b</sup>

<sup>a</sup>complex 5.3; <sup>b</sup>not determined because of solubility of complexes 5.1 and 5.2.

**Table 5.12.** Mean  $|\tau_H^{-1} - \tau_D^{-1}|_{IS}$  values for THF.

% (v/v) of H <sub>2</sub> O or D <sub>2</sub> O in THF	$ \tau_H^{-1} - \tau_D^{-1} _{IS}$ (ms <sup>-1</sup> )			
	<b>5.3</b> (w = 1)	<b>5.5</b> (w = 2)	<b>5.6</b> (w = 3)	Eu(OTf) <sub>3</sub> (w = 9)
100	0.80 <sup>a</sup>	1.64	2.44	7.49
90	0.80 <sup>a</sup>	1.58	2.36	7.25
80	0.78 <sup>a</sup>	1.58	2.33	7.15
70	0.78 <sup>a</sup>	1.46	2.36	7.18
60	0.79 <sup>a</sup>	1.49	2.34	7.15
50	0.74 <sup>a</sup>	1.35	2.34	7.08
40	0.75 <sup>a</sup>	1.36	2.40	7.06
30	0.74 <sup>a</sup>	1.36	2.43	7.11
20	0.77 <sup>a</sup>	1.38	2.42	7.15
10	0.79 <sup>a</sup>	1.32	2.42	6.92
9	0.75 <sup>a</sup>	1.27	2.35	6.74
8	0.76 <sup>a</sup>	1.33	2.42	6.77
7	0.76 <sup>a</sup>	1.28	2.41	6.80
6	0.78 <sup>a</sup>	1.35	2.47	6.83
5	0.79 <sup>a</sup>	1.32	2.45	6.67
4	nd <sup>b</sup>	nd <sup>b</sup>	nd <sup>b</sup>	nd <sup>b</sup>
3	nd <sup>b</sup>	nd <sup>b</sup>	nd <sup>b</sup>	nd <sup>b</sup>
2	nd <sup>b</sup>	nd <sup>b</sup>	nd <sup>b</sup>	nd <sup>b</sup>
1	nd <sup>b</sup>	nd <sup>b</sup>	nd <sup>b</sup>	nd <sup>b</sup>

<sup>a</sup>complex **5.3**; <sup>b</sup>not determined because of solubility of complexes **5.1** and **5.2**.

**Table 5.13.** Mean  $|\tau_H^{-1} - \tau_D^{-1}|_{IS}$  values for acetonitrile.

% (v/v) of H <sub>2</sub> O or D <sub>2</sub> O in acetonitrile	$ \tau_H^{-1} - \tau_D^{-1} _{IS}$ (ms <sup>-1</sup> )			
	<b>5.3 or 5.4</b> (w = 1)	<b>5.5</b> (w = 2)	<b>5.6</b> (w = 3)	Eu(OTf) <sub>3</sub> (w = 9)
100	0.80 <sup>a</sup>	1.64	2.44	7.49
90	0.75 <sup>a</sup>	1.49	2.45	7.28
80	0.77 <sup>a</sup>	1.24	2.46	7.21
70	0.76 <sup>a</sup>	1.28	2.44	7.21
60	0.72 <sup>a</sup>	1.20	2.44	7.18
50	0.76 <sup>a</sup>	1.14	2.46	7.18
40	0.75 <sup>a</sup>	1.08	2.43	7.15
30	0.76 <sup>a</sup>	1.09	2.41	7.15
20	0.76 <sup>a</sup>	1.06	2.40	7.13
10	0.81 <sup>a</sup>	0.86	2.40	6.95
9	0.79 <sup>a</sup>	0.87	2.28	6.82
8	0.79 <sup>a</sup>	0.86	2.15	6.67
7	0.76 <sup>a</sup>	0.85	2.12	6.55
6	0.77 <sup>a</sup>	0.87	2.08	6.35
5	0.72 <sup>a</sup>	nd <sup>c</sup>	1.86	6.40
4	0.73 <sup>b</sup>	nd <sup>c</sup>	1.88	6.39
3	nd <sup>c</sup>	nd <sup>c</sup>	nd <sup>c</sup>	nd <sup>c</sup>
2	nd <sup>c</sup>	nd <sup>c</sup>	nd <sup>c</sup>	nd <sup>c</sup>
1	nd <sup>c</sup>	nd <sup>c</sup>	nd <sup>c</sup>	nd <sup>c</sup>

<sup>a</sup>complex **5.3**; <sup>b</sup>complex **5.4**; <sup>c</sup> not determined because of solubility of complexes **5.1** and **5.2**.

**Table 5.14.** Mean  $|\tau_H^{-1} - \tau_D^{-1}|_{IS}$  values for DMF and DMF-*d*<sub>7</sub>.

% (v/v) of H <sub>2</sub> O in DMF or D <sub>2</sub> O in DMF- <i>d</i> <sub>7</sub>	$ \tau_H^{-1} - \tau_D^{-1} _{IS}$ (ms <sup>-1</sup> )			
	<b>5.3</b> (w = 1)	<b>5.5</b> (w = 2)	<b>5.6</b> (w = 3)	Eu(OTf) <sub>3</sub> (w = 9)
100	0.80	1.64	2.44	7.49
90	0.72	1.32	1.78	6.23
60	0.62	0.98	1.32	4.85
20	0.32	0.59	0.96	3.89
9	0.25	0.49	0.85	3.78
5	0.20	0.45	0.86	3.65
3	0.09	0.38	0.53	2.29
1	0.11	0.37	0.54	2.07

**Step 4:** Determine the inner-sphere decay rate difference per molecule in the absence of water. To determine the values of the per molecule decay rate differences in **Eq 5.5**, one of the two differences was set to zero. First, I set  $q'$  to 0 in **Eq 5.5** by using each cosolvent in the absence of water (**Eq 5.6**).

$$\mathbf{Eq\ 5.6} \quad \left| \tau_H^{-1} - \tau_D^{-1} \right|_{IS} = n \left| \tau_H^{-1} - \tau_D^{-1} \right|_{IS\ solvent}$$

In **Eq 5.6**,  $n$  can be replaced by  $w$  when  $q'$  is equal to 0, using the relationship shown in **Eq 5.7**, where  $w$  equals the total number of coordinated water and solvent molecules. When  $n$  was replaced by  $w$ , **Eq 5.8** was obtained, and  $\left| \tau_H^{-1} - \tau_D^{-1} \right|_{IS\ solvent}$  for each complex was divided by the  $w$  value of each complex (**Eq 5.9**) to calculate the inner-sphere decay rate per solvent molecule for all of the solvents studied. The calculated  $\left| \tau_H^{-1} - \tau_D^{-1} \right|_{IS\ solvent}$  values are listed in **Table 5.15**.

$$\mathbf{Eq\ 5.7} \quad q' + n = w$$

$$\mathbf{Eq\ 5.8} \quad \left| \tau_H^{-1} - \tau_D^{-1} \right|_{IS} = w \left| \tau_H^{-1} - \tau_D^{-1} \right|_{IS\ solvent}$$

$$\mathbf{Eq\ 5.9} \quad \frac{\left| \tau_H^{-1} - \tau_D^{-1} \right|_{IS}}{w} = \left| \tau_H^{-1} - \tau_D^{-1} \right|_{IS\ solvent}$$

**Table 5.15.** Calculated decay per inner-sphere solvent molecule.

solvent	$\left  \tau_H^{-1} - \tau_D^{-1} \right _{IS_{solvent}}$
water	0.83*
methanol	0.41
ethanol	0.44
DMSO	0
acetone	0
THF	0
acetonitrile	0
DMF	0

$$* \left| \tau_H^{-1} - \tau_D^{-1} \right|_{IS_{water}}$$

I observed values of zero for the decay per inner-sphere solvent molecule for THF, DMSO, DMF, acetonitrile, and acetone. This result is likely because these solvents do not contain vibrational oscillators capable of quenching the  $\text{Eu}^{3+}$  excited state energy. For MeOH and EtOH, the decay- per- inner-sphere- solvent- molecule values were greater than zero due to the presence of O–H oscillators.

**Step 5:** Repeat **Step 4** using 100% water to determine inner-sphere decay rate per water molecule when no cosolvent is present ( $n = 0$  from **Eq 5.5**). Here,  $q'$  in **Eq 5.5** was replaced by  $w$  to obtain **Eq 5.10**, and **Eq 5.11** shows the rearrangement of **Eq 5.10** used to calculate the inner-sphere decay rate per water molecule. The calculated  $\left| \tau_H^{-1} - \tau_D^{-1} \right|_{IS_{water}}$  value is listed in **Table 5.15**. The decay per inner-sphere solvent molecule for MeOH and EtOH was approximately half that of inner-sphere water (**Table 5.16**). This observation is not surprising because there are half as many O–H oscillators in MeOH or EtOH as there are in water.

$$\text{Eq 5.10} \quad \left| \tau_H^{-1} - \tau_D^{-1} \right|_{IS} = w \left| \tau_H^{-1} - \tau_D^{-1} \right|_{IS_{water}}$$



$$\text{Eq 5.11} \quad \frac{|\tau_H^{-1} - \tau_D^{-1}|_{IS}}{w} = |\tau_H^{-1} - \tau_D^{-1}|_{IS\ water}$$

**Step 6:** Determine  $q'$  and  $n$  by combining **Eqs 5.5** and **5.12** for each complex in all the studied solvent systems. This determination is important because solving for  $q'$  in binary solvent systems is the key step to determination of  $\alpha$  and  $A$  (**Figure 5.3**). However, the measured luminescence rates were due to the experimental number of coordination sites not occupied by a multidentate ligand,  $w'$ . This experimental  $w'$  is different than  $w$  because many of the  $w$  values were determined in a static environment using X-ray crystallography while  $w'$  is measured in a dynamic environment. The experimental  $w'$  was calculated for each studied complex by dividing the  $|\tau_H^{-1} - \tau_D^{-1}|_{IS}$  values in 100% water by  $|\tau_H^{-1} - \tau_D^{-1}|_{IS\ water}$ . All measured  $w'$  values are less than or equal to the respective  $w$  values (**Table 5.16**). Using  $w'$ , I re-wrote **Eq 5.7** as **Eq 5.12** to account for solution dynamics. **Eq 5.12** was used with **Eq 5.5** and the data from **Tables 5.8–5.14** to create a system of two equations and two variables ( $q'$  and  $n$ ). This system allowed for  $q'$  and  $n$  to be solved for in all of the solvent systems studied. The calculated values of  $q'$  and  $n$  in the DMSO/water binary system are shown in **Table 5.17** as a representative system. The  $q'$  and  $n$  values for each complex in all of the studied solvent systems are shown in Appendix B. The maximum calculated  $q'$  value was obtained in 100% water for each complex, and these values decreased with decreasing concentration of water. Further, the maximum calculated  $n$  values were observed at the lowest water percentages.

$$\text{Eq 5.12} \quad q' + n = w'$$

**Table 5.16.** values of  $w'$  for complexes **5.1–5.5** and  $\text{Eu}(\text{OTf})_3$ .

complex	$w$	$w'$
<b>5.1</b>	0	0
<b>5.2</b>	0	0
<b>5.3</b>	1	0.96
<b>5.4</b>	1	0.96
<b>5.5</b>	2	1.97
<b>5.6</b>	3	2.95
$\text{Eu}(\text{OTf})_3$	9	9.00

**Table 5.17.** Calculated  $q'$  and  $n$  values for DMSO binary systems.

% (v/v) of H <sub>2</sub> O in DMSO or D <sub>2</sub> O in DMSO	<b>5.3</b> ( $w = 1$ )		<b>5.5</b> ( $w = 2$ )		<b>5.6</b> ( $w = 3$ )		Eu(OTf) <sub>3</sub> ( $w = 9$ )	
	$q'$	$n$	$q'$	$n$	$q'$	$n$	$q'$	$n$
100	0.96	0.00	1.97	0.00	2.95	0.00	9.00	0.00
90	0.84	0.12	1.68	0.29	1.94	1.01	7.66	1.34
80	0.78	0.18	1.50	0.47	1.48	1.47	7.24	1.76
70	0.79	0.17	1.16	0.81	1.57	1.38	6.25	2.75
60	0.84	0.12	0.94	1.03	1.64	1.31	5.13	3.87
50	0.65	0.31	0.78	1.19	1.41	1.54	4.37	4.63
40	0.61	0.35	0.57	1.40	1.31	1.64	3.91	5.09
30	0.62	0.34	0.46	1.51	0.94	2.01	2.98	6.02
20	0.73	0.23	0.59	1.38	0.70	2.25	1.30	7.70
10	0.72	0.24	0.68	1.29	0.28	2.67	0.68	8.32
9	0.75	0.21	0.61	1.36	0.28	2.67	0.68	8.32
8	0.85	0.11	0.71	1.26	0.27	2.68	0.70	8.30
7	0.85	0.11	0.79	1.18	0.26	2.69	0.68	8.32
6	0.86	0.10	0.74	1.23	0.30	2.65	0.69	8.31
5	0.75	0.21	0.62	1.35	0.23	2.72	0.54	8.46
4	0.74	0.22	0.64	1.33	0.11	2.84	0.34	8.66
3	0.74	0.22	0.69	1.28	0.08	2.87	0.24	8.76
2	0.72	0.24	0.63	1.34	0.05	2.90	0.18	8.82
1	0.69	0.27	0.60	1.37	0.04	2.91	0.15	8.85

#### 5.4 Derivation of $\alpha$ and $A$ for binary solvent systems

After calculating  $q'$  values, I made plots to derive  $\alpha$  and  $A$  using the same strategy as Horrocks and coworkers. To achieve this goal, the  $|\tau_H^{-1} - \tau_D^{-1}|_m$  values from Step 1 were plotted against the  $q'$  values for complexes **5.1–5.6** as well as Eu(OTf)<sub>3</sub> in all of the binary mixtures studied. For complexes in MeOH and EtOH,  $|\tau_H^{-1} - \tau_D^{-1}|_m$  values were plotted against  $(q' + \frac{n}{2})$  because these solvents have a decay per solvent molecule that is approximately half that of one water molecule. A representative plot is shown in **Figure 5.4** using the DMSO binary solvent

system with 60% water (v/v). The remaining  $|\tau_H^{-1} - \tau_D^{-1}|_m$  versus  $q'$  and  $|\tau_H^{-1} - \tau_D^{-1}|_m$  versus  $(q' + \frac{n}{2})$  plots are shown in Appendix B.

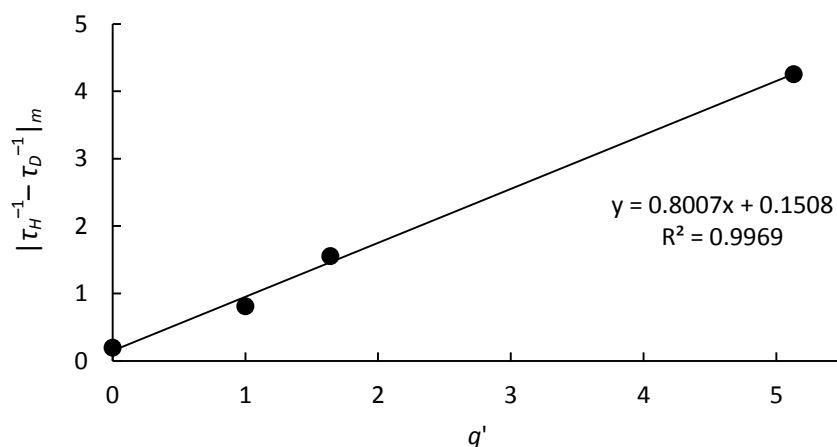


**Figure 5.4.**  $|\tau_H^{-1} - \tau_D^{-1}|_m$  versus  $q'$  for 60% H<sub>2</sub>O (v/v) in DMSO.

The data in **Figure 5.4** and Appendix B indicate that decay rates have a linear dependence on  $q'$  values in all of the measured solvent systems. Because complexes **5.1–5.6** do not contain non-solvent ligand-based O–H oscillators, the intercept of these plots can be used to determine changes outside of the inner-sphere ( $\alpha$  in **Eq 5.1**) for each unique binary solvent system (**Table 5.18**). Additionally, the  $A$  value was calculated as 1.2 using the reciprocal of the slope of the best fit line of the plots, and this value was independent of solvent system.

**Table 5.18.**  $\alpha$  values for each binary solvent system studied.

H <sub>2</sub> O% (v/v)	methanol	ethanol	DMSO	acetone	THF	acetonitrile	DMF
100	0.35	0.35	0.35	0.35	0.35	0.35	0.35
90	0.35	0.33	0.30	0.30	0.30	0.31	0.35
80	0.36	0.32	0.29	0.29	0.30	0.30	nd*
70	0.34	0.32	0.24	0.30	0.30	0.29	nd*
60	0.31	0.29	0.20	0.29	0.29	0.29	0.31
50	0.31	0.29	0.19	0.24	0.28	0.25	nd*
40	0.31	0.27	0.18	0.26	0.27	0.24	nd*
30	0.30	0.26	0.17	0.25	0.25	0.23	nd*
20	0.26	0.25	0.12	0.21	0.23	0.21	0.29
10	0.23	0.23	0.12	0.20	0.19	0.19	nd*
9	0.22	0.22	0.12	0.19	0.19	0.18	0.24
8	0.15	0.14	0.09	0.18	0.16	0.18	nd*
7	0.11	0.13	0.08	0.18	0.16	0.17	nd*
6	0.12	0.13	0.06	0.16	0.14	0.17	nd*
5	0.13	0.12	0.04	0.16	0.11	0.13	0.24
4	0.11	0.11	0.01	nd	nd	0.11	nd*
3	0.10	0.11	0.01	nd	nd	nd	0.14
2	0.09	0.11	0.01	nd	nd	nd	nd*
1	0.07	0.11	0.01	nd	nd	nd	0.10

nd = not determined due to insolubility.

nd\* = not determined because of the high price of DMF-*d*<sub>7</sub>.

The results in **Table 5.18** indicate that the maximum value for the outer-sphere contribution to luminescence decay,  $\alpha$ , was obtained in 100% water. This is likely because water molecules have more efficient vibrational quenchers (two O–H oscillators) than the other solvents studied. Furthermore, values of  $\alpha$  tend to decrease with decreasing water percentage in each solvent system, and this reduction is proportional to the relative affinity of the solvents to the Eu<sup>3+</sup> center.<sup>22</sup> Interestingly, values of  $\alpha$  for solvents without O–H oscillators were not equivalent. This difference is likely due to the different strengths of the interactions of these solvents with water leading to changes in the vibrations of the water molecules.<sup>67–70</sup> Because

these vibrations are responsible for quenching in the outersphere, changes to these vibrations from hydrogen bonding, density, or van der Waals interactions are expected to influence  $\alpha$ . To enable the determination of  $\alpha$  at any water percentage as opposed to the 19 set values in this study, the  $\alpha$  values from **Table 5.18** were plotted against water percentage (v/v) for each solvent system. These plots were fitted using Microsoft Excel version 2007 using exponential, linear, logarithmic, polynomial, and power trend-line options, and the best fit equations for each solvent are shown in **Table 5.19**.

**Table 5.19.** Equations describing  $\alpha$  as a function of water percentage for each binary solvent system studied. The variable  $x$  is the water percentage (v/v).

cosolvent	$\alpha$ *
methanol	$0.0722 \ln x + 0.0285$
ethanol	$0.0598 \ln x + 0.055$
DMSO ( $x = 1-9$ )	$0.0018x^2 - 0.0033x + 0.0092$
DMSO ( $x = 10-100$ )	$10^{-5x^2} + 0.001x + 0.1051$
acetone	$0.1132x^{0.2219}$
THF	$0.064 \ln x + 0.0301$
acetonitrile	$0.0587 \ln x + 0.0427$
DMF	$0.0523 \ln x + 0.1123$

### 5.5 Validation of empirically derived $\alpha$ equations

To validate my empirically derived equations for  $\alpha$  (**Table 5.19**) relative to the values obtained using Horrocks's equation in 100% water (**Eq 5.1**), I recalculated  $\alpha$  with  $x = 100$  using the equations in **Table 5.19**. My empirically derived  $\alpha$  values for 100% water are within the range of 0.31–0.36 (**Table 5.20**). I subsequently recalculated the number of inner-sphere water molecules in 100% H<sub>2</sub>O for all of the complexes that I studied using the  $\alpha$  value that I obtained

for 100% H<sub>2</sub>O (Results for  $q'$  determinations were rounded to two significant figures).<sup>71</sup> This comparison enabled me to determine the accuracy of  $q'$  values derived from our equations compared to  $w$  values that were obtained from published values.<sup>61-66</sup> Further, I extended my recalculations of inner-sphere water molecules in nonwater solvent systems, by using  $x = 100$  (100% H<sub>2</sub>O) in my new empirically derived equations for  $\alpha$ . **Table 5.20** shows the resulting values that display at most  $\pm 0.1$  water molecules of uncertainty relative to  $w$ . For comparison, I analyzed my data from the 100% water system (water in **Table 5.20**) using the commonly accepted Horrocks equation<sup>20</sup> and found  $w$  values of 0.12, 1.1, 1.8, 2.7, and 8.3 for **5.1**, **5.3**, **5.5**, **5.6**, and Eu(OTf)<sub>3</sub>, respectively. This comparison demonstrates that the calculated values using my equations more closely ( $\pm 0.1$  vs  $\pm 0.7$ ) reflect the actual system ( $w$ ) than the Horrocks equation. It should be noted that my equations can be used with systems for  $w \leq 9$ , where Horrocks's equations are only applicable to complexes  $w \leq 1$  ( $\alpha = 0.25$ ) and for  $1 < w \leq 6$  ( $\alpha = 0.31$ ).<sup>20</sup> My range is extended because I extended the determination of  $q'$  up to nine free coordination sites for Eu<sup>3+</sup> complexes where other studies have stopped at six.<sup>20</sup> It is also worth noting that ligand systems that contain aromatic groups in close proximity to the Eu<sup>3+</sup> ion might display back energy transfer and lead to less accurate determinations of  $q'$ ;<sup>72</sup> however, I did not observe this problem for complex **5.2**.

**Table 5.20.** Recalculated  $\alpha$  values and number of inner-sphere water molecules in 100% H<sub>2</sub>O for all the complexes.

solvent	$\alpha$	<b>5.1</b> ( $w = 0$ )	<b>5.3</b> ( $w = 1$ )	<b>5.5</b> ( $w = 2$ )	<b>5.6</b> ( $w = 3$ )	Eu(OTf) <sub>3</sub> ( $w = 9$ )
water	0.35	0.00	0.96	1.97	2.93	8.99
DMF	0.35	0.00	0.96	1.96	2.93	8.99
acetonitrile	0.31	0.05	1.00	2.01	2.98	9.03
THF	0.32	0.03	0.99	2.00	2.97	9.02
acetone	0.31	0.05	1.00	2.01	2.98	9.03
DMSO	0.31	0.05	1.00	2.01	2.98	9.03
ethanol	0.33	0.02	0.98	1.99	2.96	9.01
methanol	0.36	0.00	0.95	1.95	2.92	8.97

To demonstrate an application of my empirically derived equations, I recalculated the water-coordination measurements from an earlier study.<sup>24</sup> **Figure 5.5** shows the previously published  $q$  and recalculated  $q'$  values of the first reaction coordinate of Eu<sup>3+</sup> in the catalytic cycle of the Mukaiyama aldol reaction. The recalculated  $q'$  values were significantly different at a 95% confidence interval (student's  $t$  test) from the published  $q$  values. Further, an increase of upto 0.86 in water-coordination number was observed upon application of my empirically derived  $A$  and  $\alpha$  values to determine  $q'$ . The increased  $q'$  values at low water percentages are due to both reduced  $\alpha$  values and an increased  $A$  value. The observed increase of  $q'$  values at higher water percentages is due to increased  $A$  value. However, the use of my recalculated  $q'$  values are more appropriate for THF/water binary system because of the consideration of solvent effects.



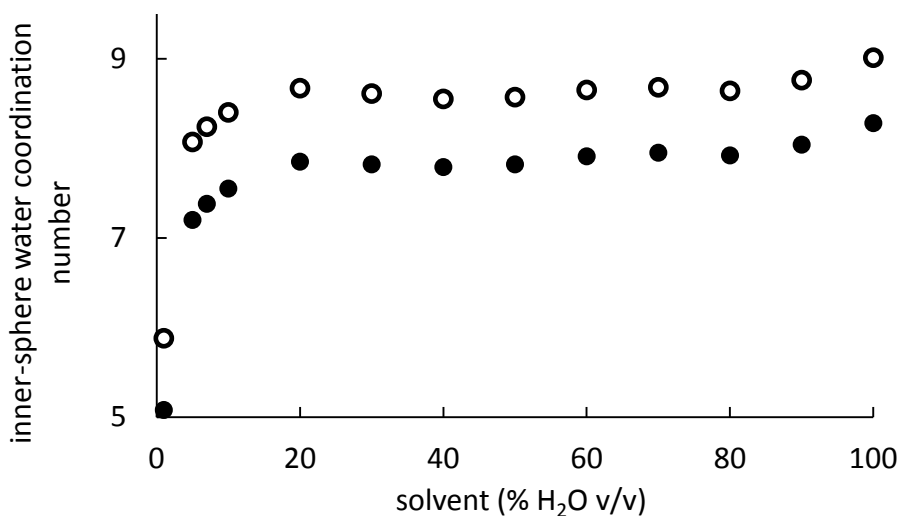


**Figure 5.5.** Comparison between published  $q$  values taken from reference 7 (●) and recalculated  $q'$  (○) of  $\text{Eu}^{3+}$  in the first reaction coordinate of the catalytic cycle. Standard error bars are smaller than the size of the dots.

Finally, I derived a simple three-step procedure for applying my results to the study of lanthanide-catalyzed reactions. The equations listed in **Table 5.20** can be applied easily to study the water-coordination number of any  $\text{Ln}^{3+}$ -based precatalysts that are soluble in any water percentage in the binary systems in this study using the three-step flowchart in **Figure 5.6**. The results of this chapter can also be easily calculated using the ‘ $\alpha$  calculator’ that I have developed using java applets, which can be found at <http://chem.wayne.edu/allengroup/teaching.html>.

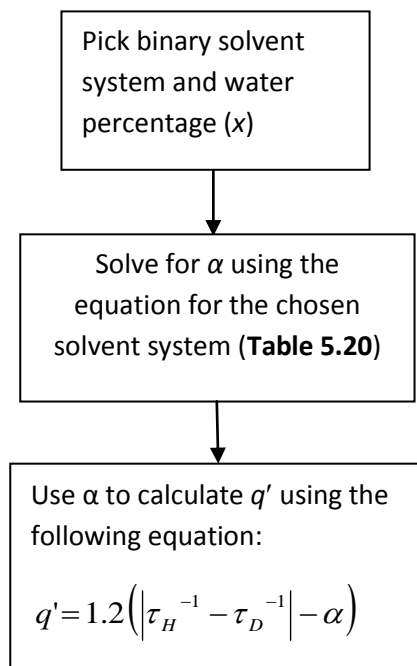


**Figure 5.6.** Flowchart description of my method to determine the number of inner-sphere water molecules of a  $\text{Eu}^{3+}$  complex in a binary solvent system.

## 5.6 Conclusion

I have empirically derived equations that enable fast and accurate determination of the water-coordination number of lanthanides in synthetically useful binary solvent systems. This determination is extremely important to understand the dynamics of the inner- and outer-sphere environments of  $\text{Ln}^{3+}$ -based precatalysts in aqueous solvent mixtures that can enable the easy acquisition of mechanistic and structural information regarding water-tolerant catalysts. The present work opens a gateway for the study of any lanthanide-catalyzed reactions and is a powerful tool for catalyst design.

## 5.7 Experimental Section

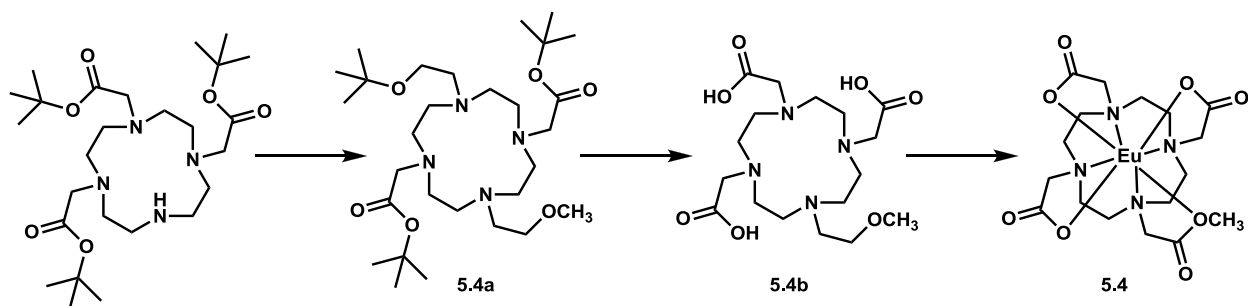
**Materials.** Commercial chemicals were of reagent-grade purity or better and were used without purification unless otherwise noted. Water was purified using a PURELAB Ultra Mk2 water purification system (ELGA). THF was purified using a solvent purification system (Vacuum Atmospheres Company). Ethanol was distilled from calcium hydride.<sup>73</sup> Tris (2,6-pyridinedicarboxylate)europium(III) **(5.1)**,<sup>74</sup> 1,4,7,10-tetraazacyclododecane-1,4,7,10-tetrayltetramethylenetetra(benzylphosphinate)europium(III) **(5.2)**,<sup>61</sup> 2,2',2'',2'''-(1,4,7,10-tetraazacyclododecane-1,4,7,10-tetrayl)tetraacetoeuropium(III) **(5.3)**,<sup>75</sup> 2,2',2''-(1,4,7,10-tetraazacyclododecane-1,4,7-triyl)triacetoeuropium(III) **(5.5)**,<sup>76</sup> and 2,2'-(1,7-dioxa-4,10-diazacyclododecane-4,10-diyl)dipropanoeuropium(III) **(5.6)**<sup>47</sup> were synthesized following published procedures.

**Characterization.** <sup>1</sup>H NMR spectra were obtained using a Varian Mercury 400 (400 MHz) spectrometer, and <sup>13</sup>C NMR spectra were obtained using a Varian Mercury 400 (101 MHz) or a Varian Mercury 500 (125 MHz) spectrometer. Chemical shifts are reported relative to residual solvent signals unless otherwise noted (CDCl<sub>3</sub>: <sup>1</sup>H: δ 7.27, <sup>13</sup>C: δ 77.23; D<sub>2</sub>O: <sup>1</sup>H: δ 4.79, <sup>13</sup>C: δ 39.51 for an internal standard of dimethyl sulfoxide-*d*<sub>6</sub>). <sup>1</sup>H NMR data are assumed to be first order with apparent singlets, and multiplets reported as “s” and “m”, respectively. Italicized elements are those that are responsible for the shifts. High-resolution electrospray ionization mass spectra (HRESIMS) were obtained on an electrospray time-of-flight high-resolution Waters Micromass LCT Premier XE mass spectrometer. IR spectra were measured using KBr pellets from 4000 to 400 cm<sup>-1</sup> on a Bruker TENSOR 27 FTIR spectrophotometer. IR maximum absorption peaks are reported in cm<sup>-1</sup> where the absorptions are s, strong; vs, very strong; and br,

broad. Liquid chromatography and mass spectrometry (LC–MS) analysis was performed on a Shimadzu LC–MS system equipped with a C18 column (Restek International, Viva C18, 5  $\mu$ m, 250  $\times$  4.6 mm) equilibrated with formic acid (0.4% v/v), using a binary gradient method (pump A: water; pump B: acetonitrile; 5–95% B over 70 min; flow rate: 1 mL/min). Exponential, linear, logarithmic, polynomial, and power trend line options as well as best fit equations were obtained using Microsoft Excel version 2007.

**2,2',2''-(10-(2-Methoxyethyl)-1,4,7,10-tetraazacyclododecane-1,4,7-triyl)triacetoeuropium(III) (5.4) (Scheme 5.1):**

To a mixture of *tert*-butyl 2,2',2''-(1,4,7,10-tetraazacyclododecane-1,4,7-triyl)triacetate (179 mg, 0.348 mmol, 1 equiv) and anhydrous K<sub>2</sub>CO<sub>3</sub> (247 mg, 1.79 mmol, 5 equiv) in anhydrous acetonitrile (10 mL) under an atmosphere of Ar was added 2-bromoethylmethylether (164  $\mu$ L, 1.75 mmol, 5 equiv). The resulting mixture was stirred at 70 °C for 12 h. After cooling to ambient temperature and removing solids by filtration, the solvent was removed under reduced pressure. The crude product was purified using silica gel chromatography (10:1 dichloromethane/methanol) to yield 194 mg (97%) of the methoxyethyl-functionalized product **5.4a** as a light yellow oil. <sup>1</sup>H NMR (400 MHz, CDCl<sub>3</sub>,  $\delta$ ): 1.20–1.50 (m, CH<sub>3</sub>, 27H), 1.60–3.60 (m, CH<sub>3</sub> and CH<sub>2</sub>, 29H); <sup>13</sup>C NMR (101 MHz, CDCl<sub>3</sub>,  $\delta$ ): 27.9 (CH<sub>3</sub>), 28.0 (CH<sub>3</sub>), 53.0 (CH<sub>2</sub>), 56.9 (CH<sub>2</sub>), 57.2 (CH<sub>2</sub>), 58.9 (CH<sub>3</sub>), 68.6 (C(CH<sub>3</sub>)<sub>3</sub>), 81.9 (CH<sub>2</sub>), 82.0 (CH<sub>2</sub>), 171.9; TLC: *R<sub>f</sub>* = 0.36 (18:1 dichloromethane/methanol); HRESIMS (*m/z*): [M + H]<sup>+</sup> calcd for C<sub>29</sub>H<sub>57</sub>N<sub>4</sub>O<sub>7</sub>, 573.4227; found, 573.4215.

**Scheme 5.1** Synthetic route to complex **5.4**

A solution of the methoxyethyl-functionalized product **5.4a** (99 mg, 0.17 mmol) in concentrated HCl (7.5 mL) was stirred at ambient temperature for 2 h. The reaction mixture was concentrated under reduced pressure, and the resulting residue was dissolved in H<sub>2</sub>O (3 mL) and freeze dried to afford 70 mg (99%) of the ligand for complex **5.4b** as a white solid. <sup>1</sup>H NMR (400 MHz, D<sub>2</sub>O, δ): 2.90–3.22 (m, CH<sub>2</sub>, 8H), 3.26–3.28 (m, CH<sub>3</sub>, 3H), 3.32–3.66 (m, CH<sub>2</sub>, 14H), 3.68–3.76 (m, CH<sub>2</sub>, 2H), 4.17 (s, CH<sub>2</sub>, 2H); <sup>13</sup>C NMR (101 MHz, D<sub>2</sub>O, δ): 49.4 (CH<sub>2</sub>), 49.9 (CH<sub>2</sub>), 52.4 (CH<sub>2</sub>), 53.4 (CH<sub>2</sub>), 54.4 (CH<sub>2</sub>), 55.0 (CH<sub>2</sub>), 56.1 (CH<sub>2</sub>), 60.2 (CH<sub>3</sub>), 67.3 (CH<sub>2</sub>), 170.0, 175.6; HRESIMS (*m/z*): [M – H]<sup>–</sup> calcd for C<sub>17</sub>H<sub>31</sub>N<sub>4</sub>O<sub>7</sub>, 403.2193; found, 403.2205.

To a solution of the ligand **5.4b** (20 mg, 48 μmol, 1 equiv) in H<sub>2</sub>O (3 mL) was added EuCl<sub>3</sub>·6H<sub>2</sub>O (39.0 mg, 106 μmol, 2.2 equiv), and the resulting reaction mixture was stirred at ambient temperature for 24 h. The pH of the reaction mixture was maintained between 6.9 and 7.1 with dropwise addition of 0.1 M aqueous NH<sub>4</sub>OH. When the pH of the mixture was constant for 24 h it was increased to 12 to precipitate excess Eu<sup>III</sup> as Eu(OH)<sub>3</sub>. The Eu(OH)<sub>3</sub> was removed by filtering through a 0.2 μm filter (Millipore, IC Millex-LG), and the remaining filtrate was freeze dried. The resulting white solid was dialyzed against H<sub>2</sub>O (cellulose ester, 100–500 dalton molecular weight cut off, Spectra/Por Biotech). The entire dialysate volume was changed after 3, 7, and 17 h. After dialysis, the solution inside the membrane was freeze dried to yield 26 mg

(83%) of **5.4** as a white solid. The purity of the product was confirmed by LC–MS (supporting information); HRESIMS ( $m/z$ ):  $[M + H]^+$  calcd for  $C_{17}H_{30}N_4O_7^{151}Eu$ , 553.1317; found 553.1313.

### Luminescence-decay measurements to determine $q'$

Luminescence-decay measurements were performed using a HORIBA Jobin Yvon Fluoromax-4 spectrofluorometer. Solutions of  $Eu(OTf)_3$  (1 mM) as well as each  $Eu^{3+}$  complex **5.1–5.6** were prepared using binary aqueous mixtures as solvents. Cosolvents included tetrahydrofuran (THF), EtOH, MeOH, dimethylsulfoxide (DMSO), acetone, or acetonitrile. Water was used at 1, 2, 3, 4, 5, 6, 7, 8, 9, 10, 20, 30, 40, 50, 60, 70, 80, 90, and 100% (v/v) with each cosolvent for a total of 109 unique solvent systems. This sample preparation was repeated with  $D_2O$  mixtures of THF, ethanol- $d$ , methanol- $d_4$ , DMSO, acetone, and acetonitrile. Prior to dissolving the  $Eu^{III}$ -containing samples in deuterated solvent systems, the samples were repeatedly (3 $\times$ ) dissolved in  $D_2O$  and concentrated to dryness under reduced pressure. The sample preparation was also repeated with DMF/ $H_2O$  and DMF- $d_7$ / $D_2O$  at 1, 3, 5, 9, 20, 60, 90, and 100% (v/v)  $H_2O$  or  $D_2O$ , respectively.

Samples were sealed in cuvettes that were purged with Ar prior to filling. Luminescence-decay measurements were acquired using the excitation ( $\lambda_{ex}$ ) and emission ( $\lambda_{em}$ ) wavelengths listed in **Table 5.22**. All other parameters were kept constant during the luminescence-decay measurements (excitation and emission slit widths (5 nm), flash count (100), initial delay (0.001 ms), maximum delay (2 ms), and delay increment (0.02 ms)). The decay rates ( $\tau^{-1}$ ) were obtained as the slopes of plots of the natural log of luminescence intensity versus time. This

procedure was performed for every solution, and all solutions were independently prepared and measured three to nine times. The resulting mean decay rates have standard errors  $\leq 0.05 \text{ s}^{-1}$ .

**Table 5.21.** Wavelengths ( $\lambda_{\text{ex}}$  and  $\lambda_{\text{em}}$ ) used in the determination of inner-sphere water-coordination numbers.

complex	$\lambda_{\text{ex}}$ (nm)	$\lambda_{\text{em}}$ (nm)
<b>5.1</b>	397	593
<b>5.2</b>	395	595
<b>5.3</b>	395	594
<b>5.4</b>	395	594
<b>5.5</b>	395	592
<b>5.6</b>	394	591
Eu(OTf) <sub>3</sub>	394	591

## CHAPTER SIX

### Adaptations of $^{17}\text{O}$ NMR spectroscopy to the determination of exchange rates of the Ln-based catalytic cycles

#### 6.1 Introduction

This chapter contains an introduction to the properties of  $^{17}\text{O}$  nuclei that is needed to understand a second analytical tool that I adapted to study lanthanide-catalyzed carbon–carbon bond-forming reactions in aqueous systems: variable temperature (VT)  $^{17}\text{O}$  NMR spectroscopy. In this chapter, I also summarize previous research that used  $^{17}\text{O}$  NMR spectroscopy to determine water-exchange rates. Finally, I describe my efforts towards the use of this technique to determine substrate-binding and product-dissociation rates of Ln-based catalytic cycles.

#### 6.2 $^{17}\text{O}$ nuclear properties

Oxygen has three isotopes ( $^{16}\text{O}$ ,  $^{17}\text{O}$ , and  $^{18}\text{O}$ ), but only the  $^{17}\text{O}$  nucleus is NMR active. The  $^{17}\text{O}$  nucleus has a nuclear spin,  $I$ , of  $5/2$  and possesses a quadrupolar magnetic moment ( $Q$ ).<sup>77–78</sup> Because of the asymmetric distribution of electrons around quadrupolar nuclei, electric field gradients are generated. The quadrupolar magnetic moment interacts with these electric field gradients resulting in quadrupolar relaxation. The quadrupolar relaxation rate influences the longitudinal relaxation rate,  $\frac{1}{T_1}$ , which can be determined using **Eq 6.1**, where  $I$  is the nuclear spin,  $\eta$  is the term describing the asymmetry of the electric field,  $Q$  is the quadrupole moment,  $E$  is the electric field gradient,  $\tau_c$  is the rotational correlation time,  $e$  is the charge of the electron, and  $\hbar$  is the reduced Planck constant that is equal to  $h/2\pi$ .<sup>77–78</sup> In solution, electric field gradients



are negligible; hence, quadrupolar relaxation is averaged to zero, and  $^{17}\text{O}$  frequencies are determined by chemical shielding and  $J$ -coupling interactions.<sup>77</sup>

$$\text{Eq 6.1} \quad \frac{1}{T_1} = \frac{3}{40} \frac{2I+3}{I^2(2I-1)} \left( 1 + \frac{\eta^2}{3} \right) \left( \frac{e^2EQ}{\hbar} \right)^2 \tau_c$$

Quadrupolar relaxation causes  $^{17}\text{O}$  signals to be relatively broad with low signal intensity compared to  $^1\text{H}$  and  $^{13}\text{C}$  NMR signals. Moreover, larger molecules with less symmetry produce large quadrupolar moments, and consequently, fast relaxation of quadrupolar nuclei occurs resulting in broad signals.<sup>78</sup> This quadrupolar relaxation coupled with a low natural abundance (0.037%) makes high concentrations (molar) or  $^{17}\text{O}$ -enrichment necessary to acquire spectra with good signal-to-noise ratios. However, there is a wide chemical shift range for  $^{17}\text{O}$ -containing functional groups, and this property is useful to differentiate broad peaks (**Figure 6.1**).<sup>77,79</sup>

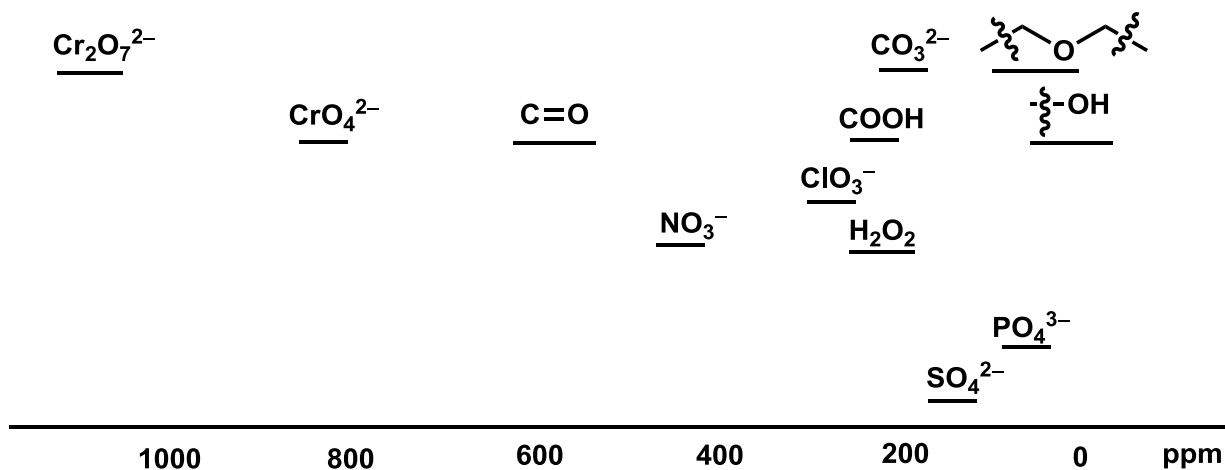


**Figure 6.1** Chemical shift range for  $^{17}\text{O}$  nuclei in different functional groups.<sup>77,79</sup>

Applications of quadrupolar relaxation include the determination of protein hydration dynamics in aqueous medium;<sup>80</sup> the study of hydrogen bonding;<sup>81</sup> the structural determination of oligopeptides and polymers; the study of organic molecules,<sup>81–82</sup> nucleic acids, and amino acids;<sup>81</sup> water mobility and binding studies;<sup>83</sup> the investigation of the hydration of ionic surfactant micelles;<sup>84</sup> and the study of the dynamics of water in electrolyte-containing solutions.<sup>85</sup> In addition to the many applications of  $^{17}\text{O}$  quadrupolar relaxation, the transverse relaxation of  $^{17}\text{O}$  is also coupled with various clinical and biomedical applications as well as structure–function determinations.<sup>86</sup> Because the determination of ligand exchange rates of lanthanide ions related to catalysis was one of my goals, section **6.2.1** gives a brief review of the determination of water-exchange rates in the presence of paramagnetic ions using  $^{17}\text{O}$  transverse relaxation.

### **6.2.1 $^{17}\text{O}$ transverse relaxation in the presence of paramagnetic ions**

Paramagnets have a positive magnetic susceptibility that can change the orientation of the magnetic moment of nearby  $^{17}\text{O}$  nuclei. To determine the effect of paramagnetic ions on the relaxation rate of  $^{17}\text{O}$  in water, Poulson and coworkers measured the line width (width at half height) obtained for  $^{17}\text{O}$  NMR peaks at room temperature with a natural abundance of  $^{17}\text{O}$  in water in solutions containing paramagnetic transition metal ions (**Table 6.1**).<sup>87</sup>

**Table 6.1.** Line widths for  $^{17}\text{O}$  NMR peaks in paramagnetic solutions.<sup>87</sup>

Added substance <sup>a</sup>	concentration (mM)	relative intensity	linewidth (ppm)
no added salt		4.4	12
MnCl <sub>2</sub>	10	2.1	16
CuSO <sub>4</sub>	1	1.4	14
Fe(NO <sub>3</sub> ) <sub>3</sub>	2	2.3	17
Fe(NO <sub>3</sub> ) <sub>3</sub>	4	1.2	28
CoCl <sub>2</sub>	0.1	1.8	20
NiCl <sub>2</sub>	0.01	1.3	25
CrCl <sub>3</sub>	1000	2.0	15

<sup>a</sup> All solutions, except CrCl<sub>3</sub>, contained 10 mM HClO<sub>4</sub>.

Adapted with permission from *J. Chem. Phys.* **1959**, *30*, 759–761; doi: 10.1063/1.1730039.

Copyright 1959, American Institute of Physics.

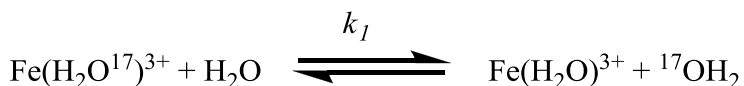
The line broadening that Poulson and coworkers observed for salt solutions relative to water with no added salt is a qualitative indication of an increased transverse relaxation rate in the presence of salts. However, the data in **Table 6.1** show that Cr<sup>3+</sup> salts have a smaller effect on line broadening than other metals. This result was in agreement with Hunt's observations that inner-sphere water molecules of Cr<sup>3+</sup> ions exhibit slow exchange with bulk water.<sup>88</sup> Further, Stover and coworkers assumed that the transverse relaxation of the spin of the  $^{17}\text{O}$  nucleus is influenced by two independent changes: changes of the residency lifetime of the  $^{17}\text{O}$  nucleus at the metal,  $T_{2P}$ , and changes of the relaxation time in the diamagnetic bulk water in the absence of paramagnetic ion,  $T_{2D}$  (**Eq 6.2**).  $T_2$  was calculated using **Eq 6.3**, where  $\Delta\omega$  is the width from peak to peak in the derivative curve.<sup>89</sup> Poulson and coworkers performed simple calculations to

determine the lower limit for water-exchange rates by substituting the value of  $T_2$  obtained from **Eq 6.3** ( $2.0 \times 10^{-3} \text{ s}^{-1}$ ) into **Eq 6.2**. Assuming that  $\text{Fe}^{3+}$  in a 4 mM solution of  $\text{Fe}(\text{NO}_3)_3$  is hexacoordinated, they calculated total concentration of inner-sphere water to be  $6 \times 4 \times 10^{-3}$  mM. Therefore, the  $T_{2P}$  value obtained for a water molecule was determined by dividing total inner-sphere water concentration by 55.5 M bulk water, and calculated  $T_{2P}$  value was  $9 \times 10^{-7} \text{ s}$  ( $[2.0 \times 10^{-3} \times 6 \times 4 \times 10^{-3}]/55.5$ ). The rate constant  $k_1$  for the equilibrium shown in **Scheme 6.1** was determined to be as  $1/T_{2P}$ , which is  $1.1 \times 10^6 \text{ s}^{-1}$ .<sup>87</sup>

$$\text{Eq 6.2} \quad \frac{1}{T_2} = \frac{1}{T_{2D}} + \frac{1}{T_{2P}}$$

$$\text{Eq 6.3} \quad T_2 = \frac{2}{\sqrt{3}\Delta\omega}$$

**Scheme 6.1** The equilibrium for water exchange between bulk and inner-sphere water, where  $k_1$  is the rate constant for water exchange.



Later, Stover and coworkers re-measured this preliminary data, which was obtained using the natural abundance of  $^{17}\text{O}$  in water, using  $^{17}\text{O}$ -enriched water,<sup>89</sup> and the rate constant values,  $k_1$ , obtained from both experiments are shown in **Table 6.2**. The major limitation for these experiments was that only lower limits for the rate constants were obtained. The reason for lower limit determination was the lack of knowledge about the overall relaxation, specifically, whether the speed of water exchange between inner-sphere and outer-sphere or the speed of  $^{17}\text{O}$  nuclear relaxation in the inner-sphere limits overall relaxation.

**Table 6.2** Comparison of  $k_1$  values obtained from samples containing  $^{17}\text{O}$  -enriched water versus natural abundance water.<sup>87,89</sup>

Solution	$k_1 (\text{s}^{-1})^{68}$	$k_1 (\text{s}^{-1})^{71}$
$\text{Cu}(\text{ClO}_4)_2$	$3.3 \times 10^6$	$6 \times 10^6$
$\text{Fe}(\text{ClO}_4)_3$	$2.4 \times 10^4$	$1.1 \times 10^6$
$\text{Mn}(\text{ClO}_4)_2$	$2.2 \times 10^7$	$1 \times 10^7$
$\text{Ni}(\text{ClO}_4)_2$	$3.2 \times 10^4$	$4 \times 10^4$
$\text{Co}(\text{ClO}_4)_2$	$3.1 \times 10^5$	$2 \times 10^5$

To resolve this limitation, Connick and coworkers further studied the rate constants using temperature studies.<sup>90</sup> They considered the experiments done by Bernheim and coworkers to determine the temperature dependence of proton longitudinal and transverse relaxation times in aqueous solutions of paramagnetic ions.<sup>91</sup> Bernheim studied the contributions of dipolar and scalar interactions to  $T_1$  and  $T_2$  relaxation times. In this study, the Bloembergen–Solomon equation was extended to include a temperature term to correlate the dependence of  $T_1$  and  $T_2$  on temperature.<sup>91</sup> Bernheim and coworkers made the assumptions that  $T_1$  is governed by a dipolar mechanism and that  $T_2$  is mainly controlled by a scalar mechanism. With the knowledge of Bernheim's investigations, Connick and coworkers used the apparatus shown in **Figure 6.2** for their temperature studies. Heated air was passed through the coil for the elevated temperature studies (the upper limit was 100 °C), and dry cooled  $\text{N}_2$  was used for low temperature studies (the lower limit was 0 °C).<sup>90</sup>

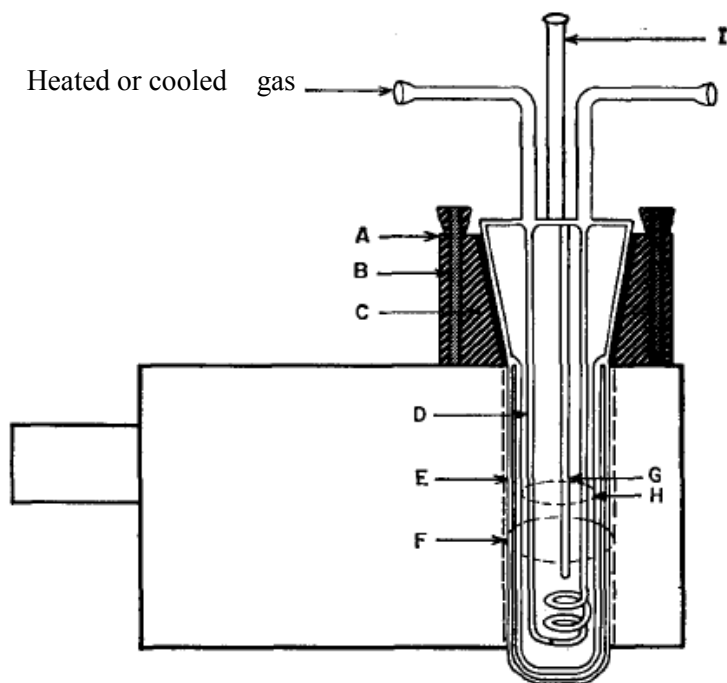


**Figure 6.2** Cross section of the all-glass sample holder employed in the temperature studies, drawn bolted into an NMR probe. The lettered parts are (A) a brass block; (B) a brass bolt welded to the probe; (C) a rubber gasket; (D) a glass coil (2 mm outer diameter); (E) a nonsilvered Dewar; (F) a receiver coil; (G) a thermocouple well; (H) a solution surface; and (I) a orifice for filling and evacuating. Reprinted with permission from *J. Chem. Phys.* **1962**, 37, 307–320; Copyright 1962, American Institute of Physics.

In this study, Connick and coworkers investigated the temperature dependence of  $T_1$  and  $T_2$  for  $^{17}\text{O}$ -enriched water containing  $\text{Mn}^{2+}$ ,  $\text{Fe}^{2+}$ ,  $\text{Co}^{2+}$ ,  $\text{Ni}^{2+}$ , or  $\text{Cu}^{2+}$ .<sup>90</sup> They derived **Eq 6.4** for paramagnetic solutions in water and used this equation to determine the water-exchange rate for the ions in their experiment. In **Eq 6.4**,  $\frac{1}{T_{2r}}$  is equal to  $\left(\frac{1}{T_2} - \frac{1}{T_{2D}}\right)$ ,  $\frac{1}{T_2}$  is the measured  $^{17}\text{O}$

NMR relaxation rate of the paramagnetic solution,  $\frac{1}{T_{2D}}$  is the measured  $^{17}\text{O}$  NMR relaxation rate

of a diamagnetic solution,  $\frac{1}{T_{2r}}$  is the reduced transverse  $^{17}\text{O}$  relaxation rate,  $T_{2m}^{-1}$  is the relaxation rate of the inner-sphere  $^{17}\text{O}$  water molecule, and  $\Delta\omega_m$  is the chemical shift difference between bound water and bulk water.<sup>90</sup>

$$\text{Eq 6.4} \quad \frac{1}{T_{2r}} = \frac{1}{\tau_m} \frac{T_{2m}^{-2} + \tau_m^{-1} T_{2m}^{-1} + \Delta\omega_m^2}{(\tau_m^{-1} + T_{2m}^{-1})^2 + \Delta\omega_m^2}$$

Based on **Eq 6.4**, there are two mechanisms for the relaxation process, in one process  $T_{2m}$  is involved, and in the other process  $\Delta\omega_m$  is involved. Because Connick and coworkers were doing temperature-dependence studies, they derived **Eq 6.5** and **Eq 6.6** to depict the correlations between  $\tau_m$  and temperature and between  $\Delta\omega_m$  and temperature, where  $\Delta H^\ddagger$  and  $\Delta S^\ddagger$  are the enthalpy and entropy for the activation of water exchange between the bulk and the inner-coordination sphere, respectively;  $I$  and  $S$  are the spins of the nucleus of the paramagnetic ion and the electron, respectively;  $\gamma_e$  and  $\gamma_N$  are the gyromagnetic ratios for the nuclei and for the electron, respectively;  $A$  is the Arrhenius constant; and  $k_B$  is the Boltzmann constant.<sup>90</sup>

$$\text{Eq 6.5} \quad \frac{\Delta\omega}{\omega} = \frac{4I(I+1)S(S+1)\gamma_e A}{9k_B T \gamma_N}$$

$$\text{Eq 6.6} \quad \tau_m = \left( \frac{k_B T}{h} \right)^{-1} \exp \left( \frac{\Delta H^\ddagger}{RT} - \frac{\Delta S^\ddagger}{R} \right)$$

**Eqs 6.4–6.6** can be used to determine water-exchange rates, but these equations were derived only for dilute solutions. Fiat and coworkers suggested that to determine the water-exchange rates for solutions containing paramagnetic ions, more concentrated solutions must be used to obtain meaningful data.<sup>92</sup> Fiat's argument was that in the presence of paramagnetic lanthanide ions, larger chemical shifts could be obtained and less line broadening would occur, except for  $\text{Gd}^{3+}$  ions (the relaxation of unpaired electron spins of  $\text{Gd}^{3+}$  is relatively slow).

Therefore, they suggested that the Connik and Swift equations (**Eqs 6.4–6.6**) are inappropriate for water-exchange analysis of lanthanide solutions and derived equations that are applicable to concentrated lanthanide solutions with fast exchange rates.

Fiat and coworkers used spherical cells for the measurements to minimize line broadening due to inhomogeneities of the magnetic field at the edges of solution. Their spherical cell was attached to a sample holder using a glass joint. They measured  $^{17}\text{O}$  line widths for acidified perchlorate solutions containing  $\text{Pr}^{3+}$ ,  $\text{Nd}^{3+}$ ,  $\text{Sm}^{3+}$ ,  $\text{Eu}^{3+}$ ,  $\text{Tb}^{3+}$ ,  $\text{Dy}^{3+}$ ,  $\text{Ho}^{3+}$ ,  $\text{Er}^{3+}$ ,  $\text{Tm}^{3+}$ , or  $\text{Yb}^{3+}$ .<sup>92</sup> After analyzing the correlation between concentration and  $^{17}\text{O}$  line width, they obtained reasonable estimations of water-exchange rates using **Eq 6.7**, where  $n$  is the number of water molecules coordinated to the metal ion and  $C_m$  is the ratio between metal molar concentration,  $c$ , and water concentration, 55.5 ( $C_m = c/55.5$ ).

$$\text{Eq 6.7} \quad \frac{1}{T_{2r}} = \frac{1 - nC_m}{T_{2D}} + \frac{nC_m}{T_{2P}} + (1 - nC_m)^2 nC_m \tau_m \Delta\omega_m^2$$

To minimize the effect of paramagnetic line broadening in concentrated samples, Fiat and coworkers analyzed diamagnetic samples including  $\text{La}^{3+}$ ,  $\text{Lu}^{3+}$ , and  $\text{Y}^{3+}$  at a variety of concentrations (**Figure 6.3**).<sup>92</sup> Because  $\text{Lu}^{3+}$  had the maximum linewidth for a given temperature, smaller ionic radii were suggested to cause more line broadening. To account for the contribution from ionic radius on  $T_2$ , equation **Eq 6.8** was used, where  $r$  is the ionic radius in angstroms.



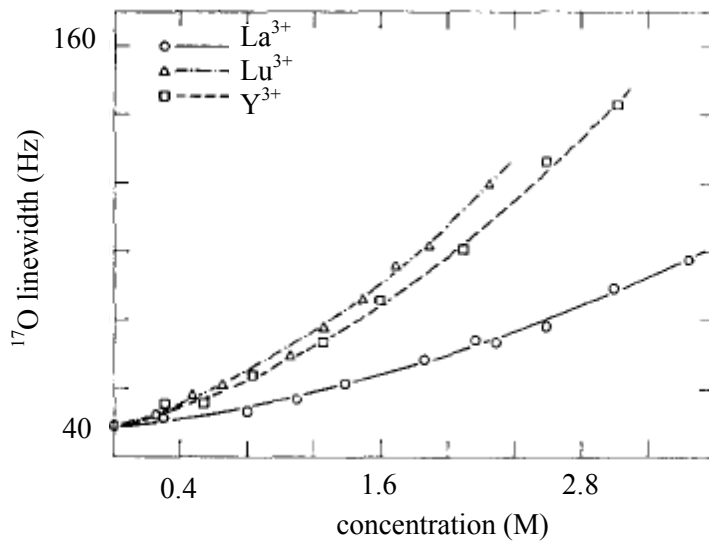


**Figure 6.3** The concentration dependence of the  $^{17}\text{O}$  linewidth in acidified solutions of  $\text{La}^{3+}$ ,  $\text{Lu}^{3+}$ , and  $\text{Y}^{3+}$  perchlorates. Adapted with permission from *J. Chem. Phys.* **1969**, *51*, 4918–4927 ; doi: 10.1063/1.1671884. Copyright 1969 American Institute of Physics.

$$\text{Eq 6.8} \quad \frac{1}{\pi T_2} = 48.6 + 6.60 r^{-4.6} c + 3.59 r^{-4.6} c^2$$

In this investigation of the temperature dependence of the  $^{17}\text{O}$  linewidth, results were normalized using **Eq 6.8** to eliminate the effect of ionic radius on linewidth and two temperature regions were observed: a region from 15 to 100 °C with a lower activation energy (2 kcal/mol) and a low temperature region down to about –20 °C with a higher activation energy (10 kcal/mol) (**Figure 6.4**). Fiat and coworkers suggested that linewidth increases with decreasing temperature because exchange rates are slower at lower temperatures; consequently,  $T_2$  is mainly influenced by  $\tau_m$ . Therefore, to determine the effect of  $\tau_m$  on the linewidth, they compared the correlation of temperature and  $^{17}\text{O}$  relaxation rate in pure water, in a diamagnetic lanthanum

perchlorate solution and in paramagnetic solutions. Their results suggest that the effect of  $\tau_m$  on linewidth is negligible.<sup>92</sup>

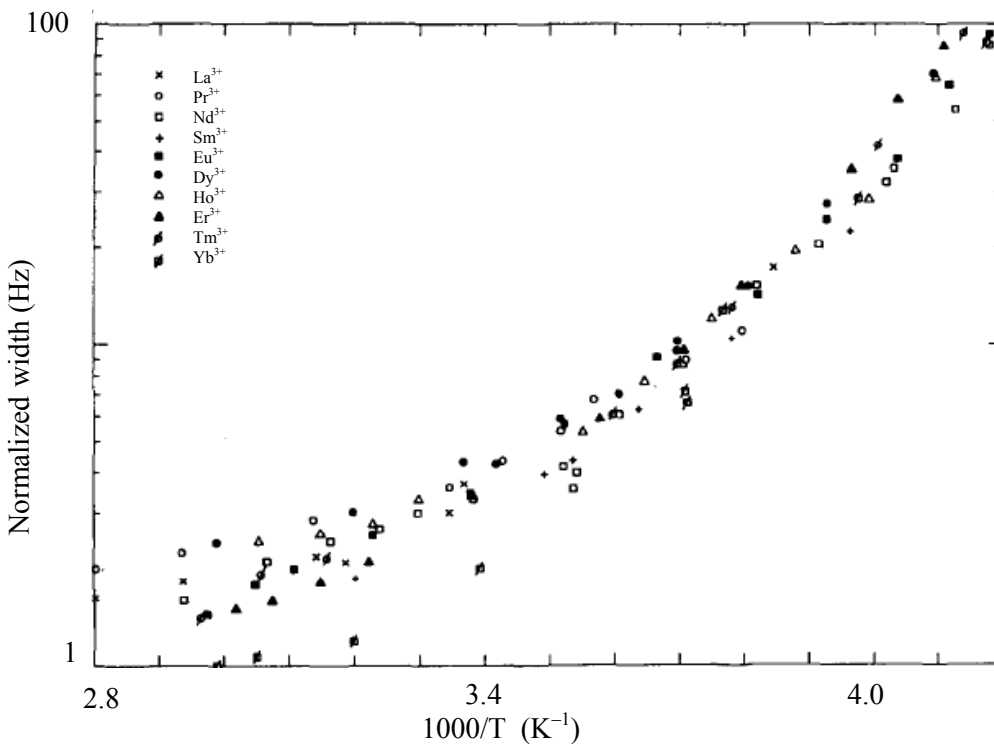


**Figure 6.4** ‘Normalized’  $^{17}\text{O}$  linewidth in perchlorate solutions containing paramagnetic ions versus  $1000/T$ . Adapted with permission from *J. Chem. Phys.* **1969**, *51*, 4918–4927; doi: 10.1063/1.1671884. Copyright 1969, American Institute of Physics.

A ‘microdynamic behavior of water’ model was used to interpret the results in **Figure 6.4** with an assumption that the  $^{17}\text{O}$  quadrupolar coupling constant is temperature independent. According to this model, there is a group of water molecules that are “free” and not hydrogen bonded. These free water molecules need less activation energy for the exchange process at elevated temperatures. The number of free molecules is smaller at low temperature because of increased hydrogen bonding resulting in the observation of higher activation energy at low temperatures.<sup>92</sup>

However, the work done by Fiat and coworkers is limited by the low magnetic field (1.4 T) and the high concentrations necessary to acquire signals with high signal-to-noise ratios. Merbach and coworkers used high field strength magnets, 4.7 and 8.5 T, for VT studies to determine water-exchange rates using less concentrated samples.<sup>93</sup> **Eq 6.4** was modified by adding the outer-sphere contribution to the relaxation,  $\frac{1}{T_{2os}}$  (**Eq 6.9**). In this equation,  $P_m$  is the molar fraction of the bound water  $^{17}\text{O}$  nuclei, and calculations of water-exchange rates were performed using nine for the coordination number of  $\text{Ln}^{3+}$  in dilute perchlorate solutions. Merbach and coworkers determined the water-exchange rates,  $k^{298}$ , for several  $\text{Ln}^{3+}$  ions as perchlorate solutions at 298.15 K (**Table 6.3**).<sup>93</sup> A gradual decrease of  $k^{298}$  was observed with decreasing ionic radius, suggesting that an increase of charge density in  $\text{Ln}^{3+}$  ions causes longer water-residency lifetimes. The advantage of using high field strength magnets is that the kinetic contribution to relaxation is maximized. Magnetic inhomogeneity was taken into account by applying a Carr–Purcell pulse sequence.

$$\text{Eq 6.9} \quad \frac{1}{T_{2r}} = \frac{1}{P_m} \left( \frac{1}{T_2} - \frac{1}{T_{2A}} \right) = \frac{1}{\tau_m} \frac{T_{2m}^{-2} + \tau_m^{-1} T_{2m}^{-1} + \Delta\omega_m^2}{(\tau_m^{-1} + T_{2m}^{-1})^2 + \Delta\omega_m^2} + \frac{1}{T_{2os}}$$

**Table 6.3** Calculated water-exchange rates for  $\text{Ln}^{3+}$  perchlorate solutions at 298.15 K.<sup>93</sup>

$\text{Ln}^{3+}$	$k^{298} (\text{s}^{-1})$
Tb <sup>3+</sup>	$5.0 \times 10^8$
Dy <sup>3+</sup>	$3.9 \times 10^8$
Ho <sup>3+</sup>	$1.9 \times 10^8$
Er <sup>3+</sup>	$1.2 \times 10^8$
Tm <sup>3+</sup>	$8.1 \times 10^7$
Yb <sup>3+</sup>	$4.1 \times 10^7$

Later, Merbach and coworkers showed that outer-sphere contributions to water-exchange rate are negligible by using a control complex with no inner-sphere water molecules,  $\text{Gd}[(\text{TETA})]^-$  ( $\text{TETA}^{4-} = 1,4,8,11\text{-tetraazacyclotetradecane-}N,N',N'',N'''\text{-tetraacetate}$ ).<sup>94</sup> They measured  $1/T_1$  and  $1/T_{2A}$  as a function of temperature for  $\text{Gd}[(\text{TETA})]^-$  and compared their results with the data obtained for  $\text{Gd}^{3+}$ -containing complexes with one inner-sphere water molecule;  $[\text{Gd}(\text{DTPA})(\text{H}_2\text{O})]^{2-}$  and  $[\text{Gd}(\text{DOTA})(\text{H}_2\text{O})]^-$  (**Figure 6.5**).<sup>94</sup> They observed a negligible increase in the transverse relaxation rate for  $\text{Gd}[(\text{TETA})]^-$  and concluded that the outer-sphere contribution to water-exchange rates is negligible.

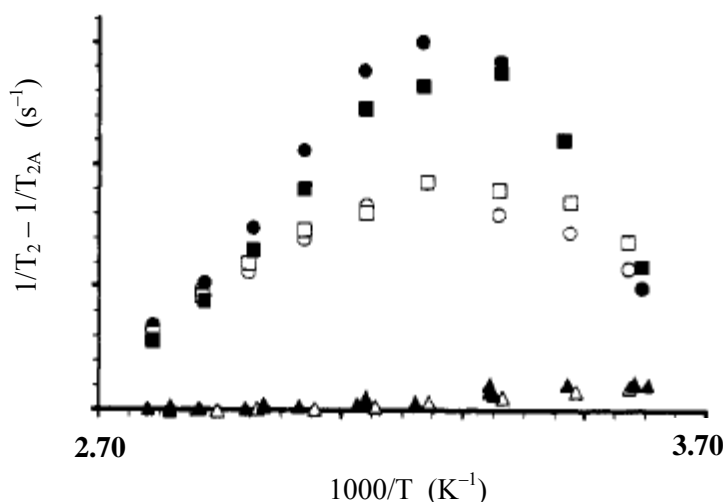


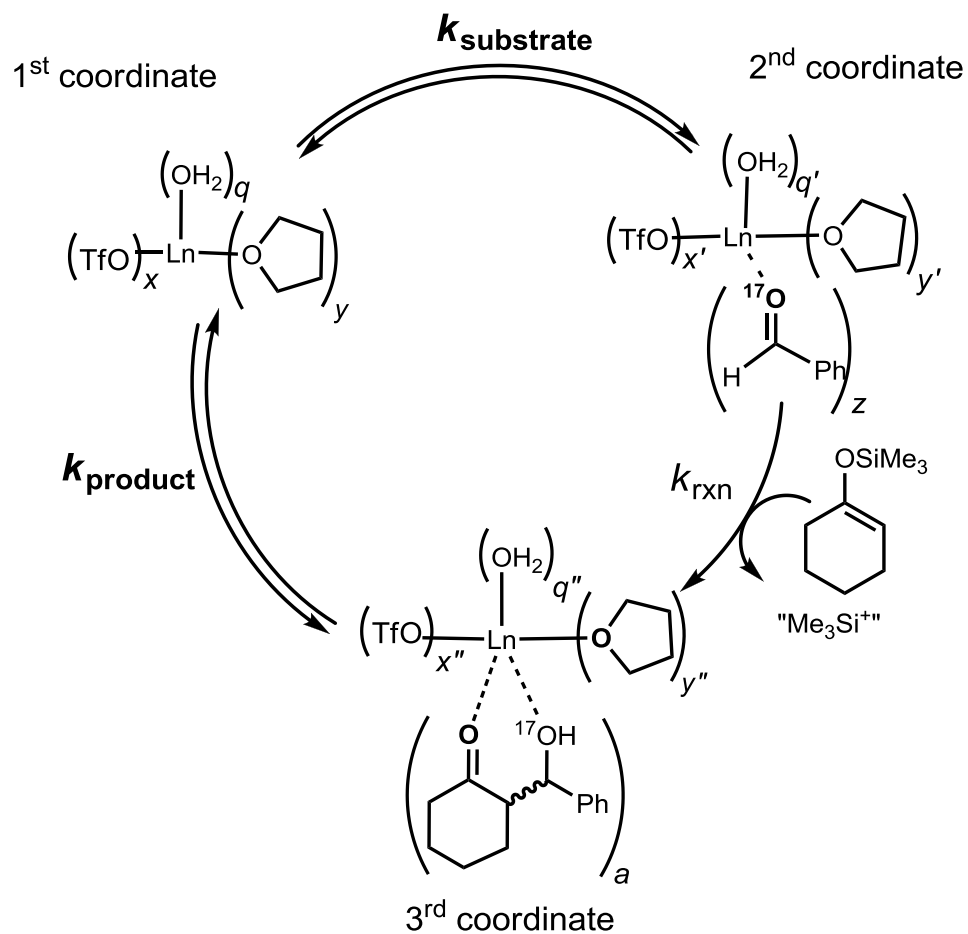
**Figure 6.5** Temperature dependence of  $^{17}\text{O}$  NMR transverse relaxation rates due to the presence of  $[\text{Gd}(\text{DTPA})(\text{H}_2\text{O})]^{2-}$  ( $\bullet$ ,  $\circ$ ),  $[\text{Gd}(\text{DOTA})(\text{H}_2\text{O})]^-$  ( $\blacksquare$ ,  $\square$ ), and  $[\text{Gd}(\text{TETA})]^-$  ( $\blacktriangle$ ,  $\triangle$ ). Filled and open symbols correspond to measurements at 9.4 and 4.7 T, respectively. Adapted with permission from Micskei, K.; Helm, L.; Brücher, E.; Merbach, A. E. *Inorg. Chem.* **1993**, 32, 3844–3850. Copyright 1993 American Chemical Society.

As described throughout the section **6.2.1**, many investigations have been performed to determine accurate water-exchange rates in the presence of paramagnetic lanthanide ions, resulting in the derivation of complex equations such as **Eq 6.9**. In section **6.2.2**, I describe my investigations to adapt VT  $^{17}\text{O}$  NMR measurements to determine exchange rates important to lanthanide catalytic cycles.

### **6.2.2 Determination of substrate- and product-exchange rates of lanthanide catalytic cycles using $^{17}\text{O}$ transverse relaxation.**

As described in the previous section, it is well known that the rate of exchange between an inner-sphere water molecule and bulk water is related to the transverse relaxation rate of  $^{17}\text{O}$  in water, and this value can be estimated using  $^{17}\text{O}$  NMR spectroscopy performed at variable temperatures.<sup>21</sup> Based on this concept, I proposed that substrate exchange rates ( $k_{\text{substate}}$ ) and product dissociation rates ( $k_{\text{product}}$ ) can be studied using  $^{17}\text{O}$  NMR spectroscopy using  $^{17}\text{O}$ -labeled substrates and products (**Scheme 6.2**). Using  $^{17}\text{O}$ -labeled benzaldehyde, I attempted this study for the same Mukaiyama aldol reaction that I studied using luminescence-decay measurements (Chapters 4 and 5, **Scheme 1.1**).

**Scheme 6.2** Simplified catalytic cycle of the Mukaiyama aldol reaction showing rates of exchange between bound and unbound substrate ( $k_{\text{substrate}}$ ) and product ( $k_{\text{product}}$ ).<sup>a</sup>



<sup>a</sup> The subscripts  $a$ ,  $q$ ,  $x$ ,  $y$ , and  $z$  represent the number of 2-(hydroxyphenylmethyl) cyclohexanone, water, triflate, THF, and benzaldehyde ligands, respectively. Charges have been omitted for simplification.

To master the technique of VT  $^{17}\text{O}$  NMR spectroscopy, my initial studies were carried out using  $\text{Gd}[(\text{DOTA})(\text{H}_2\text{O})]^-$ . This complex was chosen because the water-exchange rate ( $k_{\text{ex}}$ ) of the coordinated water molecule is reported in the literature.<sup>21</sup> I measured the  $^{17}\text{O}$  linewidth at half maximum ( $\nu_{1/2}$ ) of  $^{17}\text{OH}_2$  in  $\text{Gd}[(\text{DOTA})(\text{H}_2\text{O})]^-$  (10 mM) in 100% water) with respect to temperature. I used the relationship between the residence life time of the bound water molecule

( $\tau_m$ ) and the spectral linewidth at half maximum to calculate  $\tau_m$  using **Eq 6.10**, and Origin non-linear fitting. In **Eq 6.10**,  $\nu_{1/2}^{agent}$  is the spectral linewidth at half maximum for  $Gd[(DOTA)(H_2O)]^-$ , and I measured this value at 15 temperatures ranging from 5 to 75 °C. In the  $^{17}O$  measurements, an external reference is used, which is a solution of an analogous diamagnetic complex of the same concentration and pH as the paramagnetic sample. For this purpose, I used  $Y^{3+}$  because it is the best choice because of its similar size and charge to  $Gd^{3+}$ . In **Eq 6.10**,  $\nu_{1/2}^{H_2O}$  are the spectral linewidths at half maximum for the reference complex at the same temperatures as  $\nu_{1/2}^{agent}$ . I use the term “reduced transverse ( $R_2$ )  $^{17}O$  relaxation rate” in the rest of this chapter, where  $R_2$  is  $\pi(\nu_{1/2}^{agent} - \nu_{1/2}^{H_2O})$ . In **Eq 6.10**,  $T_{2m}$  is the relaxation time of the bound water, and  $\tau_m$  is the residency life time of the bound water, which can be used to calculate  $k_{ex}$  ( $\tau_m = 1/k_{ex}$ ). For my VT  $^{17}O$  measurements, I used an NMR tube with a coaxial insert that contained a locking solution (**Figure 6.6**). The resulting spectral linewidths at half maximum for  $Gd[(DOTA)(H_2O)]^-$  and  $Y[(DOTA)(H_2O)]^-$  are shown in **Table 6.4**. After reaching a specific temperature, I waited 7–10 min to allow the sample temperature to reach equilibrium. As expected, linewidths increased gradually from 5 to 35 °C and decreased with increasing temperature from 35 to 75 °C. This linewidth pattern is common for  $Ln^{3+}$ -containing complexes with one inner-sphere water molecule.<sup>21</sup>

Eq 6.10

$$\pi(u_{1/2}^{GSE} - u_{1/2}^{H_2O}) = \left( \frac{q[Gd]}{[H_2O]} \right) \left\{ \left( \frac{S(S+1)}{3} \right) \left( \frac{A}{\hbar} \right)^2 \right\}^{-1} \left[ \left( \frac{k_{ex}^{298} T}{298.15} e^{\left[ \frac{\Delta H}{R} \left( \frac{1}{298.15} - \frac{1}{T} \right) \right]} \right) + \left( \frac{1}{T_{le}^{298}} e^{\left( \frac{\Delta E_{ex}}{R} \left( \frac{1}{T} - \frac{1}{298.15} \right) \right)} \right) + \left( \frac{k_{ex}^{298} T}{298.15} e^{\left[ \frac{\Delta H}{R} \left( \frac{1}{298.15} - \frac{1}{T} \right) \right]} \right)^{-1} \right]$$



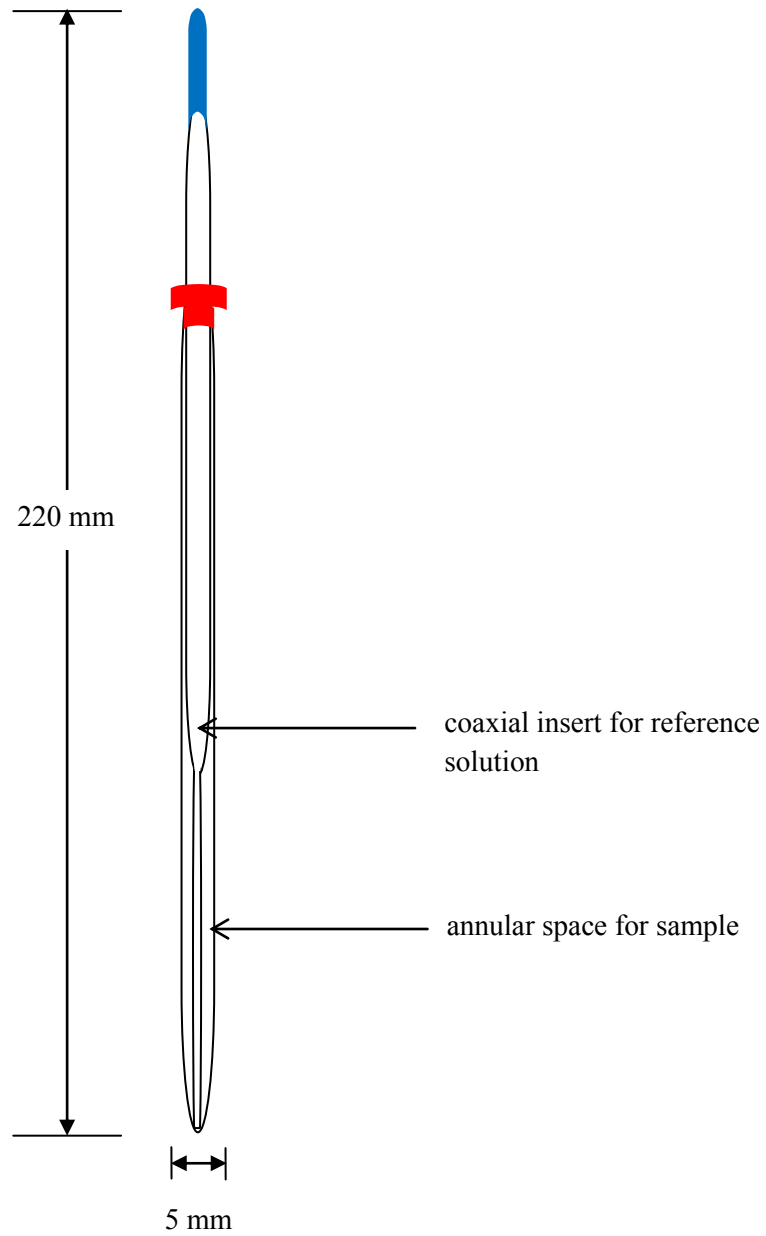


**Figure 6.6** Schematic drawing of an NMR tube with a coaxial insert.

**Table 6.4** Measured  $^{17}\text{O}$  spectral linewidths.

Temperature ( $^{\circ}\text{C}$ )	linewidth			
	Gd(DOTA) $^{-}$ (ppm)	Y(DOTA) $^{-}$ (ppm)	Gd(OTf) $_3$ (ppm)	Y(OTf) $_3$ (ppm)
5	226	87	389	105
10	232	76	368	93
15	243	66	349	79
20	268	58	315	68
25	282	52	277	60
30	291	46	234	51
35	294	42	207	47
40	278	38	175	42
45	254	35	148	37
50	225	32	124	33
55	192	30	103	31
60	156	28	87	28
65	132	26	73	25
70	110	25	62	23
75	93	23	54	22

Using my measurements of spectral linewidths at half maximum for Gd(DOTA) $^{-}$  and Y(DOTA) $^{-}$ , I calculated the reduced transverse ( $R_2$ )  $^{17}\text{O}$  relaxation rates. After plotting  $R_2$  versus

temperature as shown in **Figure 6.7**, I determined the  $k_{ex}$  of water for  $Gd[(DOTA)(H_2O)]^-$  to be  $6 \times 10^6 \text{ s}^{-1}$  (literature value:  $4 \times 10^6 \text{ s}^{-1}$ ).<sup>21</sup> I then analyzed  $Gd(OTf)_3$  to determine the  $k_{ex}$  of coordinated water molecules and obtained a  $k_{ex}$  value of  $806 \times 10^6 \text{ s}^{-1}$  (literature value:  $804 \times 10^6 \text{ s}^{-1}$ ).<sup>21</sup> The linewidths at half maximum for  $Gd(OTf)_3$  and  $Y(OTf)_3$  decreased with increasing temperature which is common for complexes with more than one inner-sphere water molecule (**Table 6.4**).<sup>21</sup>

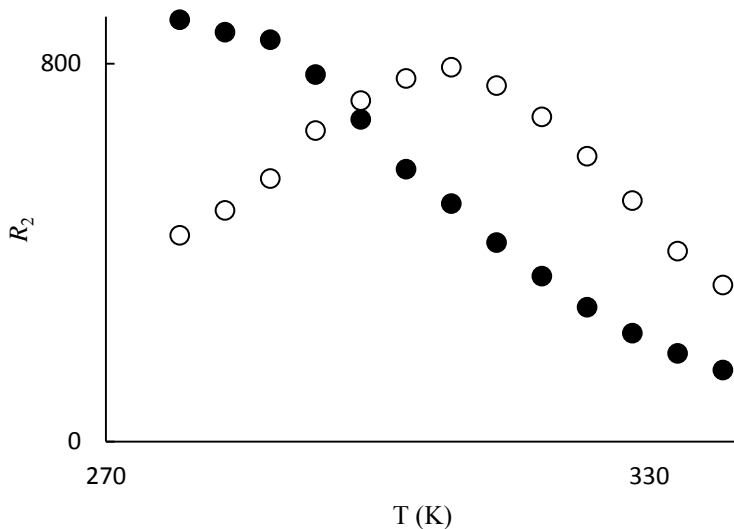


**Figure 6.7** Reduced transverse  $^{17}\text{O}$  relaxation rates versus temperature for  $Gd(DOTA)^-$  ( $\circ$ ) and  $Gd(OTf)_3$  ( $\bullet$ ).

After successfully reproducing exchange rates reported in literature, I attempted to determine the exchange rate  $^{17}\text{O}$ -labeled benzaldehyde ( $k_{\text{substrate}}$ , **Scheme 6.2**) using the VT  $^{17}\text{O}$  NMR spectroscopy. For this determination, I synthesized  $^{17}\text{O}$ -labeled benzaldehyde as described at the end of this chapter.  $^{17}\text{O}$ -labeled benzaldehyde (90 mM) was dissolved in 15%  $\text{H}_2\text{O}$  in THF (v/v) in which 10 mM  $\text{Eu}(OTf)_3$  was present (sample **6.1**, **Figure 6.8**). This sample was used because with  $\text{Eu}(OTf)_3$ , optimal initial reaction rates were observed in 15% water.<sup>57</sup> However,

with this sample, I observed four  $^{17}\text{O}$  peaks (**Figure 6.8**, peaks A, B, C, and D), which were due to the presence of  $^{17}\text{O}$ -labeled benzaldehyde, the natural abundance of  $^{17}\text{O}$  in water, the natural abundance of  $^{17}\text{O}$  in  $\text{D}_2\text{O}$ , and the natural abundance of  $^{17}\text{O}$  in THF. To differentiate these peaks, I prepared a series of samples that separated the components of the mixture in sample **6.1**: sample **6.2** contained water only; sample **6.3** contained water and  $\text{D}_2\text{O}$ ; and sample **6.4** contained water,  $\text{D}_2\text{O}$ , and THF. I identified the  $^{17}\text{OH}_2$  peak by acquiring the spectrum of a sample containing  $^{17}\text{OH}_2$  in the insert and water (sample **6.2**, **Figure 6.9**) in the annular space. For this sample, I observed a peak for  $^{17}\text{OH}_2$  that I referenced to zero. By replacing water in annular space with  $\text{D}_2\text{O}$ , I prepared sample **6.3** (**Figure 6.9**). The introduction of  $\text{D}_2\text{O}$  to the annular space led to the observation of two peaks, and I assigned them as  $^{17}\text{OD}_2$  and  $^{17}\text{OH}_2$ . Sample **6.4** (not shown) was prepared by adding THF and  $^{17}\text{OH}_2$  to the annular space, and this sample was used to assign the  $^{17}\text{O}$ -THF peak (3.38 ppm). The chemical shift that I obtained for  $^{17}\text{O}$ -benzaldehyde peak (563 ppm) was comparable to the literature value (564 ppm).<sup>77</sup>

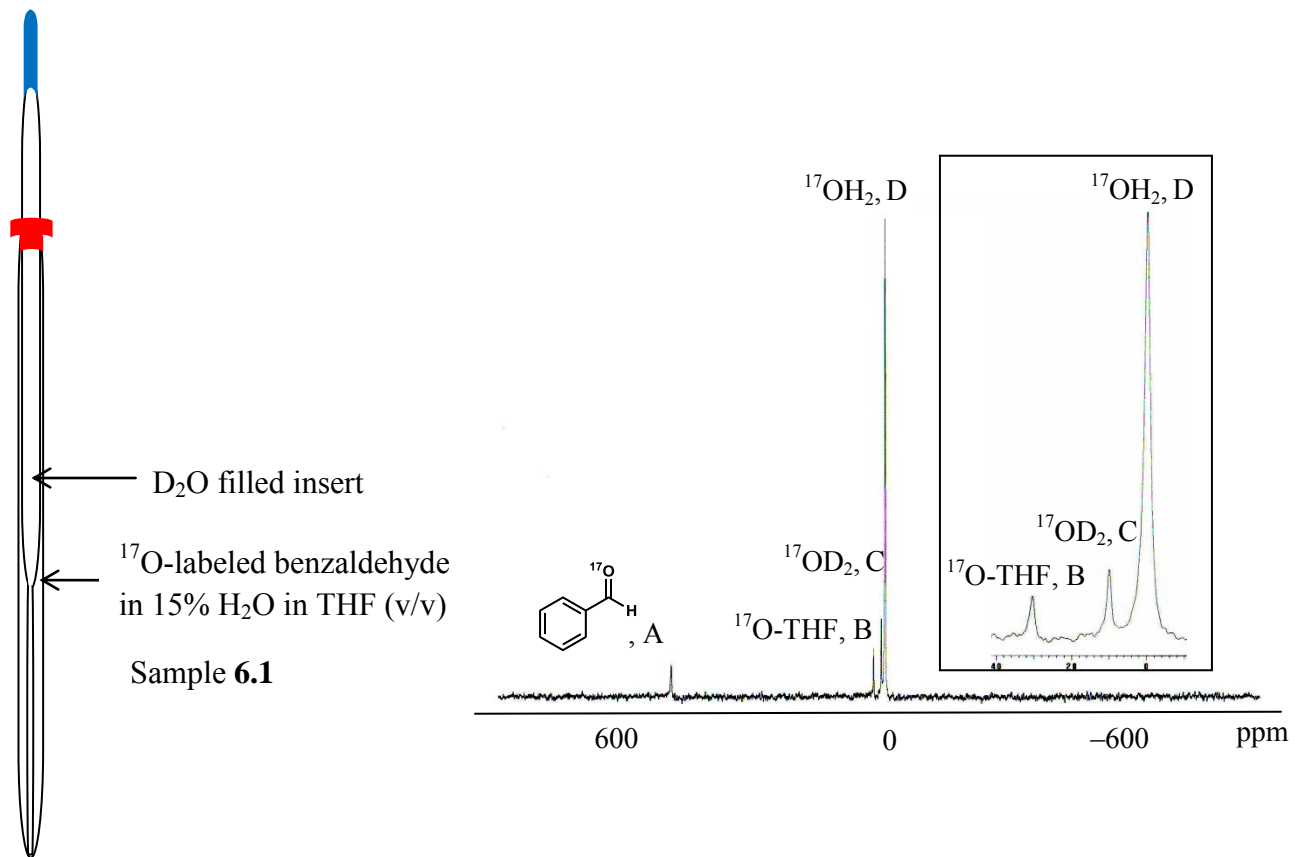


**Figure 6.8** (Left) Schematic drawing of an NMR tube containing sample **6.1**; (Right) <sup>17</sup>O NMR spectrum obtained for solution **6.1** where the insert shows portion of the spectrum that contains peaks B, C, and D.

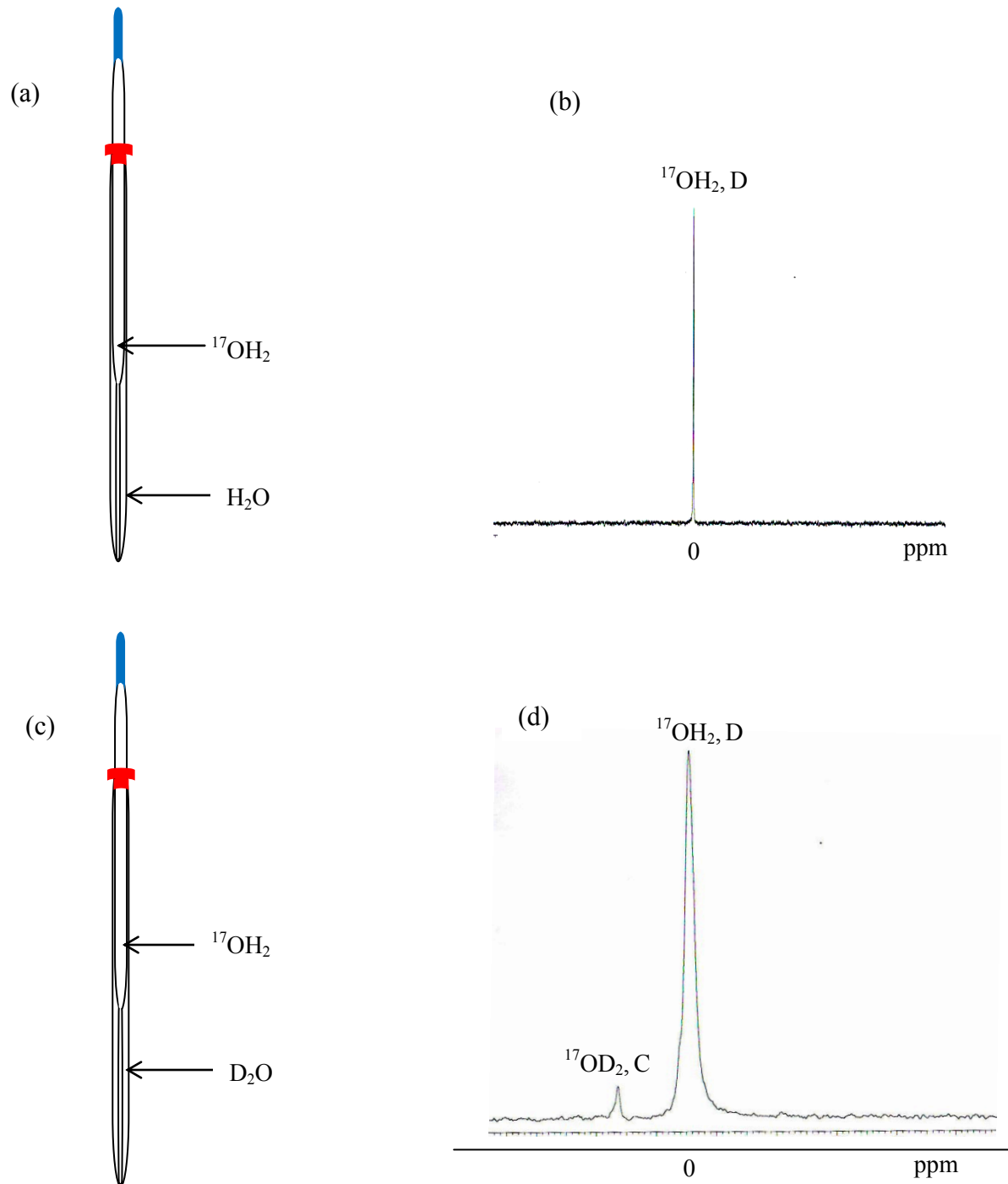


**Figure 6.9** (a) Schematic of an NMR tube containing sample **6.2** (water only), (b)  $^{17}\text{O}$  NMR spectrum obtained for sample **6.1**, (c) schematic of an NMR tube containing sample **6.3** (water and  $\text{D}_2\text{O}$  only), (d)  $^{17}\text{O}$  NMR spectrum obtained for sample **6.2**. The letters C and D correspond to the peak labels in **Figure 6.8**.

After assigning  $^{17}\text{O}$  NMR peaks, I performed VT- $^{17}\text{O}$  NMR experiments with sample **6.1** at temperatures ranging from 15 to 55 °C. The maximum temperature was 55 °C to avoid boiling of the water–THF binary solvent system. I did not perform experiments below 15 °C to avoid freezing the solution. Compared to the results shown in **Table 6.4** for  $^{17}\text{O}$ -labeled benzaldehyde in 15%  $\text{H}_2\text{O}$  in THF (v/v) containing 10 mM  $\text{Eu}(\text{OTf})_3$ , the observed linewidths at halfmax for the peak from  $^{17}\text{O}$ -labeled benzaldehyde did not consistently increase or decrease as a function of temperature (**Figure 6.10**). These observations led me to consider of the possible equilibria in the sample (**Scheme 6.3**):

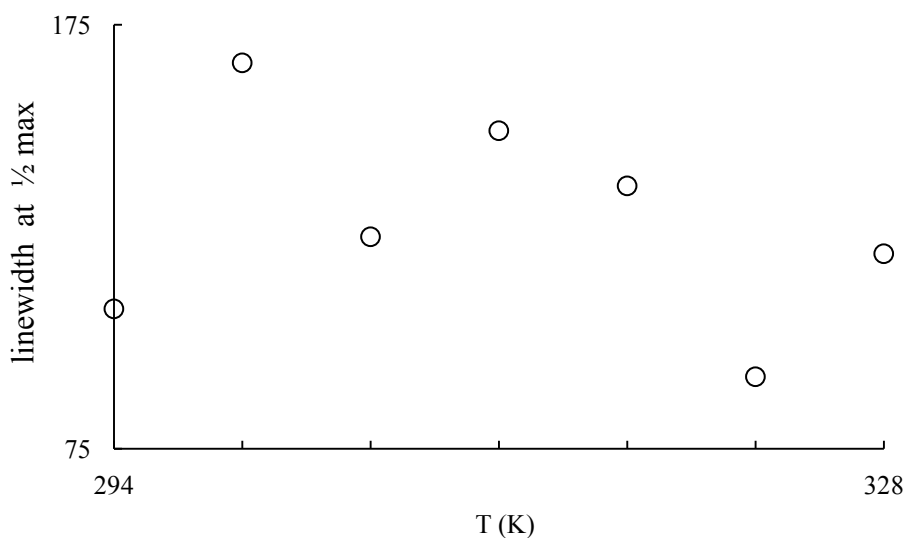
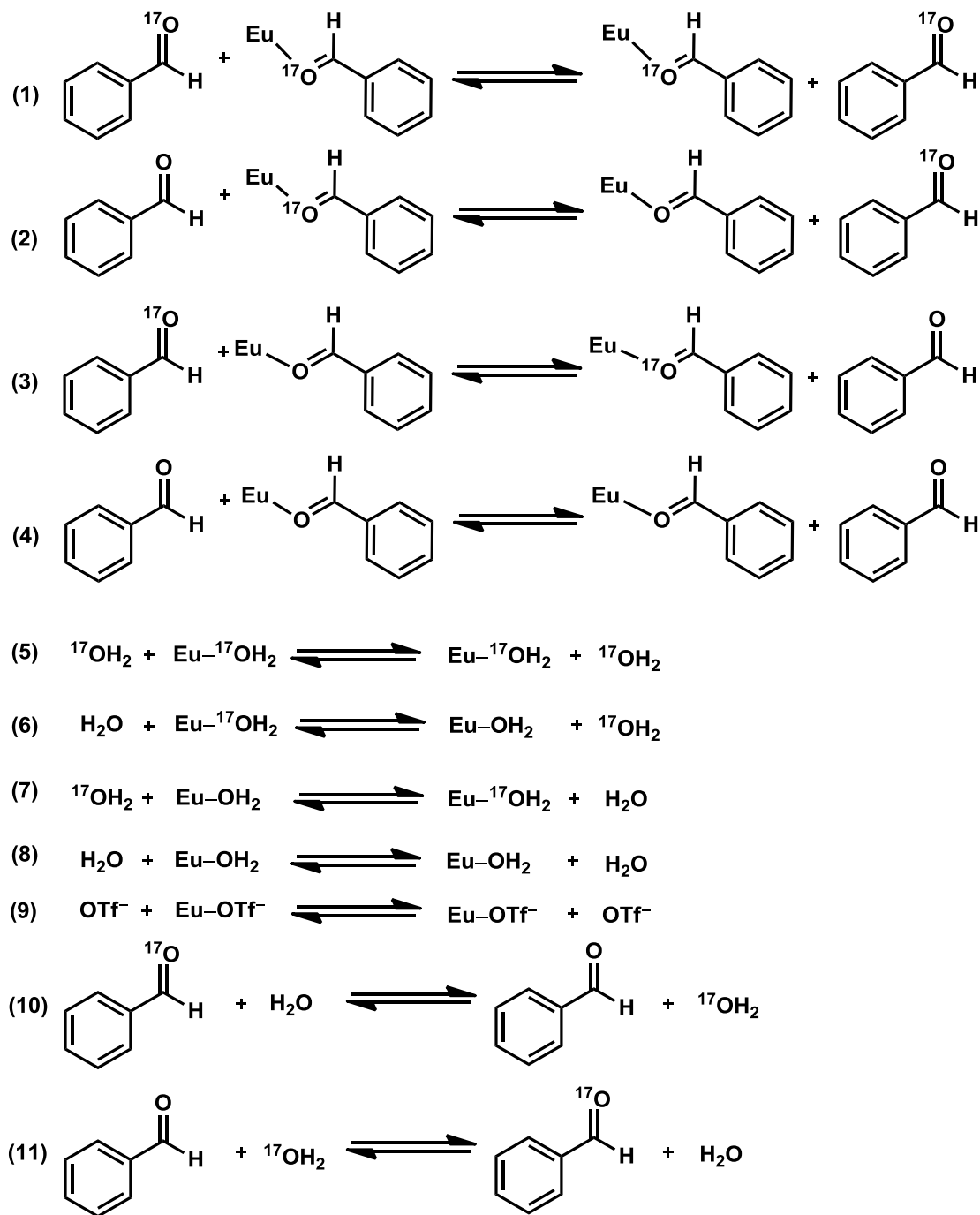


**Figure 6.10** Observed linewidths for the  $^{17}\text{O}$ -labeled benzaldehyde peak in sample **6.1** plotted as a function of temperature.

**Scheme 6.3** Possible equilibria in a solution of  $^{17}\text{O}$ -labeled benzaldehyde in 15%  $\text{H}_2\text{O}$  in THF (v/v) containing 10 mM  $\text{Eu}(\text{OTf})_3$ . Charges have been omitted for simplicity. Oxygen atoms not labeled as  $^{17}\text{O}$  represent  $^{16}\text{O}$ .





To deconvolute the complicated system depicted in **Scheme 6.3**, I simplified the system by isolating equilibrium involving only  $\text{Eu}^{3+}$  and water. I did this by performing  $^{17}\text{O}$  NMR spectroscopy on a solution of 100% water containing  $\text{Eu}(\text{OTf})_3$  (10 mM). For this sample, I observed decreasing linewidths with increasing temperature increments for  $^{17}\text{OH}_2$  linewidths (similar to the linewidth pattern that I observed for  $\text{Gd}(\text{OTf})_3$  in 100% water shown in **Table 6.4**). Surprisingly, upon addition of THF (5–95% v/v) I observed a random fluctuation of linewidth for all  $^{17}\text{O}$  peaks (similar to **Figure 6.10**). This observation of an inconsistent linewidth pattern for the  $\text{H}_2\text{O}$ –THF binary system, led me replicate the VT experiments, to see if the fluctuations that I observed were within the error of the measurements. With the repetition of VT experiments using the  $\text{H}_2\text{O}$ –THF binary system, I obtained large error bars (**Figure 6.11**), suggesting that the observed fluctuations were due to random errors likely due to the complexity of the several equilibria in the studied system. Further, I investigated other water-miscible binary systems including  $\text{H}_2\text{O}$ – $\text{CH}_3\text{CN}$  and  $\text{H}_2\text{O}$ – $\text{C}_2\text{H}_5\text{OH}$ . In these systems, I observed fluctuating linewidths as a function of temperature for  $\text{H}_2\text{O}$ – $\text{CH}_3\text{CN}$ ; however, for  $\text{H}_2\text{O}$ – $\text{C}_2\text{H}_5\text{OH}$ , I observed a trend of decreasing linewidth with increasing temperature (**Table 6.5**, **Figure 6.11**). The reason for this observation may due to the temperature dependence of formation of a hydrogen-bond network in water–water miscible binary systems. Due to the random linewidths as a function of temperature, I was unable to determine substrate-exchange rates or product-exchange rates for lanthanide-based catalytic cycles in aqueous media.

**Table 6.5** Measured  $^{17}\text{O}$  spectral linewidths.

temperature ( $^{\circ}\text{C}$ )	linewidth (ppm)	
	$^{17}\text{OH}_2$ in $\text{H}_2\text{O}-\text{CH}_3\text{CN}$	$^{17}\text{OH}_2$ in $\text{H}_2\text{O}-\text{C}_2\text{H}_5\text{OH}$
	(10% $\text{H}_2\text{O}$ v/v)	(10% $\text{H}_2\text{O}$ v/v)
21	109	277
25	132	252
30	166	279
35	126	311
40	151	214
45	138	235
50	93	132
55	122	130

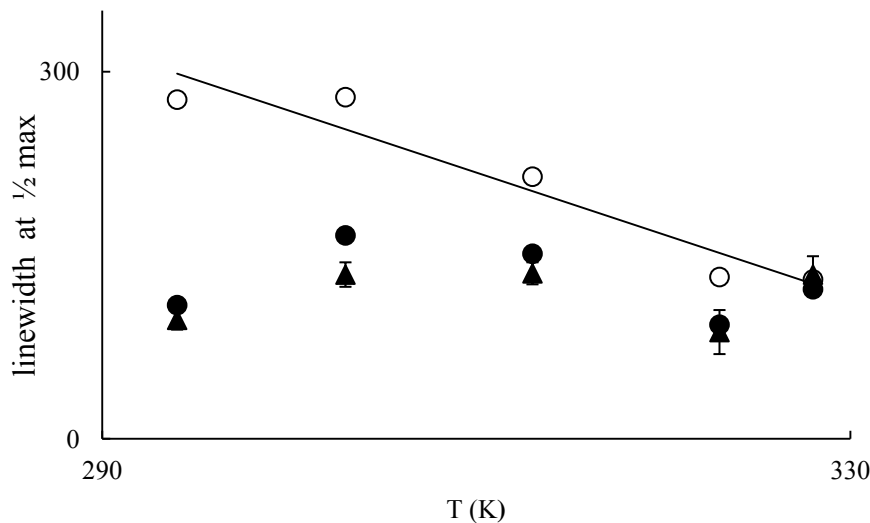


**Figure 6.11** Observed linewidths obtained for  $^{17}\text{OH}_2$  in  $\text{H}_2\text{O}-\text{CH}_3\text{CN}$  (●),  $^{17}\text{OH}_2$  in  $\text{H}_2\text{O}-\text{C}_2\text{H}_5\text{OH}$  (○), and  $^{17}\text{OH}_2$  in  $\text{H}_2\text{O}-\text{THF}$  (▲). Error bars represent the standard error of the measurements for the  $\text{H}_2\text{O}-\text{THF}$  system. Measurements for the  $\text{H}_2\text{O}-\text{CH}_3\text{CN}$  and  $\text{H}_2\text{O}-\text{C}_2\text{H}_5\text{OH}$  systems were not repeated. The regression type for the  $\text{H}_2\text{O}-\text{C}_2\text{H}_5\text{OH}$  system is linear.

### 6.3 Conclusion

This chapter describes the basic properties of  $^{17}\text{O}$  nuclei, investigations regarding its application in various fields of chemistry, biotechnology, and medicinal science, and my attempt to adapt  $^{17}\text{O}$  NMR spectroscopy to determine exchange rates important to catalysis. However, due to the complexity of my samples, I was unable to determine the desired exchange rates. I propose that the solvent interactions with lanthanide ions should be studied in the absence of substrate using  $^{17}\text{O}$  NMR investigations to set a baseline for more complex systems. This suggestion is based on the observation of changes in  $^{17}\text{O}$  chemical shift of a variety of molecules

as a function of solvent composition.<sup>95</sup> Based on my observations with ethanol-containing systems, I think that measurements might be possible at lower temperatures with good hydrogen bonding solvents. I suggest that the information obtained from the following proposed investigations (Part A–F) would be helpful to determine important exchange rates of water-tolerant Ln<sup>3+</sup>-based catalysis:

Part A: Monitor the <sup>17</sup>O chemical shift of OH<sub>2</sub> in commonly used aqueous binary systems, including water–THF, water–acetone, water–acetonitrile, water–DMSO, water–DMF in a range of water percentages (0–100% water v/v).

Part B: Investigate the effect of Eu(OTf)<sub>3</sub> on the <sup>17</sup>O chemical shifts of the solutions mentioned in Part A.

Part C: Repeat Parts A and B using the <sup>1</sup>H and <sup>13</sup>C chemical shifts of solvents to obtain a thorough understanding of the solvent effect on chemical shift.

Part D: Introduce carbonyl-containing functional groups to the solutions of Parts B and C and repeat the same experiments to study the changes in linewidth as a function of temperature.

Part E: Determine the <sup>17</sup>O, <sup>13</sup>C, and <sup>1</sup>H chemical shifts with respect to temperature using VT experiments for binary solvent mixtures.

Part F: Determine the linewidth changes with respect to temperature for neat solvents and for binary solutions using <sup>17</sup>O, <sup>13</sup>C, and <sup>1</sup>H NMR spectroscopy for the samples from Parts A, B, and D.

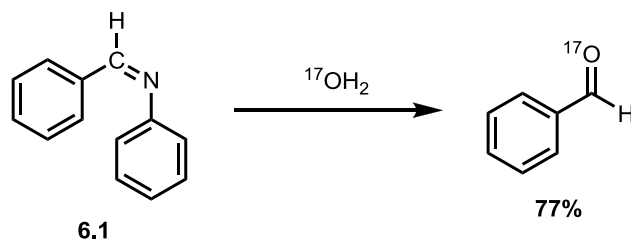
## 6.4 Experimental Section

**Materials.** Commercial chemicals were of reagent-grade purity or better and were used without purification unless otherwise noted. Water was purified using a PURELAB Ultra Mk2 water purification system (ELGA). THF was purified using a solvent purification system (Vacuum Atmospheres Company). Ethanol was distilled from calcium hydride.<sup>73</sup>

**Characterization.** <sup>1</sup>H NMR spectra were obtained using a Varian Mercury 400 (400 MHz) spectrometer, and <sup>13</sup>C NMR spectra were obtained using a Varian Mercury 400 (101 MHz) or a Varian Mercury 500 (125 MHz) spectrometer. VT experiments were done using a Varian Mercury 500 (76.18 MHz) spectrometer. Chemical shifts are reported relative to residual solvent signals unless otherwise noted (CDCl<sub>3</sub>: <sup>1</sup>H: δ 7.27, <sup>13</sup>C: δ 77.23, <sup>17</sup>O: δ of water was set to 0). <sup>1</sup>H NMR data are assumed to be first order with apparent singlets, doublets, and triplets reported as “s”, “d”, and “t”, respectively. Italicized elements are those that are responsible for the shifts. High-resolution electrospray ionization mass spectra (HRESIMS) were obtained on an electrospray time-of-flight high-resolution Waters Micromass LCT Premier XE mass spectrometer.

### Synthesis of <sup>17</sup>O-labeled benzaldehyde (Scheme 6.4):

**Scheme 6.4.** Route used to synthesize <sup>17</sup>O-labeled benzaldehyde.



To a solution of benzylideneaniline **6.1** (181 mg, 1 mmol, 1 equiv) in anhydrous THF (3.5 mL) was added 20% enriched  $^{17}\text{OH}_2$  (22.5  $\mu\text{L}$ , 1.25 mmol, 1.25 equiv). The resulting mixture was stirred at ambient temperature for 30 min and then saturated with anhydrous HCl at ambient temperature until the precipitation of benzylideneanilinium chloride was complete. The reaction mixture was further stirred for 15 min, and anilinium chloride was filtered off using a celite plug. The filtrate was concentrated under a stream of  $\text{N}_2$ . The residue was passed through a silica gel plug using THF as mobile phase and concentrated under a stream of  $\text{N}_2$  to remove the solvent to yield 83 mg (77%) of  $\text{O}^{17}$  labeled benzaldehyde as a light yellow liquid.  $^1\text{H}$  NMR (400 MHz,  $\text{CDCl}_3$ ,  $\delta$ ): 7.48–7.54 (t, CH, 3H), 7.58–7.64 (t, CH, H), 7.84–7.88(d, CH, 2H), 10.00(s, HC=O, 1H);  $^{13}\text{C}$  NMR (101 MHz,  $\text{CDCl}_3$ ,  $\delta$ ): 129.1 (CH), 129.9 (CH), 134.6 (CH), 136.6 (CH), 192.6 (HC=O);  $^{17}\text{O}$  NMR (76.18 MHz,  $\text{CDCl}_3$ ,  $\delta$ ): 563 ppm; HRESIMS ( $m/z$ ):  $[\text{M} + \text{H}]^+$  calcd for  $\text{C}_7\text{H}_6^{17}\text{O}$ , 108.0539; found, 108.0527.

## Summary of Findings

I demonstrated the applicability of luminescence-decay measurements as a dynamic tool that is useful in mechanistic studies of water-tolerant lanthanide-based catalytic systems. Using this technique, I demonstrated that the inner-coordination sphere of solvated  $\text{Ln}^{3+}$  ions is dependent on the coordination properties (denticity of the ligand), leaving group ability of the counter anion, water-saturation level of the  $\text{Ln}^{3+}$ , composition of the surrounding medium, and the solubilizing properties of the surrounding medium.

With luminescence-decay measurements, I was able to determine equilibrium constants. Furthermore, I obtained structural information using these measurements that led to a hypothesis of a mechanism for potent chiral precatalysts for carbon-carbon bond-forming reactions in aqueous media.

My use of luminescence-decay measurements to probe the coordination environment of europium-based precatalysts in solution enabled the study of the influence of precatalyst coordination environment on reaction yield. I expect these results to be useful in the design of new precatalysts for aqueous, enantioselective, lanthanide-catalyzed bond-forming reactions.

To increase the impact of my findings, I investigated variations of inner- and outer-sphere dynamics with respect to commonly used organic solvents. I empirically derived equations that enable fast and accurate determination of the water-coordination number of lanthanides in synthetically useful binary solvent systems. This determination is important to understand the dynamics of the inner- and outer-sphere environments of  $\text{Ln}^{3+}$ -based precatalysts in aqueous solvent mixtures that can enable the easy acquisition of mechanistic and structural information regarding water-tolerant catalysts. This work opens a gateway for the study of any lanthanide-catalyzed reactions and is a powerful tool for catalyst design.

Finally, I attempted to adapt  $^{17}\text{O}$  NMR spectroscopy to determine exchange rates important to catalysis. However, due to the complexity of my samples, I could not determine the desired exchange rates. I propose that the solvent interactions with lanthanide ions should be studied in the absence of substrate using  $^{17}\text{O}$  NMR investigations to set a baseline for more complex systems.



## Future Outlook

Water-tolerant lanthanide-based Lewis acid catalysts are of great interest in organic synthesis because they can catalyze a wide range of important carbon–carbon and carbon–heteroatom bond-forming reactions such as the aldol, nitro-aldol, Mannich, Diels–Alder, Michael, Mukaiyama aldol, and Friedel–Crafts reactions. The compatibility with water, ease of handling, reusability, and low cost of these catalysts have attracted tremendous interest despite the mechanism of the catalysis in aqueous systems being poorly understood. Specifically, identification of the active catalytic species and understanding its interactions with reactants and products are of paramount importance.

I adapted powerful analytical tools including luminescence-decay measurements and  $^{17}\text{O}$  NMR spectroscopy to study of the dynamic behavior of the inner-sphere composition and reaction rates of lanthanide-based precatalysts. Through my studies, the scientific community is able to gain mechanistic insight with respect to the influence of counter ion coordination, the effect of solvent coordination, and the identification of intermediates in lanthanide-based catalytic cycles in aqueous media. This knowledge should aid in the design of more powerful catalysts with respect to enantioselectivity and substrate scope.

For the past four years, I have focused on the Mukaiyama aldol reaction as a starting point for the luminescence-decay studies of counter anion displacement, of the influence of binary solutions, and of the structure–activity relationships of chiral lanthanide complexes. However, other carbon–carbon bond-forming transformations including the aldol, nitro-aldol, Mannich, Michael, Diels–Alder, and Friedel–Crafts reactions, which are catalyzed by water-tolerant lanthanide catalysts could be investigated using luminescence-decay studies with respect

to inner-sphere composition, the identification of intermediates in lanthanide-based catalytic cycles. These studies would help to determine the differences in reaction mechanisms in the presence of water relative to under anhydrous conditions.

Moreover, because my studies used the phosphorescence-decay mode on our spectrofluorometer, my studies cannot be reproduced on every spectrofluorometer because this is not a standard method. However, it is known that the lifetime of  $^5D_0$  excited state of  $Eu^{3+}$  can be directly calculated using the information obtained from the emission spectra of lanthanides.<sup>96</sup> Knowing the fact that the excited-state lifetime of a lanthanide is inversely proportional to its decay rate (either in protic or deuterated media), the steady state fluorescence studies could be used to gain the similar information obtained using luminescence-decay measurements. Using steady state fluorescence studies, the contribution from each transition to the total emission which is influenced by the change of coordination environment (electric dipole transitions) of lanthanide ion, which is known as the branching ratio, can be calculated. The area of the peak due to an individual transition is divided by the total area of the emission spectrum to calculate the branching ratio. Interestingly, because the quantum yield of  $Eu^{3+}$  emission is independent of the initially populated excited state, specific transitions (for example,  $^7F_0 \rightarrow ^5D_0$ ) are not necessary; hence, instead of a laser source, commonly used flash lamps (Xe lamps) can be used to determine the branching ratio.<sup>96</sup> With the use of the relative contribution from each transition to total emission, the lifetime of  $^5D_0$  excited state of  $Eu^{3+}$  can be calculated using equations from Judd–Oflet theory.<sup>96</sup> Further, information regarding the excited-state lifetime of lanthanide ions other than  $Eu^{3+}$  can be obtained using the absorption spectra that relate to known luminescent transitions. The results obtained using steady state fluorescence studies would be an analytical

tool that can be more widely used for the study of the inner-sphere composition of lanthanide-based precatalysts.

In addition to luminescence-based studies, there is exciting areas of research that include  $^{17}\text{O}$  NMR spectroscopy. In my adaptations of  $^{17}\text{O}$  NMR spectroscopy with variable temperature studies, I was unable to determine  $^{17}\text{O}$ -labeled benzaldehyde exchange rates because of the complexity of the  $\text{H}_2\text{O}$ –THF binary system that resulted in high fluctuations in the observed linewidths. However, for the  $\text{H}_2\text{O}$ – $\text{C}_2\text{H}_5\text{OH}$  system, linewidth fluctuations were small. Therefore, I hypothesize that the linewidth data with higher precision can be obtained in hydrogen-bonding solvents, like ethanol, compared to non-hydrogen-bonding solvents, like THF. Consequently, I expect that  $^{17}\text{O}$  linewidth studies in hydrogen-bonding binary solvents can be performed as a function of temperature to obtain the  $^{17}\text{O}$ -labeled benzaldehyde exchange rates that I was unable to obtain in THF. However due to the reaction between  $^{17}\text{O}$  present in  $^{17}\text{O}$ -labeled benzaldehyde and water, the concentration of  $^{17}\text{O}$ -labeled benzaldehyde may change with time. Based on my observations, I hypothesized that if  $^{17}\text{OH}_2$  is pre-added to the solution there will be less opportunity to the loss of  $^{17}\text{O}$ -labeled benzaldehyde. For my preliminary studies, I obtained  $^{17}\text{O}$  spectra for three samples with  $^{17}\text{OH}_2$  (5, 15, and 30  $\mu\text{L}$ ) added to  $^{17}\text{O}$ -labeled benzaldehyde (90 mM) in 15%  $\text{H}_2\text{O}$  in THF (v/v) containing 10 mM  $\text{Eu}(\text{OTf})_3$ . I measured the linewidth for the peak from  $^{17}\text{O}$ -labeled benzaldehyde at 22  $^\circ\text{C}$ , 10 min and 24 h after the addition of  $^{17}\text{OH}_2$ . I obtained constant linewidths for  $^{17}\text{O}$ -labeled benzaldehyde peaks in all the samples, suggesting that the  $^{17}\text{O}$ -labeled benzaldehyde concentration did not change in the studied time period. Using these preliminary observations, I suggest that hydrogen-bonding binary solvents with optimized benzaldehyde concentration, where the  $^{17}\text{O}$ -labeled benzaldehyde concentration is not changing, can be used to obtain  $^{17}\text{O}$ -labeled substance exchange rates.

Apart from exchange studies, direct information on solute-solvent interactions can be obtained using  $^{17}\text{O}$  NMR studies.<sup>95</sup> Although this technique is not used widely relative to  $^{13}\text{C}$  NMR due to low natural abundance and relatively high cost of  $^{17}\text{O}$ -labeled substances,  $^{17}\text{O}$ 's sensitivity is higher, and the synthesis of  $^{17}\text{O}$ -enriched substances is generally trivial. Further, due to its quadrupole moment,  $^{17}\text{O}$  relaxes fast (ms), therefore, with a rapid pulse, thousands of scans can be collected using less time relative to acquiring  $^{13}\text{C}$  spectrum. Investigations into changes in chemical shift of  $^{17}\text{O}$ -enriched substance, in commonly used binary solvent systems can be used to study effect of solvent, temperature, and solvent concentration  $^{17}\text{O}$  relaxation rate.<sup>95</sup>

**APPENDIX A**

---

<b>Page</b>	<b>Contents</b>
136	Table of Contents
137–140	Tables of $q$ Values
141–144	$^1\text{H}$ and $^{13}\text{C}$ NMR Spectra

---

**Table A1.** Number of H<sub>2</sub>O molecules,  $q$ , coordinated to Eu<sup>3+</sup> for the control complex, **4.3**.

% of solvent composed of H <sub>2</sub> O	$q$
1	0.99
2	1.07
3	1.02
4	1.03
5	1.05
6	1.08
7	1.03
8	1.09
9	1.05
10	1.02
20	1.05
30	1.09
40	1.07
50	1.07
60	1.06
70	1.09
80	1.08
90	1.06
100	1.04

**Table A2.** Number of H<sub>2</sub>O molecules,  $q$ , coordinated to Eu<sup>3+</sup> in the first reaction coordinate of the catalytic cycle.

% of solvent composed of H <sub>2</sub> O	$q$ (mean)	$q$ (standard error)
1	5.08	0.03
2	5.45	0.03
3	7.29	0.04
4	7.27	0.03
5	7.20	0.03
6	7.39	0.03
7	7.38	0.04
8	7.35	0.04
9	7.35	0.02
10	7.55	0.03
20	7.85	0.03
30	7.82	0.03
40	7.79	0.06
50	7.82	0.03
60	7.91	0.03
70	7.95	0.03
80	7.92	0.05
90	8.04	0.03
100	8.28	0.03

**Table A3.** Number of H<sub>2</sub>O molecules,  $q$ , coordinated to Eu<sup>3+</sup> in the second reaction coordinate of the catalytic cycle.

% of solvent composed of H <sub>2</sub> O	$q$ (mean)	$q$ (standard error)
1	5.05	0.03
2	5.33	0.02
3	7.17	0.02
4	7.17	0.03
5	7.02	0.03
6	7.27	0.03
7	7.26	0.02
8	7.21	0.03
9	7.21	0.05
10	7.39	0.03
20	7.51	0.03
30	7.64	0.03
40	7.61	0.04
50	7.61	0.06
60	7.70	0.05
70	7.76	0.03
80	7.73	0.03
90	7.91	0.03
100	8.20*	0.03

\* benzaldehyde was not completely dissolved.

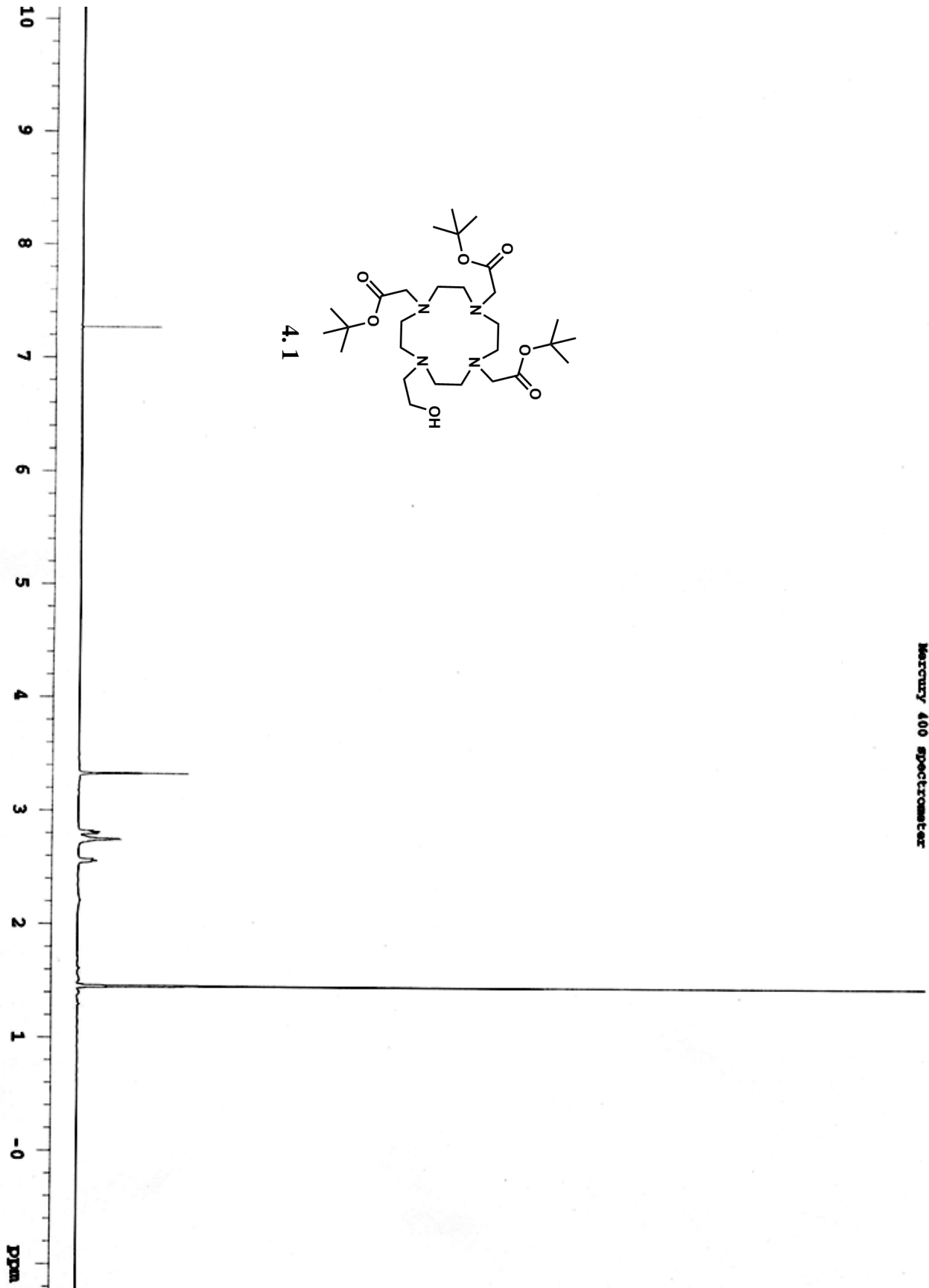


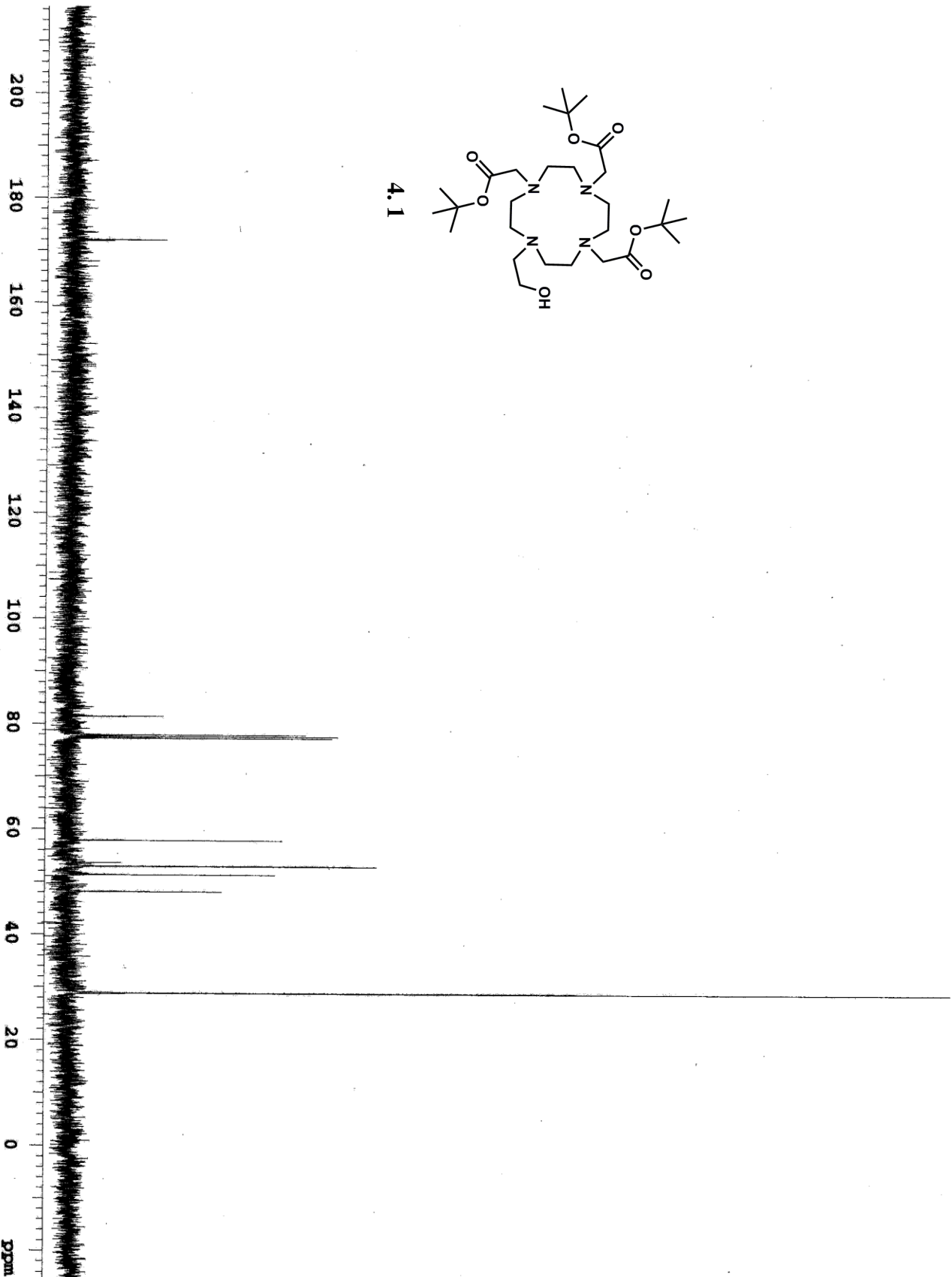
**Table A4.** Number of H<sub>2</sub>O molecules,  $q$ , coordinated to Eu<sup>3+</sup> in the third reaction coordinate of the catalytic cycle.

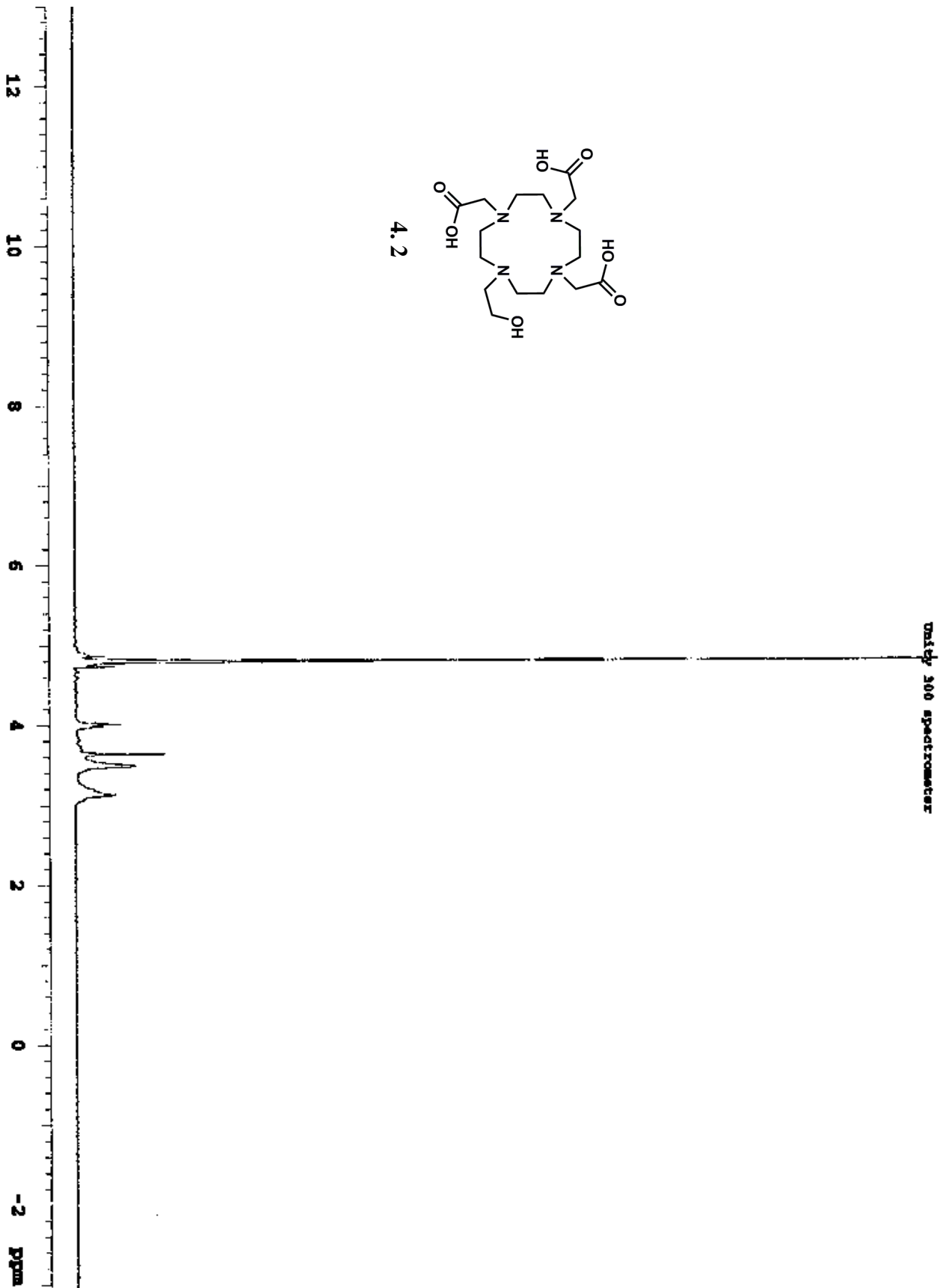
% of solvent composed of H <sub>2</sub> O	$q$ (mean)	$q$ (standard error)
1	5.08	0.03
2	5.45	0.03
3	7.30	0.05
4	7.26	0.07
5	7.20	0.03
6	7.38	0.03
7	7.36	0.03
8	7.35	0.03
9	7.36	0.03
10	7.55	0.03
20	7.79	0.05
30	7.73	0.06
40	7.76	0.03
50	7.79	0.06
60	7.91	0.06
70	7.91	0.03
80	7.91*	0.03
90	8.01*	0.06
100	8.26**	0.05

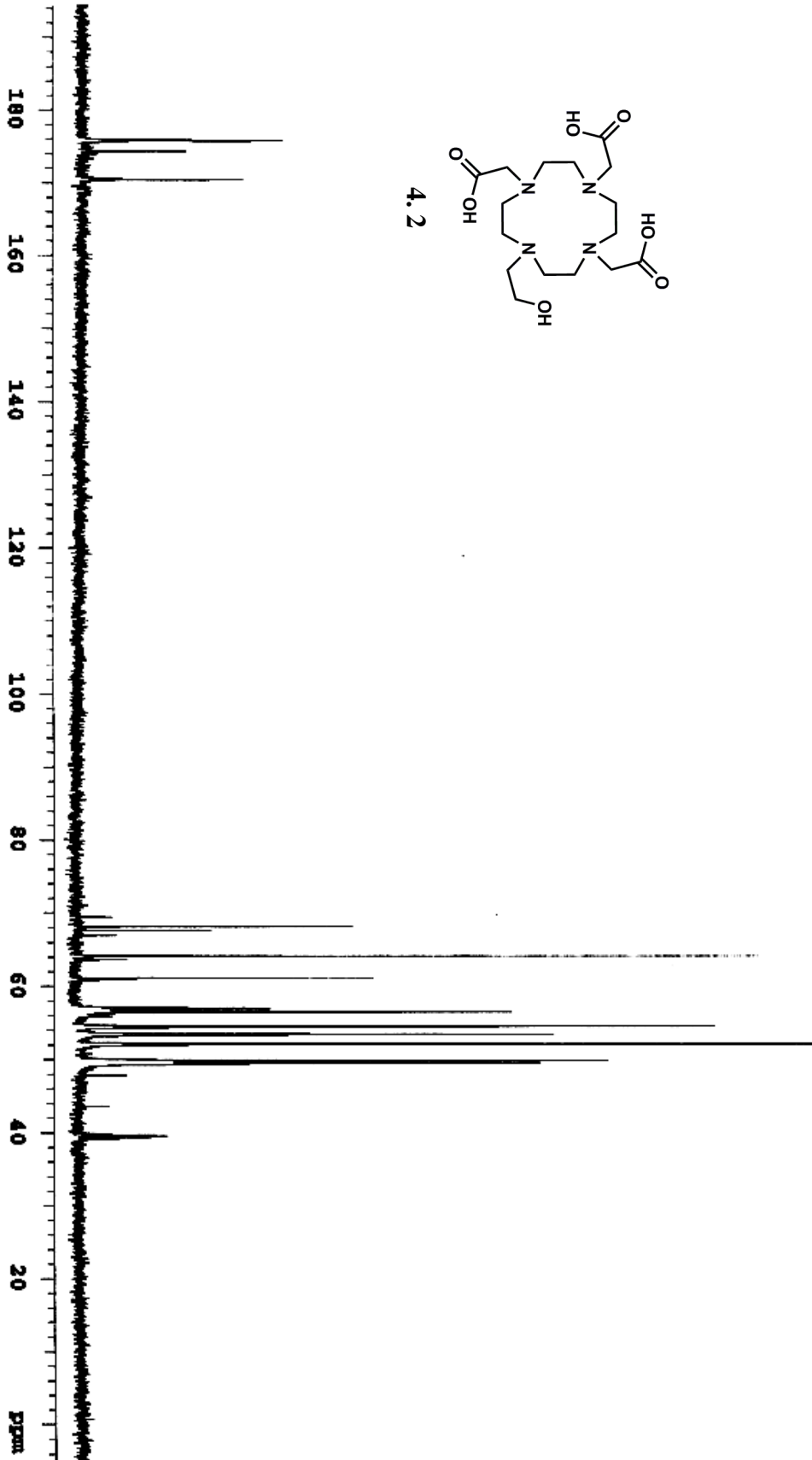
\* Eu<sup>3+</sup>:2-(hydroxyphenylmethyl)cyclohexanone ratio was 1:1.

\*\* Eu<sup>3+</sup>:2-(hydroxyphenylmethyl)cyclohexanone ratio was 1:1, and the solution was sonicated.









Varian 500 MHz spectrometer

## APPENDIX B

---

<b>Page</b>	<b>Contents</b>
145	Table of contents
146–150	Mean $ \tau_H^{-1} - \tau_D^{-1} _s$ values for binary systems
151–155	Calculated $q'$ and $n$ values for binary systems
156–171	$ \tau_H^{-1} - \tau_D^{-1} _m$ versus $q'$ for binary systems
172–173	Intercept verses solvent (%H <sub>2</sub> O v/v) for binary systems

---

**Table B1.** Mean  $|\tau_H^{-1} - \tau_D^{-1}|_{IS}$  values for MeOH and methanol- $d_4$ .

% (v/v) of H <sub>2</sub> O in MeOH or D <sub>2</sub> O in methanol- $d_4$	$ \tau_H^{-1} - \tau_D^{-1} _{IS}$ (ms <sup>-1</sup> )			
	<b>5.3</b> ( $w = 1$ )	<b>5.5</b> ( $w = 2$ )	<b>5.6</b> ( $w = 3$ )	Eu(OTf) <sub>3</sub> ( $w = 9$ )
100	0.76	1.54	2.44	7.49
90	0.76	1.53	1.91	7.21
80	0.74	1.45	1.80	7.08
70	0.74	1.31	1.80	6.88
60	0.76	1.22	1.80	6.62
50	0.68	1.15	1.79	6.41
40	0.67	1.06	1.78	6.19
30	0.67	1.01	1.78	6.07
20	0.72	1.07	1.79	6.06
10	0.71	1.11	1.79	5.96
9	0.72	1.08	1.79	5.86
8	0.77	1.12	1.80	5.76
7	0.83	1.15	1.78	5.70
6	0.81	1.13	1.72	5.68
5	0.72	1.08	1.72	5.30
4	0.72	1.09	1.71	5.33
3	0.72	1.11	1.72	5.25
2	0.71	1.08	1.70	4.90
1	0.70	1.07	1.71	4.67

**Table B2.** Mean  $|\tau_H^{-1} - \tau_D^{-1}|_{IS}$  values for EtOH and ethanol-*d*.

% (v/v) of H <sub>2</sub> O in EtOH or D <sub>2</sub> O in ethanol- <i>d</i>	$ \tau_H^{-1} - \tau_D^{-1} _{IS}$ (ms <sup>-1</sup> )			
	<b>5.3</b> ( <i>w</i> = 1)	<b>5.5</b> ( <i>w</i> = 2)	<b>5.6</b> ( <i>w</i> = 3)	Eu(OTf) <sub>3</sub> ( <i>w</i> = 9)
100	0.80	1.64	2.44	7.49
90	0.73	1.48	2.36	7.22
80	0.73	1.36	2.34	7.14
70	0.68	1.31	2.29	7.00
60	0.70	1.30	2.29	6.98
50	0.66	1.27	2.28	6.94
40	0.68	1.25	2.27	6.81
30	0.69	1.27	2.22	6.76
20	0.66	1.23	2.16	6.52
10	0.62	1.20	2.21	6.31
9	0.63	1.11	2.22	6.17
8	0.74	1.20	2.37	6.27
7	0.71	1.22	2.36	6.27
6	0.75	1.21	2.34	6.29
5	0.65	1.21	2.24	5.98
4	0.65	1.05	2.12	5.46
3	0.67	1.08	1.80	5.13
2	0.66	1.06	1.78	5.05
1	0.65	1.05	1.77	5.05



**Table B3.** Mean  $|\tau_H^{-1} - \tau_D^{-1}|_{IS}$  values for acetone.

% (v/v of H <sub>2</sub> O or D <sub>2</sub> O in acetone)	$ \tau_H^{-1} - \tau_D^{-1} _{IS}$ (ms <sup>-1</sup> )			
	5.3 or 5.4 (w = 1)	5.5 (w = 2)	5.6 (w = 3)	Eu(OTf) <sub>3</sub> (w = 9)
100	0.80 <sup>a</sup>	1.64	2.44	7.49
90	0.75 <sup>a</sup>	1.54	2.47	7.30
80	0.75 <sup>a</sup>	1.51	2.41	7.24
70	0.74 <sup>a</sup>	1.47	2.36	7.21
60	0.75 <sup>a</sup>	1.46	2.32	7.07
50	0.74 <sup>a</sup>	1.44	2.32	6.89
40	0.76 <sup>a</sup>	1.44	2.28	6.68
30	0.73 <sup>a</sup>	1.44	2.24	6.52
20	0.75 <sup>a</sup>	1.43	2.26	6.58
10	0.76 <sup>a</sup>	1.39	2.24	6.59
9	0.76 <sup>a</sup>	1.27	2.20	6.61
8	0.76 <sup>a</sup>	1.19	2.16	6.62
7	0.69 <sup>a</sup>	1.12	2.07	6.51
6	0.68 <sup>a</sup>	1.13	2.06	6.46
5	0.70 <sup>a</sup>	1.10	2.04	6.47
4	nd <sup>b</sup>	nd <sup>b</sup>	nd <sup>b</sup>	nd <sup>b</sup>
3	nd <sup>b</sup>	nd <sup>b</sup>	nd <sup>b</sup>	nd <sup>b</sup>
2	nd <sup>b</sup>	nd <sup>b</sup>	nd <sup>b</sup>	nd <sup>b</sup>
1	nd <sup>b</sup>	nd <sup>b</sup>	nd <sup>b</sup>	nd <sup>b</sup>

<sup>a</sup>complex **3**; <sup>b</sup>not determined because of solubility of complexes **1** and **2**.

**Table B4.** Mean  $|\tau_H^{-1} - \tau_D^{-1}|_{IS}$  values for THF.

% (v/v) of H <sub>2</sub> O or D <sub>2</sub> O in THF	$ \tau_H^{-1} - \tau_D^{-1} _{IS}$ (ms <sup>-1</sup> )			
	<b>5.3</b> ( <i>w</i> = 1)	<b>5.5</b> ( <i>w</i> = 2)	<b>5.6</b> ( <i>w</i> = 3)	Eu(OTf) <sub>3</sub> ( <i>w</i> = 9)
100	0.80 <sup>a</sup>	1.64	2.44	7.49
90	0.80 <sup>a</sup>	1.58	2.36	7.25
80	0.78 <sup>a</sup>	1.58	2.33	7.15
70	0.78 <sup>a</sup>	1.46	2.36	7.18
60	0.79 <sup>a</sup>	1.49	2.34	7.15
50	0.74 <sup>a</sup>	1.35	2.34	7.08
40	0.75 <sup>a</sup>	1.36	2.40	7.06
30	0.74 <sup>a</sup>	1.36	2.43	7.11
20	0.77 <sup>a</sup>	1.38	2.42	7.15
10	0.79 <sup>a</sup>	1.32	2.42	6.92
9	0.75 <sup>a</sup>	1.27	2.35	6.74
8	0.76 <sup>a</sup>	1.33	2.42	6.77
7	0.76 <sup>a</sup>	1.28	2.41	6.80
6	0.78 <sup>a</sup>	1.35	2.47	6.83
5	0.79 <sup>a</sup>	1.32	2.45	6.67
4	nd <sup>b</sup>	nd <sup>b</sup>	nd <sup>b</sup>	nd <sup>b</sup>
3	nd <sup>b</sup>	nd <sup>b</sup>	nd <sup>b</sup>	nd <sup>b</sup>
2	nd <sup>b</sup>	nd <sup>b</sup>	nd <sup>b</sup>	nd <sup>b</sup>
1	nd <sup>b</sup>	nd <sup>b</sup>	nd <sup>b</sup>	nd <sup>b</sup>

<sup>a</sup>complex **5.3**; <sup>b</sup>not determined because of solubility of complexes **5.1** and **5.2**.

**Table B5.** Mean  $|\tau_H^{-1} - \tau_D^{-1}|_{IS}$  values for acetonitrile.

% (v/v) of H <sub>2</sub> O or D <sub>2</sub> O in acetonitrile	$ \tau_H^{-1} - \tau_D^{-1} _{IS}$ (ms <sup>-1</sup> )			
	<b>5.3 or 5.4</b> (w = 1)	<b>5.5</b> (w = 2)	<b>5.6</b> (w = 3)	Eu(OTf) <sub>3</sub> (w = 9)
100	0.80 <sup>a</sup>	1.64	2.44	7.49
90	0.75 <sup>a</sup>	1.49	2.45	7.28
80	0.77 <sup>a</sup>	1.24	2.46	7.21
70	0.76 <sup>a</sup>	1.28	2.44	7.21
60	0.72 <sup>a</sup>	1.20	2.44	7.18
50	0.76 <sup>a</sup>	1.14	2.46	7.18
40	0.75 <sup>a</sup>	1.08	2.43	7.15
30	0.76 <sup>a</sup>	1.09	2.41	7.15
20	0.76 <sup>a</sup>	1.06	2.40	7.13
10	0.81 <sup>a</sup>	0.86	2.40	6.95
9	0.79 <sup>a</sup>	0.87	2.28	6.82
8	0.79 <sup>a</sup>	0.86	2.15	6.67
7	0.76 <sup>a</sup>	0.85	2.12	6.55
6	0.77 <sup>a</sup>	0.87	2.08	6.35
5	0.72 <sup>a</sup>	nd <sup>c</sup>	1.86	6.40
4	0.73 <sup>b</sup>	nd <sup>c</sup>	1.88	6.39
3	nd <sup>c</sup>	nd <sup>c</sup>	nd <sup>c</sup>	nd <sup>c</sup>
2	nd <sup>c</sup>	nd <sup>c</sup>	nd <sup>c</sup>	nd <sup>c</sup>
1	nd <sup>c</sup>	nd <sup>c</sup>	nd <sup>c</sup>	nd <sup>c</sup>

<sup>a</sup>complex 3; <sup>b</sup>complex 4; <sup>c</sup> not determined because of solubility of complexes 1 and 2.

**Table B6.** Mean  $|\tau_H^{-1} - \tau_D^{-1}|_{IS}$  values for DMF and DMF-d<sub>7</sub>.

% (v/v) of H <sub>2</sub> O in DMF or D <sub>2</sub> O in DMF- d <sub>7</sub>	$ \tau_H^{-1} - \tau_D^{-1} _{IS}$ (ms <sup>-1</sup> )			
	<b>5.3</b> (w = 1)	<b>5.5</b> (w = 2)	<b>5.6</b> (w = 3)	Eu(OTf) <sub>3</sub> (w = 9)
100	0.80	1.64	2.44	7.49
90	0.72	1.32	1.78	6.23
60	0.62	0.98	1.32	4.85
20	0.32	0.59	0.96	3.89
9	0.25	0.49	0.85	3.78
5	0.20	0.45	0.86	3.65
3	0.09	0.38	0.53	2.29
1	0.11	0.37	0.54	2.07

**Table B7.** Calculated  $q'$  and  $n$  values for THF binary systems.

% (v/v) of H <sub>2</sub> O or D <sub>2</sub> O in THF	<b>5.3</b> ( $w = 1$ )		<b>5.5</b> ( $w = 2$ )		<b>5.6</b> ( $w = 3$ )		Eu(OTf) <sub>3</sub> ( $w = 9$ )	
	$q'$	$n$	$q'$	$n$	$q'$	$n$	$q'$	$n$
100	0.96	0.00	1.97	0.00	2.95	0.00	9.00	0.00
90	0.96	0.00	1.90	0.07	2.83	0.12	8.71	0.29
80	0.94	0.02	1.89	0.08	2.79	0.16	8.58	0.42
70	0.94	0.02	1.74	0.23	2.83	0.12	8.63	0.37
60	0.95	0.01	1.78	0.19	2.81	0.14	8.59	0.41
50	0.90	0.00	1.63	0.34	2.82	0.13	8.51	0.49
40	0.91	0.00	1.64	0.33	2.89	0.06	8.49	0.51
30	0.89	0.00	1.63	0.34	2.91	0.04	8.53	0.47
20	0.93	0.00	1.67	0.30	2.91	0.04	8.60	0.40
10	0.95	0.01	1.58	0.39	2.90	0.05	8.32	0.68
9	0.90	0.06	1.52	0.45	2.83	0.12	8.10	0.90
8	0.92	0.04	1.59	0.38	2.90	0.05	8.13	0.87
7	0.92	0.04	1.54	0.43	2.91	0.04	8.17	0.83
6	0.94	0.02	1.62	0.35	2.95	0.00	8.21	0.79
5	0.95	0.01	1.59	0.38	2.95	0.00	8.02	0.98
4	nd	nd	nd	nd	nd	nd	nd	nd
3	nd	nd	nd	nd	nd	nd	nd	nd
2	nd	nd	nd	nd	nd	nd	nd	nd
1	nd	nd	nd	nd	nd	nd	nd	nd

nd = not determined

**Table B8.** Calculated  $q'$  and  $n$  values for DMF binary systems.

% (v/v) of H <sub>2</sub> O in DMF or D <sub>2</sub> O in DMF- <i>d</i> <sub>7</sub>	<b>5.3</b> ( $w = 1$ )		<b>5.5</b> ( $w = 2$ )		<b>5.6</b> ( $w = 3$ )		Eu(OTf) <sub>3</sub> ( $w = 9$ )	
	$q'$	$n$	$q'$	$n$	$q'$	$n$	$q'$	$n$
100	0.96	0.00	1.97	0.00	2.95	0.00	9.00	0.00
90	0.87	0.10	1.59	0.38	2.14	0.81	7.50	1.50
60	0.75	0.22	1.18	0.79	1.60	1.35	5.83	3.17
20	0.39	0.58	0.71	1.26	1.16	1.79	4.68	4.32
9	0.31	0.66	0.59	1.38	1.03	1.92	4.55	4.45
5	0.25	0.72	0.55	1.42	1.03	1.92	4.39	4.61
3	0.11	0.86	0.46	1.51	0.64	2.31	2.75	6.25
1	0.13	0.84	0.44	1.53	0.64	2.31	2.48	6.52

**Table B9.** Calculated  $q'$  and  $n$  values for acetonitrile binary systems.

% (v/v) of H <sub>2</sub> O or D <sub>2</sub> O in acetonitrile	<b>5.3</b> ( $w = 1$ )		<b>5.5</b> ( $w = 2$ )		<b>5.6</b> ( $w = 3$ )		Eu(OTf) <sub>3</sub> ( $w = 9$ )	
	$q'$	$n$	$q'$	$n$	$q'$	$n$	$q'$	$n$
100	0.96	0.00	1.80	0.17	2.95	0.00	9.00	0.00
90	0.05	0.05	1.80	0.17	2.94	0.01	8.75	0.25
80	0.03	0.03	1.49	0.48	2.94	0.01	8.66	0.34
70	0.05	0.05	1.54	0.43	2.93	0.02	8.66	0.34
60	0.09	0.09	1.44	0.53	2.94	0.01	8.63	0.37
50	0.05	0.05	1.37	0.60	2.92	0.03	8.63	0.37
40	0.06	0.06	1.30	0.67	2.91	0.04	8.59	0.41
30	0.04	0.04	1.30	0.67	2.89	0.06	8.59	0.41
20	0.04	0.04	1.28	0.69	2.88	0.07	8.56	0.44
10	0.01	0.01	1.03	0.94	2.91	0.04	8.35	0.65
9	0.01	0.01	1.04	0.93	2.74	0.21	8.20	0.80
8	0.00	0.00	1.04	0.93	2.58	0.37	8.01	0.99
7	0.04	0.04	1.02	0.95	2.55	0.40	7.87	1.13
6	0.03	0.03	1.05	0.92	2.50	0.45	7.63	1.37
5	0.09	0.09	nd	nd	2.24	0.71	7.69	1.31
4	0.08	0.08	nd	nd	2.26	0.69	7.68	1.32
3	nd	nd	nd	nd	nd	nd	nd	nd
2	nd	nd	nd	nd	nd	nd	nd	nd
1	nd	nd	nd	nd	nd	nd	nd	nd

nd = not determined

**Table B10.** Calculated  $q'$  and  $n$  values for acetone binary systems.

% (v/v) of H <sub>2</sub> O or D <sub>2</sub> O in acetone	<b>5.3</b> ( $w = 1$ )		<b>5.5</b> ( $w = 2$ )		<b>5.6</b> ( $w = 3$ )		Eu(OTf) <sub>3</sub> ( $w = 9$ )	
	$q'$	$n$	$q'$	$n$	$q'$	$n$	$q'$	$n$
100	0.96	0.00	1.97	0.00	2.95	0.00	9.00	0.00
90	0.89	0.07	1.85	0.12	2.94	0.01	8.77	0.23
80	0.91	0.05	1.82	0.15	2.90	0.05	8.71	0.29
70	0.89	0.07	1.77	0.20	2.83	0.12	8.66	0.34
60	0.90	0.06	1.76	0.21	2.79	0.16	8.50	0.50
50	0.90	0.06	1.74	0.23	2.79	0.16	8.28	0.72
40	0.92	0.04	1.73	0.24	2.74	0.21	8.03	0.97
30	0.88	0.08	1.73	0.24	2.69	0.26	7.84	1.16
20	0.90	0.06	1.72	0.25	2.71	0.24	7.91	1.09
10	0.92	0.04	1.67	0.30	2.69	0.26	7.92	1.08
9	0.92	0.04	1.53	0.44	2.64	0.31	7.95	1.05
8	0.92	0.04	1.43	0.54	2.60	0.35	7.95	1.05
7	0.83	0.13	1.35	0.62	2.49	0.46	7.82	1.18
6	0.82	0.14	1.36	0.61	2.47	0.48	7.77	1.23
5	0.84	0.12	1.32	0.65	2.45	0.50	7.77	1.23
4	nd	nd	nd	nd	nd	nd	nd	nd
3	nd	nd	nd	nd	nd	nd	nd	nd
2	nd	nd	nd	nd	nd	nd	nd	nd
1	nd	nd	nd	nd	nd	nd	nd	nd

nd = not determined

**Table B11.** Calculated  $q'$  and  $n$  values for ethanol binary systems.

% (v/v) of H <sub>2</sub> O in ethanol or D <sub>2</sub> O in ethanol- <i>d</i> )	<b>5.3</b> ( $w = 1$ )		<b>5.5</b> ( $w = 2$ )		<b>5.6</b> ( $w = 3$ )		Eu(OTf) <sub>3</sub> ( $w = 9$ )	
	$q'$	$n$	$q'$	$n$	$q'$	$n$	$q'$	$n$
100	0.96	0.00	1.97	0.00	2.95	0.00	9.00	0.00
90	0.78	0.18	1.57	0.40	2.69	0.26	8.42	0.58
80	0.75	0.21	1.28	0.69	2.63	0.32	8.20	0.80
70	0.63	0.33	1.18	0.80	2.51	0.44	7.87	1.13
60	0.69	0.27	1.13	0.84	2.52	0.43	7.82	1.18
50	0.61	0.35	1.08	0.89	2.51	0.44	7.74	1.26
40	0.65	0.31	1.01	0.96	2.48	0.47	7.43	1.57
30	0.67	0.29	1.08	0.89	2.36	0.59	7.31	1.69
20	0.58	0.38	0.97	1.00	2.21	0.74	6.73	2.27
10	0.50	0.46	0.90	1.07	2.22	0.73	6.23	2.77
9	0.52	0.44	0.70	1.27	2.36	0.59	5.90	3.10
8	0.78	0.18	0.92	1.05	2.72	0.23	6.16	2.84
7	0.72	0.24	0.96	1.01	2.69	0.26	6.16	2.84
6	0.80	0.16	0.92	1.05	2.63	0.32	6.18	2.82
5	0.57	0.39	0.93	1.04	2.41	0.54	5.46	3.54
4	0.58	0.38	0.56	1.41	2.12	0.83	4.21	4.79
3	0.74	0.22	0.69	1.28	1.36	0.59	3.45	8.76
2	0.72	0.24	0.63	1.34	1.31	0.64	3.24	8.82
1	0.69	0.27	0.60	1.37	1.28	0.67	3.24	8.85

**Table B12.** Calculated  $q'$  and  $n$  values for methanol binary systems.

% (v/v) of H <sub>2</sub> O in methanol or D <sub>2</sub> O in methanol- <i>d</i> <sub>4</sub> )	<b>5.3</b> ( $w = 1$ )		<b>5.5</b> ( $w = 2$ )		<b>5.6</b> ( $w = 3$ )		Eu(OTf) <sub>3</sub> ( $w = 9$ )	
	$q'$	$n$	$q'$	$n$	$q'$	$n$	$q'$	$n$
100	0.96	0.00	1.97	0.00	2.95	0.00	9.00	0.00
90	0.90	0.06	1.83	0.14	2.75	0.20	8.69	0.31
80	0.87	0.09	1.73	0.24	2.74	0.21	8.53	0.47
70	0.87	0.09	1.57	0.40	2.75	0.20	8.29	0.71
60	0.90	0.06	1.46	0.51	2.62	0.33	8.23	0.77
50	0.80	0.16	1.38	0.59	2.61	0.34	8.22	0.78
40	0.79	0.17	1.27	0.70	2.48	0.47	8.19	0.81
30	0.79	0.17	1.21	0.76	2.48	0.47	8.05	0.95
20	0.84	0.12	1.28	0.69	2.49	0.46	7.92	1.08
10	0.83	0.13	1.32	0.65	2.49	0.46	7.56	1.44
9	0.84	0.12	1.29	0.68	2.51	0.44	7.44	1.56
8	0.85	0.11	1.34	0.63	2.50	0.45	7.44	1.56
7	0.87	0.09	1.38	0.59	2.60	0.35	7.37	1.63
6	0.85	0.11	1.36	0.61	2.52	0.43	7.35	1.65
5	0.85	0.11	1.30	0.67	2.53	0.42	7.02	1.98
4	0.85	0.11	1.31	0.66	2.40	0.55	6.45	2.55
3	0.85	0.11	1.33	0.64	2.17	0.78	6.36	2.64
2	0.84	0.12	1.30	0.67	2.11	0.84	5.94	3.06
1	0.83	0.13	1.28	0.69	2.08	0.87	5.79	3.21



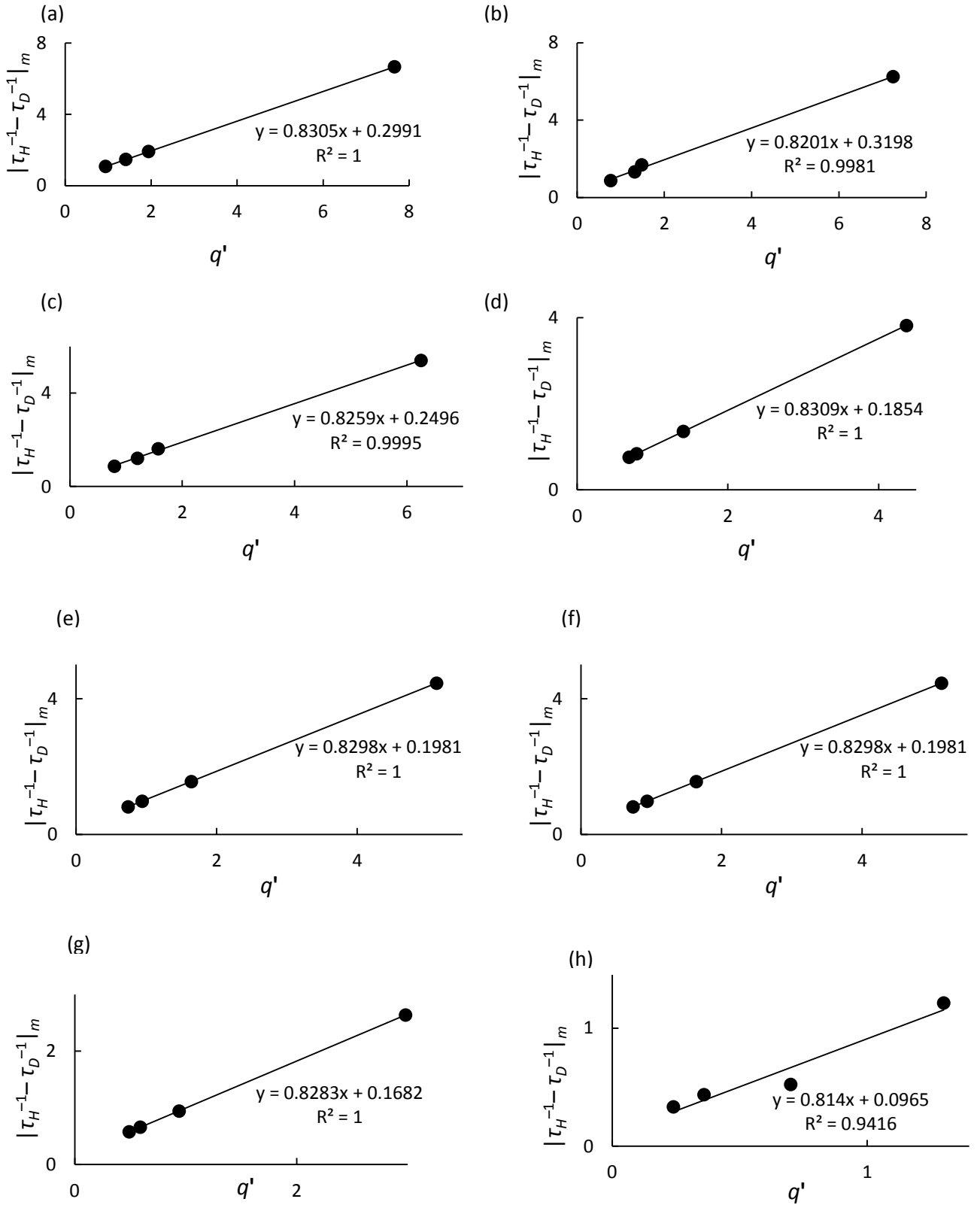


Figure B2. Continued on next page. See next page for caption.

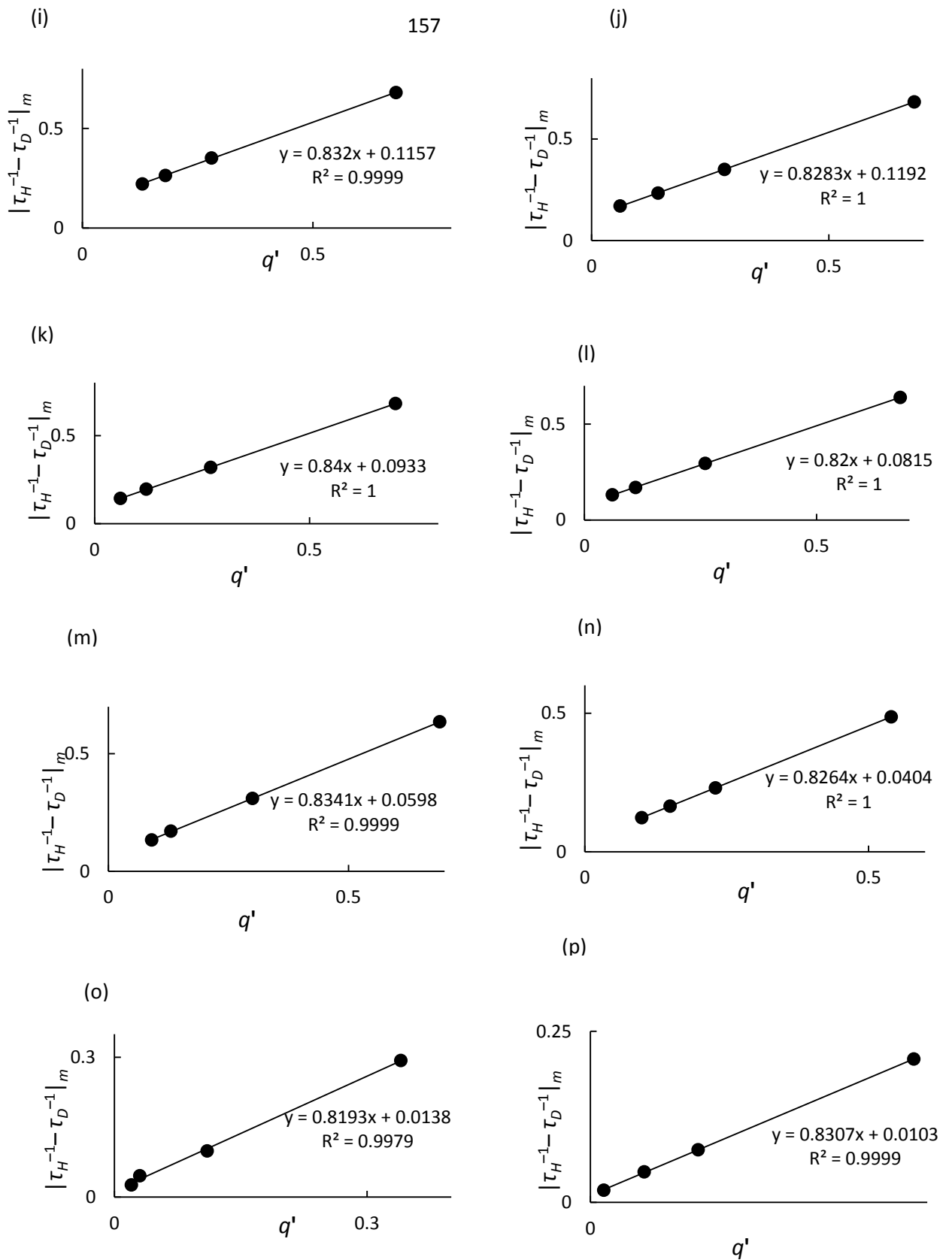
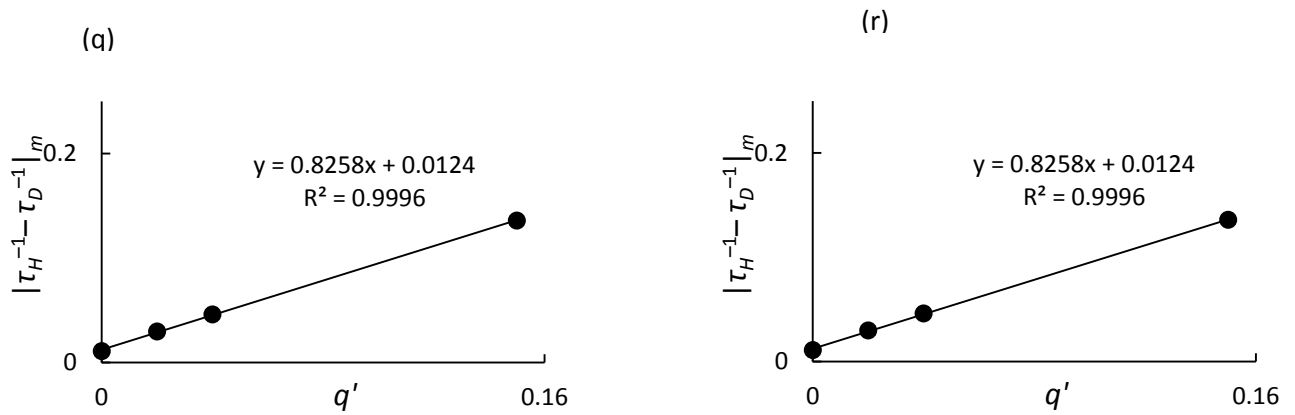


Figure B2. Continued on next page. See next page for caption.



**Figure B2.** Continued from previous page.  $|\tau_H^{-1} - \tau_D^{-1}|_m$  versus  $q'$  for (a) 90%; (b) 80%; (c) 70%; (d) 60%; (e) 50%; (f) 40%; (g) 20%; (i) 10%; (j) 9%; (k) 8%; (l) 7%; (m) 6%; (n) 5%; (o) 4%; (p) 3%; (q) 2%; and (r) 1% H<sub>2</sub>O (v/v) in DMSO.

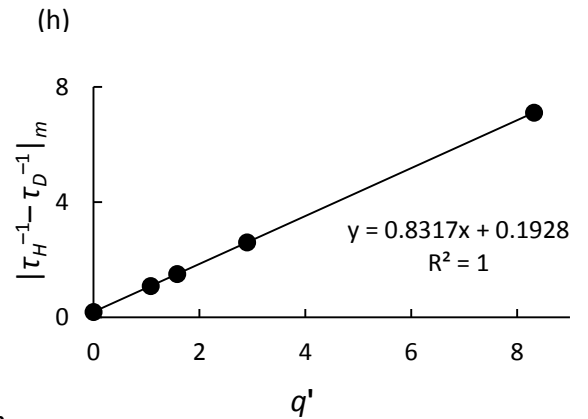
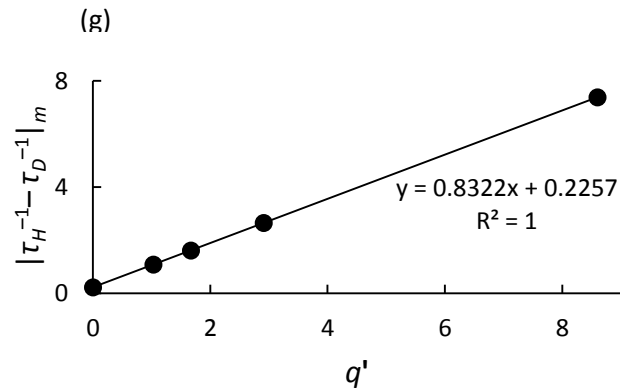
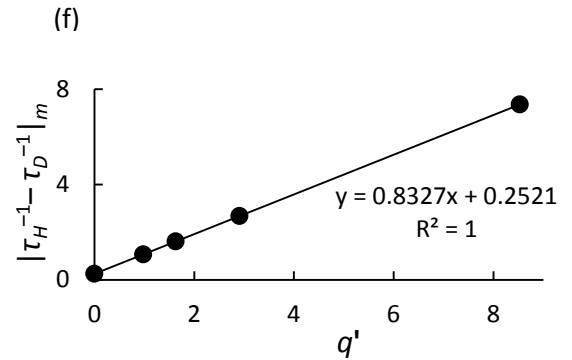
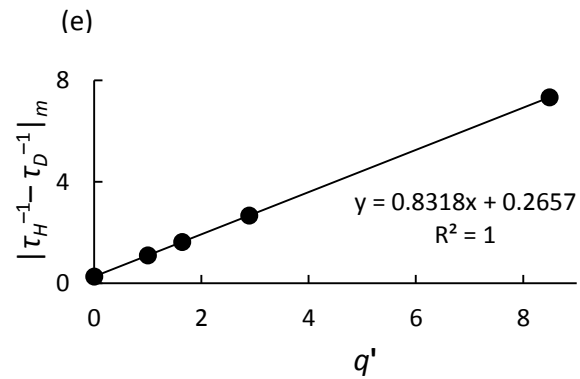
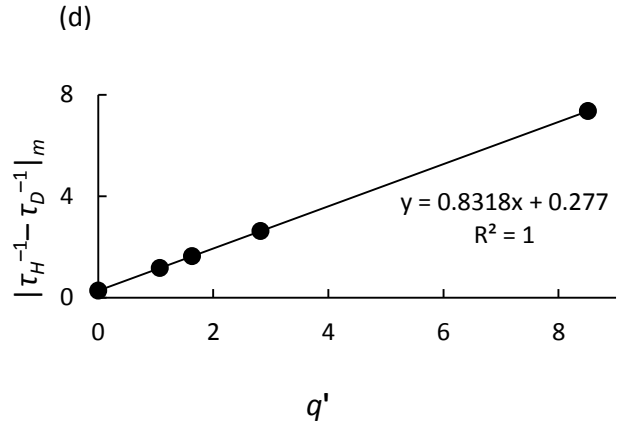
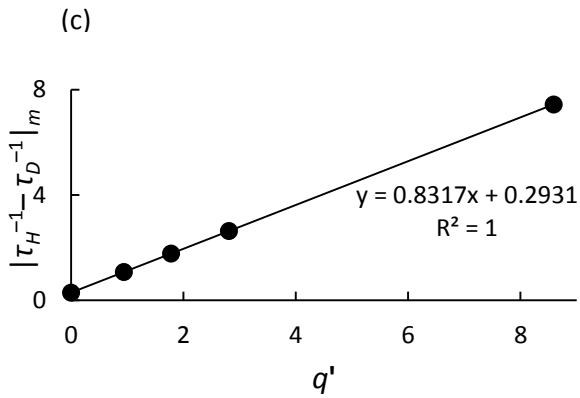
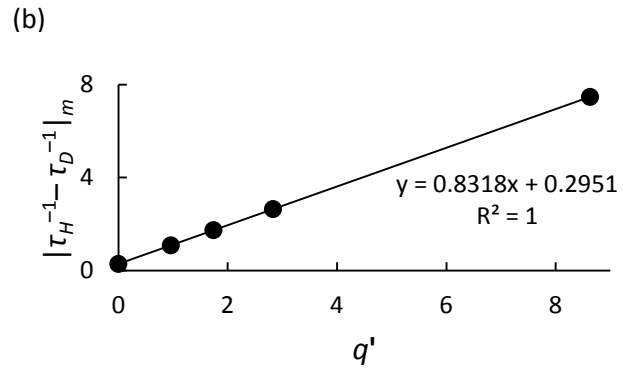
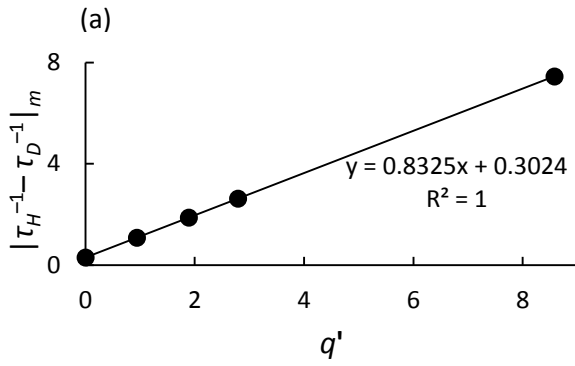
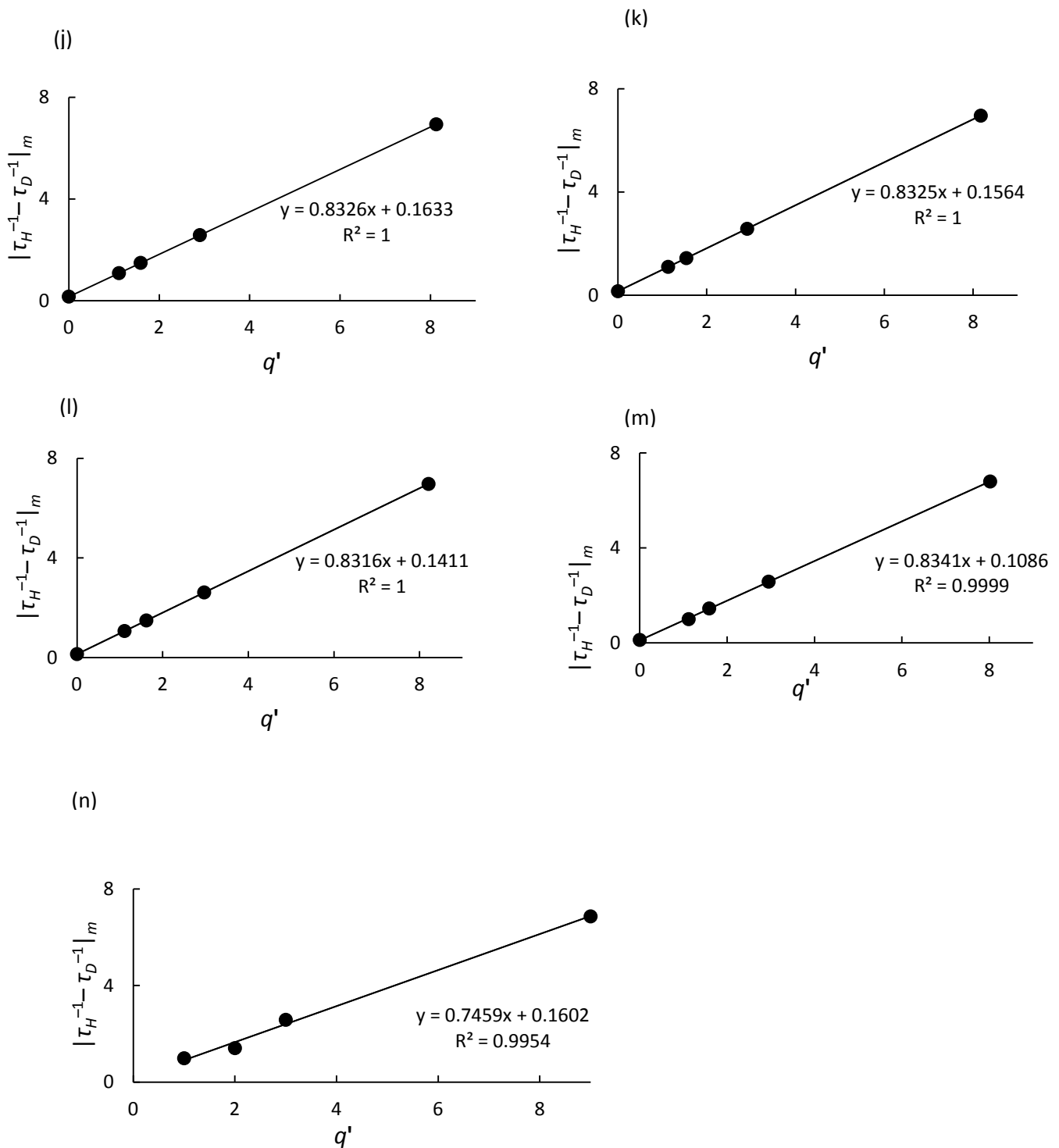
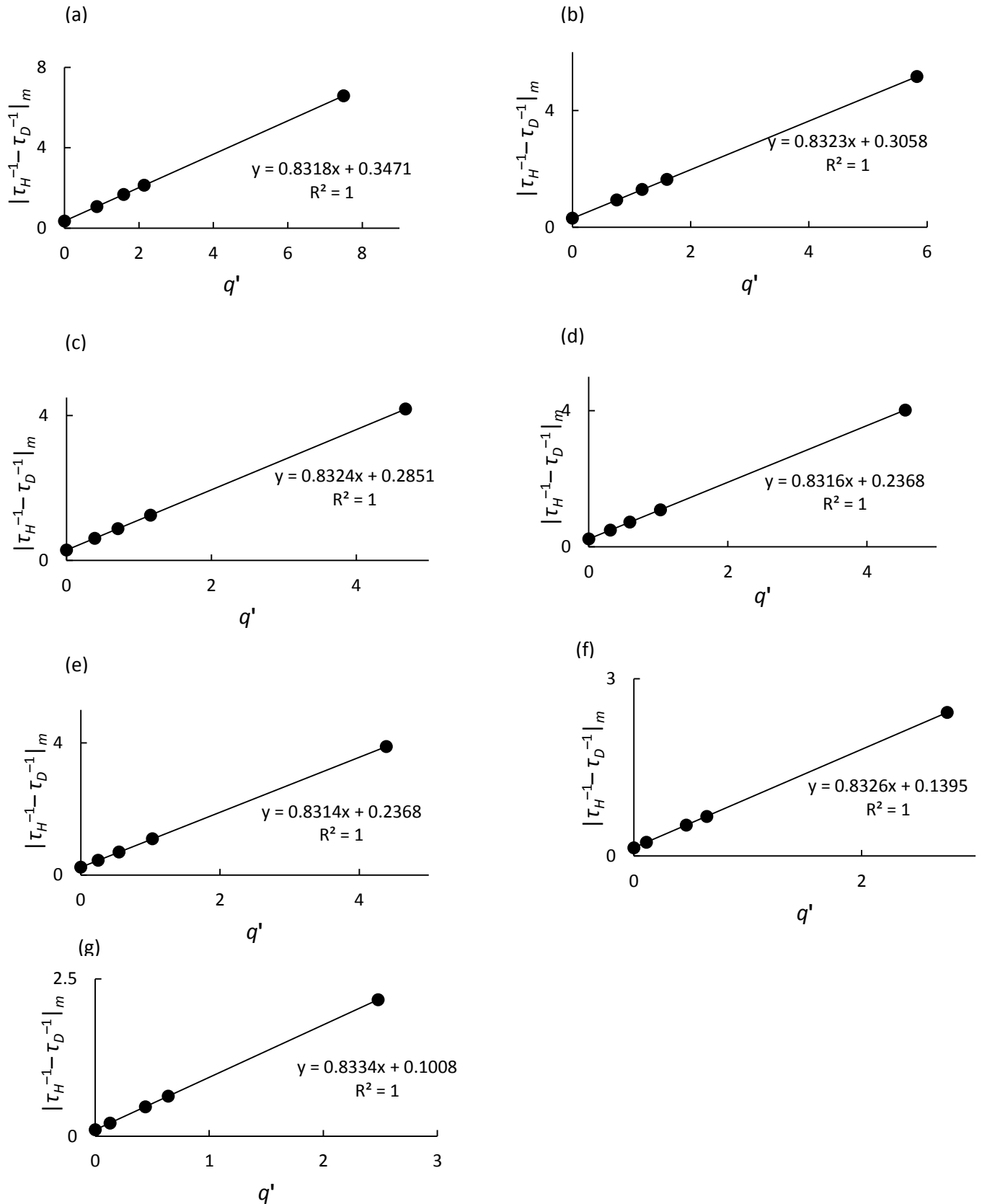


Figure B3. Continued on next page. See next page for caption.



**Figure B3.** Continued from previous page.  $|\tau_H^{-1} - \tau_D^{-1}|_m$  versus  $q'$  for (a) 90%; (b) 80%; (c) 70%; (d) 60%; (e) 50%; (f) 40%; (g) 20%; (i) 10%; (j) 9%; (k) 8%; (l) 7%; (m) 6%; and (n) 5% H<sub>2</sub>O (v/v) in THF.



**Figure B4.**  $|\tau_H^{-1} - \tau_D^{-1}|_m$  versus  $q'$  for (a) 90% H<sub>2</sub>O; (b) 60% H<sub>2</sub>O; (c) 20% H<sub>2</sub>O; (d) 9% H<sub>2</sub>O; (e) 5% H<sub>2</sub>O; (f) 3% H<sub>2</sub>O; (g) 1% H<sub>2</sub>O; (v/v) in DMF.

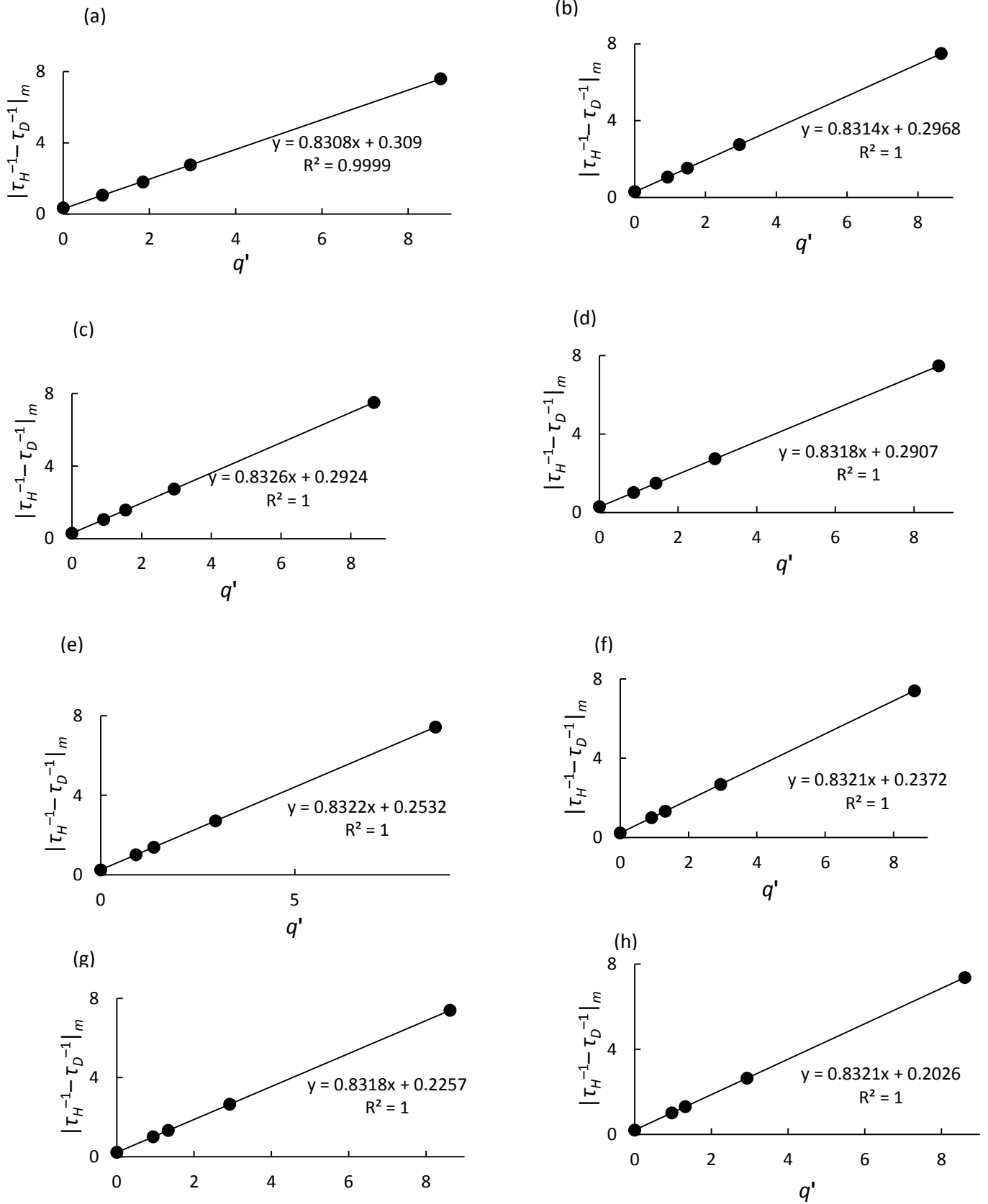
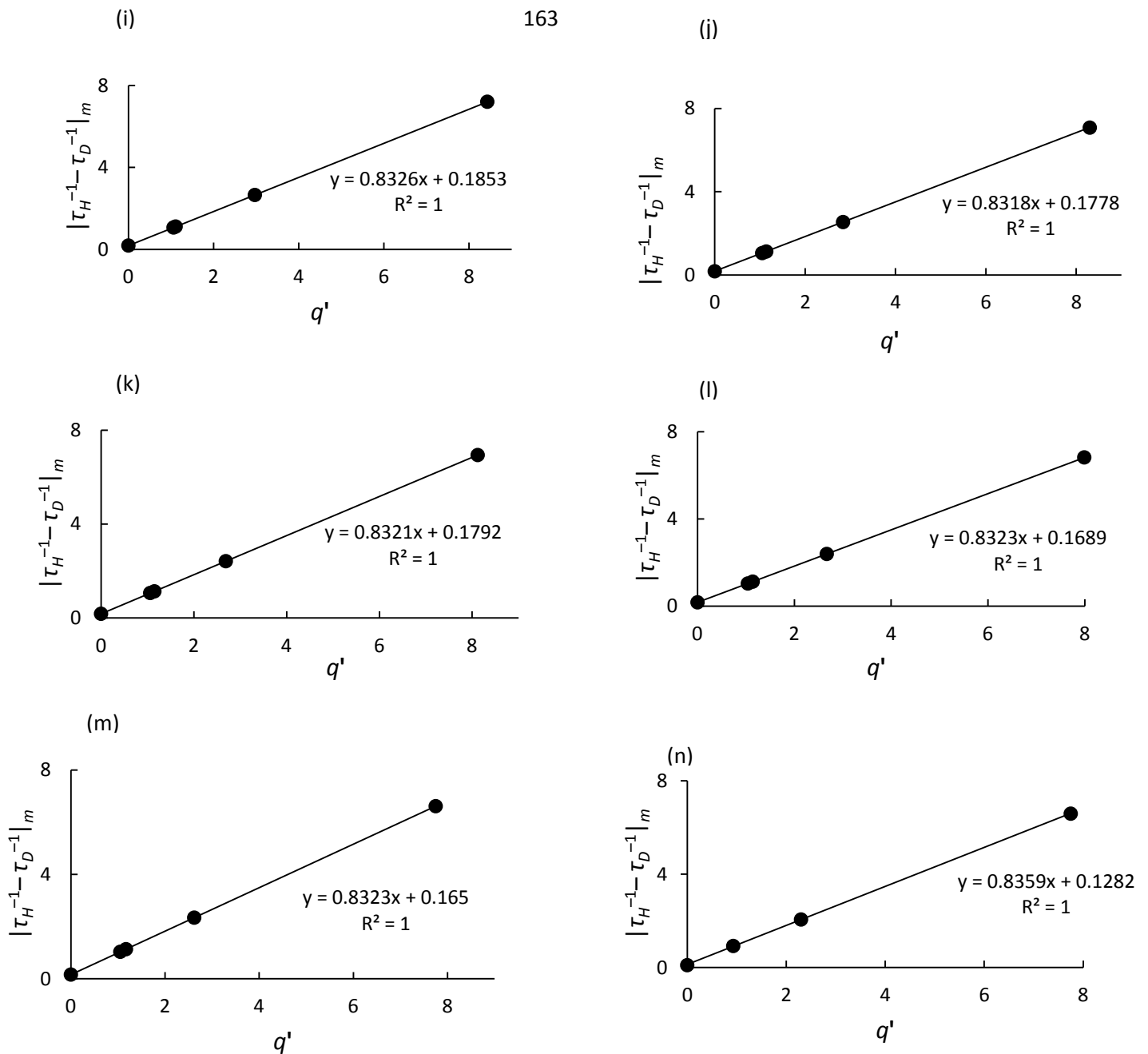


Figure B5. Continued on next page. See next page for caption.



**Figure B5** Continued from previous page.  $|\tau_H^{-1} - \tau_D^{-1}|_m$  versus  $q'$  for (a) 90%; (b) 80%; (c) 70%; (d) 60%; (e) 50%; (f) 40%; (g) 20%; (i) 10%; (j) 9%; (k) 8%; (l) 7%; (m) 6%; and (n) 5% H<sub>2</sub>O (v/v) in acetonitrile.



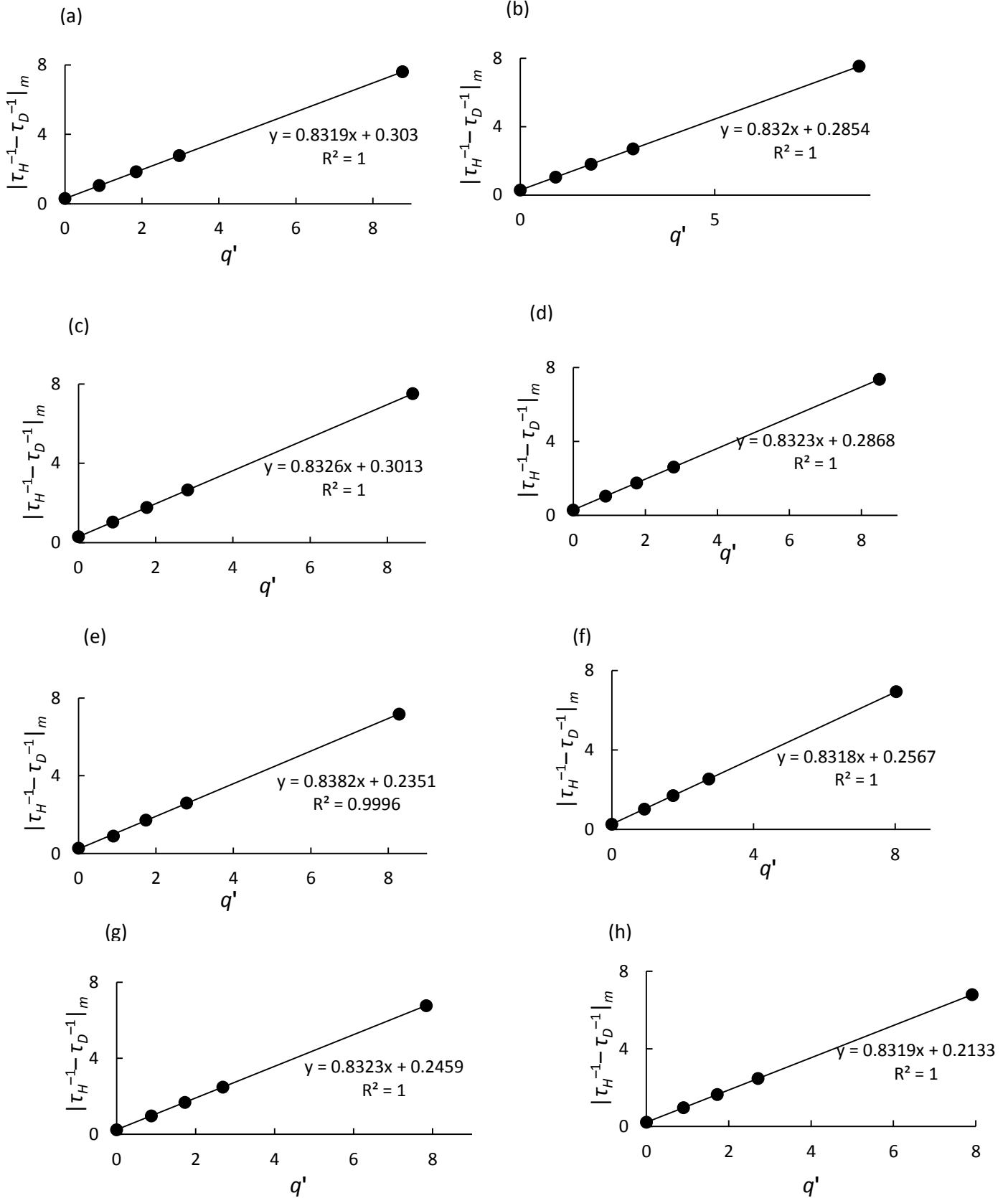
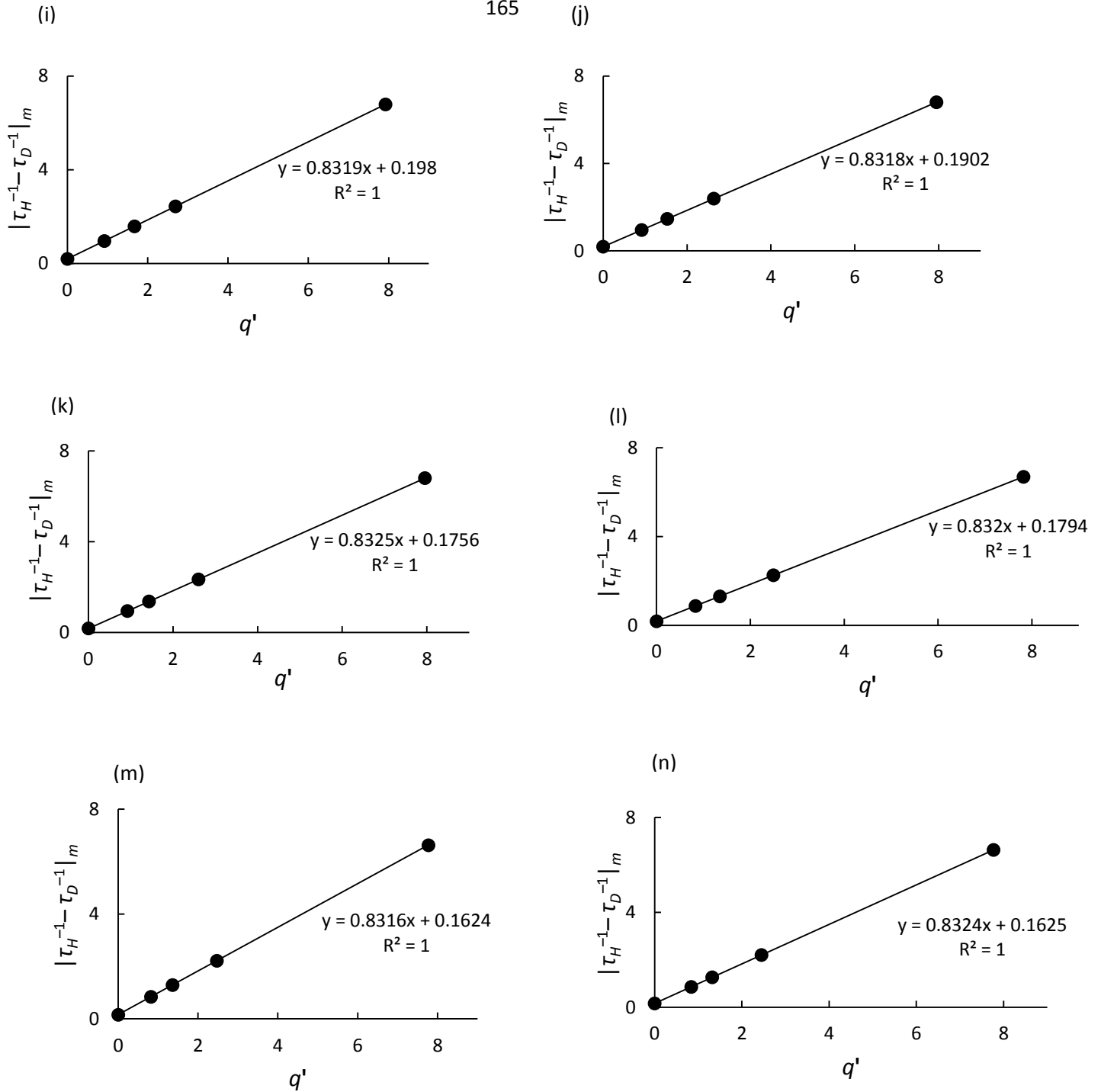
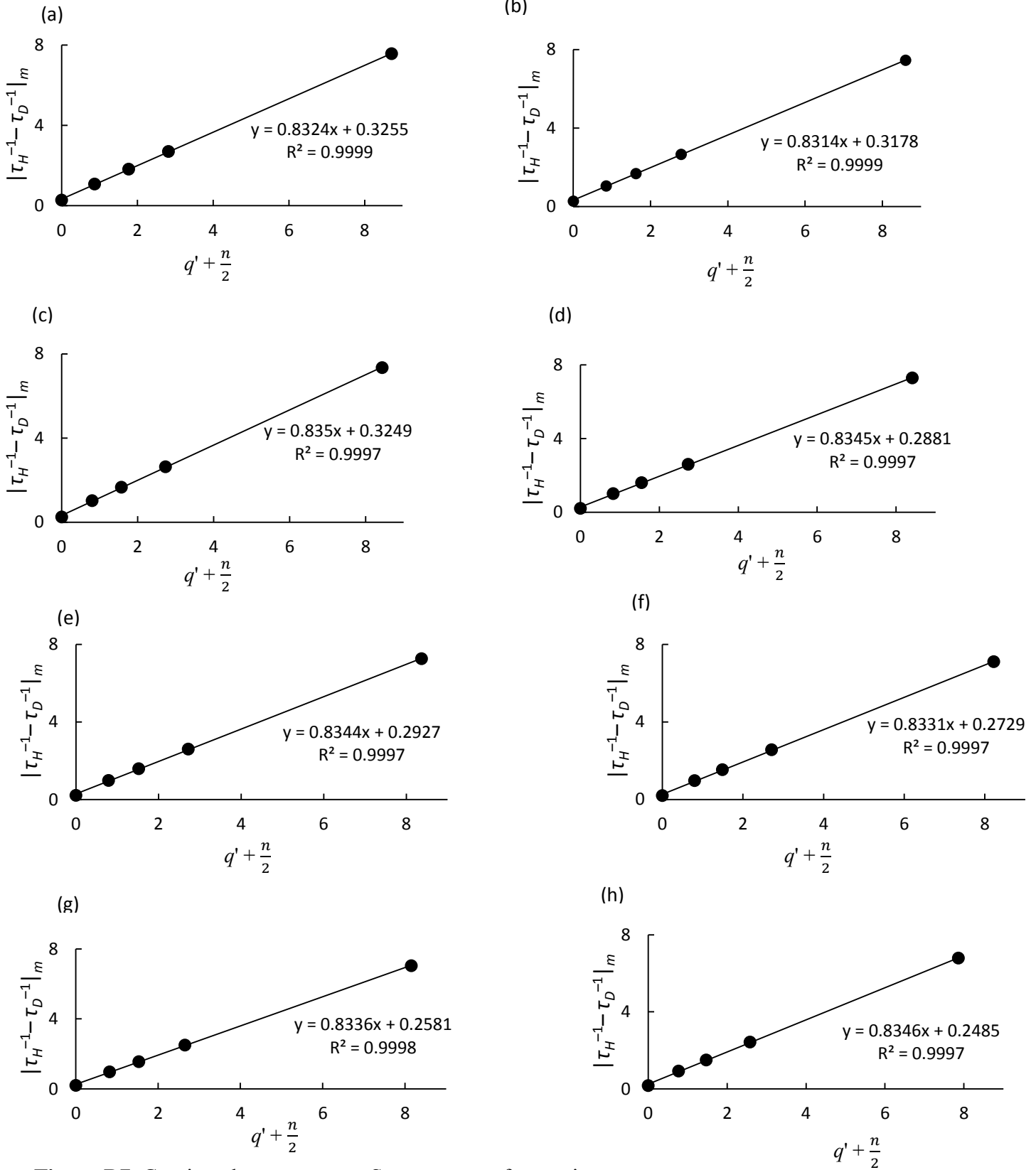


Figure B6. Continued on next page. See next page for caption.



**Figure B6.** Continued from previous page.  $|\tau_H^{-1} - \tau_D^{-1}|_m$  versus  $q'$  for (a) 90%; (b) 80%; (c) 70%; (d) 60%; (e) 50%; (f) 40%; (g) 20%; (i) 10%; (j) 9%; (k) 8%; (l) 7%; (m) 6%; and (n) 5% H<sub>2</sub>O (v/v) in acetone.



**Figure B7.** Continued on next page. See next page for caption.

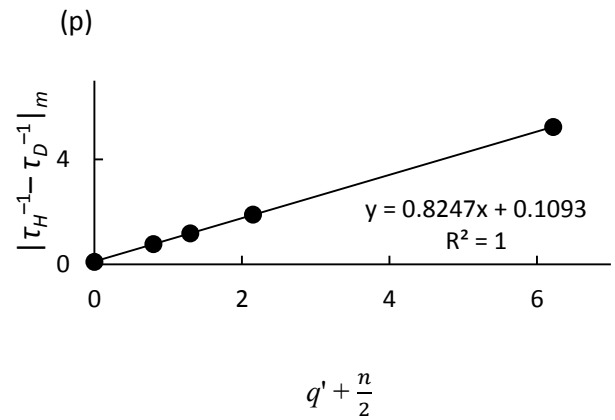
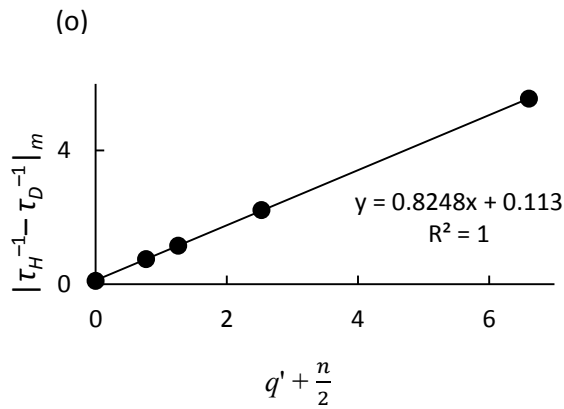
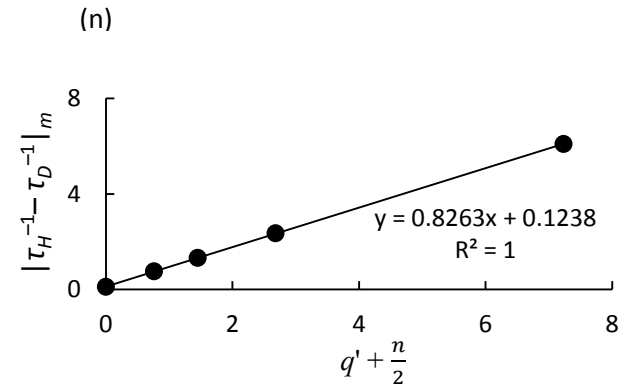
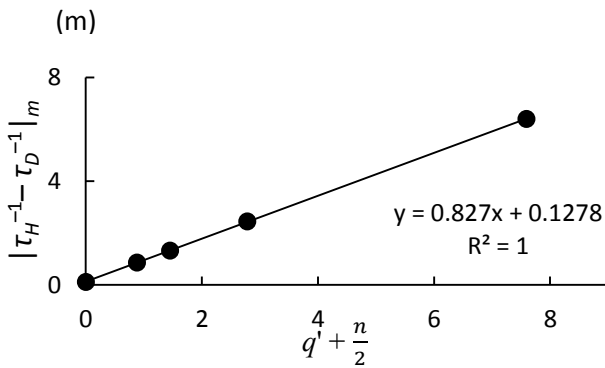
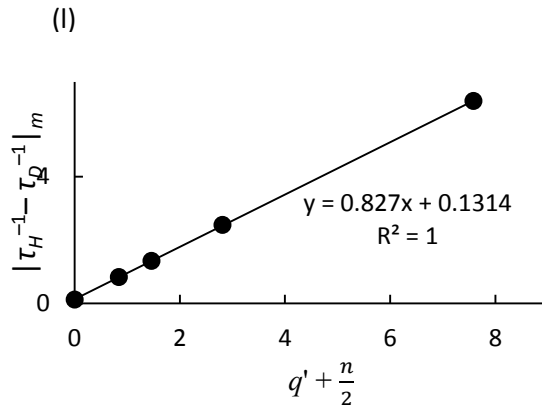
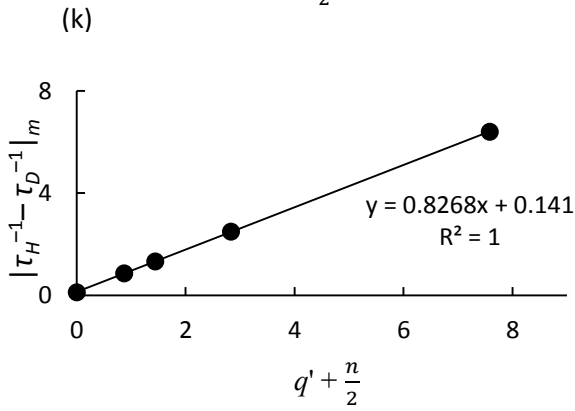
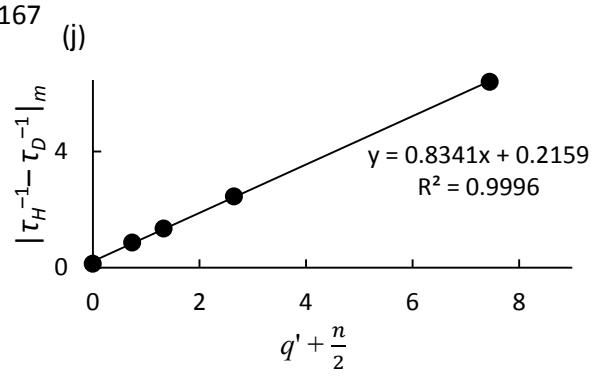
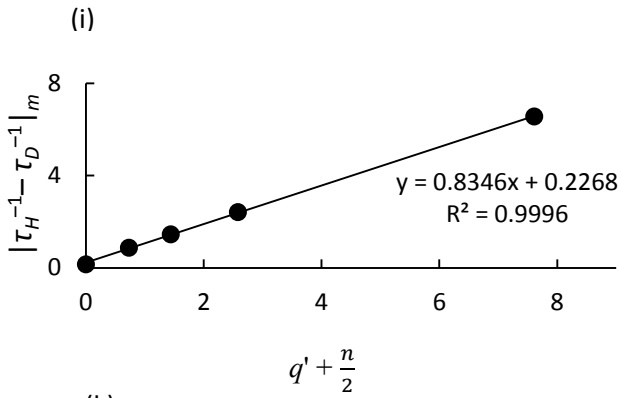
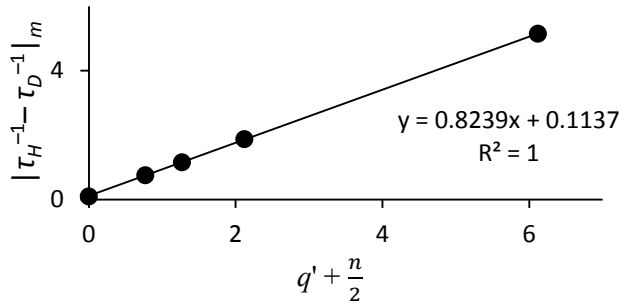
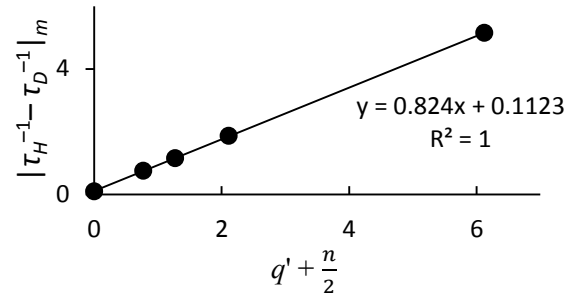


Figure B7. Continued on next page. See next page for caption.

(q)



(r)



**Figure B7.** Continued from previous page.  $|\tau_H^{-1} - \tau_D^{-1}|_m$  versus  $q'$  for (a) 90%; (b) 80%; (c) 70%; (d) 60%; (e) 50%; (f) 40%; (g) 20%; (i) 10%; (j) 9%; (k) 8%; (l) 7%; (m) 6%; (n) 5% H<sub>2</sub>O (o) 4% H<sub>2</sub>O; (p) 3% H<sub>2</sub>O; (q) 2% H<sub>2</sub>O; and (r) 1% H<sub>2</sub>O (v/v) in ethanol.

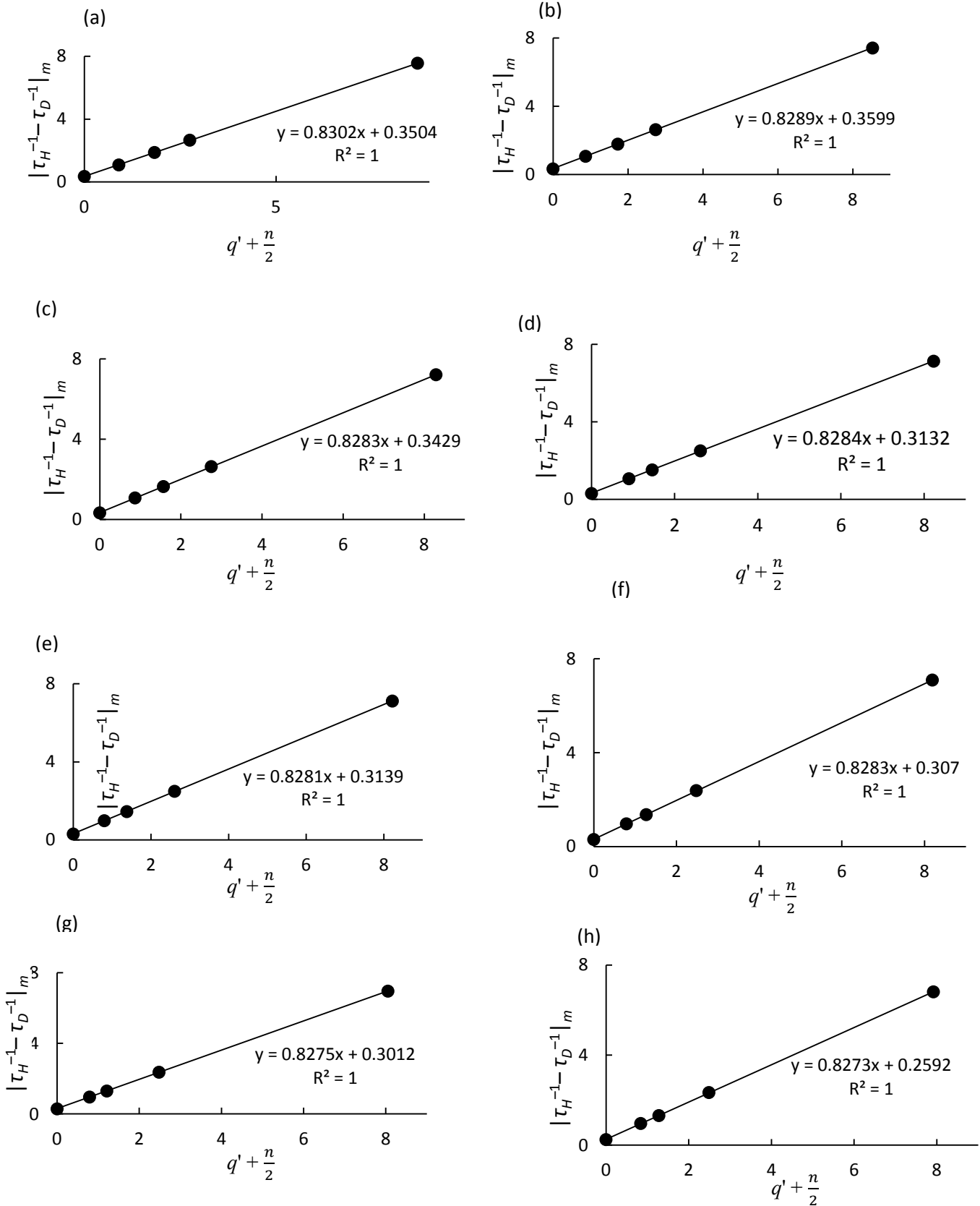


Figure B8. Continued on next page. See next page for caption.

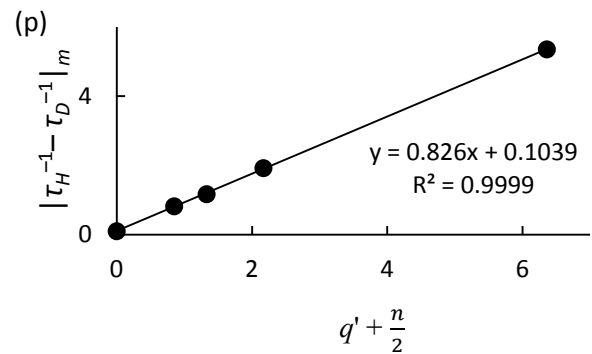
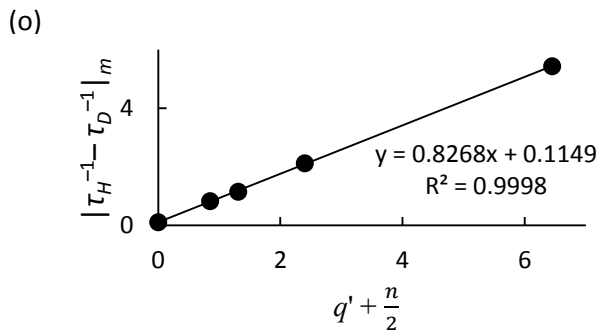
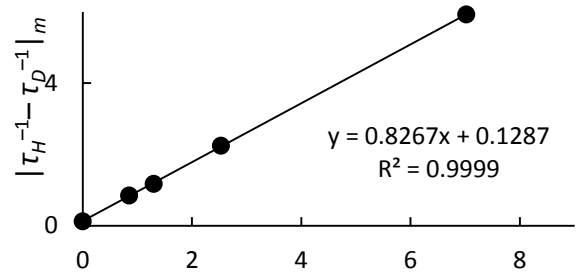
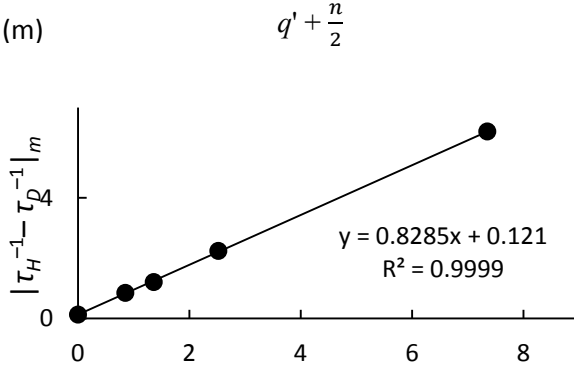
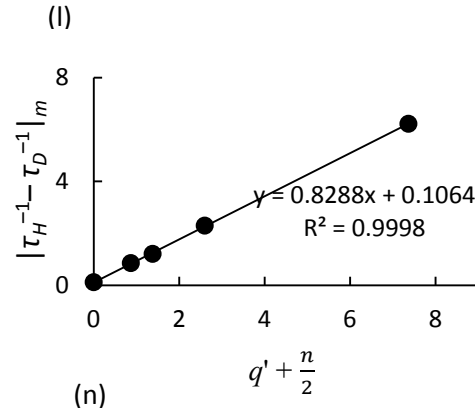
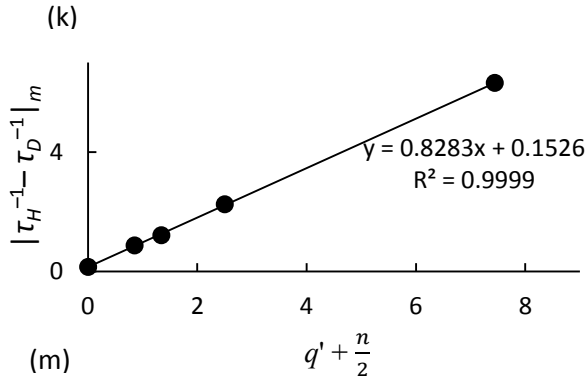
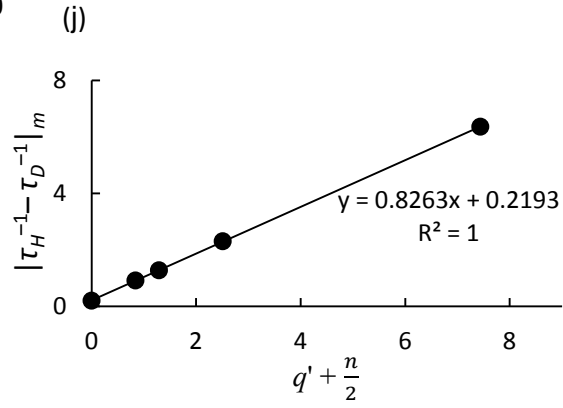
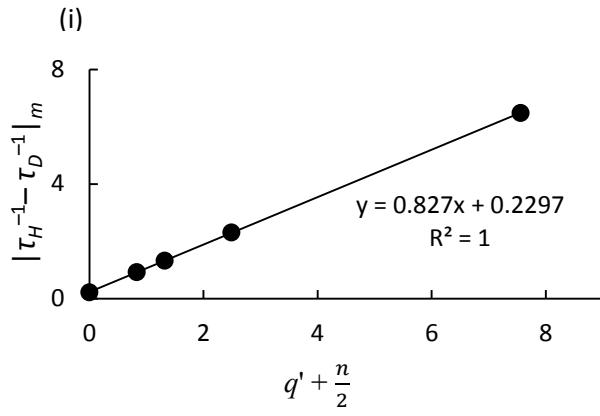
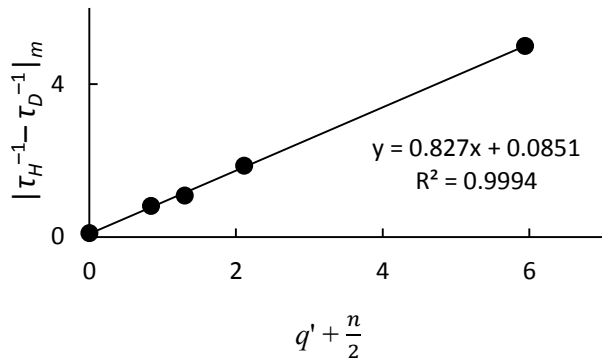
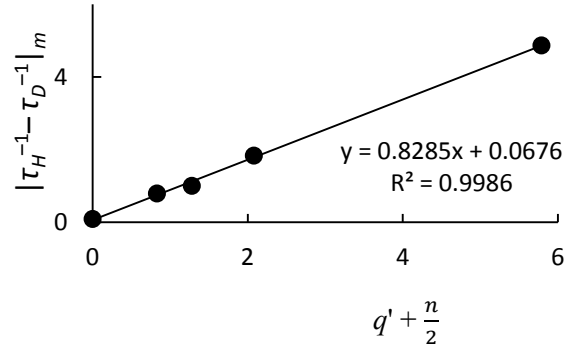


Figure B8. Continued on next page. See next page for caption.

(q)



(r)



**Figure B8.** Continued from previous page.  $|\tau_H^{-1} - \tau_D^{-1}|_m$  versus  $q'$  for (a) 90%; (b) 80%; (c) 70%; (d) 60%; (e) 50%; (f) 40%; (g) 20%; (i) 10%; (j) 9%; (k) 8%; (l) 7%; (m) 6%; (n) 5% H<sub>2</sub>O (o) 4% H<sub>2</sub>O; (p) 3% H<sub>2</sub>O; (q) 2% H<sub>2</sub>O; and (r) 1% H<sub>2</sub>O (v/v) in methanol.



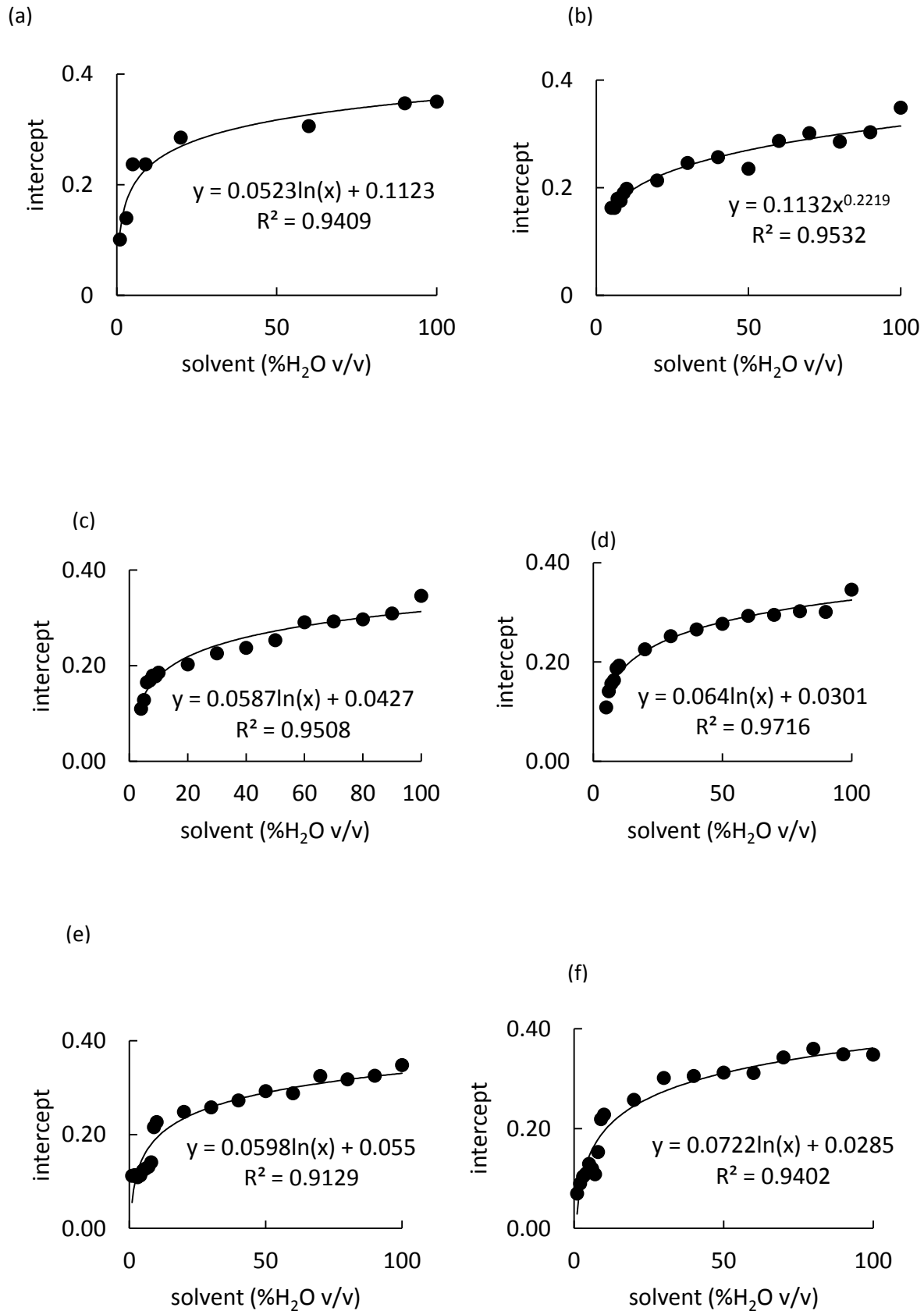


**Figure B9.** Continued on next page. See next page for caption.

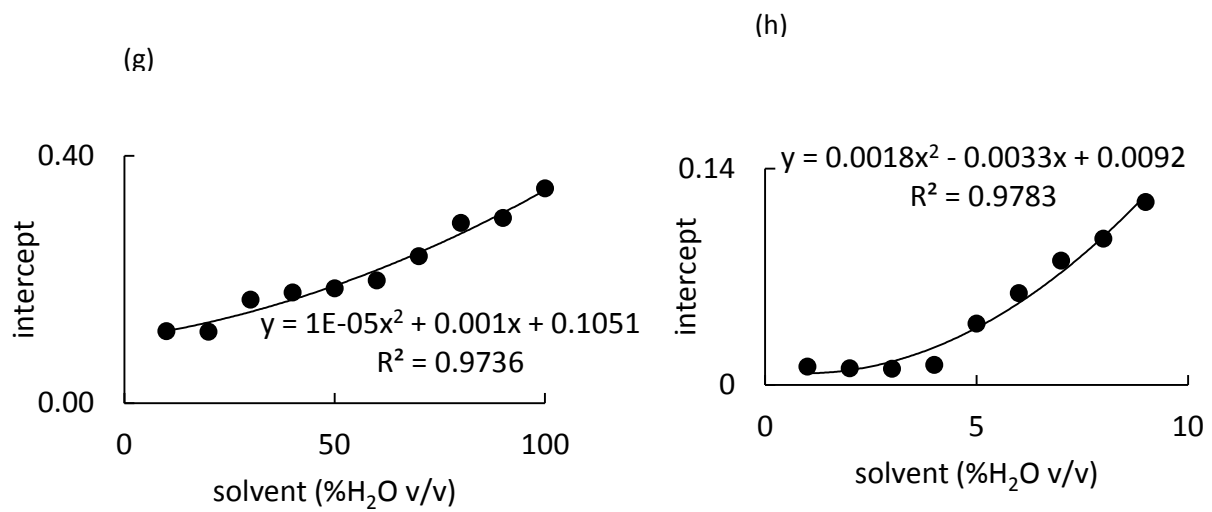


**Figure B9.** Continued from previous page. Intercept versus solvent (%H<sub>2</sub>O v/v) for (a) DMF; (b) acetone; (c) THF; (d) acetonitrile; (e) ethanol%; (f) methanol; (g) DMSO (10–100 (%H<sub>2</sub>O v/v); (h) DMSO (1–9 (%H<sub>2</sub>O v/v).

**APPENDIX C**

---

<b>Page</b>	<b>Contents</b>
174	Table of contents
175	Copyright permission for Reference 10
176–182	Copyright permission for Reference 11
183–188	Copyright permission for Reference 14
189	Copyright permission for Reference 24
190	Copyright permission for Reference 25
191	Copyright permission for Reference 47
192	Copyright permission for Reference 57
193–195	Copyright permission for Reference 87
196–198	Copyright permission for Reference 90
199–201	Copyright permission for Reference 92

---

**Science of Synthesis copyright permission**

Dear Mr. Dissanayake,

Please note that this query has now been forwarded to the permissions department (permission@thieme.de) at Thieme and you should receive a response soon.

Best regards,

Fiona Shortt de Hernandez

Dear Mr. Dissanayake,

Having consulted with the permissions department I can now confirm that this is ok. Please cite the source as:

Dissanayake, P.; Averill, D. J.; Allen, M. J., Science of Synthesis Knowledge Updates, (2011) 4, 1.

Best regards,

Fiona Shortt de Hernandez

**ELSEVIER LICENSE  
TERMS AND CONDITIONS**

Mar 01, 2012

---

---

This is a License Agreement between Prabani L Dissanayake ("You") and Elsevier ("Elsevier") provided by Copyright Clearance Center ("CCC"). The license consists of your order details, the terms and conditions provided by Elsevier, and the payment terms and conditions.

**All payments must be made in full to CCC. For payment instructions, please see information listed at the bottom of this form.**

Supplier	Elsevier Limited The Boulevard, Langford Lane Kidlington, Oxford, OX5 1GB, UK
Registered Company Number	1982084
Customer name	Prabani L Dissanayake
Customer address	Department of Chemistry  Detroit, MI 48201
License number	2845440153315
License date	Feb 10, 2012
Licensed content publisher	Elsevier
Licensed content publication	Inorganica Chimica Acta
Licensed content title	Competitive equilibria in lanthanide trifluoromethanesulfonate solutions in propylene carbonate containing a 15-crown-5

	177
	ether
Licensed content author	Francis Pilloud, Jean-Claude G. Bünzli
Licensed content date	1 December 1987
Licensed content volume number	139
Licensed content issue number	1–2
Number of pages	2
Start Page	153
End Page	154
Type of Use	reuse in a thesis/dissertation
Intended publisher of new work	other
Portion	figures/tables/illustrations
Number of figures/tables/illustrations	1
Format	both print and electronic
Are you the author of this Elsevier article?	No
Will you be translating?	No
Order reference number	
Title of your thesis/dissertation	New Adaptations of Analytical Tools for the Study of Dynamic Interactions of Lanthanide-based Catalysis in Aqueous Media
Expected completion date	May 2012

Estimated size (number of pages)	300
Elsevier VAT number	GB 494 6272 12
Permissions price	0.00 USD
VAT/Local Sales Tax	0.0 USD / 0.0 GBP
Total	0.00 USD

Terms and Conditions

## INTRODUCTION

1. The publisher for this copyrighted material is Elsevier. By clicking "accept" in connection with completing this licensing transaction, you agree that the following terms and conditions apply to this transaction (along with the Billing and Payment terms and conditions established by Copyright Clearance Center, Inc. ("CCC"), at the time that you opened your Rightslink account and that are available at any time at <http://myaccount.copyright.com>).

## GENERAL TERMS

2. Elsevier hereby grants you permission to reproduce the aforementioned material subject to the terms and conditions indicated.

3. Acknowledgement: If any part of the material to be used (for example, figures) has appeared in our publication with credit or acknowledgement to another source, permission must also be sought from that source. If such permission is not obtained then that material may not be included in your publication/copies. Suitable acknowledgement to the source must be made, either as a footnote or in a reference list at the end of your publication, as follows:

“Reprinted from Publication title, Vol /edition number, Author(s), Title of article / title of chapter, Pages No., Copyright (Year), with permission from Elsevier [OR APPLICABLE SOCIETY COPYRIGHT OWNER].” Also Lancet special credit - “Reprinted from The Lancet, Vol. number, Author(s), Title of article, Pages No., Copyright (Year), with permission from Elsevier.”

4. Reproduction of this material is confined to the purpose and/or media for which permission is hereby given.

5. Altering/Modifying Material: Not Permitted. However figures and illustrations may be altered/adapted minimally to serve your work. Any other abbreviations, additions, deletions and/or any other alterations shall be made only with prior written authorization of Elsevier Ltd.

(Please contact Elsevier at [permissions@elsevier.com](mailto:permissions@elsevier.com))

6. If the permission fee for the requested use of our material is waived in this instance, please be advised that your future requests for Elsevier materials may attract a fee.

7. Reservation of Rights: Publisher reserves all rights not specifically granted in the combination of (i) the license details provided by you and accepted in the course of this licensing transaction, (ii) these terms and conditions and (iii) CCC's Billing and Payment terms and conditions.

8. License Contingent Upon Payment: While you may exercise the rights licensed immediately upon issuance of the license at the end of the licensing process for the transaction, provided that you have disclosed complete and accurate details of your proposed use, no license is finally effective unless and until full payment is received from you (either by publisher or by CCC) as provided in CCC's Billing and Payment terms and conditions. If full payment is not received on a timely basis, then any license preliminarily granted shall be deemed automatically revoked and shall be void as if never granted. Further, in the event that you breach any of these terms and conditions or any of CCC's Billing and Payment terms and conditions, the license is automatically revoked and shall be void as if never granted. Use of materials as described in a revoked license, as well as any use of the materials beyond the scope of an unrevoked license, may constitute copyright infringement and publisher reserves the right to take any and all action to protect its copyright in the materials.

9. Warranties: Publisher makes no representations or warranties with respect to the licensed material.

10. Indemnity: You hereby indemnify and agree to hold harmless publisher and CCC, and their respective officers, directors, employees and agents, from and against any and all claims arising out of your use of the licensed material other than as specifically authorized pursuant to this license.

11. No Transfer of License: This license is personal to you and may not be sublicensed, assigned, or transferred by you to any other person without publisher's written permission.

12. No Amendment Except in Writing: This license may not be amended except in a writing signed by both parties (or, in the case of publisher, by CCC on publisher's behalf).

13. Objection to Contrary Terms: Publisher hereby objects to any terms contained in any purchase order, acknowledgment, check endorsement or other writing prepared by you, which terms are inconsistent with these terms and conditions or CCC's Billing and Payment terms and conditions. These terms and conditions, together with CCC's Billing and Payment terms and conditions (which are incorporated herein), comprise the entire agreement between you and publisher (and CCC) concerning this licensing transaction. In the event of any conflict between your obligations established by these terms and conditions and those established by CCC's Billing and Payment



terms and conditions, these terms and conditions shall control.

14. **Revocation:** Elsevier or Copyright Clearance Center may deny the permissions described in this License at their sole discretion, for any reason or no reason, with a full refund payable to you. Notice of such denial will be made using the contact information provided by you. Failure to receive such notice will not alter or invalidate the denial. In no event will Elsevier or Copyright Clearance Center be responsible or liable for any costs, expenses or damage incurred by you as a result of a denial of your permission request, other than a refund of the amount(s) paid by you to Elsevier and/or Copyright Clearance Center for denied permissions.

#### LIMITED LICENSE

The following terms and conditions apply only to specific license types:

15. **Translation:** This permission is granted for non-exclusive world **English** rights only unless your license was granted for translation rights. If you licensed translation rights you may only translate this content into the languages you requested. A professional translator must perform all translations and reproduce the content word for word preserving the integrity of the article. If this license is to re-use 1 or 2 figures then permission is granted for non-exclusive world rights in all languages.

16. **Website:** The following terms and conditions apply to electronic reserve and author websites:

**Electronic reserve:** If licensed material is to be posted to website, the web site is to be password-protected and made available only to bona fide students registered on a relevant course if:

This license was made in connection with a course,

This permission is granted for 1 year only. You may obtain a license for future website posting,

All content posted to the web site must maintain the copyright information line on the bottom of each image,

A hyper-text must be included to the Homepage of the journal from which you are licensing at <http://www.sciencedirect.com/science/journal/xxxx> or the Elsevier homepage for books at <http://www.elsevier.com> , and

Central Storage: This license does not include permission for a scanned version of the material to be stored in a central repository such as that provided by Heron/XanEdu.

17. **Author website** for journals with the following additional clauses:

All content posted to the web site must maintain the copyright information line on the bottom of each image, and

the permission granted is limited to the personal version of your paper. You are not allowed to download and post the published electronic version of your article (whether PDF or HTML, proof or final version), nor may you scan the printed edition to create an electronic version,

A hyper-text must be included to the Homepage of the journal from which you are licensing at <http://www.sciencedirect.com/science/journal/xxxx> , As part of our normal production

process, you will receive an e-mail notice when your article appears on Elsevier's online service ScienceDirect ([www.sciencedirect.com](http://www.sciencedirect.com)). That e-mail will include the article's Digital Object Identifier (DOI). This number provides the electronic link to the published article and should be included in the posting of your personal version. We ask that you wait until you receive this e-mail and have the DOI to do any posting.

Central Storage: This license does not include permission for a scanned version of the material to be stored in a central repository such as that provided by Heron/XanEdu.

**18. Author website** for books with the following additional clauses:

Authors are permitted to place a brief summary of their work online only.

A hyper-text must be included to the Elsevier homepage at <http://www.elsevier.com>

All content posted to the web site must maintain the copyright information line on the bottom of each image

You are not allowed to download and post the published electronic version of your chapter, nor may you scan the printed edition to create an electronic version.

Central Storage: This license does not include permission for a scanned version of the material to be stored in a central repository such as that provided by Heron/XanEdu.

**19. Website** (regular and for author): A hyper-text must be included to the Homepage of the journal from which you are licensing at <http://www.sciencedirect.com/science/journal/xxxx>. or for books to the Elsevier homepage at <http://www.elsevier.com>

**20. Thesis/Dissertation:** If your license is for use in a thesis/dissertation your thesis may be submitted to your institution in either print or electronic form. Should your thesis be published commercially, please reapply for permission. These requirements include permission for the Library and Archives of Canada to supply single copies, on demand, of the complete thesis and include permission for UMI to supply single copies, on demand, of the complete thesis. Should your thesis be published commercially, please reapply for permission.

**21. Other Conditions:**

v1.6

**If you would like to pay for this license now, please remit this license along with your payment made payable to "COPYRIGHT CLEARANCE CENTER" otherwise you will be invoiced within 48 hours of the license date. Payment should be in the form of a check or money order referencing your account number and this invoice number RLNK500716831.**

**Once you receive your invoice for this order, you may pay your invoice by credit card. Please**

follow instructions provided at that time.

**Make Payment To:**  
**Copyright Clearance Center**  
**Dept 001**  
**P.O. Box 843006**  
**Boston, MA 02284-3006**

For suggestions or comments regarding this order, contact RightsLink Customer Support: [customercare@copyright.com](mailto:customercare@copyright.com) or +1-877-622-5543 (toll free in the US) or +1-978-646-2777.

Gratis licenses (referencing \$0 in the Total field) are free. Please retain this printable license for your reference. No payment is required.

---

**ELSEVIER LICENSE  
TERMS AND CONDITIONS**

Mar 01, 2012

---

---

This is a License Agreement between Prabani L Dissanayake ("You") and Elsevier ("Elsevier") provided by Copyright Clearance Center ("CCC"). The license consists of your order details, the terms and conditions provided by Elsevier, and the payment terms and conditions.

**All payments must be made in full to CCC. For payment instructions, please see information listed at the bottom of this form.**

Supplier Elsevier Limited  
The Boulevard, Langford Lane  
Kidlington, Oxford, OX5 1GB, UK

Registered Company Number 1982084

Customer name Prabani L Dissanayake

Customer address Department of Chemistry  
Detroit, MI 48201

License number 2845440636484

License date Feb 10, 2012

Licensed content publisher Elsevier

Licensed content publication Inorganica Chimica Acta

Licensed content title Lanthanide(III) trifluoromethanesulfonate complexes in anhydrous acetonitrile

Licensed content author Plinio Di Bernardo, Gregory R. Choppin, Roberto Portanova, Pier Luigi Zanonato

Licensed content date 1 May 1993

Licensed content volume number 207

Licensed content issue number 1

Number of pages 7

Start Page 85

End Page 91

Type of Use reuse in a thesis/dissertation

Intended publisher of new work other

Portion figures/tables/illustrations

Number of figures/tables/illustrations 3

Format both print and electronic

Are you the author of this Elsevier article? No

Will you be translating? No

Order reference number

Title of your thesis/dissertation

New Adaptations of Analytical Tools for the Study of Dynamic Interactions of Lanthanide-based Catalysis in Aqueous Media

Expected completion date May 2012

Estimated size (number of pages) 300

Elsevier VAT number GB 494 6272 12

Permissions price 0.00 USD

VAT/Local Sales Tax 0.0 USD / 0.0 GBP

Total 0.00 USD

Terms and Conditions

## INTRODUCTION

1. The publisher for this copyrighted material is Elsevier. By clicking "accept" in connection with completing this licensing transaction, you agree that the following terms and conditions apply to this transaction (along with the Billing and Payment terms and conditions established by Copyright Clearance Center, Inc. ("CCC"), at the time that you opened your Rightslink account and that are available at any time at <http://myaccount.copyright.com>).

## GENERAL TERMS

2. Elsevier hereby grants you permission to reproduce the aforementioned material subject to the terms and conditions indicated.

3. Acknowledgement: If any part of the material to be used (for example, figures) has appeared in our publication with credit or acknowledgement to another source, permission must also be sought from that source. If such permission is not obtained then that material may not be included in your publication/copies. Suitable acknowledgement to the source must be made, either as a footnote or in a reference list at the end of your publication, as follows:

“Reprinted from Publication title, Vol /edition number, Author(s), Title of article / title of chapter, Pages No., Copyright (Year), with permission from Elsevier [OR APPLICABLE SOCIETY COPYRIGHT OWNER].”  
Also Lancet special credit - “Reprinted from The Lancet, Vol. number, Author(s), Title of article, Pages No., Copyright (Year), with permission from Elsevier.”

4. Reproduction of this material is confined to the purpose and/or media for which permission is hereby given.

5. Altering/Modifying Material: Not Permitted. However figures and illustrations may be altered/adapted minimally to serve your work. Any other abbreviations, additions, deletions and/or any other alterations shall be made only with prior written authorization of Elsevier Ltd. (Please contact Elsevier at [permissions@elsevier.com](mailto:permissions@elsevier.com))

6. If the permission fee for the requested use of our material is waived in this instance, please be advised that your future requests for Elsevier materials may attract a fee.

7. Reservation of Rights: Publisher reserves all rights not specifically granted in the combination of (i) the license details provided by you and accepted in the course of this licensing transaction, (ii) these terms and conditions and (iii) CCC's Billing and Payment terms and conditions.

8. License Contingent Upon Payment: While you may exercise the rights licensed immediately upon issuance of the license at the end of the licensing process for the transaction, provided that you have disclosed complete and accurate details of your proposed use, no license is finally effective unless and until full payment is received from you (either by publisher or by CCC) as provided in CCC's Billing and Payment terms and conditions. If full payment is not received on a timely basis, then any license preliminarily granted shall be deemed automatically revoked and shall be void as if never granted. Further, in the event that you breach any of these terms and conditions or any of CCC's Billing and Payment terms and conditions, the license is automatically revoked and shall be void as if never granted. Use of materials as described in a revoked license, as well as any use of the materials beyond the scope of an unrevoked license, may constitute copyright infringement and publisher reserves the right to take any and all action to protect its copyright in the materials.

9. Warranties: Publisher makes no representations or warranties with respect to the licensed material.

10. **Indemnity:** You hereby indemnify and agree to hold harmless publisher and CCC, and their respective officers, directors, employees and agents, from and against any and all claims arising out of your use of the licensed material other than as specifically authorized pursuant to this license.

11. **No Transfer of License:** This license is personal to you and may not be sublicensed, assigned, or transferred by you to any other person without publisher's written permission.

12. **No Amendment Except in Writing:** This license may not be amended except in a writing signed by both parties (or, in the case of publisher, by CCC on publisher's behalf).

13. **Objection to Contrary Terms:** Publisher hereby objects to any terms contained in any purchase order, acknowledgment, check endorsement or other writing prepared by you, which terms are inconsistent with these terms and conditions or CCC's Billing and Payment terms and conditions. These terms and conditions, together with CCC's Billing and Payment terms and conditions (which are incorporated herein), comprise the entire agreement between you and publisher (and CCC) concerning this licensing transaction. In the event of any conflict between your obligations established by these terms and conditions and those established by CCC's Billing and Payment terms and conditions, these terms and conditions shall control.

14. **Revocation:** Elsevier or Copyright Clearance Center may deny the permissions described in this License at their sole discretion, for any reason or no reason, with a full refund payable to you. Notice of such denial will be made using the contact information provided by you. Failure to receive such notice will not alter or invalidate the denial. In no event will Elsevier or Copyright Clearance Center be responsible or liable for any costs, expenses or damage incurred by you as a result of a denial of your permission request, other than a refund of the amount(s) paid by you to Elsevier and/or Copyright Clearance Center for denied permissions.

#### **LIMITED LICENSE**

The following terms and conditions apply only to specific license types:

15. **Translation:** This permission is granted for non-exclusive world **English** rights only unless your license was granted for translation rights. If you licensed translation rights you may only translate this content into the languages you requested. A professional translator must perform all translations and reproduce the content word for word preserving the integrity of the article. If this license is to re-use 1 or 2 figures then permission is granted for non-exclusive world rights in all languages.

16. **Website:** The following terms and conditions apply to electronic reserve and author websites:

**Electronic reserve:** If licensed material is to be posted to website, the web site is to be password-protected and made available only to bona fide students registered on a relevant course if:

This license was made in connection with a course,

This permission is granted for 1 year only. You may obtain a license for future website posting,

All content posted to the web site must maintain the copyright information line on the bottom of each image,

A hyper-text must be included to the Homepage of the journal from which you are licensing at <http://www.sciencedirect.com/science/journal/xxxx> or the Elsevier homepage for books at <http://www.elsevier.com> , and

Central Storage: This license does not include permission for a scanned version of the material to be stored in a central repository such as that provided by Heron/XanEdu.

17. **Author website** for journals with the following additional clauses:

All content posted to the web site must maintain the copyright information line on the bottom of each image, and

the permission granted is limited to the personal version of your paper. You are not allowed to download and post the published electronic version of your article (whether PDF or HTML, proof or final version), nor may you scan the printed edition to create an electronic version,

A hyper-text must be included to the Homepage of the journal from which you are licensing at <http://www.sciencedirect.com/science/journal/xxxx> , As part of our normal production process, you will receive an e-mail notice when your article appears on Elsevier's online service ScienceDirect ([www.sciencedirect.com](http://www.sciencedirect.com)). That e-mail will include the article's Digital Object Identifier (DOI). This number provides the electronic link to the published article and should be included in the posting of your personal version. We ask that you wait until you receive this e-mail and have the DOI to do any posting.

Central Storage: This license does not include permission for a scanned version of the material to be stored in a central repository such as that provided by Heron/XanEdu.

18. **Author website** for books with the following additional clauses:

Authors are permitted to place a brief summary of their work online only.

A hyper-text must be included to the Elsevier homepage at <http://www.elsevier.com>

All content posted to the web site must maintain the copyright information line on the bottom of each image

You are not allowed to download and post the published electronic version of your chapter, nor may you scan the printed edition to create an electronic version.

Central Storage: This license does not include permission for a scanned version of the material to be stored in a central repository such as that provided by Heron/XanEdu.

19. **Website** (regular and for author): A hyper-text must be included to the Homepage of the journal from which you are licensing at <http://www.sciencedirect.com/science/journal/xxxx>. or for books to the Elsevier homepage at <http://www.elsevier.com>

20. **Thesis/Dissertation**: If your license is for use in a thesis/dissertation your thesis may be submitted to your institution in either print or electronic form. Should your thesis be published commercially, please reapply for permission. These requirements include permission for the Library and Archives of Canada to supply single copies, on demand, of the complete thesis and include permission for UMI to supply single



copies, on demand, of the complete thesis. Should your thesis be published commercially, please reapply for permission.

**21. Other Conditions:**

v1.6

**If you would like to pay for this license now, please remit this license along with your payment made payable to "COPYRIGHT CLEARANCE CENTER" otherwise you will be invoiced within 48 hours of the license date. Payment should be in the form of a check or money order referencing your account number and this invoice number RLNK500716835.**

**Once you receive your invoice for this order, you may pay your invoice by credit card. Please follow instructions provided at that time.**

**Make Payment To:**

**Copyright Clearance Center**

**Dept 001**

**P.O. Box 843006**

**Boston, MA 02284-3006**

**For suggestions or comments regarding this order, contact RightsLink Customer**

**Support:**[customercare@copyright.com](mailto:customercare@copyright.com) or +1-877-622-5543 (toll free in the US) or +1-978-646-2777.

**Gratis licenses (referencing \$0 in the Total field) are free. Please retain this printable license for your reference. No payment is required.**

---

---



RightsLink®

Home

Account  
Info

Help



ACS Publications  
High quality. High impact.

**Title:** Dynamic Measurements of Aqueous Lanthanide Triflate-Catalyzed Reactions Using Luminescence Decay

**Author:** Prabani Dissanayake et al.

**Publication:** Journal of the American Chemical Society

**Publisher:** American Chemical Society

**Date:** May 1, 2009

Copyright © 2009, American Chemical Society

Logged in as:

Prabani Dissanayake

Account #:

3000401852

LOGOUT

### PERMISSION/LICENSE IS GRANTED FOR YOUR ORDER AT NO CHARGE

This type of permission/license, instead of the standard Terms & Conditions, is sent to you because no fee is being charged for your order. Please note the following:

- Permission is granted for your request in both print and electronic formats.
- If figures and/or tables were requested, they may be adapted or used in part.
- Please print this page for your records and send a copy of it to your publisher/graduate school.
- Appropriate credit for the requested material should be given as follows: "Reprinted (adapted) with permission from (COMPLETE REFERENCE CITATION). Copyright (YEAR) American Chemical Society." Insert appropriate information in place of the capitalized words.
- One-time permission is granted only for the use specified in your request. No additional uses are granted (such as derivative works or other editions). For any other uses, please submit a new request.

BACK

CLOSE WINDOW

Copyright © 2012 [Copyright Clearance Center, Inc.](#) All Rights

Reserved. [Privacy statement](#).  
Comments? We would like to hear  
from you. E-mail us  
at [customercare@copyright.com](mailto:customercare@copyright.com)



RightsLink®

Home

Account  
Info

Help



ACS Publications  
High quality. High impact.

**Title:** Luminescence-Decay as an  
Easy-to-Use Tool for the  
Study of Lanthanide-  
Containing Catalysts in  
Aqueous Solutions

**Author:** Prabani Dissanayake et al.

**Publication:** ACS Catalysis

**Publisher:** American Chemical Society

**Date:** Oct 1, 2011

Copyright © 2011, American Chemical  
Society

Logged in as:  
Prabani Dissanayake  
Account #:  
3000401852

LOGOUT

### PERMISSION/LICENSE IS GRANTED FOR YOUR ORDER AT NO CHARGE

This type of permission/license, instead of the standard Terms & Conditions, is sent to you because no fee is being charged for your order. Please note the following:

- Permission is granted for your request in both print and electronic formats.
- If figures and/or tables were requested, they may be adapted or used in part.
- Please print this page for your records and send a copy of it to your publisher/graduate school.
- Appropriate credit for the requested material should be given as follows: "Reprinted (adapted) with permission from (COMPLETE REFERENCE CITATION). Copyright (YEAR) American Chemical Society." Insert appropriate information in place of the capitalized words.
- One-time permission is granted only for the use specified in your request. No additional uses are granted (such as derivative works or other editions). For any other uses, please submit a new request.

BACK

CLOSE WINDOW

Copyright © 2012 [Copyright Clearance Center, Inc.](#) All Rights Reserved. [Privacy statement](#).  
Comments? We would like to hear from you. E-mail us at [customercare@copyright.com](mailto:customercare@copyright.com)



RightsLink®

Home

Account  
Info

Help



ACS Publications  
High quality. High impact.

**Title:** A New Class of Ligands for Aqueous, Lanthanide-Catalyzed, Enantioselective Mukaiyama Aldol Reactions

**Author:** Yujiang Mei et al.

**Publication:** Journal of the American Chemical Society

**Publisher:** American Chemical Society

**Date:** Sep 1, 2010

Copyright © 2010, American Chemical Society

Logged in as:  
Prabani Dissanayake  
Account #:  
3000401852

LOGOUT

### PERMISSION/LICENSE IS GRANTED FOR YOUR ORDER AT NO CHARGE

This type of permission/license, instead of the standard Terms & Conditions, is sent to you because no fee is being charged for your order. Please note the following:

- Permission is granted for your request in both print and electronic formats.
- If figures and/or tables were requested, they may be adapted or used in part.
- Please print this page for your records and send a copy of it to your publisher/graduate school.
- Appropriate credit for the requested material should be given as follows: "Reprinted (adapted) with permission from (COMPLETE REFERENCE CITATION). Copyright (YEAR) American Chemical Society." Insert appropriate information in place of the capitalized words.
- One-time permission is granted only for the use specified in your request. No additional uses are granted (such as derivative works or other editions). For any other uses, please submit a new request.

BACK

CLOSE WINDOW

Copyright © 2012 [Copyright Clearance Center, Inc.](#) All Rights Reserved. [Privacy statement.](#)  
Comments? We would like to hear from you. E-mail us at [customercare@copyright.com](mailto:customercare@copyright.com)

**Molecules copyright permission**

Dear Dr. Dissanayake,

Thank you very much for your request. As we are Open Access journal, we follow the Creative Commons Attribution License 3.0. This means you may use these materials freely from our side, on condition that "proper accreditation of the source and original publisher" is made

Please feel free to let us know if we can provide any further assistance.

Kind regards,  
Jessica Bai  
Assistant Editor  
Molecules (<http://www.mdpi.org/molecules/>)

--

Ms. Jessica Bai, M. Sc.  
MDPI Branch Office, Beijing  
Tel. +86 10 59011068; Fax: +86 10 59011089  
E-mail: [jessica.bai@mdpi.com](mailto:jessica.bai@mdpi.com)

Editor-in-Chief, Molecules:  
Dr. Derek J. McPhee  
E-Mail: <<mailto:mcphee@mdpi.org>>[mcphee@mdpi.org](mailto:mcphee@mdpi.org)

Molecules Editorial Office  
Molecular Diversity Preservation International (MDPI),  
Kandererstrasse 25, CH-4057 Basel, Switzerland;  
Tel. +41 61 683 77 34 (office); Fax +41 61 302 89 18  
E-mail: <<mailto:molecules@mdpi.org>>[molecules@mdpi.org](mailto:molecules@mdpi.org)  
<http://www.mdpi.com/journal/molecules>

## AMERICAN INSTITUTE OF PHYSICS LICENSE TERMS AND CONDITIONS

Mar 01, 2012

---



---

Click [here](#) for Payment Terms and Conditions.

**All payments must be made in full to CCC. For payment instructions, please see information listed at the bottom of this form.**

License Number	2845471177905
Order Date	Feb 10, 2012
Publisher	American Institute of Physics
Publication	Journal of Chemical Physics
Article Title	Effect of Paramagnetic Ions on the Nuclear Magnetic Resonance of O17 in Water and the Rate of Elimination of Water Molecules from the First Coordination Sphere of Cations
Author	Robert E. Connick, Richard E. Poulson
Online Publication Date	Mar 1, 1959
Volume number	30
Issue number	3
Type of Use	Thesis/Dissertation
Requestor type	Student
Format	Print and electronic
Portion	Figure/Table
Number of figures/tables	1
Title of your thesis / dissertation	New Adaptations of Analytical Tools for the Study of Dynamic Interactions of Lanthanide-based Catalysis in Aqueous Media
Expected completion date	May 2012
Estimated size (number of pages)	300
Total	0.00 USD
Terms and Conditions	

## American Institute of Physics -- Terms and Conditions: Permissions Uses

American Institute of Physics ("AIP") hereby grants to you the non-exclusive right and license to use and/or distribute the Material according to the use specified in your order, on a one-time basis, for the specified term, with a maximum distribution equal to the number that you have ordered. Any links or other content accompanying the Material are not the subject of this license.

1. You agree to include the following copyright and permission notice with the reproduction of the Material: "Reprinted with permission from [FULL CITATION]. Copyright [PUBLICATION YEAR], American Institute of Physics." For an article, the copyright and permission notice must be printed on the first page of the article or book chapter. For photographs, covers, or tables, the copyright and permission notice may appear with the Material, in a footnote, or in the reference list.
2. If you have licensed reuse of a figure, photograph, cover, or table, it is your responsibility to ensure that the material is original to AIP and does not contain the copyright of another entity, and that the copyright notice of the figure, photograph, cover, or table does not indicate that it was reprinted by AIP, with permission, from another source. Under no circumstances does AIP, purport or intend to grant permission to reuse material to which it does not hold copyright.
3. You may not alter or modify the Material in any manner. You may translate the Material into another language only if you have licensed translation rights. You may not use the Material for promotional purposes. AIP reserves all rights not specifically granted herein.
4. The foregoing license shall not take effect unless and until AIP or its agent, Copyright Clearance Center, receives the Payment in accordance with Copyright Clearance Center Billing and Payment Terms and Conditions, which are incorporated herein by reference.
5. AIP or the Copyright Clearance Center may, within two business days of granting this license, revoke the license for any reason whatsoever, with a full refund payable to you. Should you violate the terms of this license at any time, AIP, American Institute of Physics, or Copyright Clearance Center may revoke the license with no refund to you. Notice of such revocation will be made using the contact information provided by you. Failure to receive such notice will not nullify the revocation.
6. AIP makes no representations or warranties with respect to the Material. You agree to indemnify and hold harmless AIP, American Institute of Physics, and their officers, directors, employees or agents from and against any and all claims arising out of your use of the Material other than as specifically authorized herein.
7. The permission granted herein is personal to you and is not transferable or assignable without the prior written permission of AIP. This license may not be amended except in a writing signed by the party to be charged.
8. If purchase orders, acknowledgments or check endorsements are issued on any forms containing terms and conditions which are inconsistent with these provisions, such inconsistent terms and conditions shall be of no force and effect. This document, including the CCC Billing and Payment Terms and Conditions, shall be the entire agreement between the parties relating to the subject matter hereof.

This Agreement shall be governed by and construed in accordance with the laws of the

State of New York. Both parties hereby submit to the jurisdiction of the courts of New York County for purposes of resolving any disputes that may arise hereunder.

**If you would like to pay for this license now, please remit this license along with your payment made payable to "COPYRIGHT CLEARANCE CENTER" otherwise you will be invoiced within 48 hours of the license date. Payment should be in the form of a check or money order referencing your account number and this invoice number RLNK500716891.**

**Once you receive your invoice for this order, you may pay your invoice by credit card. Please follow instructions provided at that time.**

**Make Payment To:  
Copyright Clearance Center  
Dept 001  
P.O. Box 843006  
Boston, MA 02284-3006**

**For suggestions or comments regarding this order, contact RightsLink Customer Support: [customercare@copyright.com](mailto:customercare@copyright.com) or +1-877-622-5543 (toll free in the US) or +1-978-646-2777.**

**Gratis licenses (referencing \$0 in the Total field) are free. Please retain this printable license for your reference. No payment is required.**

---



---

---

License Number	2845471476903
Order Date	Feb 10, 2012
Publisher	American Institute of Physics
Publication	Journal of Chemical Physics
Article Title	NMR-Relaxation Mechanisms of O17 in Aqueous Solutions of Paramagnetic Cations and the Lifetime of Water Molecules in the First Coordination Sphere
Author	T. J. Swift, Robert E. Connick
Online Publication Date	Jul 15, 1962
Volume number	37
Issue number	2
Type of Use	Thesis/Dissertation
Requestor type	Student
Format	Print and electronic
Portion	Figure/Table
Number of figures/tables	1
Title of your thesis / dissertation	New Adaptations of Analytical Tools for the Study of Dynamic Interactions of Lanthanide-based Catalysis in Aqueous Media
Expected completion date	May 2012
Estimated size (number of pages)	300
Total	0.00 USD

**Terms and Conditions**

American Institute of Physics -- Terms and Conditions: Permissions Uses

American Institute of Physics ("AIP") hereby grants to you the non-exclusive right and license to use and/or distribute the Material according to the use specified in your order, on a one-time basis, for the specified term, with a maximum distribution equal to the number that you have ordered. Any links or other content accompanying the Material are not the subject of this license.

1. You agree to include the following copyright and permission notice with the reproduction of the Material: "Reprinted with permission from [FULL CITATION]. Copyright [PUBLICATION YEAR], American Institute of Physics." For an article, the copyright and permission notice must be printed on the first page of the article or book chapter. For photographs, covers, or tables, the copyright and permission notice may appear with the Material, in a footnote, or in the reference list.
2. If you have licensed reuse of a figure, photograph, cover, or table, it is your responsibility to ensure that the material is original to AIP and does not contain the copyright of another entity, and that the copyright notice of the figure, photograph, cover, or table does not indicate that it was reprinted by AIP, with permission, from another source. Under no circumstances does AIP, purport or intend to grant permission to reuse material to which it does not hold copyright.
3. You may not alter or modify the Material in any manner. You may translate the Material into another language only if you have licensed translation rights. You may not use the Material for promotional purposes. AIP reserves all rights not specifically granted herein.
4. The foregoing license shall not take effect unless and until AIP or its agent, Copyright Clearance Center, receives the Payment in accordance with Copyright Clearance Center Billing and Payment Terms and Conditions, which are incorporated herein by reference.
5. AIP or the Copyright Clearance Center may, within two business days of granting this license, revoke the license for any reason whatsoever, with a full refund payable to you. Should you violate the terms of this license at any time, AIP, American Institute of Physics, or Copyright Clearance Center may revoke the license with no refund to you. Notice of such revocation will be made using the contact information provided by you. Failure to receive such notice will not nullify the revocation.
6. AIP makes no representations or warranties with respect to the Material. You agree to indemnify and hold harmless AIP, American Institute of Physics, and their officers, directors, employees or agents from and against any and all claims arising out of your use of the Material other than as specifically authorized herein.
7. The permission granted herein is personal to you and is not transferable or assignable without the prior written permission of AIP. This license may not be amended except in a writing signed by the party to be charged.
8. If purchase orders, acknowledgments or check endorsements are issued on any forms containing terms and conditions which are inconsistent with these provisions, such inconsistent terms and conditions shall be of no force and effect. This document, including the CCC Billing and Payment Terms and Conditions, shall be the entire agreement between the parties relating to the subject matter hereof.

This Agreement shall be governed by and construed in accordance with the laws of the State of New York. Both parties hereby submit to the jurisdiction of the courts of New York County for purposes of resolving any disputes that may arise hereunder.

**If you would like to pay for this license now, please remit this license along with your payment made payable to "COPYRIGHT CLEARANCE CENTER" otherwise you will be invoiced within 48 hours of the license date. Payment should be in the form of a check or money order referencing your account number and this invoice number**

**RLNK500716898.**

**Once you receive your invoice for this order, you may pay your invoice by credit card. Please follow instructions provided at that time.**

**Make Payment To:  
Copyright Clearance Center  
Dept 001  
P.O. Box 843006  
Boston, MA 02284-3006**

**For suggestions or comments regarding this order, contact RightsLink Customer Support: [customercare@copyright.com](mailto:customercare@copyright.com) or +1-877-622-5543 (toll free in the US) or +1-978-646-2777.**

**Gratis licenses (referencing \$0 in the Total field) are free. Please retain this printable license for your reference. No payment is required.**

## AMERICAN INSTITUTE OF PHYSICS LICENSE TERMS AND CONDITIONS

Mar 01, 2012

---



---

License Number	2845471326575
Order Date	Feb 10, 2012
Publisher	American Institute of Physics
Publication	Journal of Chemical Physics
Article Title	Nuclear Magnetic Resonance Studies of Solutions of the Rare-Earth Ions and Their Complexes. IV. Concentration and Temperature Dependence of the Oxygen-17 Transverse Relaxation in Aqueous Solutions
Author	Jacques Reuben, Daniel Fiat
Online Publication Date	Dec 1, 1969
Volume number	51
Issue number	11
Type of Use	Thesis/Dissertation
Requestor type	Student
Format	Print and electronic
Portion	Figure/Table
Number of figures/tables	2
Title of your thesis / dissertation	New Adaptations of Analytical Tools for the Study of Dynamic Interactions of Lanthanide-based Catalysis in Aqueous Media
Expected completion date	May 2012
Estimated size (number of pages)	300
Total	0.00 USD

Terms and Conditions

American Institute of Physics -- Terms and Conditions: Permissions Uses

American Institute of Physics ("AIP") hereby grants to you the non-exclusive right and license to use and/or distribute the Material according to the use specified in your order, on a one-time basis, for the specified term, with a maximum distribution equal to the number that you have ordered. Any links or other content accompanying the Material are not the subject of this license.

1. You agree to include the following copyright and permission notice with the reproduction of the Material: "Reprinted with permission from [FULL CITATION]. Copyright [PUBLICATION YEAR], American Institute of Physics." For an article, the copyright and permission notice must be printed on the first page of the article or book chapter. For photographs, covers, or tables, the copyright and permission notice may appear with the Material, in a footnote, or in the reference list.
2. If you have licensed reuse of a figure, photograph, cover, or table, it is your responsibility to ensure that the material is original to AIP and does not contain the copyright of another entity, and that the copyright notice of the figure, photograph, cover, or table does not indicate that it was reprinted by AIP, with permission, from another source. Under no circumstances does AIP, purport or intend to grant permission to reuse material to which it does not hold copyright.
3. You may not alter or modify the Material in any manner. You may translate the Material into another language only if you have licensed translation rights. You may not use the Material for promotional purposes. AIP reserves all rights not specifically granted herein.
4. The foregoing license shall not take effect unless and until AIP or its agent, Copyright Clearance Center, receives the Payment in accordance with Copyright Clearance Center Billing and Payment Terms and Conditions, which are incorporated herein by reference.
5. AIP or the Copyright Clearance Center may, within two business days of granting this license, revoke the license for any reason whatsoever, with a full refund payable to you. Should you violate the terms of this license at any time, AIP, American Institute of Physics, or Copyright Clearance Center may revoke the license with no refund to you. Notice of such revocation will be made using the contact information provided by you. Failure to receive such notice will not nullify the revocation.
6. AIP makes no representations or warranties with respect to the Material. You agree to indemnify and hold harmless AIP, American Institute of Physics, and their officers, directors, employees or agents from and against any and all claims arising out of your use of the Material other than as specifically authorized herein.
7. The permission granted herein is personal to you and is not transferable or assignable without the prior written permission of AIP. This license may not be amended except in a writing signed by the party to be charged.
8. If purchase orders, acknowledgments or check endorsements are issued on any forms containing terms and conditions which are inconsistent with these provisions, such inconsistent terms and conditions shall be of no force and effect. This document, including the CCC Billing and Payment Terms and Conditions, shall be the entire agreement between the parties relating to the subject matter hereof.

This Agreement shall be governed by and construed in accordance with the laws of the State of New York. Both parties hereby submit to the jurisdiction of the courts of New

York County for purposes of resolving any disputes that may arise hereunder.

**If you would like to pay for this license now, please remit this license along with your payment made payable to "COPYRIGHT CLEARANCE CENTER" otherwise you will be invoiced within 48 hours of the license date. Payment should be in the form of a check or money order referencing your account number and this invoice number RLNK500716892.**

**Once you receive your invoice for this order, you may pay your invoice by credit card. Please follow instructions provided at that time.**

**Make Payment To:  
Copyright Clearance Center  
Dept 001  
P.O. Box 843006  
Boston, MA 02284-3006**

**For suggestions or comments regarding this order, contact RightsLink Customer Support: [customercare@copyright.com](mailto:customercare@copyright.com) or +1-877-622-5543 (toll free in the US) or +1-978-646-2777.**

**Gratis licenses (referencing \$0 in the Total field) are free. Please retain this printable license for your reference. No payment is required.**

---

## REFERENCES

- (1) (a) Fay, D. P.; Litchinsky, D.; Purdie, N. *J. Phys. Chem.* **1969**, *73*, 544–552. (b) Habenschuss, A.; Spedding, F. H. *J. Chem. Phys.* **1980**, *70*, 2797–2806. (c) Habenschuss, A.; Spedding, F. H. *J. Chem. Phys.* **1980**, *73*, 442–450. (d) Johansson, G.; Wakita, H. *Inorg. Chem.* **1985**, *24*, 3047–3052. (e) Hemmila, I. *J. Alloys Compd.* **1995**, *225*, 480–485. (f) Justel, T.; Nikol, H.; Ronda, C. *Angew. Chem. Int. Ed.* **1998**, *37*, 3084–3103. (g) Adam, J.-L. *Chem. Rev.* **2002**, *102*, 2461–2476. (h) Kido, J.; Okamoto, Y. *Chem. Rev.* **2002**, *102*, 2357–2368. (i) Kaminskii, A. A. *Phys. Stat. Sol. A*, **2003**, *200*, 215–296. (j) Rocha, J.; Carlos, L. D. *Curr. Opin. Solid State Mater. Sci.* **2003**, *7*, 199–205. (k) Auzel, F. *Chem. Rev.* **2004**, *104*, 139–173. (l) Wybourne, B. G. *J. Alloys. Compd.* **2004**, *380*, 96–100. (m) Parker, D. *Chem. Soc. Rev.* **2004**, *33*, 156–165. (n) Dossing, A. *Eur. J. Inorg. Chem.* **2005**, 1425–1434.
- (2) Parker, D.; Williams, J. A. G. *J. Am. Chem. Soc. Dalton Trans.* **1996**, 3613–3628.
- (3) Cotton, S. Coordination Chemistry of the Lanthanides. *Lanthanide and Actinide Chemistry*; John Wiley & Sons, Ltd: West Sussex, **2006**; pp 35–60.
- (4) Bünzli, J.-C. G.; Piguet, C. *Chem. Soc. Rev.* **2005**, *34*, 1048–1077.
- (5) Terreno, E.; Fasano, M.; Botta, M.; Aime, S. *Chem. Soc. Rev.* **1998**, *27*, 19–29.
- (6) Kim, S.; Lim, Y. T.; Soltesz, E. G.; De Grand, A. M.; Lee, J.; Nakayama, A.; Parker, J. A.; Mihhaljevic, T.; Laurence, R. G.; Dor, D. M.; Cohn, L. H.; Bawendi, M. G.; Frangioni, J. W. *Nature Biotechno.* **2004**, *22*, 93–97.
- (7) Kobayashi, S.; Hachiya, I. *J. Org. Chem.* **1994**, *59*, 3590–3596.
- (8) Eckert, C. A.; Liotta, C.L.; Bush, D.; Brown, J. S.; Hallett, J. P. *J. Phys. Chem.* **2004**, *108*, 18108–18118.

- (9) (a) Ishitani, H.; Kobayashi, S. *Tetrahedron Lett.* **1996**, *37*, 7357–7360. (b) Kobayashi, S. Homometallic Lanthanoids in Synthesis: Lanthanide Triflate-Catalyzed Synthetic Reactions. In *Transition Metals for Organic Synthesis*, 2nd ed.; Beller, M., Bolm, C., Eds.; Wiley-VCH Verlag GmGh & Co. KGaA: Weinheim, 2004; Vol. 1, pp 335–361. (c) Matsunaga, S.; Shibasaki, M. Rare Earth-Alkali Metal Heterobimetallic Asymmetric Catalysis. In *Multimetallic Catalysis in Organic Synthesis*; Shibasaki, M., Yamamoto, Y., Eds.; Wiley-VCH Verlag GmGh & Co. KGaA: Weinheim, 2004; pp 121–142. (d) Sasai, H.; Suzuki, T.; Itoh, N.; Tanaka, K.; Date, T.; Okamura, K.; Shibasaki, M. *J. Am. Chem. Soc.* **1993**, *115*, 10372–10373. (e) Satoh, K.; Kamigaito, M.; Sawamoto, M. *Macromolecules* **2000**, *33*, 4660–4666. (f) Yu, L.; Li, J.; Ramirez, J.; Chen, D.; Wang, P. G. *J. Org. Chem.* **1997**, *62*, 903–907. (g) Dzudza, A.; Marks, T. J. *J. Org. Chem.* **2008**, *73*, 4004–4016.
- (10) Dissanayake, P.; Averill, D. J.; Allen, M. J. In *Science of Synthesis*, Knowledge Updates 2011/4; Marek, I., Ed.; Georg Thieme Verlag KG: Stuttgart, Germany, 2012; pp 1–9.
- (11) Bünzli, J.-C.G.; Merback, A.E.; Nielson, R. M. *Inorg. Chim. Acta* **1987**, *139*, 151–152.
- (12) Bünzli, J.-C. G.; Kasperek, V. *Inorg. Chim. Acta* **1991**, *182*, 101–107.
- (13) Bünzli, J.-C. G.; Mabillard, C. *Inorg. Chem.*, **1986**, *25*, 2750–2754.
- (14) Bernardo, P. D.; Choppin, G. R.; Portanova, R.; Zanonato, P. L. *Inorg. Chim. Acta* **1993**, *201*, 85–91.
- (15) Geary, W. J. *Coord. Chem. Rev.*, **1971**, *7*, 81–122.
- (16) Habenschuss, A.; Spedding, F. H. *J. Chem. Phys.* **1979**, *70*, 2797–2806.
- (17) Narten, A. H.; Hahn, R. L. *J. Chem. Phys.* **1983**, *87*, 3193–3197.
- (18) Annis, B. K.; Hahn, R. L.; Narten, A. H. *J. Chem. Phys.* **1985**, *82*, 2086–2091.
- (19) Smith, L. S.; Wertz, D. L. *J. Am. Chem. Soc.* **1975**, *97*, 2365–2368.



- (20) (a) Supkowski, R. M.; Horrocks, W. D., Jr. *Inorg. Chim. Acta* **2002**, *340*, 44–48. (b) Horrocks, W. D., Jr. and Sudnick, D. R. *J. Am. Chem. Soc.* **1979**, *101*, 334–340.
- (21) Caravan, P.; Ellison, J. J.; McMurry, T. J.; Lauffer, R. B. *Chem. Rev.* **1999**, *99*, 2293–2352.
- (22) Kimura, T.; Nagashi, R.; Kato, Y.; Yoshida, Z. *J. Alloys Compd.* **2001**, *323–324*, 164–168.
- (23) Lis, S.; Chopping, G. R. *Anal. Chem.* **1991**, *63*, 2542–2543.
- (24) Dissanayake, P.; Allen, M. J. *J. Am. Chem. Soc.*, **2009**, *131*, 6342–6343.
- (25) Dissanayake, P.; Mei, Y.; Allen, M. J. *ACS Catal.* **2011**, *1*, 1203–1212.
- (26) Mukaiyama, T.; Narasaka, K.; Banno, K. *Chem. Lett.* **1973**, 1011–1014.
- (27) (a) Altenbach, H. J. *Org. Synth. Highlights.* **1991**, 66–70. (b) Machajewski, T. D., Wong, C.-H., Lener, R. A. *Angew. Chem., Int. Ed. Engl.* **2000**, *39*, 1352–1374. (c) Carreira, E. M. *Comprehensive Asymmetric Catalysis I-III* **1999**, *3*, 997–1065.
- (28) Chan, T. H.; Aida, T.; Lan, P. W. K.; Gorys, V.; Harpp, D. N. *Tetrahedron* **1979**, 4029–4031.
- (29) Heathcock, C. H.; Davidsen, S. K.; Hug, K. T.; Flippin, L. A. *J. Org. Chem.* **1986**, *51*, 3027–3031.
- (30) Palazzi, C.; Colombo, C.; Gennari, C. *Tetrahedron Lett.* **1986**, *27*, 1735–1738.
- (31) Heathcock, C. H.; Hug, K. T.; Flippin, L. A. *Tetrahedron Lett.* **1984**, *25*, 5973–5976.
- (32) Dubois, J.-E.; Axeiotis, G.; Bertouneque, E. *Tetrahedron Lett.* **1984**, *25*, 4655–4658.
- (33) Reetz, M. T.; Kessler, K.; Jung, A. *Tetrahedron* **1984**, *40*, 4327–4326.
- (34) Mahrwald, R. *Chem. Rev.* **1999**, *99*, 1095–1120.
- (35) Panek, J. S.; Jain, N. F. *J. Org. Chem.* **2001**, *66*, 2747–2756.
- (36) Kobayashi, S.; Furuta, T.; Hayashi, T.; Nishijima, M.; Hanada, K. *J. Am. Chem. Soc.* **1998**, *120*, 908–919.

- (37) Vougioukas, A. E.; Kagan, H. B., *Tetrahedron Lett.*, **1987**, 28, 5513–5515.
- (38) Lannou, M.-I.; H\_lion, F.; Namy, J.-L., *Tetrahedron*, **2003**, 59, 10551–10554.
- (39) Giuseppone, N.; deWeghe, P. V.; Mellah, M.; Collin, J., *Tetrahedron*, **1998**, 54, 13129–13132.
- (40) Kobayashi, S., *Chem. Lett.*, 1991, 2187–2192.
- (41) Kobayashi, S.; Wakabayashi, T.; Nagayama, S.; Oyamada, H., *Tetrahedron Lett.*, **1997**, 38, 4559–4563.
- (42) Ruland, Y.; Noereuil, P.; Baltas, M., *Tetrahedron*, **2005**, 61, 8895–8898.
- (43) Uotsu, K.; Sasai, H.; Shibasaki, M., *Tetrahedron: Asymmetry*, **1995**, 6, 71–74.
- (44) Desimoni, G.; Faita, G.; Piccinini, F.; Toscanini, M., *Eur. J. Org. Chem.*, **2006**, 5228–5232.
- (45) Hamada, T.; Manabe, K.; Ishikawa, S.; Nagayama, S.; Shiro, M.; Kobayashi, S., *J. Am. Chem. Soc.*, **2003**, 125, 2989–2992.
- (46) Kobayashi, S.; Manabe, K., *Acc. Chem. Res.*, **2002**, 35, 209–211.
- (47) Mei, Y.; Dissanayake, P.; Allen, M. J., *J. Am. Chem. Soc.*, **2010**, 132, 12871–12872.
- (48) Hamada, T., Manabe, K., Ishikawa, S., Nagayama, S., Shiro, M. and Kobayashi, S. *J. Am. Chem. Soc.* **2003**, 125, 2989–2996.
- (49) Kobayashi, S., Hamada, T., Nagayama, S. and Manabe, K. *Org. Lett.* **2001**, 3, 165–167.
- (50) Alleti, R.; Perambuduru, M.; Samantha, S.; Reddy, V. P. *J. Mol. Catal. A: Chem.* **2005**, 226, 57–59.
- (51) (a) Woods, M.; Woessner, D. E.; Zhao, P.; Pasha, A.; Yang, M.-Y.; Huang, C.-H.; Vasalitiy, O.; Morrow, J. R.; Sherry, A. D. *J. Am. Chem. Soc.* **2006**, 128, 10155–10162. (b) Jocher, C. J.; Moore, E. G.; Xu, J.; Avedano, S.; Botta, M.; Aime, S.; Raymond, K. N. *Inorg. Chem.* **2007**, 46, 9182–9191.

- (52) (a) Kürti, L., Czako, B. *Strategic Applications of Named Reactions in Organic Synthesis*; Elsevier Academic Press: Burlington, 2005; pp 298–299. (b) Palomo, C., Oiarbide, M. Garcia, J. M. *Chem.—Eur. J.* **2002**, *8*, 36–44.
- (53) (a) Halpern, J. *Science* **1982**, *217*, 401–407. (b) Grenthe, I. *Kemia-Kemi* **1978**, *5*, 234–237.
- (54) (a) Denmark, S. E.; Heemstra, J. R.; Beutner, G. L. *Angew. Chem., Int. Ed.* **2005**, *44*, 4682–4698. (b) Schetter, B. and Mahrwald, R. *Angew. Chem., Int. Ed.* **2006**, *45*, 7506–7525.
- (55) Kobayashi, S. and Hachiya, I. *Tetrahedron Lett.* **1992**, *33*, 1625–1628.
- (56) (a) Corey, E. J.; Rhode, J. J.; Fischer, A.; Azimioara, M. D. *Tetrahedron Lett.* **1997**, *38*, 33–36. (b) Ishihara, K., Kondo, S., and Yamamoto, H. *J. Org. Chem.* **2000**, *65*, 9125–9128. (c) Corey, E. J. and Lee, T. W. *Chem. Commun.* **2001**, 1321–1329.
- (57) Averill, D. J.; Dissanayake, P.; Allen, M. J. *Molecules* **2012**, *17*, 2073–2081.
- (58) (a) Sreekanth, P., Kim, S.-W., Hyeon, T., Kim, B. M. *Adv. Synth. Catal.* **2003**, *345*, 936–938. (b) Takeuchi, M., Akiyama, R., Kobayashi, S. *J. Am. Chem. Soc.* **2005**, *127*, 13096–13097.
- (59) Still, C. W.; Kahn, M.; Mitra, A. *J. Org. Chem.* **1978**, *43*, 2923–2925.
- (60) Andolina, C. M.; Holthoff, W. G.; Page, P. M.; Mathews, R. A.; Morrow, J. R.; Bright, F. V. *Appl. Spectrosc.* **2009**, *63*, 483–493.
- (61) Rohovec, J.; Vojtíšek, P.; Hermann, P.; Mosinger, J.; Žák, Z.; Lukeš, I. *Dalton Trans.* **1999**, 3585–3592.
- (62) Persson, I.; D'Angelo, P.; De Panfilis, S.; Sandström, M.; Eriksson, L. *Chem.—Eur. J.* **2008**, *14*, 3056–3066.
- (63) Tóth, É.; Dhubhghaill, O. M. N.; Besson, G.; Helm, L.; Merbach, A. E. *Magn. Reson. Chem.* **1999**, *37*, 701–708.

- (64) Brayshaw, P. A.; Bünzli, J.-C. G.; Froidevaux, P.; Harrowfield, J. M.; Kim, Y.; Sobolev, A. *N. Inorg. Chem.* **1995**, *34*, 2068–2076.
- (65) Spirlet, M.-R.; Rebizant, J.; Desreux, J. F.; Loncin, M.-F. *Inorg. Chem.* **1984**, *23*, 359–363.
- (66) Silber, H. B.; Mioduski, T. *Inorg. Chem.* **1984**, *23*, 1577–1583.
- (67) Holden, C. A.; Hunnicutt, S. S.; Sánchez-Ponce, R.; Craig, J. M.; Rutan, S. C. *Appl. Spectrosc.* **2003**, *57*, 483–490.
- (68) Stangret, J. J. *Mol. Struct.* **2002**, *643*, 29–35.
- (69) Mosyak, A. A.; Prezhdo, O. V.; Rosicky, P. J. *Mol. Struct.* **1999**, *485–486*, 545–554.
- (70) Dickens, B.; Dickens, S. H. *J. Res. Natl. Inst. Stand. Technol.* **1999**, *104*, 173–183.
- (71) Andolina, C. M.; Holthoff, W. G.; Page, P. M.; Mathews, R. A.; Morrow, J. R.; Bright, F. V. *Appl. Spectrosc.* **2009**, *63*, 483–493.
- (72) Beeby, A.; Faulkner, S.; Parker, D.; Williams, J. A. G. *J. Chem. Soc., Perkin Trans. 2* **2001**, 1268–1273.
- (73) Armarego, W. L. F.; Chai, C. L. L. *Purification of Organic Chemicals. Purification of Laboratory Chemicals*, 5th ed.; Elsevier: Cornwall, Great Britain, **2003**; pp 231–232.
- (74) D'Aléo, A.; Pompidor, G.; Elena, B.; Vicat, J.; Baldeck, P. L.; Toupet, L.; Kahn, R.; Andraud, C.; Maury, O. *Chem. Phys. Chem.* **2007**, *8*, 2125–2132.
- (75) Burai, L.; Tóth, É.; Moreau, G.; Sour, A.; Scopelliti, R.; Merbach, A. E. *Chem.—Eur. J.* **2003**, *9*, 1394–1404.
- (76) Kalesse, M.; Loos, A. *Bioorg. Med. Chem. Lett.* **1996**, *17*, 2063–2068.
- (77) Boykin, D. W.; Cotton, S. Applications of  $^{17}\text{O}$  NMR spectroscopy to structural problems in organic chemistry: Torsion angle relationships.  *$^{17}\text{O}$  NMR spectroscopy in Organic Chemistry* CRC Press, Inc. Boca Raton, **1991**; pp 35–60.

- (78) (a) Hubbard, P. S. *J. Chem. Phys.* **1970**, *53*, 985–987. (b) Bull, T.E., Forsén, s., Turner, D. L. *J. Chem. Phys.* **1979**, *70*, 3106–3111. (c) Abragam, A., *The principles of Nuclear Magnetism*, Oxford, London, **1978**; 314–318 (d) Fukushima, E., Roeder, S. B.W. *Experimental Pulse NMR*, Addison-Wesley; Reading, MA, **1981**; 158–161.
- (79) <http://chem.ch.huji.ac.il/nmr/techniques/1d/row2/o.html> (accessed on Feb 21, 2012).
- (80) (a) Denisov, V. P., Halle, B. *J. Mol. Biol.* **1995**, *245*, 682–697. (b) R. Kuroki, I. Ando, A. Shoji, T. Ozaki, *Chem. Commun.* **1992**, 433–434. (c) Kuroki, S., Takahashi, A., Ando, I., Shoji, A., Ozaki, T. *J. Mol. Struct.* **1994**, *323*, 197–208. (d) Asakawa, N., Kameda, T., Kuroki, S., Kurosu, H., Ando, S., Ando, I., Shoji, A. *Annu. Rep. NMR Spectrosc.* **1998**, *35*, 55–137.
- (81) (a) Dong, S., Ida, R., Wu, G. *J. Phys. Chem. A* **2000**, *104*, 11194–11202. (b) Wu, G., Yamada, K., Dong, A., Grondey, H. *J. Am. Chem. Soc.* **2000**, *122*, 4215–4216. (c) Kuroki, S., Takahashi, A., Ando, I., Shoji, A., Ozaki, T. *J. Mol. Struct.* **1994**, *323*, 197–208.
- (82) Asakawa, N., Kameda, T., Kuroki, S., Kurosu, H., Ando, S., Ando, I., Shoji, A. *Annu. Rep. NMR Spectrosc.* **1998**, *35*, 55–137.
- (83) Richardson, S. J., Baianu I, I. C., Steinberg, M. P. *J. Agric. Food Chem.* **1966**, *34*, 17–23.
- (84) Halle, B., Carlstrom, G. *J. Phys. Chem.* **1981**, *85*, 2142–2147.
- (85) van der Maarel, J. R. C., Lankhorst, D., de Bleijser, J., Leyte, J. C. *J. Phys. Chem.* **1986**, *90*, 1470–1478.
- (86) (a) Maigut, J.; Meier, R.; Zahl, A.; Eldik, R. v. *J. Am. Chem. Soc.* **2008**, *130*, 14556–14569. (b) Zhang, S.; Wu, K.; Biewer, M. C.; Sherry, A. D. *Inorg. Chem.*, **2001**, *40*, 4284–4290. (c) Burai, L.; Tth, v.; Sour, A.; Merbach, A. E. *Inorg. Chem.*, **2005**, *44*, 3561–3568. (d) Zhang, S.; Wu, K.; Sherry, A. D. *J. Am. Chem. Soc.* **2002**, *124*, 4226–4227.
- (87) Connick, R. E.; Poulson, R. E. *J. Chem. Phys.* **1959**, *30*, 759–761.

- (88) Hunt, J.P., Taube, H. *J. Chem. Phys.* **1951**, *19*, 602–609.
- (89) Connick, R. E., Stover, E. D. rate of elimination of water molecules from cations, **1961**, *65*, 2075–2077.
- (90) Swift, T. J., Connick, R. E. *J. Chem. Phys.* **1962**, *37*, 307–320.
- (91) Bernheim, R. A., Brown, T. H., Gutowsky, H. S., Woessner, D. E. *J. Chem. Phys.* **1959**, *30*, 950–956.
- (92) Reuben, J., Fiat, D. *J. Chem. Phys.* **1969**, *51*, 4918–4927.
- (93) Cossy, C., Helm, L., Merbach, A. E. *Inorg. Chem.* **1988**, *27*, 1973–1979.
- (94) Micskei, K., Helm, L., Briücher, E., Merbach, A. E. *Inorg. Chem.* **1993**, *32*, 3844–3850.
- (95) (a) Gilboa, H., Steinschneider, A., Valentine, B., Dhawan, D., Fiat, D. *Biochimica et Biophysica Acta*, *800*, 1984, 251–257. (b) Baltzer, L., Becker, E. D. *J. Am. Chem. Soc.*, **1983**, *105*, 5730–5733. (c) Fujikara, R., Rode, B. M. *Inorganica Chimica Acta*, 1982, *60*, 99–104. (d) Schwartz, H., MacCoss, M., Danyluk, S. S. *J. Am. Chem. Soc.*, **1983**, *105*, 5901–5911.
- (96) Werts, M H. V., Jukes, R. T. F., Verhoeven, J. W. *Phys. Chem. Chem. Phys.* **2002**, *4*, 1542–1548.

**ABSTRACT****NEW ADAPTATIONS OF ANALYTICAL TOOLS FOR THE STUDY OF DYNAMIC INTERACTIONS OF LANTHANIDE-BASED CATALYSIS IN AQUEOUS MEDIA**

by

**PRABANI LAKMANTHI DISSANAYAKE****May 2012****Advisor:** Dr. Matthew J. Allen**Major:** Chemistry**Degree:** Doctor of Philosophy

Lewis acid catalyzed carbon–carbon bond-forming reactions are of great interest in organic synthesis. However, many conventional Lewis acids, and almost all enantioselective Lewis acid catalysts, must be used under strictly anhydrous conditions to avoid hydrolysis and the difficulties associated with recovery and reuse of the catalysts. Due to these drawbacks of conventional Lewis acids, there is a growing desire to perform many organic transformations using more environmentally friendly aqueous-stable catalysts. The advantages of using aqueous-stable catalysts include the ability to use unprotected functional groups, ease of product separation and catalyst recovery, and avoidance of costly solvent drying procedures. Lanthanide trifluoromethanesulfonates (triflates),  $\text{Ln}(\text{OTf})_3$ , address this goal because they are water-tolerant Lewis acid precatalysts that can catalyze a wide range of important carbon–carbon and carbon–heteroatom bond-forming reactions such as the aldol, nitro-aldol, Mannich, Diels–Alder, Michael, Mukaiyama aldol, and Friedel–Crafts reactions due to their hard, electrophilic, and hydrolysis-stable character.

Despite their favorable properties, the use of lanthanide triflates in asymmetric carbon–carbon bond formation under aqueous conditions has been limited due to lack of mechanistic understanding of these precatalysts in aqueous solution: the influence of counter ion coordination, the effect of solvent coordination, and the identification of intermediates in the catalytic cycle. Further, identification of the rate-determining step and product-dissociation rate of aqueous lanthanide triflate-based catalysis is of fundamental importance for developing more efficient catalysts.

I adapted luminescence-decay measurements to enable the study of the mechanism of lanthanide-based precatalysts in aqueous systems. Because the number of water molecules coordinated to the lanthanide ion is critical to more thoroughly understanding the nature and the reactivity of lanthanide-based precatalysts, I used luminescence-decay studies to measure the dynamics of water molecules coordinated to lanthanide-ions throughout the catalytic cycle of a selected Mukaiyama aldol reaction. Using these luminescence-decay measurements, I determined equilibrium constants as well as structural and mechanistic information regarding lanthanide-based chiral catalytic systems in aqueous medium. Furthermore, I used this analytical tool to study the influence of the coordination environment of europium-based precatalysts including europium nitrates, chlorides, and acetates on reaction rate and yield. I also empirically derived equations that enable fast and accurate determination of the water-coordination number of lanthanides in binary solvent systems. In summary, I adapted luminescence-decay measurements to probe the coordination environment of europium-based precatalysts in aqueous media and the details of my efforts are described in this thesis.

The other analytical tool described in this thesis involves the use of  $^{17}\text{O}$  NMR spectroscopy with variable temperature for the determination of important exchange rates



in lanthanide-catalyzed reactions. The results described in this thesis demonstrate the utility of these two powerful analytical tools to study aqueous, lanthanide-catalyzed bond-forming reactions.

## AUTOBIOGRAPHICAL STATEMENT

### College Education

University of Colombo, Colombo, Sri Lanka: Chemistry B.S. 2001–2005  
Wayne State University, Detroit, Michigan, USA: Chemistry Ph.D. 2007–2012

### Honors and Awards

- Bhikaji Framji Khan Gold Medal for Chemistry awarded by the senate of the University of Colombo, Sri Lanka for the Excellency of being the batch top in the chemistry special degree program 2001/2005, University of Colombo
- Professor .C. L. De Silva memorial price in Chemistry awarded by the senate of the University of Colombo, Sri Lanka: 2003
- Graduate Student Professional Travel Award, Wayne State University, Detroit, MI, 2009
- Best talk award presented at the 12<sup>th</sup> Annual Chemistry Graduate Research Symposium, Wayne State University, Detroit, MI, October 9<sup>th</sup>, 2010
- Heller Fellowship, Wayne State University, Detroit, MI, 2010–2011
- Summer Dissertation Fellowship, Wayne State University, Detroit, MI, 2011
- David F. Boltz award in Analytical chemistry in recognition of superior academic achievement, the Faculty of the Department of Chemistry, Wayne State University, Detroit, MI, April 25<sup>th</sup>, 2011

### Professional Affiliations

- Phi Lambda Upsilon (PLU) Wayne State Chapter 2008–2011  
Sri Lankan Students Association (SLSA) Wayne State University 2007–2012
- American Chemical Society, 2010

### Research Experience

University of Colombo 2001–2005, Advisor: Dr. Ranjith Mahanama  
Wayne State University 2007–2012 (Graduate Student) Advisor: Dr. Matthew J. Allen  
Assistant Lecturer, University of Colombo, 2006–2007  
Probationary Lecturer, University of Sri Jayewardanapura, Sri Lanka, April 2007–Present  
Chemistry Teacher, Colombo International School, September 2006–April 2007  
Graduate Teaching Assistant, Wayne State University, 2007–2010

### Publications

**Dissanayake, P.**; Allen, M. J. *J. Am. Chem. Soc.* **2009**, *131*, 6342–6343.  
Mei, Y.; **Dissanayake, P.**; Allen, M. J. *J. Am. Chem. Soc.* **2010**, *132*, 12871–12873.  
**Dissanayake, P.**; Mei, Y.; Allen, M. J. *ACS Catal.* **2011**, *1*, 1203–1212.  
**Dissanayake, P.**; Averill, D. J.; Allen, M. J. Lanthanide-Catalyzed Mukaiyama Aldol Reactions. In *Science of Synthesis*, Knowledge Updates 2011/4; Marek, I., Ed.; Georg Thieme Verlag KG: Stuttgart, Germany, 2012; pp 1–9. (review article)  
Averill, D. J.; **Dissanayake, P.**; Allen, M. J. *Molecules* **2012**, *17*, 2073–2081.

### Presentations (presenter is underlined)

**Dissanayake, P.**; Allen, M. J. Presented at the Tenth Graduate Research Symposium, Wayne State University, October 4, 2008; Poster.  
**Dissanayake, P.**; Allen, M. J. Presented at the 31st Annual Michigan Catalysis Society Spring Symposium, Ann Arbor, MI, May 12, 2009; Talk.  
**Dissanayake, P.**; Allen, M. J. Presented at the 238th ACS National Meeting, Washington, DC, August 16–20, 2009; Poster Abstract INOR-524.  
**Dissanayake, P.**; Allohaibi, Z.; Mei, Y.; Allen, M. J. Presented at the 11th Annual Chemistry Graduate Research Symposium, Wayne State University, October 3, 2009; Poster.  
**Dissanayake, P.**; Allen, M. J. Presented at the 12<sup>th</sup> Annual Chemistry Graduate Research Symposium, Wayne State University, Detroit, MI, October 9<sup>th</sup>, 2010; Talk.